PLEASE NOTE:

In all cases this material has been filmed in the best possible way from the available copy. Problems encountered with this document have been identified here with a check mark ✓.

1. Glossy photographs _____
2. Colored illustrations _____
3. Photographs with dark background _____
4. Illustrations are poor copy _____
5. Print shows through as there is text on both sides of page _____
6. Indistinct, broken or small print on several pages ✓ throughout 54-56 + 257
7. Tightly bound copy with print lost in spine _____
8. Computer printout pages with indistinct print _____
9. Page(s) _____ lacking when material received, and not available from school or author _____
10. Page(s) _____ seem to be missing in numbering only as text follows _____
11. Poor carbon copy _____
12. Not original copy, several pages with blurred type _____
13. Appendix pages are poor copy _____
14. Original copy with light type _____
15. Curling and wrinkled pages _____
16. Other _____

COSMOLOGICAL TESTS OF A SCALE COVARIANT THEORY OF GRAVITATION

BY

Jane Rix Owen

A dissertation submitted to the Graduate Faculty in Physics in partial fulfillment of the requirements for the degree of Doctor of Philosophy, The City University of New York

1979

This manuscript has been read and accepted for the Graduate Faculty in Physics in satisfaction of the dissertation requirement for the degree of Doctor of Philosophy.

5/24/79
Date

Professor V. Canuto V. Canuto
Chairman of Examining Committee

5/24/79
Date

Professor Frank Martino Frank Martino
Executive Officer

Prof. R. B. Stothers

Prof. C. Yuan

Prof. E. Tryon

Prof. E. Spiegel

Supervisory Committee

The City University of New York

ACKNOWLEDGEMENTS

Dr. V. Canuto suggested this work, arranged for its support and worked as principal investigator with his colleagues on the bases of the scale-covariant tests and on the final expression of all parts of this work. Through his and Dr. Jastrow s offices, I have benefited from the resources of Goddard Institute of Space Studies, N.A.S.A. Doctors Wardle and Van Flandern have generously provided some of their data.

I would like to extend my personal thanks to Doctors Arons and Wittleman in their executive capacities and to many of the teachers from whom I took courses: their disinterested application of purely scholarly standards of achievement may give me and others the (essential) luxury of investigating the fundamental questions of physics.

This work was made possible in part by N.A.S.A. grant NGL 33-013-040.

TABLE OF CONTENTS

		page
A.	Perspective	1
B.	Planetary Considerations	23
C.	Cosmological Tests in Standard, Constant-G Theory	42
D.	Cosmological Tests in Scale-Covariant Gravitational Theory	110
E.	Scale Covariance and the log N-log S Relation	219
F.	Concluding Remarks	237
Bibliography		291

TABLES

	page
Tables C	79
Tables D	137
Tables E	261

FIGURES

	page
Figures C	39
Figures D	199
Figures E	269

SECTION A

PERSPECTIVE

SECTION A: PERSPECTIVE

I. The Thesis

The purpose of this thesis is to subject the scale-covariant theory of gravitation as formulated so far to major cosmological tests and to compare its performance with that of standard, constant G cosmology.

This work is the result of a collaboration and consists of four papers which form Parts B, C, D, and E of this thesis. The division of labor is approximately as follows:

Dr. V. Canuto suggested as mentor the subject of the binned θ-z section of C and the subjects of all the other papers with the exception of DVIII. In his capacity as advisor, he edited all the papers and selected the final conclusions. In addition, he provided the written text of almost all of D and EII. He independently derived several scale-covariant bases for all parts of B, D, and E, including those used. He personally went through all the mathematics and served as principal investigator.

Dr. S.-H. Hsieh provided the final form of B. Asked to edit D, he suggested and wrote part of the text of DVIII and Appendix C and rewrote part of the Introduction. He acted as a sounding board for B and D. He principally worked on the Paper II which is referenced in these works.

J. Owen wrote C and E on all levels, with the contributions of Dr. V. Canuto above noted. She independently derived several scale-covariant bases for the other parts. She provided the calculations, numerical computations, data analysis, literature search, graphs and tables, and intermediate and final result analysis for D. She made independent calculations and acted as sounding board and sometime editor on B.

Part B is "Varying G" by V. Canuto, S.-H. Hsieh, and J. Owen.

Part C is "Radio Cosmological Tests" by J. Owen.

Part D is "Scale Covariance and G-Varying Cosmology: III, The m vs. z, Ω_m vs. z, Θ_i vs. z, and N(m) vs. m Tests" by V. Canuto, S.-H. Hsieh, and J. Owen.

Part E is "Scale Covariance and G-Varying Cosmology: IV, The log N vs. log S Test" by V. Canuto and J. Owen.

Although each part of this thesis has its own introduction and references to recent developments of scale-covariant gravitational theory, it may be appropriate to say something at this point about the motivations for such investigations and for this thesis and to describe some of the salient features of each part.

II. A Scale Covariant Theory of Gravitation

Two of the most fundamental questions ever asked may have been: "What is the geometry of the Universe?" and "What are the forces of nature?" A quasi-religious feeling for the basic unity of physics has led scientists to suspect that if the answer to one of these questions were fully appreciated, the answer to the other would be implicitly understood. Usually the problems have been attacked separately, by the relativistic astrophysicists on the one hand and by the particle physicists on the other. Occasionally pontoon bridges have been proposed between the two subjects, by Brans and Dicke, by Hoyle and Narlikar, by Dirac, among others.

Four forces are recognized in contemporary physics: strong, electromagnetic, weak, and gravitational. The strengths of their coupling constants are approximately in the ratios: 1, 10^{-2}, 10^{-5}, and 10^{-41}. Weinberg and Salam have shown that a long-range and a short-range force, the electromagnetic and weak forces may be understood as manifestations of an interaction which is unified in the high energy regime and split in the low energy regime which obtains on the average today. It is speculated that all the forces

may have acted with the same strength when the universe was young, and their divergence today might be due to the low energies involved in most of our present observations. In particular, two long range forces, the electromagnetic and gravitational, may once have had the same strength. Frameworks which might encompass such a possibility have been erected with varying degrees of success by Milne, Jordan, Gilbert, Dirac, Brans and Dicke, Hoyle and Narlikar, and Canuto et al. It is the last formulation which is used as the basis of this investigation (Paper I). It posits a scale factor $\beta(t)$ between the gravitational and atomic (electromagnetic) line elements,

$$ds_E = ds_A \, \beta(t),$$

but does not provide a dynamical equation for determining $\beta(t)$. For convenience, a parametric form

$$\beta(t) = (t/t_o)^{-\epsilon}$$

is employed, which might be valid only for large cosmological times, i.e. after decoupling. The theory is as yet incomplete and it is intentional that before attempting to construct a unified model of the gravitational and electromagnetic interactions, we try to see if the theory, as developed so far, would

have any unphysical consequences by testing its compatibility with basic astrophysical observations. Such is the program of the present dissertation. Since we are testing for ≤ 1 part in 10^{10} change per year in the gravitational constant, the field of astronomy with its cosmological time scales forms a natural arena.

The model was tested for $-1 \leq \epsilon < 1$ and for $0 \leq q_0 \leq 1$ in general. In particular, ϵ was taken to be -1, -1/2, 0, +1/2, and .92. The value 0 corresponds to standard cosmology. When $0 < \epsilon < 1$ for a given observed redshift, we are looking at much more recent gravitational history than would be indicated by the redshifts interpretation in standard cosmology. When $\epsilon < 0$, for the range of deceleration parameters investigated, a given redshift corresponds to much more distant gravitational history than indicated by standard cosmology. Other values of ϵ and q_0 were tried occasionally to test the model's dependence on these parameters but not in a serious attempt to test compatibility with the data. A value ϵ identically equal to 1 was not used because of divergences which would occur in the equations.

We shall now explain how the the choice of and q_0 is unrelated to the posited variation of G in this thesis and how their choice is related to the elements of the Dirac Large Number Hypothesis:

The scale covariant theory of gravitation can but does not have to include the relations implied by Dirac's Large Number Hypothesis. These include the variation of G itself, which is implied by the near equality of the first large numbers, the Hubble age of the universe counted in units of the time it takes light to cross the classical radius of the electron,

$$\frac{c/H_o}{e^2/m_e c^2} \cong 7 \cdot 10^{40} ,$$

and the ratio of the electromagnetic to gravitational forces,

$$\frac{e^2}{Gm_e m_p} \cong 2 \cdot 10^{39} .$$

It was decided to incorporate $G \propto 1/t$ into all the non-standard tests presented in this paper.

A third large number, the number of nucleons within the Hubble radius of the universe,

$$\frac{3}{m_p} \frac{4\pi}{3} (c/H_o)^3 \cong 10^{78} ,$$

which is taken to imply that $N \propto t^2$, was not always included. Whenever both $G/G_o = t_o/t$ (all cases) and either $\epsilon = +1$ (irrespective of the deceleration

parameter) or $\bar{q}_o = 1/2$ (irrespective of ϵ) are assumed, this third large number naturally follows within the scale-covariant theory of gravitation. Conversely, if we assume all the large number relations, then either $\bar{q}_o = 1/2$ or $\epsilon = +1$. The other cases do not incorporate $N/N_o = (t/t_o)^2$, contrary to the spirit of the Dirac Large Number Hypothesis. However, the scale-covariant theory of gravitation is not committed to the Dirac Large Number Hypothesis. The choice $\epsilon = +1$ is Dirac's ... matter creation gauge (Here, the word gauge means the choice of scalar function $\beta(t)$.) which was preferred for a time; it has the interesting feature that while a singularity (big Bang) exists in atomic units, giving the universe a finite age, it occurs only in the infinite past in gravitational or Einstein units. It brought up many troublesome questions about how and in what form the matter would be created. Furthermore, within the context of the tests developed in this thesis, we shall see that the data is not most easily interpretable within this gauge. If we reject this gauge and still want to include all the large numbers, within the scale-covariant theory of gravitation, we choose $\bar{q}_o = 1/2$. If in addition

we wish to exclude all degrees of matter creation, not only as t^2 as when $\epsilon = +1$ but in any amounts, then we assume in addition that $\epsilon \neq -1$. This is Dirac's non-matter-creation gauge, which for practical purposes is equivalent to the old additive creation case (the creation we discuss above is multiplicative creation). In this gauge, the third large number proceeds from the relative rates of growth of the horizon and the scale factor R of the universe; it is due to more matter coming within the horizon as t^2. Dirac cosmologists have independent reasons for choosing $\alpha_0 = 1/2$. Instead of using it only to predict the third large number, they are concerned that with all other deceleration parameters, if we assume no matter creation and the third large number, we can form another large number, the total mass within R^3, which would be independent of time.

III. Part B

It is shown in Part B that when β = constant, the theory reduces to standard cosmology. In this case, the product G·M is conserved, but it is possible to allow G to vary if and only if M is allowed to vary. Many authors, proceeding from the results of standard general relativity theory, have disregarded this rule and violated its foundations. Allowing only G to vary, they

have obtained the following relations for the angular frequency n and orbital distance of two massive bodies:

$$\frac{\dot{n}}{n} = 2\,\frac{\dot{G}}{G} = -2\,\frac{\dot{R}}{R} \quad .$$

They should however have used

$$\frac{\dot{n}}{n} = 2\,\frac{(GM)^{\cdot}}{GM} = -2\,\frac{\dot{R}}{R} \quad .$$

Measurements of n and R will then tell us whether standard theory is correct without telling us whether we can in addition impose as is traditional M = constant and G = constant.

In scale covariant theory we obtain the relation

$$G\,M\,\beta = \text{constant},$$

which for β = constant reduces to standard theory. Energy and angular momentum are not conserved on cosmological scales. Kepler's law of periods holds, but his law of areas does not. We then obtain

$$\frac{\dot{n}}{n} = -\frac{(GM)^{\cdot}}{GM} = \frac{\dot{\beta}}{\beta} = -\frac{\dot{R}}{R} \quad .$$

Unless we have further evidence, we can only determine how much β or the product G·M varies. The additional information might come from radar-echo

experiments or from data on the expansion or shrinkage of macroscopic bodies, but then we would have to know more about their internal structure as described in Part B. The present evidence on the period of the Moon indicates, tentatively that $\dot{G} < 0$. If we then assume that M is constant for convenience, it would imply that G is indeed decreasing with time.

It may be possible when more data are available to apply these relations to the orbital elements of two compact stellar bodies, such as neutron stars. Such bodies may be proportionately far enough apart to make tidal effects negligible, and any changes in their internal structure may be monitored through their pulse frequencies.

It can also be shown that the standard arguments against the variation of G based on the solar luminosity varying as

$$L \propto G^{+7} M^{+5}$$

suffer from the same assumption of constant mass, variable G within Einstein's equations. It is then contended that if $L \propto G^{+7}$, the Earth would have been unreasonably hot within the time of geological records. If the product $G \cdot M$ is kept constant within Einstein's theory, then $L \propto G^{-2}$ only, which is acceptable as far as the Earth temperature is concerned. The explicit G and M dependence of stellar luminosities within the scale covariant theory of gravitation has not yet been determined.

We have been describing tests involving objects which are relatively close to us. We remind the reader that standard general relativity theory has only been tested on the scale of the solar system and it remains to be shown if it is as successful on an extragalactic scale. We pass therefore in Parts C, D, and E to tests involving high redshift objects: galaxies, QSO's, and quasars. High redshift objects have already been used in standard cosmology to test the subset of cosmological models represented by different deceleration parameters. For various reasons detailed in the text, standard cosmology has not been able to come up with an unequivocable number for $\bar{q}_0$. When we are discussing early times in the gravitational history of the universe, the choice of deceleration parameter has greater influence on our predictions than when we discuss recent times. Therefore, when $\epsilon < 0$ and for a given observed redshift, we determine a larger redshift in gravitational units, the effect of $\bar{q}_0$ is very pronounced and we can distinguish readily which of its values are most compatible with the data. Conversely, when $\epsilon > 0$, the effect of $\bar{q}_0$ on our predictions is even less pronounced than it is in standard cosmology, and an observed redshift corresponds to a more recent era in gravitational history than it does in standard cosmology.

IV. Part C

In Part C we examine the high redshift tests as they perform in standard cosmology in conjunction with recent radio data. Standard Friedman models with $\Lambda = 0$ are tested for $\bar{q}_o = 10, 5, 2, 1, 0.5,$ and 0.03 and occasionally for other values. One advantage of this work is that several major cosmological tests are run with the same source population whereas the results of the tests in the literature are hard to compare because they are based on different data. The tests were repeated for both interferometric and scintillation data sets with the original intention that any acceptable cosmological conclusions drawn from the tests would have to be compatible with both data sets. In order to be suitable for all tests, the data sets consisted of sources for which redshifts, fluxes, angular diameters, and spectral indices were available. Although drawn from different surveys, the sources are found in regions of the sky all covered by the deepest survey used. This by no means eliminates selection effects, but understanding the data in terms of selection effects is part of the impetus of the work.

The results for the interferometric data are:

In general correlation tests and data distributions indicate association of small physical diameter with brightness, with flat spectral index, and with high z. At the same time, flat spectral indices are correlated weakly with high z and with dimness.

A practical result of the investigation is the recommendation that sources with flat spectral indices be used for the angular diameter-redshift test instead of steep spectral index sources as sometimes suggested in the attempt to pick out a subset of sources which could serve as standard measuring rods. Steep spectral index sources are usually the more extended ones, and these are more prevelant at low z than high z; this may be due to a selection effect or to the greater sensitivity to cosmological evolution of the extended portions of the source. Whatever the reason, the small, flat index sources are present at all redshifts and are thus more suitable for an angular diameter-redshift test.

If we plot the absolute luminosity of the sources versus the redshift, the absence of bright sources at low redshift and of dim sources at high redshift is immediately apparent at all q_o. The disappearance of the dim sources is adequately understood as a selection effect. It is not apparent whether the lack of near, bright sources is due to selection, to evolution, to a local inhomogeneity or to interpretation within a faulty cosmology. A regression fit for

$$L = L_o (1 + z)^{p'}$$

was made for all the data and for the first through fifth ranking sources in bins of increasing redshift. The evolutionary exponent g' remained non-zero even at $q_o = 50$; this would seem to eliminate interpretation of the data purely in terms of a closed universe with moderate q_o. In order to examine the possibility that the apparent evolution might be due to a local hole, the tests, ranked and unranked, were rerun for the far z data only; lesser but finite evolution persisted. Finally, instead of a plot of the absolute luminosities against redshift, a plot of absolute luminosity versus volume was made; the local hole was much less in evidence since the small redshifts of the local region correspond to only small volumes. The absolute magnitudes were then plotted against V/V_m with the result that even the bright sources seem to have a uniform distribution and there absence at small z may be due to their low space density. If this is so, most of the apparent evolution is a selection effect.

It is then shown that if we assume a physical relationship between the luminosity and linear diameter of a source of various functional forms such that the brighter sources are the smaller ones, we can use this relationship in conjunction with the luminosity-redshift correlation just discussed to predict the

upper envelope of the metric angular diameter-redshift diagram. The angular diameter-redshift test was performed for ranked and unranked sources, for all data, for steep spectral index sources only, and for flat spectral index sources only. A regression fit for real or apparent evolution of the linear diameter as

$$D = D_o (1 + z)^{-W}$$

was made. It indicated an apparent decrease of source size with cosmological distance in excess of that expected in the standard Friedman, $\Lambda = 0$, models from geometrical considerations alone. Less apparent evolution is needed in open models than in closed models. This can be understood as a selection effect if we happen to be seeing the brighter sources at high z and these happen to be the physically smaller ones. A possibility exists that at high redshifts we are mixing measures of source components into our sample of measures of "largest angular size" which is usually the distance between source components; this would account for some of the decrease of D with z. However, the source components generally have flatter spectral indices than the extended regions of the sources and a plot of the distribution of spectral indices as a function of redshift together with the weakness of the corresponding correlation factor indicates that small and large spectral indices are found about equally in the near and far regions so

this possibility doesn't seem to dominate the statistics. Therefore the flat index sources would seem to form an acceptable set and the fit was indeed better when these sources were used rather than the steep ones. When the latter are used, we are investigating the selection envolope or the apparent evolution of the extended sources to a greater degree while probing for the cosmology.

Tests with the scintillation data showed wide scatter and were inconclusive. Flat spectral index sources were progressively absent from the sample at high z so these could not be used for the tests. The scintillation technique may measure mostly component sizes. The spectral indices used are crude parameters derived from the flux data of the total sources and do not necessarily represent the spectral indices of the source regions; these are presumably flatter than the indices of the whole sources. Even so, no relationship could be determined between the scintillation angular size and the redshift. Even for the interferometric data, no relationship was determined between component size and redshift although it appeared to be approximately proportional to the square root of the largest angular size; this last relationship may depend on the fact that we can not measure very accurately the fine structure of the small components.

A word of caution with respect to the posited correlation between size and brightness is in order. Even in the sample used, it only applies loosely to the extended sources. Small sources appear with all apparent luminosities; it may be that the correlation of luminosity with steep index is derived from the the small sources and the correlation of large linear diameter with steep index and with brightness is derived from the large diameter population.

V. Part D

In Part D we pass on to the full solution to Einstein's gravitational equations in atomic units for a matter dominated universe. The solution in Einstein units remains the same as in standard theory, but when viewed through atomic measurements, they can be either magnified or reduced. The choice $G/G_o = t_o/t$ is imposed. There are now two deceleration parameters, two Hubble constants, and two universal scale factors; those defined in gravitational units and those observed in atomic units. The results are applied to the magnitude- redshift test for elliptical galaxies and QSO s, to the isophotal angle-redshift test for elliptical galaxies, to the number count- magnitude test for QSO's, and to the metric angle-redshift test for quasars.

The metric angular diameter-redshift test is the only radio test in this part, and it is here

applied to essentially the same data as employed in Part C. In scale-covariant cosmology it is possible to account for the sharp decrease of metric angular size with redshift without recourse to selection effects or evolution if an open universe and a scale function β increasing with time are chosen.

For elliptical galaxies, the evolutionary parameter e, where

$$L = L_0 \beta^e ,$$

is calculated within scale-covariant theory extending the models used in standard theory. Subject to the same uncertainties as these models, it is found that the values so obtained account adequately for the observations. When $\epsilon < 0$, it becomes apparent that an open universe fits the data better than a closed one for the e obtained. As ϵ approaches +1, the results become indifferent to q_0.

Unfortunately there is no acceptable theory for the evolution of QSO's in standard theory which we can render in scale-covariant form to determine e. The expedient used is therefore to determine what evolutionary parameter is necessary to either pass through the QSO data on the magnitude-redshift diagram or to define its

its envelope and to see whether this value is consistent with other tests, such as the number count-magnitude test. In standard theory, as we shall see, the values are not compatible. In scale covariant cosmology we obtain for the integrate number count when $q_o = 0$:

$$N \propto \frac{1}{2} \ln(1+2F) - \frac{F(1+F)}{1+2F}$$

where

$$10^{.2(m-m_o)} = F(1+2F)^{p/2}/(1-\epsilon)$$

and

$$p = (1+e\epsilon)/2/(\epsilon-1),$$

and when $q_o = 1/2$:

$$R^{1/3} = \frac{4\pi n_o}{3}^{1/3} \frac{c}{H_o} \frac{F}{(1-q_o)(1+2F)^{1/2} + q_o(1+F)}$$

where

$$F = 10^{.2(m-m_o)} G^{1/2} \beta^{e/2} H_o/H_o.$$

In standard cosmology we would have had only

$$F = 10^{.2(m-m_o)} (1+z)^{E/2}$$

where

$$L = L_o (1+z)^E.$$

Because of this difference, it becomes possible to satisfy both the magnitude-redshift test and the number count-magnitude test for the same e when $\epsilon < 0$. We emphasize that it is not the magnitude of e which is pertinent but its uniqueness across several tests. For instance when $\epsilon = .92$, $e = 0$ can simulate the $E = 4.5$ of standard cosmology in the number count test, but $e \cong 2.5$ is required in the redshift-magnitude test for the same QSO's and gauge.

VI. Part E

In Part E we examine the number count-flux test for radio sources in a scale-covariant cosmology. This part is a logical continuation of Part D, and it was given its own section only because it is so large. The data used are the same as those used in Part C. Again, there are no adequate models for predicting the evolution of the sources. We rederive the radio luminosity function and find expressions for both the integrated and differential counts. The range of e acceptable for each test is found for different assumed gauges and deceleration parameters. In standard cosmology these ranges do not overlap and complicated evolutionary assumptions must be made to save the cosmology. In scale-covariant cosmology when $\epsilon < 0$ with an open universe, it is possible to obtain the main features of both tests with the same simple evolutionary parametrization. This success is not limited to our assumption of luminosity evolution. In general, if sourced density evolution is assumed in these tests instead of luminosity evolution, it enters with an exponent equal to

3/2 the value which would have been acceptable for luminosity evolution. This is true as well in standard cosmology where it is well known that these tests do not distinguish between the two kinds of evolution and accounts for some of the confusion in the literature as to the value of the exponent. It is suggested that if a diffuse spectrum could be taken at the same frequencies at which we observe the discrete sources, since we are determining $e + s$, where s is the exponent for density evolution, in the case of the diffuse spectrum and $3e/2 + s$ in the case of the discrete spectra, a little algebra combining the results of both tests might determine e and s separately.

This preface is intended only to give the main impetus of each Part to provide benchmarks for the reader persuing this thesis whose purpose is to show that at least on this level there are no contra-indications to a scale-covariant interpretation of gravitational theory.

SECTION B

PLANETARY CONSIDERATIONS

SECTION B: PLANETARY CONSIDERATIONS

I. INTRODUCTION

Mc Crea (1978) has pointed out that there is no sense in which the standard general relativity (GR) can admit a variable "gravitational constant". It was also suggested (Mc Crea 1974) that with improved observational confirmation of Einstein's results, thus establishing the correctness of his theory of gravitation, any variation of the gravitational constant can be ruled out by inference. While we agree with the former remark, we do take issue with the latter inference. In the present paper, we shall explain how Einstein's theory of gravitation can be reconciled with a varying gravitational constant.

The value of any dimensional physical constant depends on the units one employs. In a space-time theory such as GR, the fundamental unit is a length, which is provided by some measuring procedure. However, any measuring instrument, being a physical system itself, must obey certain dynamical laws. Thus, for example, if we use the distance between orbiting gravitational bodies as a reference, we would have a gravitational unit (or Einstein unit) of length. On the other hand, if atomic instruments, whose governing physical law is quantum electrodynamics, are used, we have an atomic unit of length. A priori, there is no reason to believe that the two units of length must be a constant multiple of each other. Consequently, when the "gravitational constant" is a constant in one system of unit, it is not necessarily a constant in the other system of unit.

The idea can be better illustrated. If we write ds_A, ds_E for the line elements as measured in atomic and gravitational units respectively, we would have in general

$$ds_E = \varphi(x)\, ds_A \qquad (1)$$

it follows then that all dimensionful physical quantities in the two respective units are similarly related:

$$Q_E = \beta^{\pi} Q_A \tag{2}$$

where Q_E and Q_A may be scalars, vectors or tensors and the exponent π is given by the dimensions of Q. In particular, the "gravitational constants" in the two units are related by

$$G_E = \beta^{\pi_g} G_A \tag{3}$$

We wish to note here a subtle difference between our use of the terms "general relativity" and "Einstein's theory of Gravitation". The former assumes the strong principle of equivalence which dictates that β must be strictly constant. If one assumes only the weak equivalence principle, Einstein's theory of gravitation remains intact, and β can in general be a function of space-time. In the geometrical framework of Einstein's theory of gravitation, the Bianchi identities along with the conservation of energy and momentum demand a constant G_E, which is a proportionality factor between the geometrical Einstein tensor and the energy-momentum tensor. We note that it is G_E, and not

the "gravitational constant" in any other units which is required to be a constant, because Einstein's theory governs the dynamics of gravitational phenomena only, and it provides a geometrodynamical unit of length. Hence Einstein's field equations must be understood as written in Einstein units. In standard GR, people use these equations as though they are also valid in atomic units. It should be recognized however that this amounts to making an extra assumption, namely, that the scaling function $\beta(x)$ in Eq. (1) is a constant. Thus, one goes beyond the realm of gravitational physics and stipulates a specific relation between gravitational dynamics and atomic dynamics. If the gravitational interaction strength changes relative to electromagnetic interaction, we must expect β to be varying and therefore according to (3) G_A must also be varying. It is in this sense that we can accommodate and interpret a varying "gravitational constant". From this viewpoint of scaling between two kinds of dynamical units, G must be expressible as a functional of β as is clear from (3). However, it is important to note that for a complete determination of the variation of G, one must know not only the variation of β but also the value of π_g, as we shall explain in more details below.

With this understanding, it becomes evident that observational confirmation of Einstein's results in purely gravitational experiments can be compatible with experiments which purport to measure the variation of G, provided in the latter, atomic units are used. This in fact is what some observers have been attempting to do in the

past few years: measuring the non-gravitational variation of the orbital period of the moon in terms of atomic time. Whatever theoretical prejudice one may have for preferring a null result in the above experiments, one should keep an open mind and allow for the possibility of a non-null result.

Historically, Milne had long ago anticipated the possibility of Eq. (1). When Dirac introduced his Large Numbers Hypothesis (LNH) and proposed a varying G, he also had Eqs. (1)-(3) in mind. Unfortunately, when people study the effects of a varying gravitational constant, Newton's or Einstein's dynamical equations are used with only the modification that G_E is allowed to be a variable. As was pointed out, this is a logically inconsistent procedure.

A consistent formulation of the gravitational equations in non-gravitational units has been given in an earlier paper (Canuto et al. 1977) in which we developed the ideas outlined above: gravitational dynamics remains unchanged. When described in atomic units, the dynamical equations are obtained by conformal transformation, as required by Eq. (1), from the corresponding ones in standard GR. Clearly the a priori undetermined function β would appear in these equations. If e.g., the observational results are analyzed with these equations, β can be determined observationally. On the other hand, one could apply theoretical considerations such as Dirac's LNH to fix the functional

form of β. In this case, the conformally transformed dynamical equations are fully deterministic, and one can predict results from experiments using atomic units. In this manner, one can have a valid observational check on Dirac's ideas.

In the next section, we briefly review the framework of scale covariant gravitation introduced in an earlier paper and then illustrate the types of theoretical considerations one can use for the determination of β. In Section III, we shall show in some detail how the scale covariant framework can be used to interpret and analyze data from atomic measurements of gravitational phenomena, thus giving a description of the observational determination of β.

II. THEORETICAL DETERMINATION OF β

With the premise that Einstein's theory correctly describes gravitational phenomena, the following field equations and geodesic equations are assumed valid:

omena, the following field equations and geodesic equations are assumed valid:

$$G^{(E)}_{\mu\nu} = -\,8\pi\, C_E\, T^{(E)\mu\nu} \tag{4a}$$

$$\frac{d^2 x^\mu}{d\lambda_E^2} + \Gamma^\mu_{\nu\rho}\, \frac{dx^\nu}{d\lambda_E}\, \frac{dx^\rho}{d\lambda_E} = 0\ . \tag{5a}$$

where $d\lambda_E$ is the differential affine parameter, identifiable with the differential path length for non-null geodesics. It is therefore a length measured in Einstein units. We adopt the convention that the coordinate differential is dimensionless. Thus, given that

$$ds_E^2 = {}^{(E)}g_{\mu\nu}\, dx^\mu\, dx^\nu \quad ; \quad ds_A^2 = {}^{(A)}g_{\mu\nu}\, dx^\mu\, dx^\nu \tag{6}$$

Equation (1) implies

$${}^{(E)}g_{\mu\nu} = \beta^2\, {}^{(A)}g_{\mu\nu} \quad , \tag{7}$$

which can be readily recognized as a conformal transformation. The geometric parts of Eq. (4a) and (5a) are easily transformed. With the further assumption that the right hand side of (4a) is form invariant (see Canuto et al. 1977, for details), we get

$${}^{(A)}G_{\mu\nu} + f_{\mu\nu} = -\, 8\pi\, G_A\, {}^{(A)}T_{\mu\nu} \tag{4b}$$

with

$$f_{\mu\nu} = 2\, \frac{\beta_{\mu;\nu}}{\beta} - 4\, \frac{\beta_\mu\, \beta_\nu}{\beta^2} - {}^{(A)}g_{\mu\nu} \left(2\, \frac{\beta^\rho}{\beta}{}_{;\rho} - \frac{\beta^\rho\, \beta_\rho}{\beta^2} \right)$$

and

$$\frac{d^2 x^\mu}{d\lambda^2} + \Gamma^\mu_{\nu\rho}\, \frac{dx^\nu}{d\lambda_A}\, \frac{dx^\rho}{d\lambda_A} + \frac{\beta_\nu}{\beta} \left(\frac{dx^\mu}{d\lambda_A}\, \frac{dx^\nu}{d\lambda_A} - g^{\mu\nu}\, \frac{dx^\rho}{d\lambda_A}\, \frac{dx_\rho}{d\lambda_A} \right) = 0 \tag{5b}$$

with

$$\beta_\nu \equiv \beta_{,\nu} \ .$$

We note that $G^{(E)}_{\mu\nu}$ and $G^{(A)}_{\mu\nu}$ are the Einstein tensors constructed from $g^{(E)}_{\mu\nu}$ and $g^{(A)}_{\mu\nu}$ respectively. Covariant differentiation in (4b) is defined with respect to $g_{\mu\nu}$. Likewise, the Γ's in (5a) and (5b) are the Christoffel symbols constructed from $g^{(E)}_{\mu\nu}$ and $g^{(A)}_{\mu\nu}$ respectively.

It can be shown from (1b), using (3) that

$$T^{\mu\nu}{}_{;\nu} = (\pi_g - 2)\, T^{\mu\nu}\, (\partial_\nu \beta)_\nu + (\partial_\nu \beta)^\mu \pi^\nu_\nu \ . \tag{8}$$

(Hereafter, we drop the index A for atomic units). Hence the energy momentum conservation law in atomic units must be modified as a consequence of our assumptions. In the same spirit the modified baryon number conservation equation reads

$$(nu^\mu)_{;\mu} + (1 - \pi_g)\, n\, \frac{\dot{\beta}}{\beta} = 0 \tag{9}$$

where n is the baryon number density. The generalization given by Eq. (9) is compatible with Eq. (8) if we assume a perfect fluid form for the energy momentum tensor with $p = 0$. However, the validity of (9) is independent of this assumption.

If one writes ($p = \Gamma \rho$)

$$T^{\mu\nu} = (\rho + p)\, u^{\mu}\, u^{\nu} - p\, g^{\mu\nu} \tag{10}$$

and integrate equations (8) and (9) over a volume element V, it can be shown that Eq. (8) yields

$$\rho V^{(1+\Gamma)} \sim G^{-1}\, \beta^{-(1+3\Gamma)} \tag{11}$$

and Eq. (9) yields

$$nV \sim G^{-1}\, \beta^{-1} \tag{12}$$

where Γ has been assumed constant, and we have again made use of Eq. (3). Equations (11) and (12) give the allowed variation of total energy (in atomic units) and particle number within a co-moving volume. Obviously, the results of the standard theory are recovered if we set G and β equal to constants.

With the aid of Eqs. (11) and (12), we can indicate how cosmological considerations such as Dirac's LNH can be used for the determination of β. (A more detailed discussion and a brief review of LNH can be found in Canuto et al. 1977). We assume homogeneous cosmological models so that only functional dependence with respect to cosmic time t (in atomic units) needs to be considered.

(a) First gauge. If we assume (Dirac 1974)

$$G \sim \frac{1}{t} \quad , \quad N \equiv nV \sim t^2 \quad , \tag{13}$$

Equations (11) and (3) imply that

$$\beta \sim \frac{1}{t} \quad , \quad \pi_g = -1 \tag{14}$$

(b) Second gauge, (Dirac 1938). If we assume

$$G \sim \frac{1}{t} \quad , \quad N \equiv nV \sim t^0 = \text{constant} \quad . \tag{15}$$

Eqs. (12), (15) and (3) then yield

$$\beta \sim t \quad , \quad \pi_g = +1 \tag{16}$$

(c) From considerations of the spectrum of the background radiation (Canuto and Hsieh 1978), one may prefer to impose the auxiliary condition that radiation be adiabatically conserved. Thus with $\Gamma = \frac{4}{3}$, we find from (11) that

$$G\beta^2 = \text{constant} \tag{17}$$

Together with (13) and (3) we obtain

$$\beta \sim t^{1/2} \quad , \quad \pi_g = 2 \tag{18}$$

The common assumption among the above three cases is the Dirac hypothesis that the gravitational constant decreases as the inverse of the cosmological epoch. The hypothesis of matter creation which is incorporated only in Case (a), can be modified. Instead of specifying the time variation of the particle number within a co-moving volume, one can stipulate that the number of particles within the observer horizon increases as the square of the epoch:

$$N_{II} = \frac{\rho_m}{m} (ct)^3 \sim t^2 \quad . \tag{19}$$

We shall now show that for certain cosmological models, the assumption (19) leads back to the hypothesis on the variation of G.

For that purpose, we note first that Eq. (11) with $\Gamma = 0$ gives the variation of mass density

$$\rho_m \sim R^{-3} G^{-1} \beta^{-1} \tag{20}$$

where we have replaced the volume by R^3, R being the scale factor in the Robertson-Walker metric. Next we note that Eqs. (4a), (4b) are conformal transformation of each other and so must be their solutions. Hence, using (7) it can be shown that

$$R_E(t_E) = \beta(t) R(t) \tag{21}$$

where $R_E(t_E)$ is the scale factor of the R-W metric in Einstein units satisfying (4a). It is well known that in the matter dominated era, for $k = 0$, we have

$$R_E(t_E) \sim t_E^{2/3} \tag{22}$$

Using Eq. (1), Eq. (21) can be rewritten as

$$R(t) \sim \beta^{-1}(t) \left\{ \int_o^t \beta(t')\, dt' \right\}^{2/3} \tag{23}$$

With Eqs. (20) and (23), (19) becomes

$$N_H \sim \beta^2\, t^3\, G^{-1} \left(\int_o^t \beta(t')\, dt' \right)^{-2} \sim t^2$$

which, for simple power laws $\beta \sim t^p$, $(p \neq -1)$ yields

$$N_H \sim \frac{t}{G} \sim t^2$$

i.e. $G \sim t^{-1}$, the hypothesis on the variation of G (Dirac 1938).

III. OBSERVATIONAL DETERMINATION OF β

From standard theory, it is easy to show that

$$G_E\, M_E = \text{const.} \tag{24}$$

$$\frac{\dot{n}_E}{n_E} = 2 \frac{(G_E M_E)^{\cdot}}{G_E M_E} \tag{25}$$

$$\frac{\dot{R}_E}{R_E} = - \frac{(G_E M_E)^{\cdot}}{G_E M_E} \tag{26}$$

where R_E is the radius of the planetary orbit and $n_E = \frac{2\pi}{T_E}$, with T_E denoting the period of revolution. Without a clear distinction between different dynamical clocks, it has been tempting for observers to interpret the variation of $(\dot{n}/n)$ and $(\dot{R}/R)$, over and above that due to tidal effects, in terms of Eqs. (25) and (26). In fact, assuming a constant total mass, it is often stated that

$$\frac{\dot{n}_E}{n_E} = 2 \frac{\dot{G}_E}{G_E} = -2 \frac{\dot{R}_E}{R_E} \tag{27}$$

Observational results are often presented in terms of $\frac{\dot{G}}{G}$, using Eq. (27) (see for example Reasenberg and Shapiro 1977 and 1978). The latter is the result of what Dirac has referred to as a "primitive theory" of varying G which stipulates the same Newtonian equations of motion with G being a function of time. Such a stipulation by itself is not necessarily wrong unless one imposes also certain conservation laws which are not compatible with the assumed dynamical equations. This is most easily understood in the framework of Einstein's theory of gravitation where for a given Lagrangian, both the dynamical equations and the conservation laws are specified. Considering the Newtonian

equations as a classical limit of Einstein's theory, Eqs. (25) and (26) must be used in conjunction with the constraint (24), i.e. $G_E M_E$ = constant. Hence, the only information one can get from these two equations is that

$$\frac{dn_E}{dt_E} = 0 , \quad \frac{dR_E}{dt_E} = 0 \tag{28}$$

Thus imposition of the standard conservation law, namely, constant total mass, cannot be compatible with variable G.

On the other hand, measurements of planetary orbital parameters using atomic instruments ought not be considered as a test of Einstein's theory of gravitation per se. Rather, assuming the latter's validity, such observations should be considered a test of the constancy of β. Since the orbital period and radius are both small intervals compared to the cosmological scale, the differential scaling law, Eq. (1), applies so that

$$n_E = \frac{1}{\beta} n ; \quad R_E = \beta R \tag{29}$$

where n and R now refer to the corresponding orbital parameters measured in atomic units. With the assumed constancy of n_E and R_E, we find immediately

$$\frac{\dot{n}}{n} = \frac{\dot{\beta}}{\beta} = - \frac{\dot{R}}{R} \tag{30}$$

Thus having introduced the distinction between two dynamical clocks, a non-vanishing observational result in $\dot{n}$ and $\dot{R}$ can be easily understood. Even without reference to the constraint (24), primitive theory and the new theory can be distinguished in that they imply different ratios.

$$\frac{\dot{n}_E/n_E}{\dot{R}_E/R_E} = -2 \quad , \qquad \frac{\dot{n}/n}{\dot{R}/R} = -1$$

which can be checked by observations.

One can derive (30) in a more elaborate fashion, using the equation of motion (5b). However, as can be recognized, (5a) and (5b) are conformal transformations of each other. Results of (5b) can be obtained from those of (5a) by a conformal transformation.

To gain more information from (30), we first note that for non-relativistic matter, the energy density ρ is mostly due to the rest mass density. Hence with $\Gamma = 0$, Eq. (11) gives

$$\rho V \sim (G\beta)^{-1}$$

or

$$GM\beta = \text{constant} \quad , \tag{31}$$

which replaces Eq. (24). Clearly for $\beta = 1$, the two coincide. We now have

$$\frac{\dot{n}}{n} = -\frac{(GM)^{\cdot}}{GM} = -\frac{\dot{R}}{R} = \frac{\dot{\beta}}{\beta} \tag{32}$$

Thus, unless one makes more detailed stipulations, observational determination of the variation of β by measuring $\dot{n}$ and $\dot{R}$ gives no information about the separate variation of G and M. This is expected of all gravitational experiments dealing with geodesic motions. For the latter respond to the source strength which is always characterized by the combination GM. On the other hand, given hypotheses (a), (b) or (c) as described in the previous section, the variations of G and/or M are specified by cosmological considerations. These in turn determine $\dot{\beta}/\beta$ which can be checked, using Eq. (30), against the measured values of $\dot{n}/n$ and $\dot{R}/R$. Before making more detailed comments on such a comparison, we shall consider another effect of varying β.

If the strength of the gravitational interaction does change with respect to that of atomic dynamics, the size of a macroscopic object such as a planet or a star would be expected to vary with time. To see this, we consider a model in which matter has an equation of state of the form

$$p \sim \rho^{\gamma} \tag{33a}$$

where p and ρ are respectively the pressure and mass density. γ is called the polytropic index.

It has been shown (Canuto et al. 1977) that from (4b), the equation of hydrostatic equilibrium in the non-relativistic limit retains the standard Newtonian form

$$\frac{dp}{dr} = -\rho \frac{GM}{r^2} \tag{33b}$$

From (33a) and (33b), we get

$$GM^{2-\gamma} r^{3\gamma-4} = \text{constant} \quad ,$$

so that

$$\frac{\dot{r}}{r} = -\frac{1}{4-3\gamma} \frac{\dot{G}}{G} + \frac{2-\gamma}{4-3\gamma} \frac{\dot{M}}{M} \tag{34a}$$

Making use of (31), we can write

$$\frac{\dot{r}}{r} = \frac{\gamma-2}{4-3\gamma} \frac{\dot{\beta}}{\beta} + \frac{\gamma-1}{4-3\gamma} \frac{\dot{G}}{G} \tag{34b}$$

It is important to note that unlike the case of a planetary orbit, the variation of the radius of the kind of macroscopic object under consideration cannot be reduced to purely a variation of the product GM. Hence the two types of observations (32) and (34b) together give not only the value of $\dot{\beta}$, but $\dot{G}$ and $\dot{M}$ separately.

There has been indications (Mc Elhinny et al. 1978) that the Earth and Mars have been slowly expanding whereas Mercury has been contracting. On the other hand, no observable variation of the size of the Moon is detected. Not withstanding the difficulties of interpretating paleomagnetic data, Mc Elhinny et al.'s results cannot be directly compared with (34b) because the latter is merely a rough approximation for a simplistic polytropic model. Many geo-thermal effects which can contribute to the variation of the radius have not been included. Nevertheless, the model does point out the fact that in situations where a balance of two types of forces is at play, one can gain information on the separate variation of G and M. We therefore venture to suggest that with

sophisticated computation of stellar structure and high resolution measurement of the solar radius, one can perhaps have sufficient accuracy for a determination of $\dot{G}/G$.

Finally, we return to the observational determination of $\dot{\beta}$ using (30). The latest values of the observed total variation of n for the moon are

$$\dot{n}_a = (-23.8 \pm 4)'' \text{ cy}^{-2} \qquad \text{(Williams et. al. 1978)}$$

$$\dot{n}_a = (-24.6 \pm 1.6)'' \text{ cy}^{-2} \qquad \text{(Calame and Mulholland, 1978)}$$

$$\dot{n}_a = (-21.7 \pm 3.6)'' \text{ cy}^{-2} \qquad \text{(Van Flandern, 1978)}$$

From these one must subtract the contribution due to tidal effects (Muller, 1978).

$$\dot{n}_t = (-30.0 \pm 3)'' \text{ cy}^{-2}$$

so that the net variation can be expressed as

$$\frac{\dot{n}}{n} = \frac{1}{n} (\dot{n}_a - \dot{n}_t) \tag{35}$$

where $n = 1.73 \times 10^9$ $''$ cy^{-1}. These data indicate that

$$\frac{\dot{n}}{n} = (3.6 \pm 2.9)\ 10^{-11}/\text{yr}$$

$$= (3.1 \pm 2.0)\ 10^{-11}/\text{yr} \tag{36}$$

$$= (4.8 \pm 2.7)\ 10^{-11}/\mathrm{yr}$$

Hence from (32),

$$(GM)^{\cdot} > 0 \ , \quad \dot{\beta} > 0 \tag{37}$$

Comparison with (14), (16) and (18) shows that of the three different gauge conditions proposed for the determination of β, only Dirac's matter creation gauge (14), is excluded by present observations.

IV. CONCLUSION

We have advocated the interpretation of a varying G as a non-constant scale between atomic and gravitational clocks. Consistent dynamical equations with a varying G can thus be written and observational data should be analyzed in terms of these equations. The scaling function β is not dynamically determined. This is because the theory is as yet incomplete. In fact so far we have only expressed gravitational dynamics in terms of atomic units. When a theory of coupled atomic and gravitational dynamics will be available, we expect β to emerge naturally as a dynamical field variable.

On the other hand, observational constraints on β can be a valuable guide for the construction of such a theory. It is therefore useful to further develop the present theory to study its astrophysical and cosmological consequences. Part of this task has been accomplished (Canuto and Hsieh, 1978; Sections D and E below). It is found that currently available observations on magnitudes, angular diameters and radio-data do not exclude a varying G of one part in 10^{11} per year.

SECTION C

STANDARD TESTS

SECTION C: STANDARD TESTS

INTRODUCTION

Continuing examination of the optical and radio data for galaxies and quasi-stellar objects has not yielded a decisive preference for any cosmological model. The indeterminism is ascribed to (1) the scarcity of data, (2) the superposition of selection effects and evolutionary trends of the sources upon the cosmological functional dependence, and (3) the intrinsic statistical spread of the source parameters.

The observed parameters available for radio sources are apparent magnitude m (derived from the observed flux S), redshift z, spectral index α, and angular diameter θ determined either by interferometry or scintillation. Throughout this paper it will be assumed that the redshifts are cosmological.

The traditional tests are m-z, θ-z, m - θ, the volume test V/Vm, and the number counts N(S), N(θ), and N(z). Variations of these tests may be made with the derived quantities: absolute magnitude M(m, z), linear diameter D(θ, z), and bolometric distance $d_L(z)$ assuming a given cosmological model but are not different except formally from the tests with m, θ, and z.

The tests may be applied to optical or radio data with or without ranking. Most of the tests applied to cluster galaxies have been applied to the radio data. Bahcall and Hills (1973) and Burbidge and O'Dell (1973) have found some trend although of debatable slope in the m - z relation for radio sources using the first-rank method. Ehlers (1975 Urbino NATO Summer School) has investigated the θ-S relation, and Narlikar and Chitre (1977 Tata preprint) have applied two statistical tests to this mapping which also involve breaking up the data sets into luminosity classes, i.e. a brightness ranking principle

on N(θ) is incorporated. Sandage (1972) has applied the first-rank method to the θ - z relation for cluster galaxies. The θ - z relation for radio sources has been investigated without ranking by Wardle and Miley (1974) using interferometric angles (and interpreted assuming there is no established m - z relation), by Hewish, Readhead, and Duffet-Smith (1974) using scintillation angles, and by Readhead and Longair (1975) using the scintillation index. It is the intention of this paper to repair a hiatus in the family of testing by treating the θ - z relation for radio sources with ranking since ranking improved the picture in the m - z test.

The possibility that the surface brightness-redshift test may separate the cosmological, evolutionary, and observational effects has been discussed by Petrosian (1976), Tinsley (1976), and Disney (1976). In the present paper a functional form $(1 + z)^{g}$ is assumed for the absolute luminosity L and $(1 + z)^{-w}$ for D, the linear diameter. A regression analysis determines the best g and typical L from the ranked M - z test and the best w and typical D from the ranked θ - z test for different cosmological models. The success of the model is judged by the goodness of the fit.

The ranked θ - z test is also made assuming no evolution in order to see which purely cosmological formulation gives the best fit. The models considered are the traditional Friedman universes with $\Lambda = 0$, $\rho/\rho_c = 2\ q_0 = 20$, 10, 4, 2, 1, and .06 and the steady state universe, $q_0 = -1$. The correlation functions of the observed θ with z and of θ with the theoretical angle φ, where φ is the best fit of the θ - z data for a given cosmological model, were also used as tests of the cosmological θ - z relation.

The problem of the intrinsic variance of source parameters is attacked by searching for correlations among z, θ, D, S, m, M, and α which might allow

selection of a subset with less intrinsic variance. In fact it is the M - D correlation which allows us to rank sources by their luminosity and then use the first brightest, second brightest, etc. in the θ - z test and find a lesser spread in angular diameter. Comparative ranking of the sources by θ, D, m, and M is also used to test the M - D correlation. The correlation of diameter with spectral index allows us to obtain a cleaner picture of the unranked θ - z mapping by choosing only the sources with flat spectra; it had alternately been suggested that steep sources would illustrate the cosmological trend best,but it appears that these sources cloud the issue with their evolution.

In order to investigate luminosity and number density evolution problems and selection effects in the data set used, the radio V/Vm test is presented and gives results statistically close to .5 or a uniform distribution. Graphs of M as a function of z, of volume V in sphere z, and of V/Vm as well as of V/Vm as a function of z show however at least some preponderance of the dimmer sources near us which is not satisfactorily explained.

The M-z test shows the best fit (and least implied luminosity evolution) for closed models. If we assume no intrinsic linear diameter evolution, the θ - z test in general shows the best fit for the open models. It is apparent then that no one traditional deceleration parameter q_o fits both the m and θ data without some evolution or strong selection effects. Now if the universe is closed, there is less residual dependence of the luminosity on redshift but there is a lot of diameter evolution at such high q_o. We shall see that the correlation of brightness with small linear sizes is even greater at high q_o than at low q_o, and,using the D - M relation and accepting the residual M - z dependence, we can predict in a very general fashion the D - z dependence.

Since we are not considering the D - M relation to be z dependent at this level of analysis, only a reduced dependence such as the M - z one, which is at least partly due to selection effects such as Scotts (1951) and the superposition of optical and radio limitations, may need an explanation. Also at high q_o, the Magnitude vs Volume graph shows a surprisingly uniform distribution of sources per unit volume. We note that when the $D \sim (1 + z)^{-W}$ dependence is simultaneously found with the best fit to the θ - z curve, the best fitting θ - z model shows no preference for high or low q_o although the θ - z test without evolution gave favor to low q_o. If we choose very open models, it is not necessary to consider any great diameter evolution but there is a heavy luminosity dependence on redshift and since the M - D correlation is reduced somewhat at low q_o, we can rely even less on this source characteristic to explain it. There may be other reasons such as the deuterium density and Mass-Luminosity Ratio, (Gott et al., 1974), to prefer low q_o. The main problem is the luminosity distribution. The D - z distribution is understandable; there may be just as many large diameters at high z as at low z; we just don't seem them because of their low luminosity; we see at small z both large and small diameters. However the M vs V/Vm curve shows a slightly closer distribution of the dimmer sources than the brighter ones and the M - z curve shows a lack of bright sources near us. We may be in an evolved "vacuole" in a uniform universe, but the "vacuole" would be larger than the local supercluster or about the size of the z-anisotropy region. On the other hand, adding one strong source at z = o, putting ourselves in the middle of it, would improve the graph. The θ and m data might be reconciled in a non-traditional cosmology which shortened the effective bolometric distances to the sources relative to the angular distances, making distant sources appear brighter than expected. Another possibility is that θ is not measuring the metric width of the same parts of the sources at different z.

This preview has of necessity been very general. Because the reader must be familiar with the details of many varied but interconnected pieces of evidence, they are presented in separate paragraphs as follows:

I The Data

II Correlations

III $\theta - z$

a) General

b) Flats

c) Ranking

IV $M - z$

V Volume test

VI $D - M$

VII $D - z$

VIII Spectral Index

IX Component Size

X Scintillation Data

XI Conclusion

I. THE DATA

Two sets of data are used: that compiled by Miley (1972) and by Wardle and Miley (1973) with angular data given at 3.7 cm and 11.1 cm (NRAO) and augmented by Riley and Pooley (1975) at 6 cm with the Cambridge 5-km telescope with fluxes given by the 179 MHz (168 cm) survey in addition to flux and angular data at 962 MHz (Stannard and Neal, 1977), referred to as the interferometric data; and that reported by Readhead and Hewish (1974) by the scintillation technique at 81.5 MHz (368 cm). The data are quite different for the two sets and so provide a check on each other.

The bolometric correction for nonthermal sources is made according to the argument given by Schmidt (1968). When occasionally no spectral index was available, it was calculated from available data or arbitrarily set equal to .71 (.7 is considered about average). For the Riley and Pooley data the spectral index is calculated over the large range of 5000 MHz to 179 MHz. In some cases the spectral index had to be used to have a value of the flux at 179 or 81.5 MHz. However no translation of angles to the values they would appear to have at the new frequency was made.

The number of sources in the data sample used is designated by "SET". For ranking tests the data are placed in order of increasing redshift and divided into bins containing 'N' members. The program was run for SET = 96 (N = 12, 16), 115 (N = 23), 165 (N = 15, 11), 182 (N = 13, 14), and 209 (N = 20) for interferometric data and for SET = 66 (N = 11) and SET = 110 (N = 11) for scintillation data, providing a check on the constancy of the statistics.

In our data the absence of small scintillation angles for $.7 < z < 1.6$ reported by Hewish et al. (1974) is not in evidence; the significance of the previous observation

is doubtful since their sample does not include many small angles anywhere and the present includes a few scattered everywhere even at low z.

An attempt is made to take advantage of a greater number of observations available today. However, the samples are purposely limited to those sources for which θ, S, and z are all known so that all tests are made on the same population.

II. CORRELATIONS

For any pair of variables x and y a correlation function r(x,y) is defined as follows:

$$r(x,y) = \frac{\text{SET } \Sigma xy \; - \; \Sigma x \, \Sigma y}{\sqrt{(\text{SET } \Sigma x^2 \; - \; \Sigma x \, \Sigma x)\,(\text{SET } \Sigma y^2 \; - \; \Sigma y \, \Sigma y)}}$$

From r we can form the function $w = .5 \, \ell n \left(\frac{1+r}{1-r} \right)$ which is expected to be normally distributed with standard deviation $SD = 1/\sqrt{SET - 3}$.

The correlations of the spectral index α with redshift z, linear diameter D, absolute magnitude M, and observed flux S are presented in Table I in terms of the number of standard deviations. It appears that a steep spectrum is correlated with low z, intrinsic brightness (less so for low q_o) and large linear diameter (more so for low q_o). The α - D correlation is substantial enough to suggest that one may pick out a subset with less intrinsic D variance for the θ - z test by using only sources with chosen spectral indices.

Table I also lists the D - z and M - D correlations. For the interferometric data we tried restricting the sums to those sources with D > 100 kpc because preliminary inspection of the data showed small diameter sources with every luminosity and redshift whereas the large diameter sources were less apparent at high z or bright M. Thus we are investigating the upper "evolutionary" band of the D distribution. This discrimination allows us to avoid the region of selection where the angle

subtended becomes unresolvable $D(\theta = 1'', z = .25) = 5.2$ kpc and $D(\theta = 1'', z = 3) = 12.7$ kpc. It is found that large width is correlated with dimness and low z (more so for high q_0). The effect is still present but less pronounced when all sources are included. This property of the sources allows us to pick out sources with generally smaller diameters and less statistical spread by picking the brightest for the $\theta - z$ test.

III. θ - Z TEST

A. General

If we assume no evolution we find that a source with a typical diameter D in kpc should subtend an angle ϕ in arcsecs given by (we take $H_o = 50$ km/sec/Mpc throughout this paper)

$$\phi = .03438\ D(1+z)^2 / d_L$$

where d_L is the bolometric distance to the source

$$d_L = \frac{c}{H_o}\left[q_o z + (q_o - 1)\left(\sqrt{2q_o z + 1} - 1\right)\right] / q_o^2$$

for Friedman models and

$$d_L = \frac{c}{H_o}(1+z)z$$

for Steady State model. If we assume for the evolution of the physical diameter a form

$$D \sim (1+z)^{-W} ,$$

we then find

$$\phi_{ev} \sim (1+z)^{-W}\ \phi$$

It is here assumed that the LAS (largest angular size) of radio sources represents the metric angular diameter since the hottest spots of double radio sources are often near their maximum diameter, and the component (which might have a luminosity function on which to construct an isophotal angle - metric angle ratio) is only a fraction of the LAS; it is the inner regions which may fade out first and we just do not have yet a good brightness law to determine the isophotal-metric ratio.

We have used the correlation of θ and z to test the significance of the data we are trying to fit and that of θ and ϕ as a test of the goodness of our model. We find that $w(\theta, z) = -5.61$ SD, and $w(\theta, \phi)$ for the various models is given in Table II. In general low densities are favored.

The observed angular sizes θ for all sources are plotted as a function of redshift z in Figure 1 and fitted assuming no evolution. We note that the scatter about a mean value of θ at each z is not constant; the "curve" is of varying width or variance σ. This will still be true when we look at only flat sources. Still we calculate as test of the fit one statistical estimate of error SEE = $\sqrt{(\Sigma(\theta - \phi)^2/(n - 2))}$ where ϕ is the theoretical fitted angle, θ is the experimental value and n is the number of sources in the test. A low SEE indicates a good fit and using this as criterion, low densities are favored (Table II). In many tests throughout this paper the SEE vary only slightly from case to case, but usually in a consistent manner as q_0 changes and in the same way for the many samples used, and so are presented.

B. Flat Spectra

Assuming no evolution, a fit to the $\theta - z$ graph for sources with flat spectra only ($\alpha < .7$ and $\alpha < .4$) is made; the case $\alpha < .7$ is presented in Figure IIa and the SEE are shown in Table III. Again, the lower densities give a better fit. Just to make sure that there is not less scatter for flat sources than for all sources merely because we have less sources, we looked at steep sources ($\alpha > .7$ and $\alpha > .85$) and found we had increased scatter (Figures II b and II c). Since the steep sources tend to be the large ones which tend to be even larger at low z than high z, their angles show an even steeper drop with z then the flats; this is probably why when there was even less data than there is now and any set of angles which would show an average drop with z seemed to support a cosmological $\theta - z$ rela[illegible] it was sometimes suggested that the steep sources be chosen. We see that this [illegible] only further entwines the problems of selection and evolution into the scatter.

C. Ranking

The ranking method involves putting the SET sources in order of z into SET/N bins containing N sources each still in order of z. A typical source is chosen from each bin and its magnitude or angular size plotted as a function of the average ℓn z for that bin. In the case of the magnitude - redshift test, the first brightest (or second or fifth brightest) source is chosen in general as typical; in that case, discrimination is on the basis of the same quantity (apparent magnitude) as is being investigated. The first ranking test was first applied to clusters of galaxies which formed natural bins whereas here the bins contain widely separated sources. In this paper we will choose the typical source as discussed below, make a best regression fit obtaining a typical diameter and, if evolution is assumed, an evolutionary exponent w, and find the SEE for the fit.

Since Kaheall and Hills (1972) did not find their computer sampling B correction significant in their m - z test, such a procedure was not imitated here. In fact our fit of M - z, which should include evolutionary and selection effects, shows a much stronger z dependence than their B correction and reflects the difference in results.

The bin technique has been refined by adjusting the angles chosen to the values they would have had if located at $z = 10^{<\lg z>}$ where they are plotted instead of at their particular locations. Since this did not improve the results, we have dropped this feature from the work presented here.

The tests were run for a variety of sample and bin sizes without any effect except that when there are fewer bins, there is a deceptively easier fit.

Table IV shows the fitted diameter and SEE for various trials without evolution and Table V the same with evolution. These results were obtained by choosing the

sources with the first brightest (then second through fifth brightest) absolute magnitudes, designated by rank R = 1 - 5.

Before discussing the results, we note that we repeated the ...s choosing sources by apparent bolometric magnitude instead of by absolute ... gle. If the objects in the bin were all of the same redshift, there would be no ...nce in the apparent and absolute magnitude rankings; therefore changes in the ...ources chosen would be a comment on the effectiveness of the z grouping in bins of objects which are not physically associated like cluster galaxies. The result was that almost the same sources were chosen with more change in the fainter series where the magnitudes are not so different from each other, and the angle of the newly picked source didn't in general improve the $\theta - z$ trend. This reports favorably on the z grouping.

For similar reasons we tried choosing the sources representing the bins by their angular diameters themselves since this is a closer analogy to the $m - z$ bin method where the brightest sources are chosen and brightness is plotted. Whether the largest or fifth largest quasar can serve as a standard measuring rod is open to at least as much discussion as whether the brightest or fifth brightest can serve as a standard candle. At any rate discrimination by θ itself did not change the results.

As in the case of discrimination by magnitudes there may be some difference in using θ (angular diameter) or D (linear diameter) as a width discriminant because of dispersion within the z bin; but a trial discrimination by linear diameter did not change the result. Even within a bin, the order of sources (largest to fifth largest) by angular diameter is almost the same as the order of sources by linear diameter and the order of sources by apparent bolometric magnitude (first to fifth brightest) almost the same as the order by absolute magnitude.

However, if within a bin we rank the sources by size, we find that we are choosing dimmer than average sources. Conversely, if we rank the sources by magnitude, we find that the brightest sources are smaller than average. This corroborates the M - D correlation and occasions the choice of small sources when we pull out the first or fifth brightest for the bin method. In this way less evolutionary trend (wide sources at low z) is expressed in the θ - z graph when it is ranked.

Disposing of these scruples we present an example of a binned θ - z without evolution graph in Figure III. Table IV shows that the SEE are usually smaller for low densities when evolution is not included. With evolution, Table V shows no consistent q_o preference of the SEE's. If we exclude the nearest sixty sources from our sample (SET = 140, N = 14), we find assuming evolution that the brighter classes show marginal preference for the closed models with the diameter even increasing with z for some cases, but here w doesn't change monotonically with q_o ; the typical diameters for the non-local set are much smaller than those for the total sample as might be surmised.

IV. M - z

Let S_o be the observed magnitude in flux units μ 10^{-26} $W/m^2/Hz$ and $S = S_o(1+z)^{\alpha-1}$ be the bolometrically corrected flux. If we assume that the absolute luminosity of the source L varies as $L_o(1+z)^{\beta}$ then the absolute magnitude of the standard L_o is $M_o = M - 2.5g \lg(1+z)$ where f is the observation frequency in MHz and the absolute magnitude is $M = -2.5 \lg (f \cdot S) - 5 \lg d_L - 12.888$.

Figure IV shows absolute magnitude as a function of redshift. Here we should see a combination of selection and evolutionary effects if the model used in computing M from m is correct. If the cosmological model is inadequate, we hope to distinguish the discrepancy. The graph shows that M becomes brighter with z as expected from selection. The dimmest absolute magnitude necessary to observe 2 μ at cosmological z was plotted and the data follows the curve very well as expected since the spread of M - z plot in the M direction is a fairly uniform band (instead of narrowing markedly with increasing z as expected) and the same equation raises the observed flux and the 2 μ . But it is only the lower bound of the data which we expect to follow the 2 μ line as long as there are no dim sources missing. The Scott effect (1951) is expected to lift the lower values of M at high z, not decrease the upper values of M at low z if all bright sources are assumed to be known for small z. There is a curious local paucity of intrinsically bright objects. Even if the average local brightness were lower, we should still see some brighter near sources. The uniform width of this curve might be taken as an argument for non-cosmological z or a non-traditional cosmology in which the "effective" bolometric distance, which relates m and M, has only a weak z dependence.

A best regression fit of M vs $\ell n(1 + z)$ for all sources shown in Figure V in terms of the absolute luminosity resulted in $L = 132(1 + z)^{4.23}$ for $q_o = 1$ and $L = 121(1 + z)^{5.43}$ for $q_o = .03$. The function $L \sim (1 + z)^g$ is steeper for low q_o.

An F test on the variances for $q_o = 1$ and $q_o = .03$ shows the values to be significantly different at the 1% level for M indicating that the cosmological model is not swamped by variance in M.

A by-product of the bin technique in $\theta - z$ is an application of that same method to M - z, investigated by Zotov and Davidson (1973). The analysis gives some prejudice in favor of luminosity evolution. The tables under Figure III include the absolute magnitude of the first through fifth brightest sources in each bin with its given bin average log z. We see that M generally increases with $\langle \lg z \rangle$ although not monotonically.

We have used these binned values of M to fit $L \sim L_o(1 + z)^g$ and M_o and g and the SEE of the fit are shown in Table VI and Figure VI. We see that the best fit and least evolution is indicated for high q_o. For $q_o = 10$, rank 1, $g = 2.5$. For $q_o = -1$, rank 3, $g = 6.3$. Thinking that this high value of g (which persisted at about 2 for $q_o = 40$ and 50) might be due to local behavior, trials were made for the last 140 sources of the SIT = 200 sample with N = 20; the ranked fitted test yield a reduced g of 4.7 for $q_o = -1$, 1.2 for $q_o = 10$ and .8 for $q_o = 40$.

V. VOLUME TEST

Assume that objects with property f(V) are distributed uniformly in space with density ρ. Here V is the volume of a sphere with an object on its surface and an observer at its center. The number of objects found in V is $N = \rho V$. Assume there is a limiting fm corresponding to Vm and Nm. Then the average $\langle f \rangle / fm =$

$$(1/fm) \int_0^{N_m} f \, dN/Nm.$$

For a power law $f \sim V^n$, we find $\langle f \rangle / fm = 1/(n+1)$.

If $f = V$ itself, $n = 1$ and $\langle V/Vm \rangle = .5$ is expected for a uniform distribution, so a test of uniformity consists in forming this average where Vm is the volume corresponding to an object-observer bolometric distance d_{Lm} such that the observed radiation flux from d_{Lm} would be Sm, the limiting flux of the survey averaged.

We here follow the procedure laid out by Sandage (1961) and use Wegstein's iteration scheme. We have calculated the statistical estimate of error:

$$SEE = \sqrt{(\Sigma (V/Vm - \langle V/Vm \rangle)^2 / SEV/SET - 1))}$$

since it gives a physical feeling of the dispersion even though such a parameter usually describes a normal distribution and our basic physical assumption is that the values of V/Vm would be spread out evenly from 0 to 1 and this has turned out to not be inconsistent with the data.

The results are presented in Table VII and are finally favorable to the hypothesis of uniformity. The reader is warned that this is the radio average and the optical average is higher for optically limited samples.

Unfortunately the test is very sensitive to the choice of a minimum flux and great care must be taken if one dares to mix surveys as we have done here. We have chosen the minimum flux to be $2\overset{f}{.}u$ for the interferometric set and $4\overset{f}{.}u$ for the scintillation set. These values correspond approximately to the lowest values observed in the sets and survey lower limits. We note that only the region $\delta > 77$ is not covered by all surveys used and we did not include any sources from this area. Our sample is thus complete only in the sense that our data comes from overlapping regions of the surveys. It is incomplete in the sense that it selects only those objects for which angular diameters and redshifts are available. The superposition of the visual magnitude selection upon the radio selection can lower the V/Vm. It is only the improbability that all these improprieties should combine to give such happy results which speaks in their favor.

We have plotted absolute magnitude M vs volume V (arbitrary units) in Figure VII because an M - z graph gives the small local volume too much visual importance; quite aside from the Scott and radio-optical survey limitation effects, it is more probable to find a bright source at large z where there are more sources (volume) than at low z, and this can be effective assuming a rather low over-all density of bright sources (McCrea, 1966). The M - V plot can be read to form number densities $\mu = \Delta N(M)/\Delta M$ and $\nu = \Delta N(V)/\Delta V$ albeit encumbered with selection effects. The gross ν declines only slowly with V. This, of course, could come about directly from a secular decline in source density. (Longair & MacDonald (1969), observing the preponderance of high z objects and assuming the bright sources to be young, quantified this by a source birthrate decreasing as perhaps $(1+z)^{-1.25}$ with no sources created prior to $z = 2.5$). The decline in $\nu(V)$ could also result from only a not improbable decrease in $\mu(M)$ with M, a decrease however which cannot be seen from the empirical

μ(M) directly. Similarly we have plotted V/Vm vs z (Figure VIII) and M vs V/Vm (Figure IX) and finally in this slice, the local paucity of high magnitudes appears much less important but cannot yet be said not to exist.

VI. D - M

We have already noted the association of small linear size with brightness by means of the correlation function. The association is even closer for high q_o.

Even for the components Mackay (1973) has noted that of two outer components, the brighter is usually closer to the center, smaller in linear diameter and flatter in spectrum.

Figure X shows a graph of D - M for $q_o = .03$.

For all sources (and also in trials with D > 100 kpc but with barely changed results) we have found by regression the best linear, $D = C_1 M + C_2$, hyperbolic, $D = C_3/(C_4 - M)$, and exponential, $D = C_5 L^{-f}$ fits. These are presented in Table VIII. (When restricted to large D they represent only the upper evolutionary band). Moffet (1968) predicts f = .33 for a spectral index of .75, and at that time .33 was thought to be low. Our fitted f ranges from .336 ($q_o = 10$) to .083 ($q_o = -1$).

Ekers (1975 NATO Summer School, Urbino) has reported some success with the θ - S relationship although data sets had to be matched and spectral indices translated to 21 cm. He reports that the data flatten out too much at low S meaning that the θ for dim S are too large (to fit the cosmology but not necessarily in themselves). If these S are dim because M is dim this may be an indication that D (and therefore θ) is large for dim M. However, to be fair, if m is dim because z is large, the situation is not supportive of the D - M correlation because we usually calculate:

$$D \sim d_L \, \theta / (1+z)^2$$

and

$$L \sim d_L^2 \, S$$

implying

$$L \sim D^2 \, (1+z)^4 \, S/\theta^2$$

or

$$S/\theta^2 \sim L/D^2/(1+z)^4 \quad .$$

For

$$D \sim L^{-f} \quad ,$$

we have

$$S/\theta^2 \sim D^{-1/f-2} \, (1+z)^{-4} \sim L^{1+2f} \, (1+z)^{-4}$$

What Ekers found is that the S/θ^2 may be smaller than expected from pure cosmology at high z, where however L is large and D is small and the source properties might be expected to make the ratio even larger.

We remind the reader that ranking within the bins made for the $\theta - z$ and $M - z$ tests indicated an $M - D$ relation. However, such a relation fails to appear in an expected decrease of fitted D for each brightness class.

VII. D - z

For the interferometric data $\omega(D,z)$ increased from -1.373 SD ($q_o = 1$) to -1.679 SD ($q_o = .03$). For the steady state case $\omega(D,z)$ is -2.346 SD. A negative $\omega(D,z)$ is equivalent to saying that geometrically extended sources are characterized by low z's.

Figure XI shows the linear diameter as a function of redshift assuming a cosmological model. For the interferometric data there is a general decrease of D with increasing z even though small diameters continue to be present at all values of z. The curve representing the angular resolution limit lies so low on the scale of the graph as not to be discernible. This investigation tries to fit the upper data points which vary with z.

A gap in the linear diameter distribution between 180 and 210 kpc in Miley's data, found significant at the 4.4% level by Reinhart (1972) and discussed by Van der Kruit (1974) and somewhat present in this larger interferometric sample, is absent in the scintillation data at ... diameter, giving weight to the hypothesis that its origin is observational. If the linear size gap were real, the immediate suggestion would be that evolution in this region were fast.

If the small D at low z were a projection effect, we wouldn't expect these sources to be brighter than the large D. The projection effect is not likely to be a strong factor because there aren't too many small projections in an assumed random orientation and there are relatively many small sources in the data.

The distribution of linear diameters with redshift was partitioned for a simple χ^2 (with Yates correction) and variance test for SET = 115. The tests show the lack of many diameters greater than 200 kpc for $z = 1.25$ to be statistically significant.

If we assume that the large sources at high z are as faint as the large sources observed at low z, their absence at high z is understood because they could be as much as 5 magnitudes fainter than the 2 to 12.5 μu's observed at high z in our sample and they would thus be near or below the limit of the survey used. Their absence by selection makes it difficult to determine if the sources were uniformly produced in the past.

Using the theoretical absolute magnitude corresponding to 2μu and a given z and the D - M fits we have constructed the shape of the upper D - z distribution. This is shown in Figure XI. Among other causes selection certainly limits us to brighter sources which tend to be the ones with small linear sizes.

Table V from the ranked θ - z test already gives us the evolutionary exponent w. Rank 1 (the first brightest) gives much smaller w than others. A separate determination of w, using all sources, is shown in Figure XII where we have plotted ℓn D vs $\ell n (1 + z)$. For all sources we find $D = 181 (1 + z)^{-1.98}$ kpc for $q_o = 1$ (compare with w $\sim$ .5 to 2.6 for bins) and $D = 178 (1 + z)^{-1.37}$ kpc for $q_o = .03$ (w = . 6 to 2.3 for bins). As expected, w is smaller for low q_o.

Table IX shows the predicted w of various radio source models. Assuming that quasars are associated with early galaxies, Hills (1977) has calculated their formation times as a function of mass. Using his expressions for a galactic isothermal sphere with an inverse square density distribution, we find the radius $r = M/\Pi = 9.45$ kpc (t_f/t_o). For $q_o = .5$ this yields $r = 9.45$ kpc $(1 + z_f)^{-3/2}$. This could be the radius of the source components. If the source largest angular size D goes as the square of the component size (cf. Part IX), then $D \sim (1 + z_f)^{-3}$. We include this prediction in Table IX.

The theoretical exponent coming closest to the experimental values is $w = 2$ of the Christiansen radiation limited, B_o constant model.

VIII. SPECTRAL INDEX

We expect that the more compact sources have higher mean opacity and higher magnetic fields and consequently higher luminosities and flatter spectra (cf. Moffet, 1968).

In addition it can be shown that if a power law spectrum

$$S = I_o (\nu/\nu_o)^{-\alpha} \gamma$$

is assumed between ν_L and ν_H, and if half the power Q is emitted at $\nu < \nu_*$ and half the power Q is emitted at $\nu > \nu_*$, then ν_* is bluer for the same ν_H, ν_L and Q for a flat spectrum than a steep one:

$$\nu_H^{2-\alpha} - \nu_*^{2-\alpha} = \nu_*^{2-\alpha} - \nu_L^{2-\alpha} = Q(2-\alpha)\,\nu_o^{\alpha}/(2I_o)$$

As z increases and we see only the brighter sources, we might expect to see bluer and flatter sources.

We also note that since

$$S/S_m = (d_{Lm}/d_L)^2 (1+z)^{1-\alpha}/(1+z_m)^{1-\alpha}$$

flat spectral indices can raise the V/Vm. If uniformly distributed, the flat sources appear weaker than the steep ones after the bolometric correction and obfuscate the correlation $w(\alpha, M)$.

The data support these expectations. The steep spectra are associated with low z (-1.313 SD) and apparently bright sources (2.832 SD) and large sources (more so for low q_o) and intrinsically bright sources (less so for low q_o). This is conjoined with the association of large dimensions and dimness (less so for low q_o). Figure XIII is a good illustration of $w(\alpha, D)$.

We have already discussed the reasons for using the flat sources and not the steep ones for the α - z test.

Pacholczyk and Scott (1976) note in support that in head tail sources, after a minimum in slope (near a flux maximum and polarization minimum) the spectra seem to be steeper and dimmer as one moves down the tail away from the head. A discussion of the rise in α in the bridge between two components of the same source can be found in Gopal-Krishna and Swarup (1977).

IX. COMPONENT SIZE

The angles θ we have been using are reported as the angular distances across the entire width of composite sources. Representing the average angular width of the several components of a source by c, we have taken 42 sources with reported θ and c from Miley (1972) and arranged them in order of increasing θ, placing them in 7 bins of 6 members each and forming the average θ and c in each bin. A regression fit for these averages yielded $c \sim \theta^{.5}$.

It seems that the components as detectable regions do not expand as fast as the whole source. This question should be re-examined as the resolution of the components is improved.

The c were quite clearly an empirical function of θ whereas there was no obvious dependence of c on z.

X. SCINTILLATION DATA

The foregoing remarks apply to the interferometric data.

In Figure XV we show the θ_s scintillation angle plotted against θ_i interferometric angle for those sources which occur in both our sets. A correlation test for the two angles was performed for the 50 sources common to both sets. It was found that $r = 0.196$ and $w = 0.198 = 1.359$ SD where SD = .146 indicating somewhat less than brilliant agreement.

We find that steep spectral indices are correlated with large width but poorly (whereas the interferometric picture was clear) and with apparent brightness (.370 SD) and with absolute brightness (less so for low z) as for the interferometric data but with high z (3.02 SD) instead of with low z. Therefore, we compare a plot of α vs z for scintillation data (Figure XIVc) with the same for interferometric data (Figure XIVa). In the later case all areas of the graph are fairly well covered, but the former case reveals a markedly increasing absence of flat sources.

We next see that the correlation parameter $w(\theta, z)$ is only -.431 SD and $w(\theta, \phi)$ favors the higher q_o (and not the lower q_o as preferred in the interferometric case) at this level of insignificance. In trying to fit the $\theta - z$ curve, we can't use the flat spectrum sources because there aren't any at high z. Using the steep sources does not produce even a trend. Binning the sources produces a bad fit which is again "better" for high q_o.

Faithful to cosmology, we describe this θ behavior as a corresponding broadly scattered dependence of linear diameter on redshift. We find $w(D, z)$ associates

breadth with high z. It increased from .107 SD ($q_o = 1$) to 2.460 SD ($q_o = .03$) with 3.805 SD for the steady state. We note that Hewish, Readhead and Duffet-Smith (1974) and Readhead and Longair (1975) obtained indication of a correlation of small D with large z for scintillation data which is not obtainable from our scintillation data but would be consistent with the interferometric data. Regression fits of ℓn D vs ℓn (1 + z) show the same dependence, with steeper slope for low q_o.

Also breadth of source was positively correlated with brightness (more so for low q_o) in contradiction to the interferometric case and most source models. Of course, other factors may enter; Roeder (1975) described the absence of small D at high z in connection with a maximum in the bolometric distance even for low q_o because of inhomogeneities. However, the correlation itself is contestable. Hewish et al. (1974) state that strong scintillators have high luminosities (Readhead and Longair, in press, Mon. Not. RAS).

In way of temporary explanation of these conflicts, we suggest that we are observing increasingly steep and intrinsically broad sources with increasing z, swamping the θ - z relation; and this might occur if when z is small, components (flat) may be the right size to scintillate, and when z is large, total composite sources (steep) may be the right size. Apparent growth of D is enhanced if $\epsilon \sim \sqrt{\theta}$.

Finally in support we note that when we added 44 mostly low z, low θ sources to the 66, $w(\theta, z)$ jumped to -1.518 SD although the graph θ - z still looked like a scatter diagram.

XI. CONCLUSION

The θ's decrease with increasing z as though q_o were very low. However at least some of the drop in θ with z is due to selection effects and the circumstance that absolute luminosity and linear size are inversely correlated.

In contrast to the θ-z behavior the magnitudes decrease with z as though q_o were very high. It might be thought that by accepting high q_o and limitating θ by selection, the postulation of source evolution could be avoided. However we have manipulated the data for q_o up to 50 and even there we have found an evolutionary luminosity exponent of about 2 at $q_o = 50$ and the persistence of the local paucity of bright sources in the m-z and M-V distributions (although it becomes entirely insignificant in the $M-V/V_m$ distribution).

Therefore within the framework of a homogeneous Friedman $\Lambda = 0$ model, it seems necessary to include source evolution although less of it in a closed universe than in an open universe. The very existence of large scale source evolution rules out the simpler versions of the steady state theory even if eventually we find objects which might be used as standard candles, e.g. components with a "signature" identifying one point of their development.

FIGURE CAPTIONS

Figure 1. Angle vs. Redshift. $q_o = .03$. SET = 200.
Fitted Diameters = 210 kpc. SEE = 52.

Figure IIa. Angle vs. Redshift for flat spectrum sources.
$\alpha < .7$. $q_o = .03$. SET = 200.
Number of flat spectrum sources = 97.
Fitted Diameter = 241 kpc. SEE = 63.

Figure IIb. Angle vs. Redshift for steep spectrum sources.
$\alpha > .7$. $q_o = .03$. SET = 182.
Number of steep spectrum sources = 102.
Fitted Diameter = 192 kpc. SEE = 39.

Figure IIc. Angle vs. Redshift for steep spectrum sources.
$\alpha > .85$. $q_o = .03$. SET = 182.
Number of steep spectrum sources = 49.
Fitted Diameter = 157 kpc. SEE = 33.

Figure III. Angle vs. Redshift for ranked sources.
$q_o = .03$. SET = 182. N = 14 Rank = 4.
Fitted Diameter = 255. SEE = 38.

Figure IV. Absolute Magnitude vs. Redshift.
$q_o = .03$. SET = 182.

Figure V. Absolute Magnitude vs. $\frac{1}{2}(1 + z)$.
$q_o = .03$. SET = 182.
Regression yields a best fit
$M = -5.90\ \frac{1}{2}(1 + z) - 16.7$
with SEE = 1.15.

Figure VI. Absolute Magnitude vs $\log(1 + z)$ for ranked sources.

$q_o = 10.$ SET = N = 14. RANK = 5.

Regression yields a best fit

$M = -16.6\ (1 + z)^{2.71}$

with SEE = .595.

Figure VII. Absolute Magnitude vs. Volume.

$q_o = .03$ SET = 200.

This figure should be compared with Figure IV.

Figure VIII. Radio V/Vm vs. Redshift.

$q_o = .03$ SET = 182.

Figure IX. Absolute Magnitude vs. V/Vm.

$q_o = .03$. SET = 200.

This figure should be compared with Figures IV and VII.

Figure X. Linear Diameter vs. Absolute Magnitude.

$q_o = .03$. SET = 182.

Figure XIa. Linear Diameter vs. Redshift.

$q_o = .03$. SET = 182.

Line shows diameter of lowest luminosity source observable at a given redshift for a survey limit of 2 flux units assuming the best exponential diameter-luminosity fit $D(kpc) = 1175\ L^{-.143}$ (watts/m^2).

Figure XIb. Linear Diameter vs. Redshift

$q_o = 1.$ SET = 182.

Line shows diameter of lowest luminosity source observable at a given redshift for a survey limit of 2 flux units assuming the best hyperbolic diameter - absolute magnitude fit D(kpc) = 74.3/(16.3 + M).

Figure XIIa. ℓn Linear Diameter vs. $\ell n(1 + z)$.

$q_o = .03.$ SET = 182.

Regression yields a best fit

ℓn D(kpc) = -1.37 $\ell n(1 + z)$ + 5.18 with SEE = 1.69.

Figure XIIb. ℓn Linear Diameter vs. $\ell n(1 + z)$.

$q_o = 1.$ SET = 182.

Regression yields a best fit

ℓn D(kpc) = -1.98 $\ell n(1 + z)$ + 5.20 with SEE = 1.69. Note that this case with higher q_o is steeper, i.e., looks more evolutionary, than case a, but scatter is dominant in both cases.

Figure XIII. Spectral Index α vs. Linear Diameter

$q_o = -1.$ SET = 200.

Case $q_o = .03$ looks similar, but to be perfectly fair at least one of the sample cases presented in this paper should be from the steady state model.

Figure XIVa. Spectral Index α vs. Redshift for Interferometric Data. SET = 182.

Even though there is a non-zero correlation coefficient, $w(\alpha, z) = -1.3$ S.D., the diagram shows enormous scatter.

Figure XIVb. Spectral Index α vs. Radio V/Vm for Interferometric Data.

$q_o = .03$. SET = 177.

This figure amplifies Figure XIVa because there is a danger that bright component sources may be selected over wide double sources as z increases.

Figure XIVc. Spectral Index α vs. Redshift for Scintillation Data.

SET = 66.

Note the increasing absence of <u>low</u> spectral indices with increasing redshift which does not occur in the interferometric data shown in Figure <u>XIVa</u>.

Figure XV. Scintillation Angle vs. Interferometric Angle.

Correlation Coefficient = r = 0.196.

Normally distributed coefficient = ω = .198 = 1.359 S.D.

Figure XVI. Angle vs. Redshift for Scintillation Data

$q_o = 10$. SET = 110.

Regression yields a "best fit"

$D(kpc) = 1.689\ (1+z)^{.081}$

with SEE = .529.

TABLE I

CORRELATION ω IN STANDARD DEVIATIONS

q_o	$\omega(\alpha, D)$	$\omega(\alpha, m)$	$\omega(M, D)$	$\omega(D, z)$
-1	2.48	- .892	1.81	-2.40
.03	2.32	-1.17	2.41	-3.11
.49	2.18	-1.46	2.73	-3.64
1	2.10	-1.67	2.88	-3.91
2	2.02	-1.94	3.02	-4.20
5	1.93	-2.36	3.17	-4.57
10	1.88	-2.71	3.23	-4.82

$\omega(\alpha, z) = -1.31$

$\omega(\alpha, s) = 2.83$

TABLE II

REGRESSION FIT OF θ - Z FOR ALL SOURCES

q_o	$w(\theta, \varphi)$	SEE (no evolution)	SEE (evolution)	w
-1	7.02	54.21	56.08	1.0
.03	6.97	53.80	56.07	1.4
.49	6.93	54.12	56.08	1.8
1	6.54	54.46	56.08	1.9
2	6.23	55.11	56.07	2.2
5	5.51	56.59	56.10	2.5
10	4.59	58.01	56.22	2.7

TABLE III

STATISTICAL ESTIMATE OF ERROR

OF REGRESSION FIT OF $\theta - Z$

FOR $\alpha < .7$

q_o	SEE
-1	64.62
.03	65.18
.49	66.09
1	66.80
2	67.72
5	69.03
10	69.90

TABLE IV

Fitted Diameters to Bins for 5 Brightness Classes R
Without Assuming Evolution

Set = 182 N = 14

R	q_o	- 1.00	0.03	0.45	1.00
1	Diameter	150.408	143.919	132.840	124.078
	SEE	41.484	40.051	40.431	40.286
2	Diameter	508.885	451.409	397.901	356.797
	SEE	23.007	30.638	27.790	43.193
3	Diameter	481.737	426.965	386.819	343.579
	SEE	28.861	35.150	39.810	45.662
4	Diameter	295.867	254.897	216.403	199.514
	SEE	43.535	37.786	38.496	39.121
5	Diameter	366.331	323.395	307.484	259.596
	SEE	31.942	42.294	42.476	45.857

TABLE V

Fitted Diameters to Bins 5 Brightness Classes R

Set = 200 N = 20

R	q_o	-1.00	0.03	0.49	1.00	10.00	20.00
	Diameter	59.683	58.286	60.211	59.683	42.058	33.896
1	SEE	42.881	42.874	42.883	42.881	42.672	41.999
	w	-0.952	-0.554	-0.169	0.048	0.640	0.782
	Diameter	415.285	405.564	418.961	415.284	274.077	260.479
2	SEE	22.387	22.413	22.375	22.387	20.951	18.083
	w	2.099	2.497	2.882	3.099	3.117	3.240
	Diameter	248.741	389.831	503.125	498.771	350.618	285.572
3	SEE	39.971	25.791	21.616	21.672	27.131	27.746
	w	1.546	1.770	2.389	2.606	3.779	3.933
	Diameter	237.935	250.457	258.563	256.295	171.998	135.851
4	SEE	30.826	30.791	29.276	29.201	27.541	26.973
	w	0.313	0.775	1.462	1.679	2.367	2.430
	Diameter	383.140	357.615	295.886	101.816	53.584	79.021
5	SEE	20.629	22.676	26.276	44.053	41.866	75.370
	w	0.983	1.418	0.267	0.373	0.722	1.527

TABLE VI

Fitted Magnitudes to Bins for 5 Brightness Classes R

Set = 200 N = 20

R	q_o	- 1.00	0.03	0.49	1.00	10.00	20.00
	Magnitude	-19.115	-19.031	-19.077	-19.042	-18.250	-17.780
1	See	0.704	0.699	0.723	0.724	0.692	0.681
	g	5.744	4.999	4.255	3.842	2.490	2.216
	Magnitude	-18.501	-18.428	-18.482	-18.451	-17.657	-17.186
2	See	0.407	0.375	0.380	0.368	0.282	0.260
	g	5.781	5.001	4.225	3.796	2.431	2.153
	Magnitude	-17.938	-17.850	-17.912	-17.880	-17.095	-16.622
3	See	0.384	0.391	0.444	0.455	0.414	0.398
	g	6.074	5.311	4.550	4.133	2.775	2.499
	Magnitude	-17.855	-17.818	-17.933	-17.901	-17.051	-16.562
4	See	0.436	0.461	0.528	0.534	0.482	0.470
	g	6.030	5.193	4.321	3.904	2.627	2.374
	Magnitude	-17.822	-17.718	-17.757	-17.734	-16.954	-16.510
5	See	0.491	0.481	0.512	0.532	0.534	0.523
	g	5.772	5.058	4.353	3.917	2.527	2.215

TABLE VII

VOLUME TEST

q_o	V/VM	SEE
-1	.521	.039
.03	.453	.058
.49	.480	.058
1	.485	.059

TABLE VIII

D - M (all sources)

	$D = C_1M + C_2$		$D = C_3/(C_4 - M)$		$D = C_5L^{-f}$	
q_o	C_1	C_2	C_3	C_4	C_5	f
-1	28.8	721	193	-19.4	445.4	.068
.03	28.1	768	135	-18.3	1,175	.143
.49	32.0	809	94.2	-18.5	3,177	.197
1	33.2	806	74.3	-18.3	5,458	.230
2	33.3	774	55.8	-18.0	9,354	.265
5	30.8	677	36.1	-17.4	16,088	.310
10	27.1	571	25.6	-16.9	18,800	.336

TABLE IX

PREDICTIONS OF w

Christiansen

Lifetime Limitation	v_o Constant	H_o Constant
Expansion	3	3
Radiation	2.75	2
Compton	3.75	6

Rees & Setti: 1.5

De Young: .8

Hills Model: 3

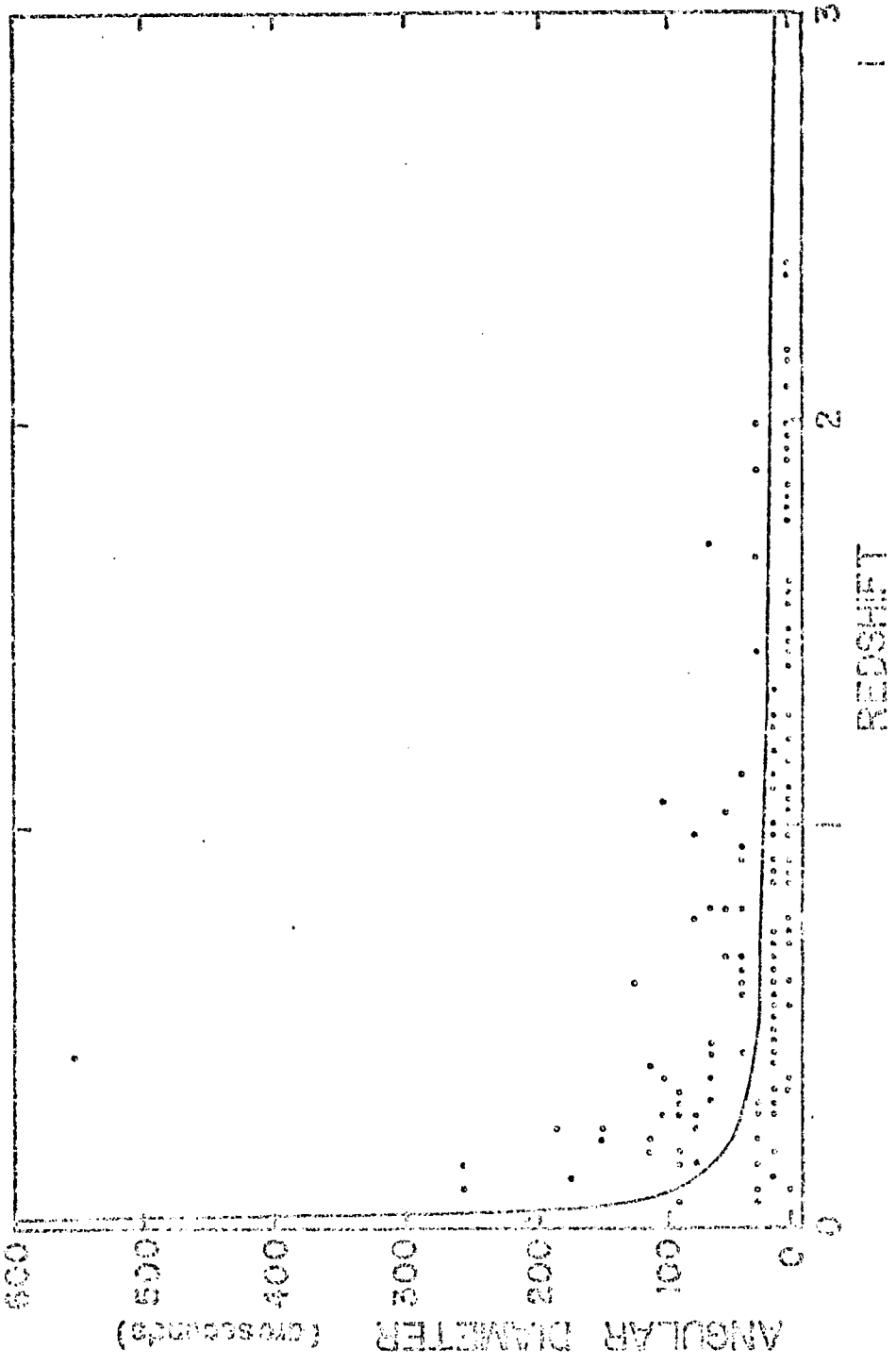
ANGULAR DIAMETER (arcseconds)
600
500
400
300
200
100
0
0
1
2
3
REDSHIFT

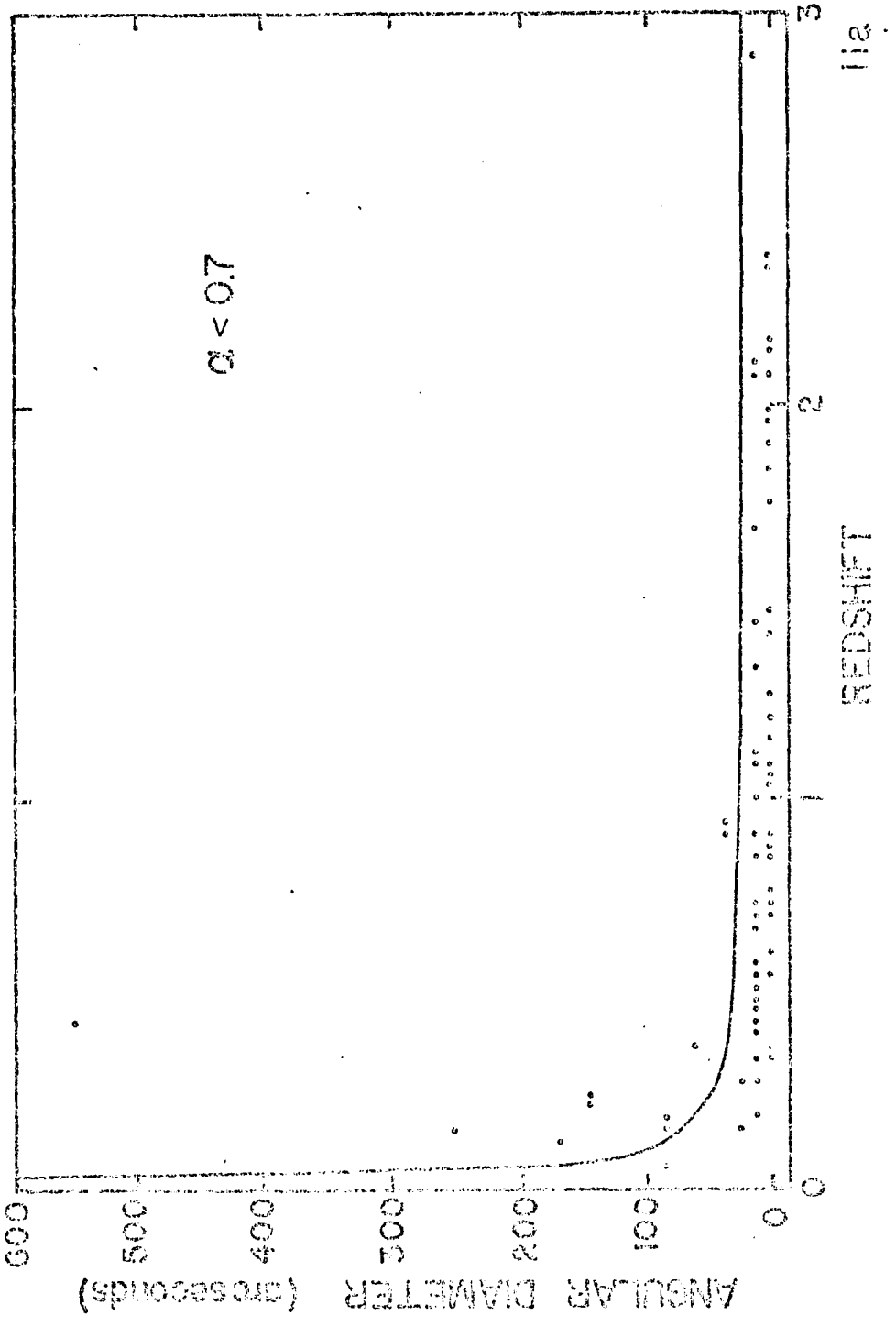
ANGULAR DIAMETER (arcseconds)
600
500
400
300
200
100
0
0
1
2
3
REDSHIFT
$q_0 = 0.7$

Fig. 11a

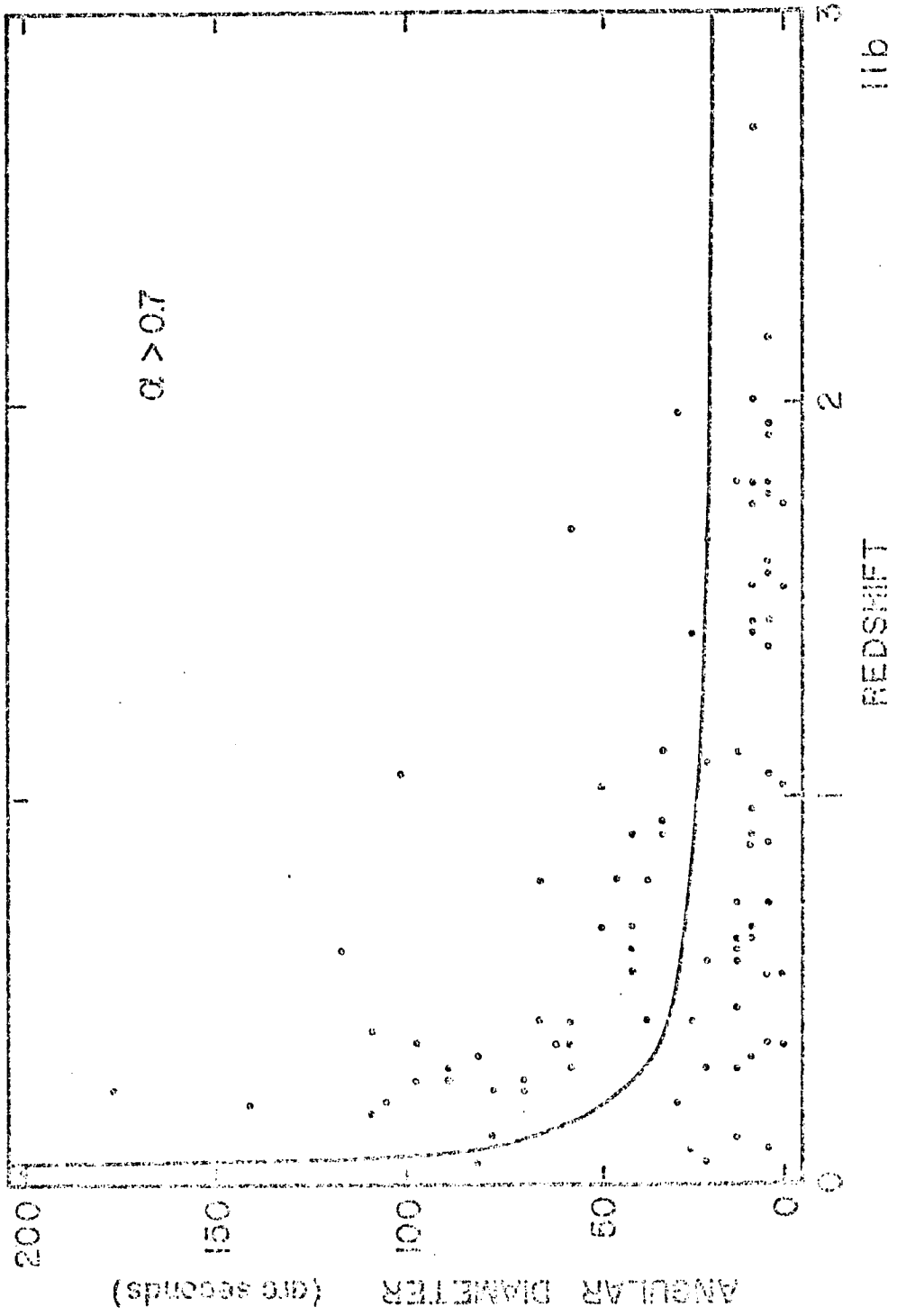
ANGULAR DIAMETER (arc seconds)
0.02
0.01
0.00
0.03
0
1
2
3
REDSHIFT
$q_0 > 0.7$

Fig. 11b

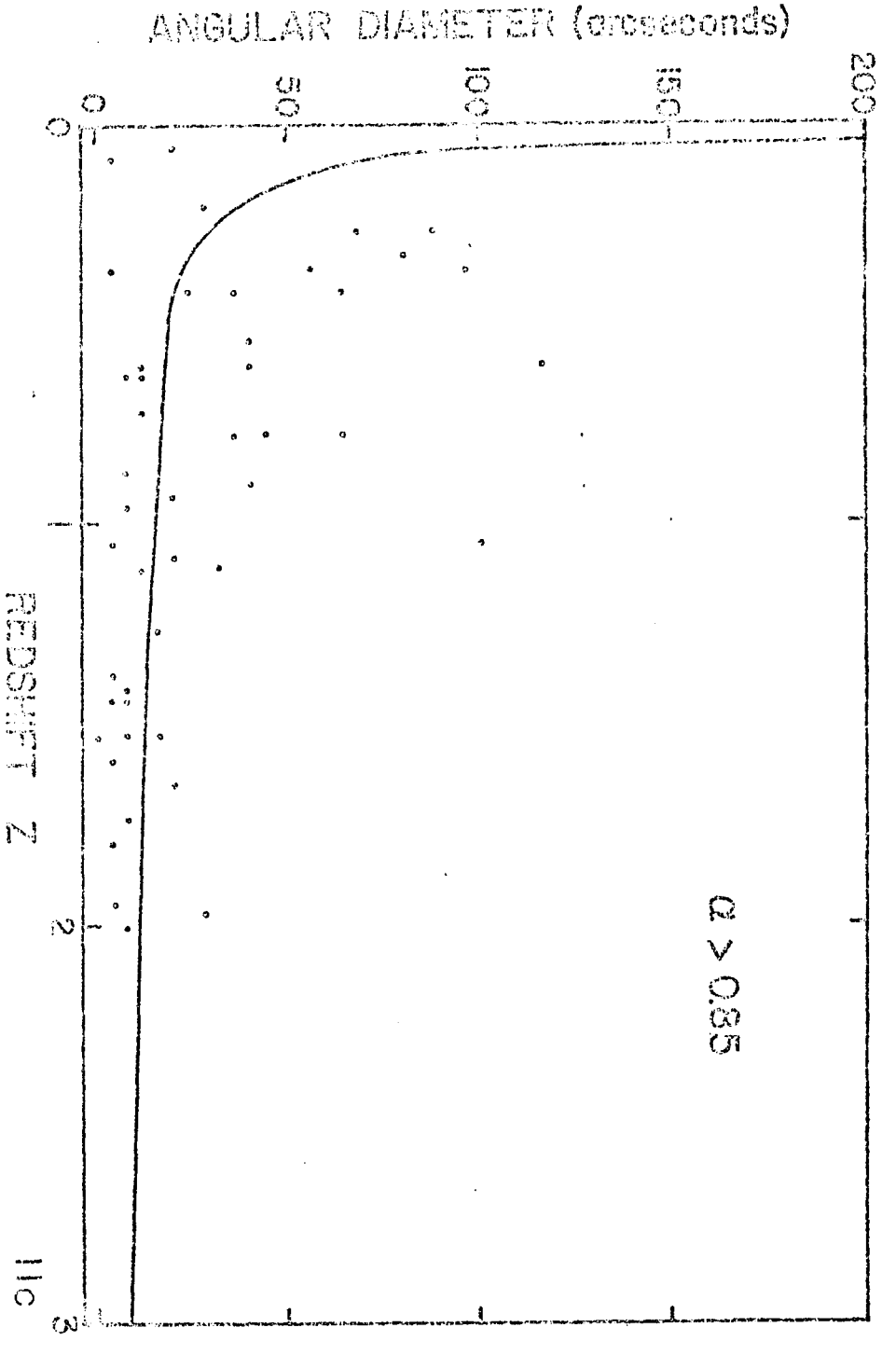
ANGULAR DIAMETER (arcseconds)
0
.005
.001
.0015
.002
RESOLUTION Z
1
2
3
110
SEEING 0.35

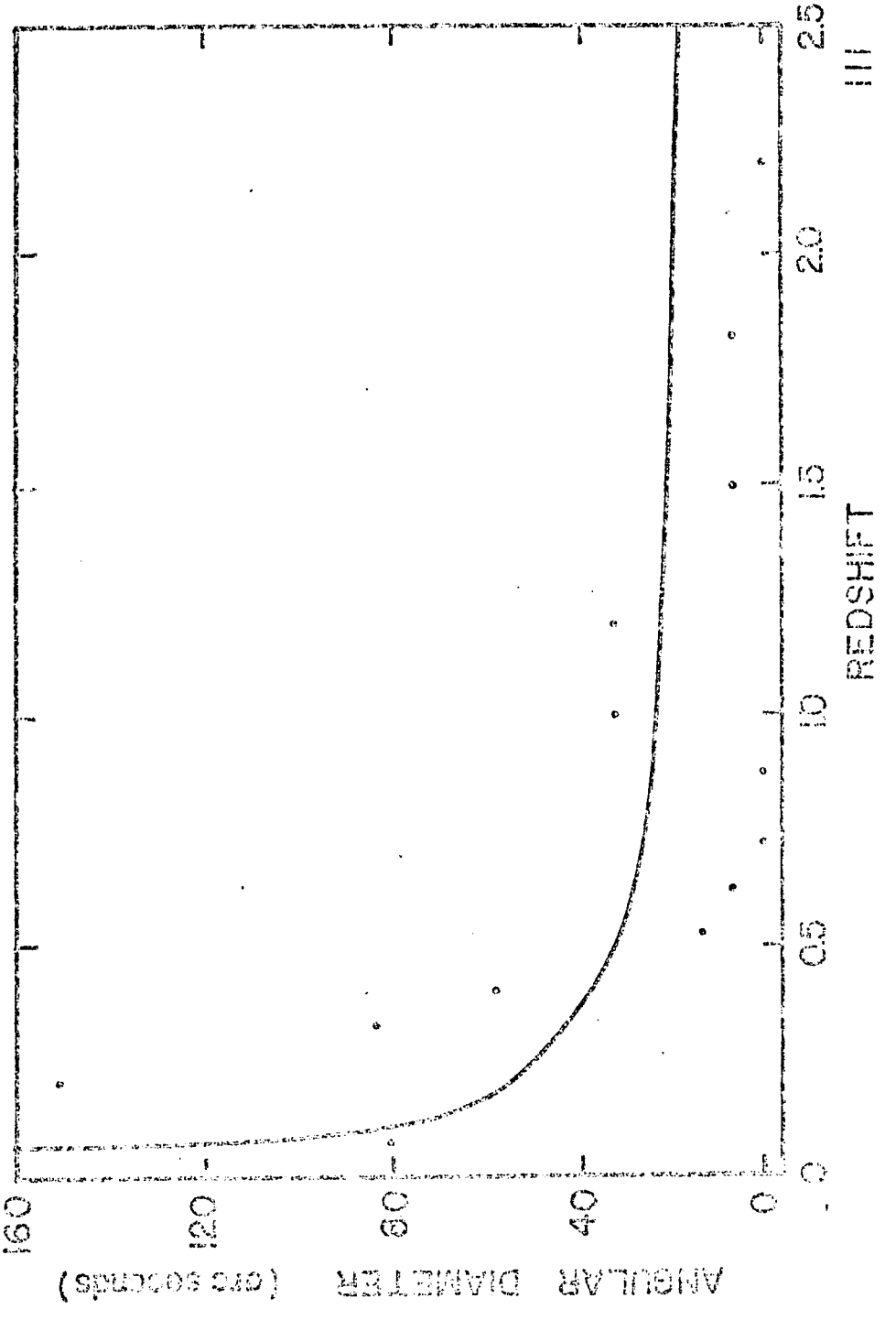
160
120
80
40
0
0
0.5
1.0
1.5
2.0
2.5
REDSHIFT
ANGULAR DIAMETER (arc seconds)

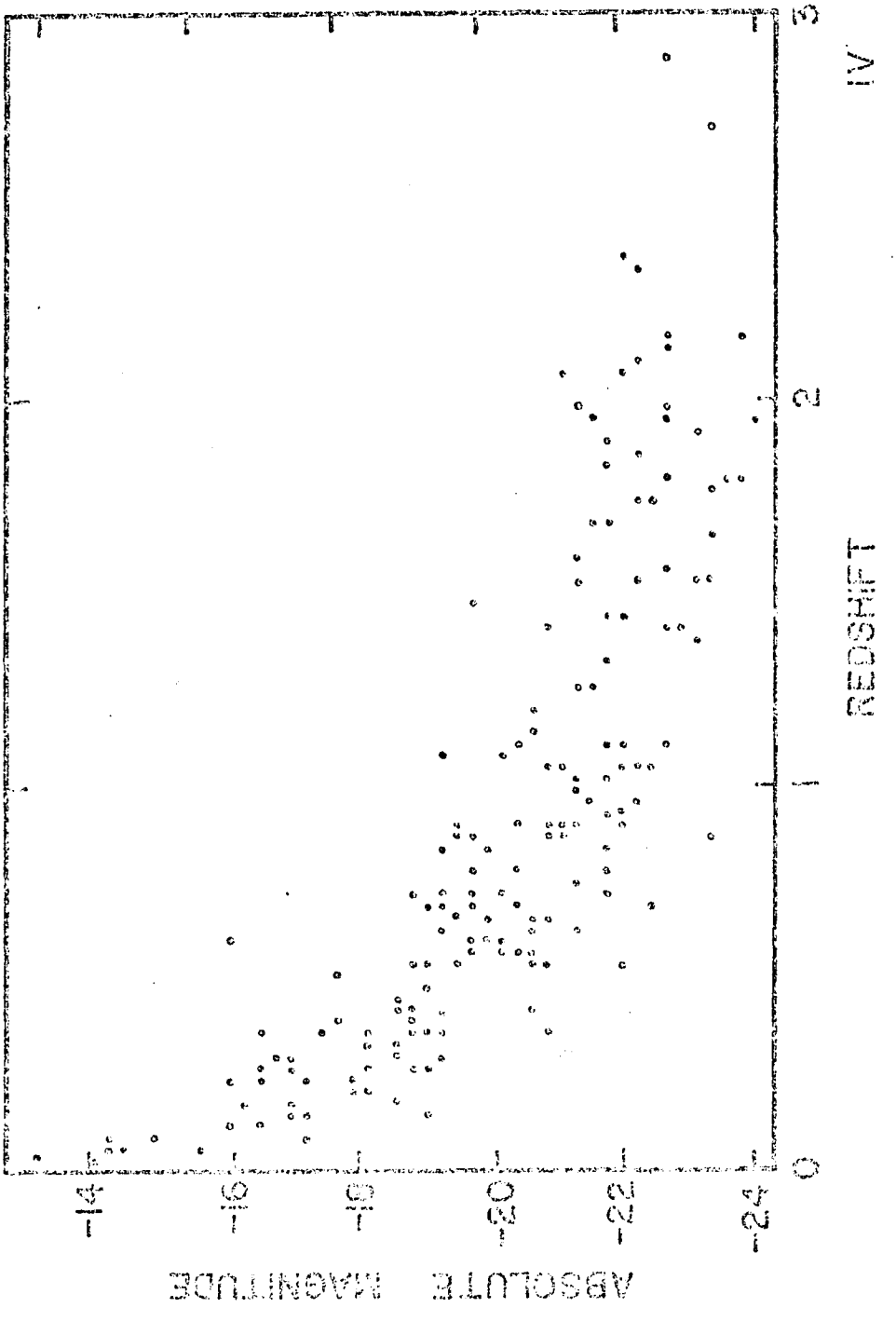
ABSOLUTE MAGNITUDE
-14
-16
-18
-20
-22
-24
0
1
2
3
REDSHIFT
AV

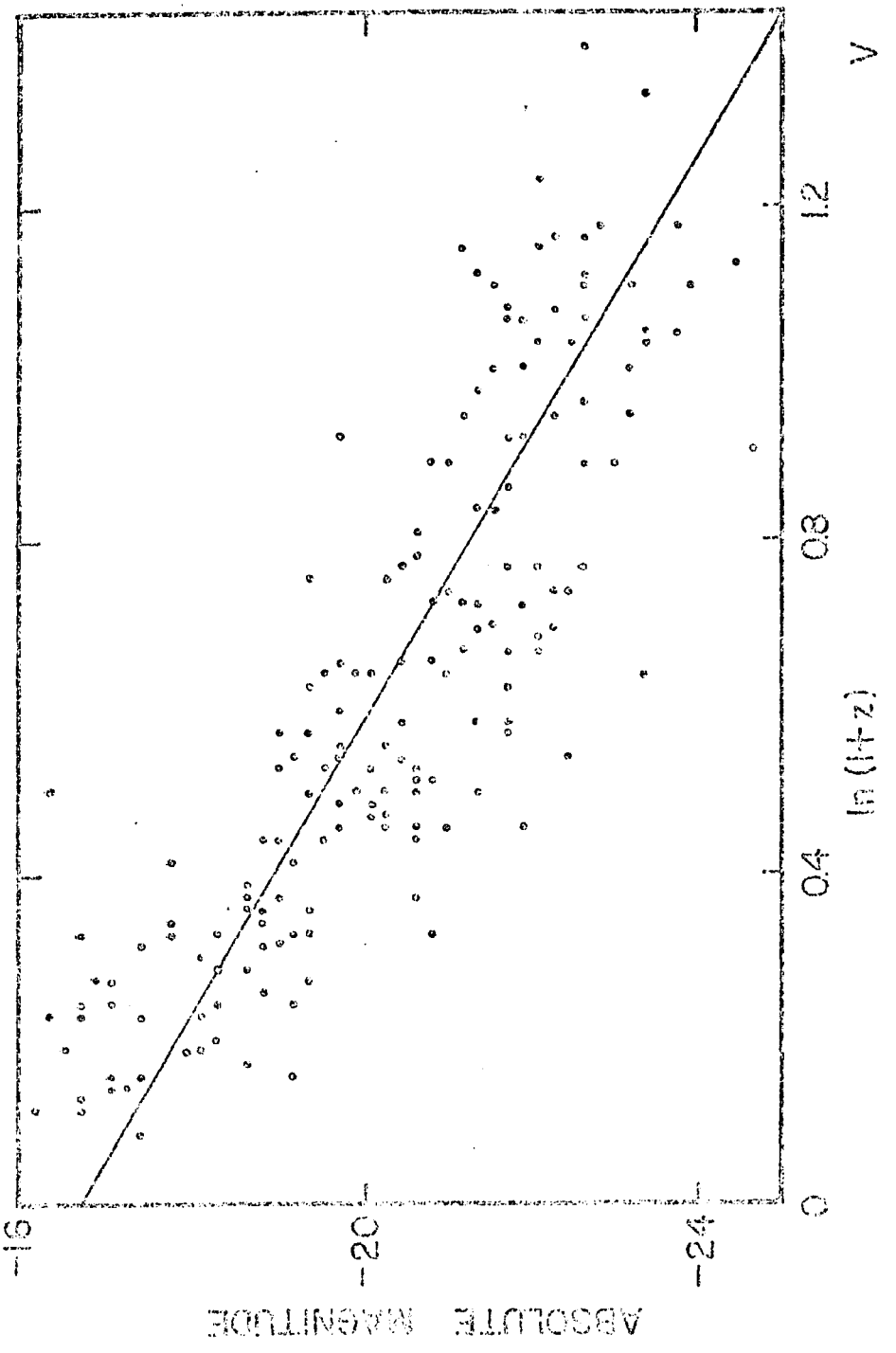
ABSOLUTE MAGNITUDE
−16
−20
−24
0
0.4
0.8
1.2
ln (1+z)
V

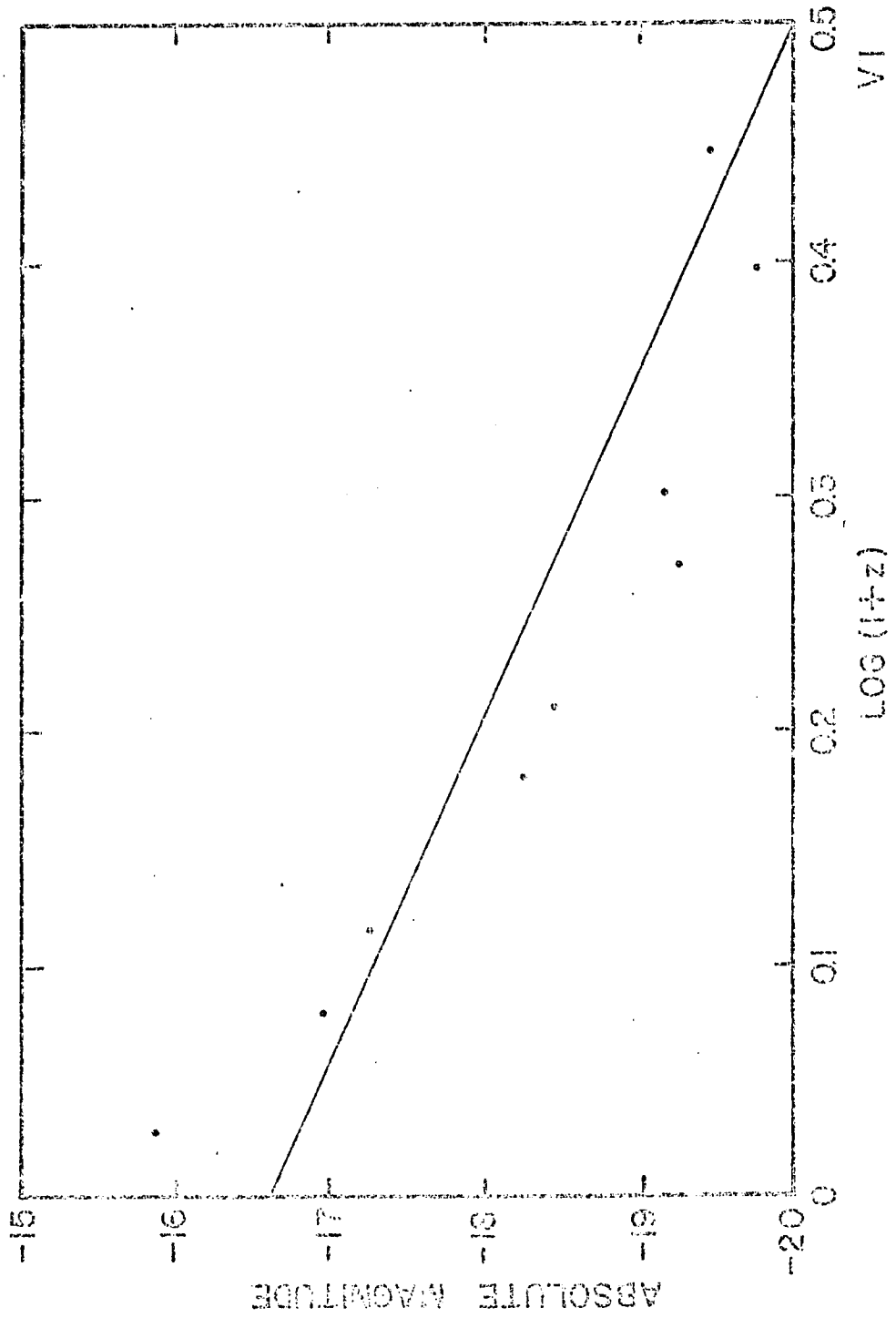
VI
0.5
0.4
0.3
0.2
0.1
0
LOG (Hz)
-20
-15
-10
-5
0
ABSOLUTE MAGNITUDE

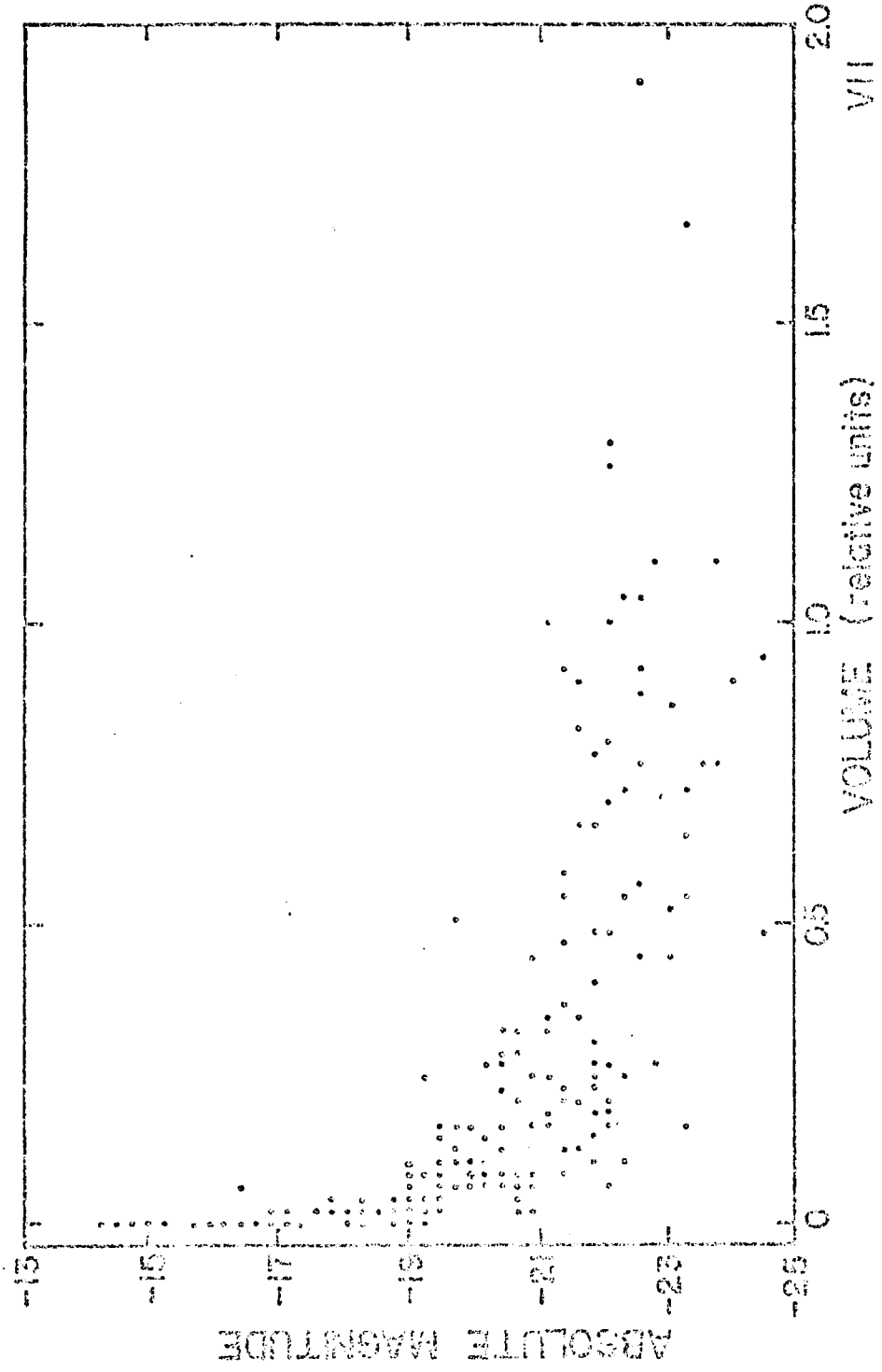
VOLUME (relative units)
0
0.5
1.0
1.5
2.0
ABSOLUTE MAGNITUDE
-15
-16
-17
-18
-19
-20
-21

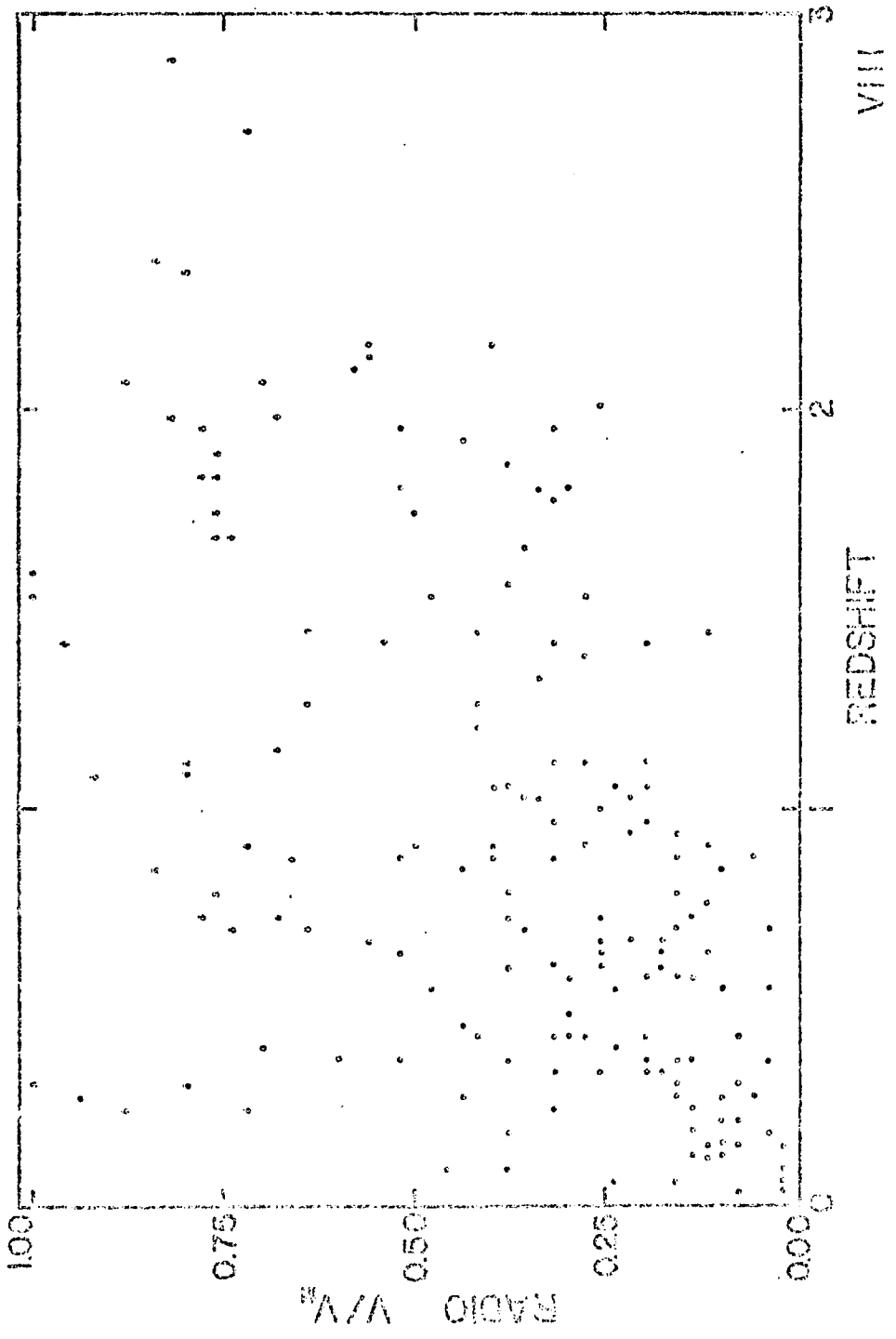
RADIO V/V_m
1.00
0.75
0.50
0.25
0.00
0
1
2
3
REDSHIFT
VIII

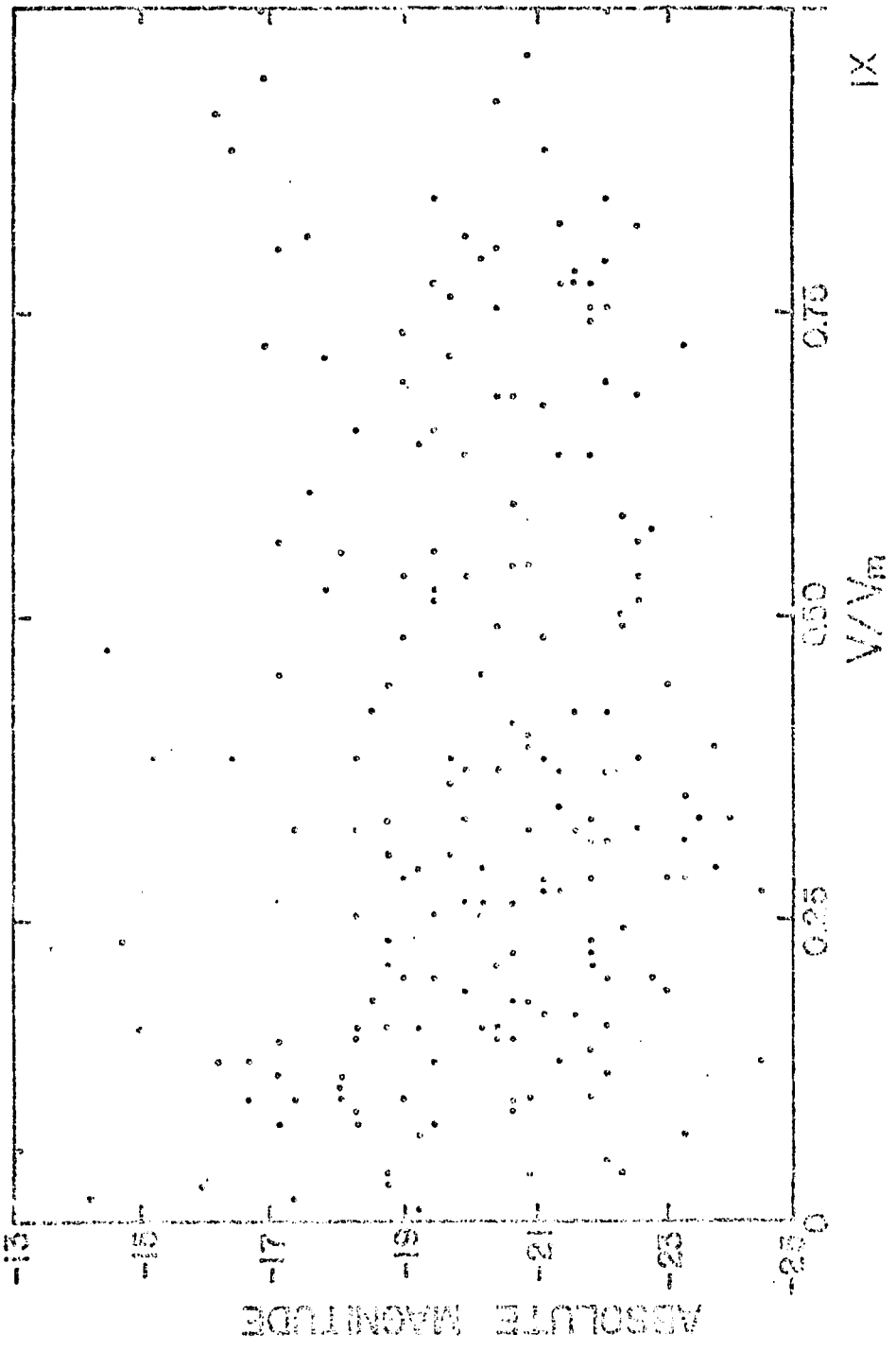
ABSOLUTE MAGNITUDE
-13
-15
-17
-19
-21
-23
-25
0
0.25
0.50
0.75
1
EW/W
IX

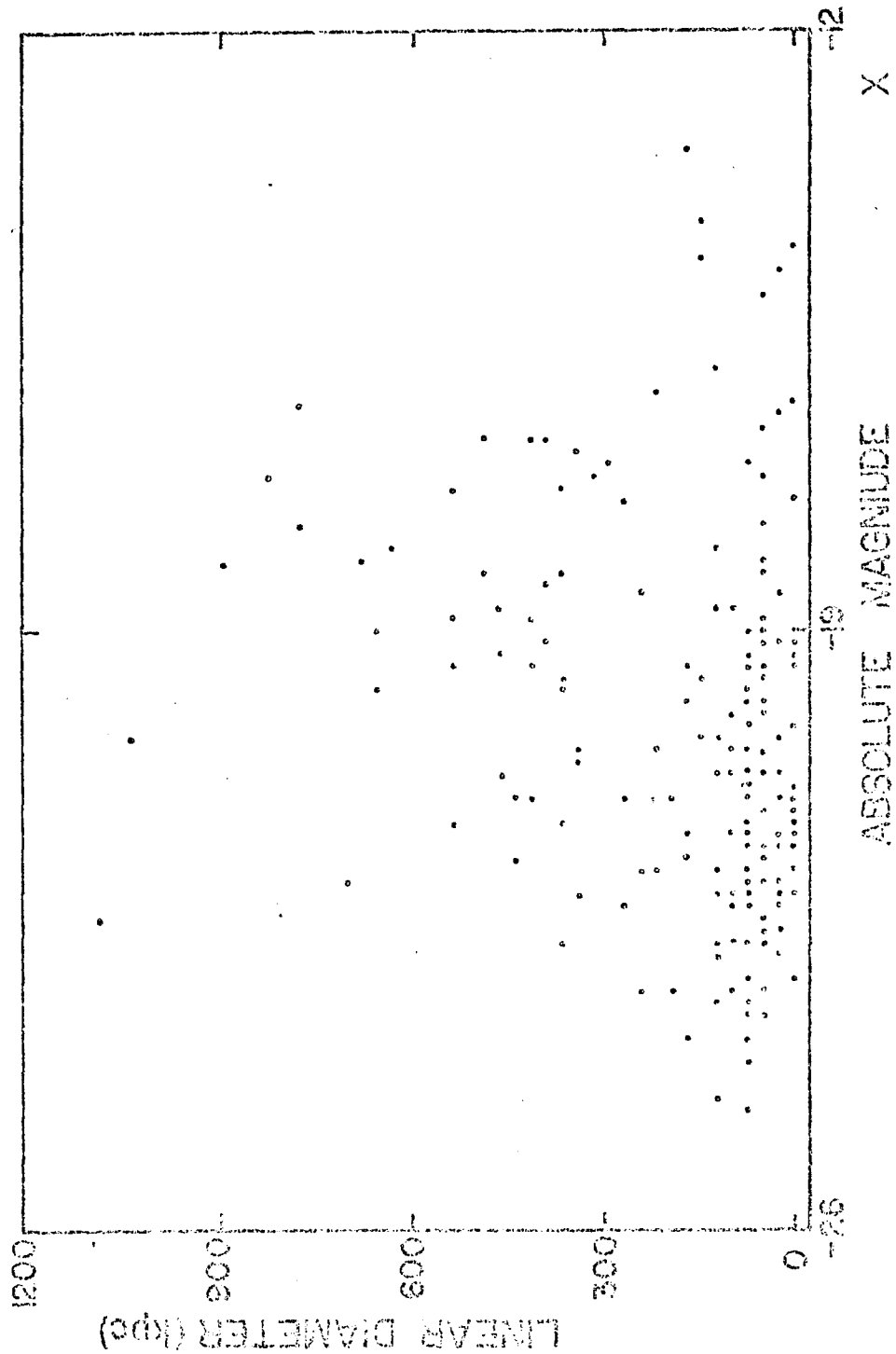
LINEAR DIAMETER (kpc)
1200
800
600
400
0
-26
-19
-12
ABSOLUTE MAGNITUDE
X

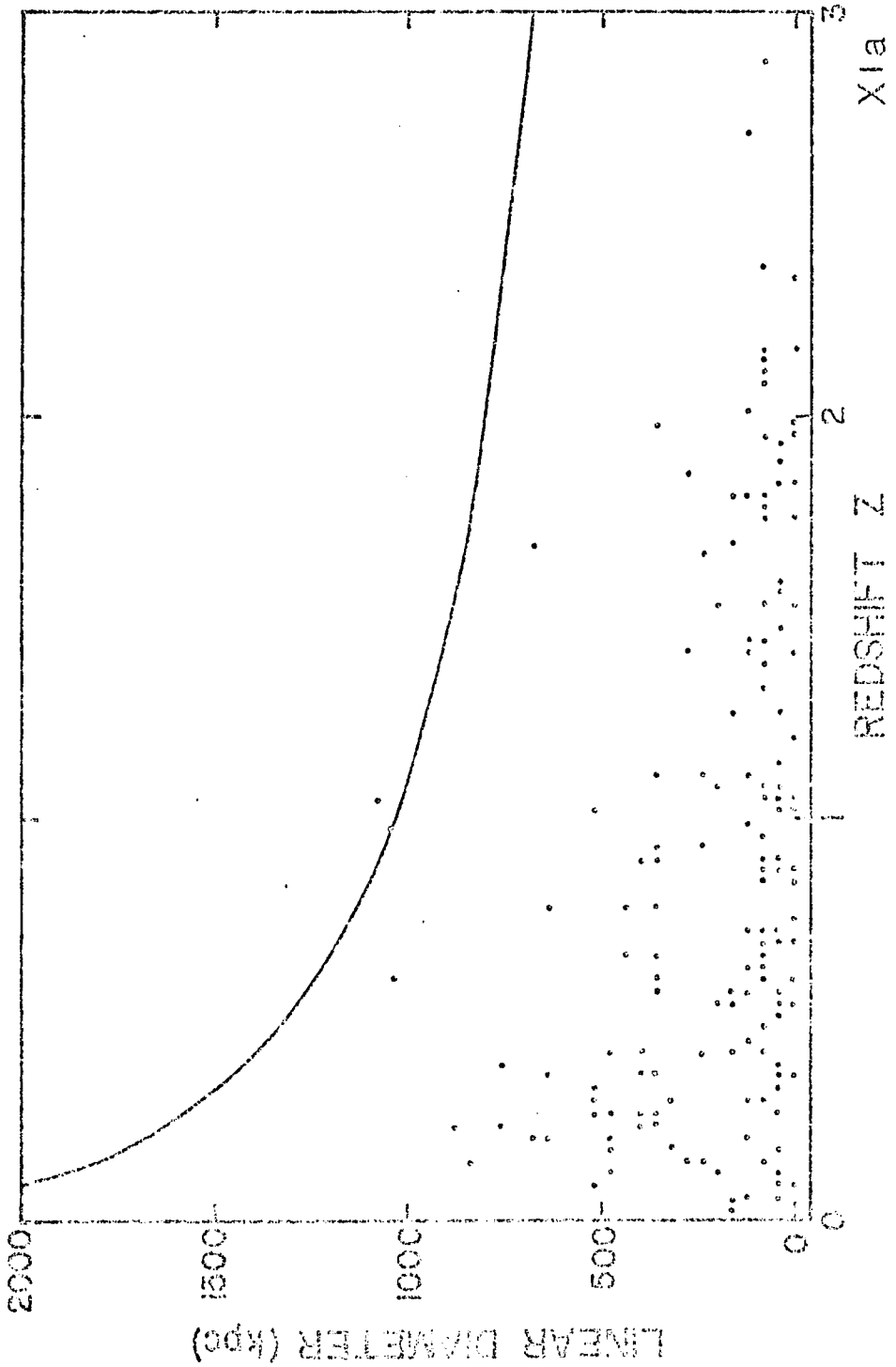
LINEAR DIAMETER (kpc)
2000
1500
1000
500
0
0
1
2
3
REDSHIFT z
XIa

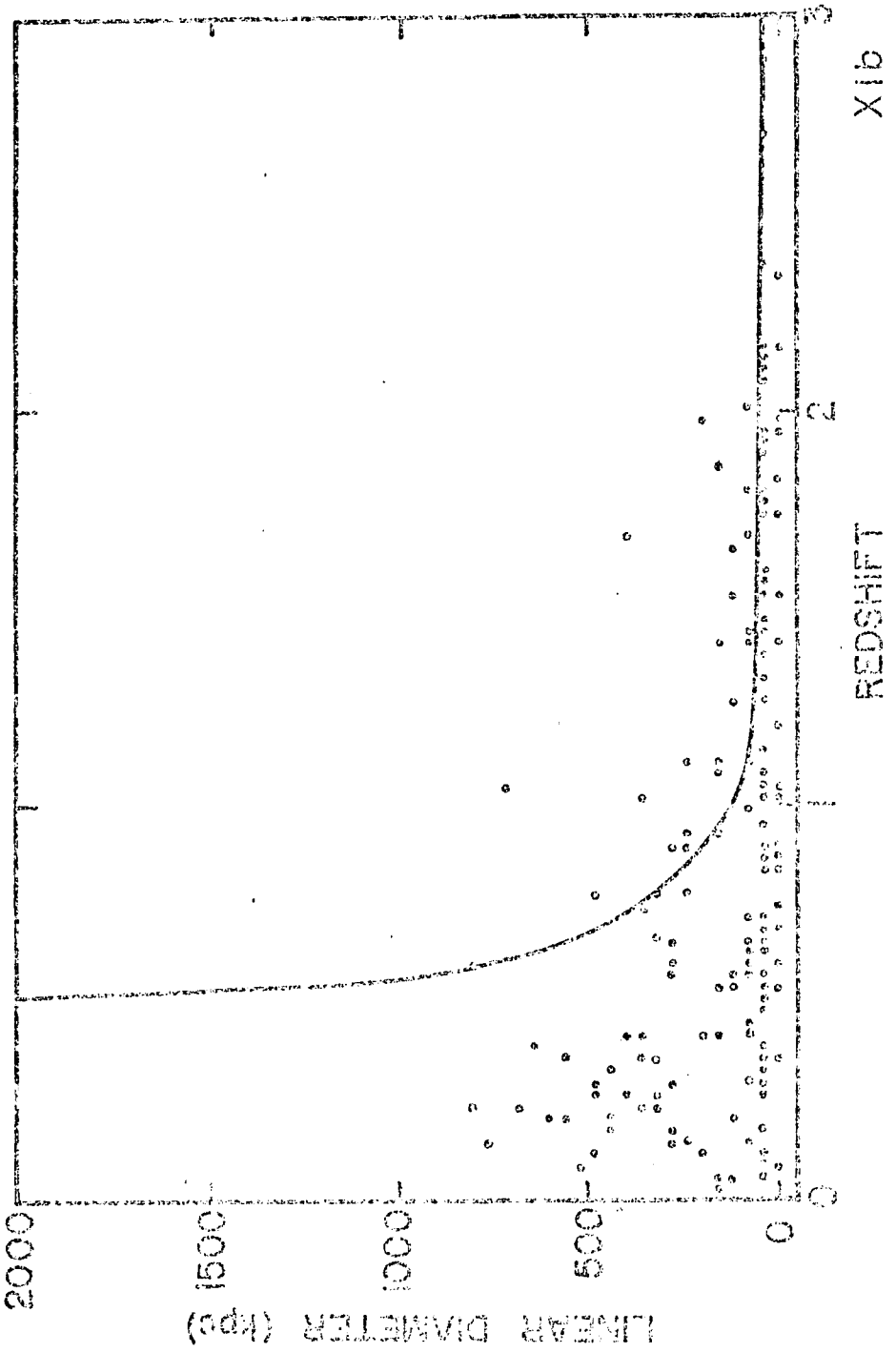
LINEAR DIAMETER (kpc)
2000
1500
1000
500
0
0
1
2
3
REDSHIFT
XIb

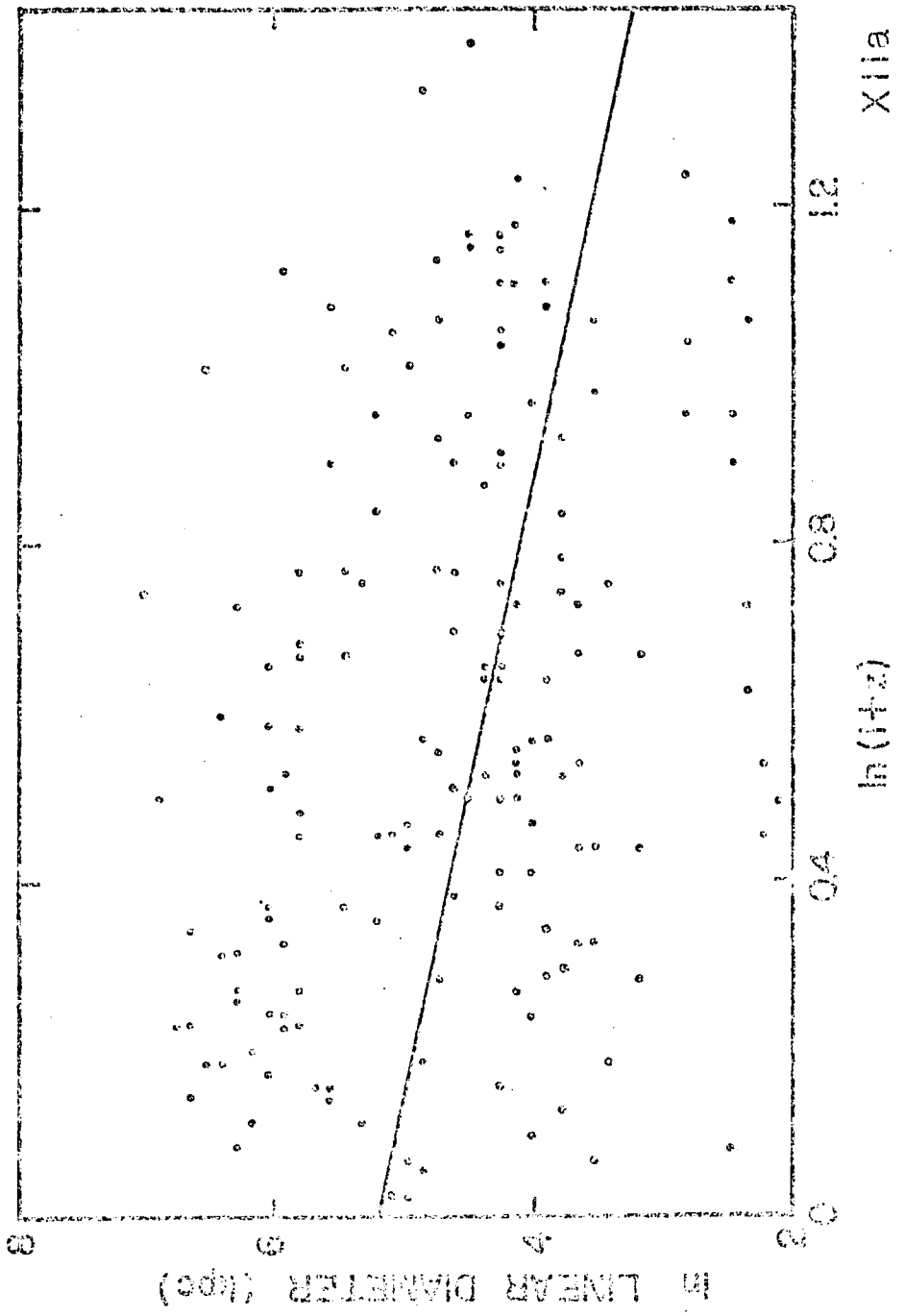
XIIa
ln (1+z)
ln LINEAR DIAMETER (kpc)

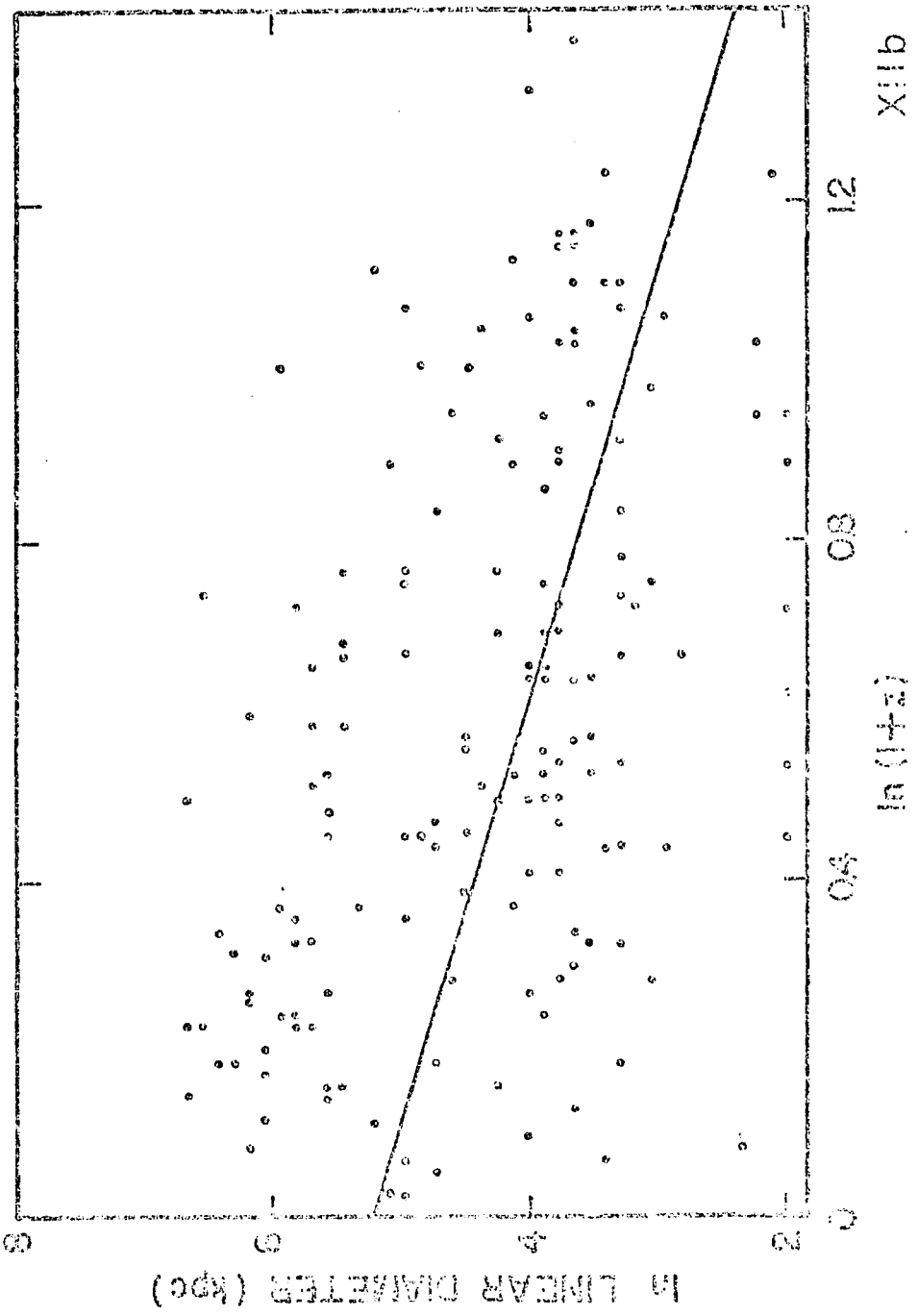
XIIb
ln (1+z)
ln LINEAR DIAMETER (kpc)

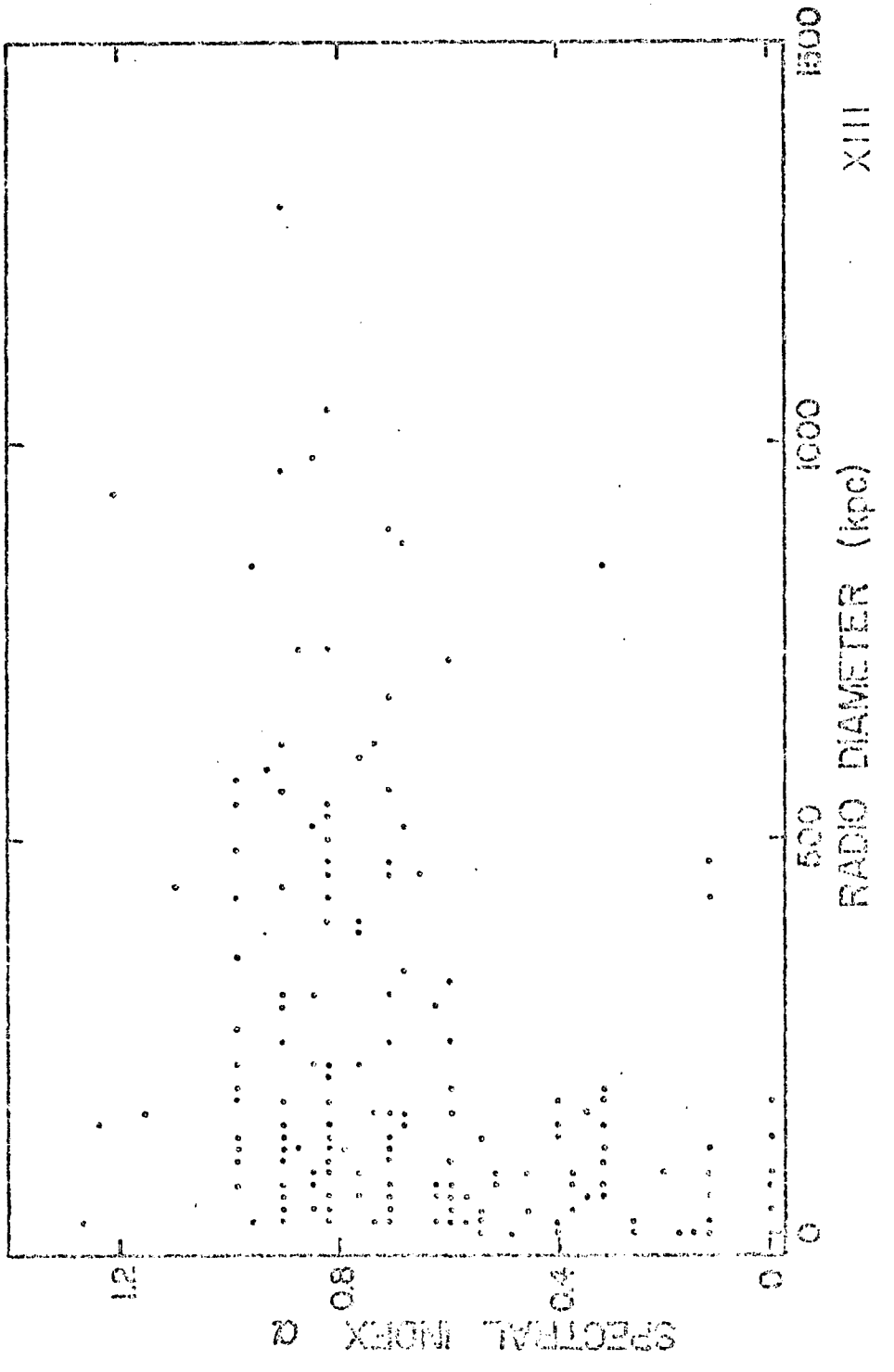
SPECTRAL INDEX α
0
.4
.8
1.2
0
600
1200
RADIO DIAMETER (kpc)
XIII

XIVa

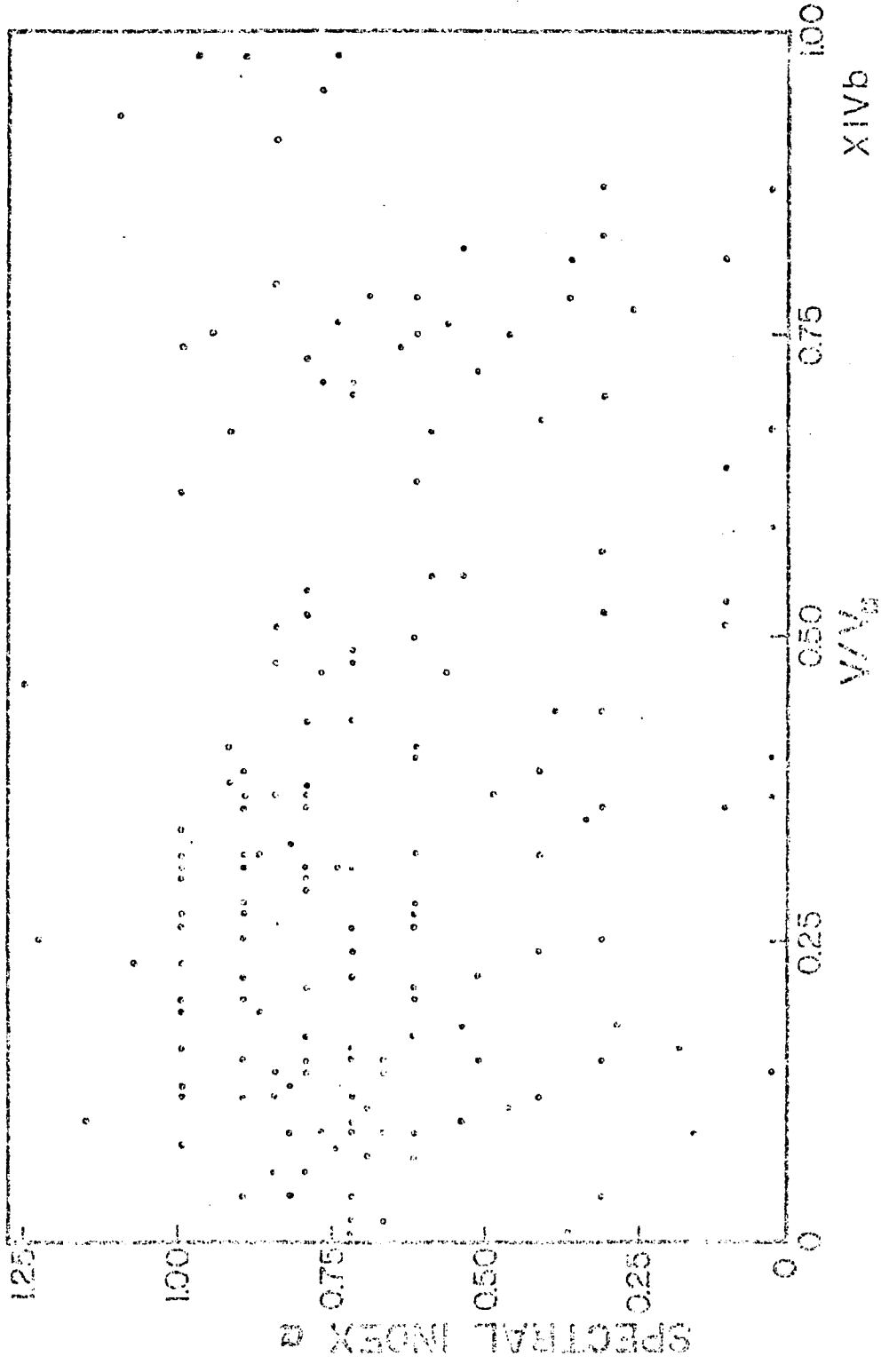
SPECTRAL INDEX α
1.25
1.00
0.75
0.50
0.25
0
0
0.25
0.50
0.75
1.00
XIVb
XIVa

SPECTRAL INDEX α
0.75
0.5
0.25
0
0
0.5
1.0
1.5
2.0
2.5
REDSHIFT
XiVc

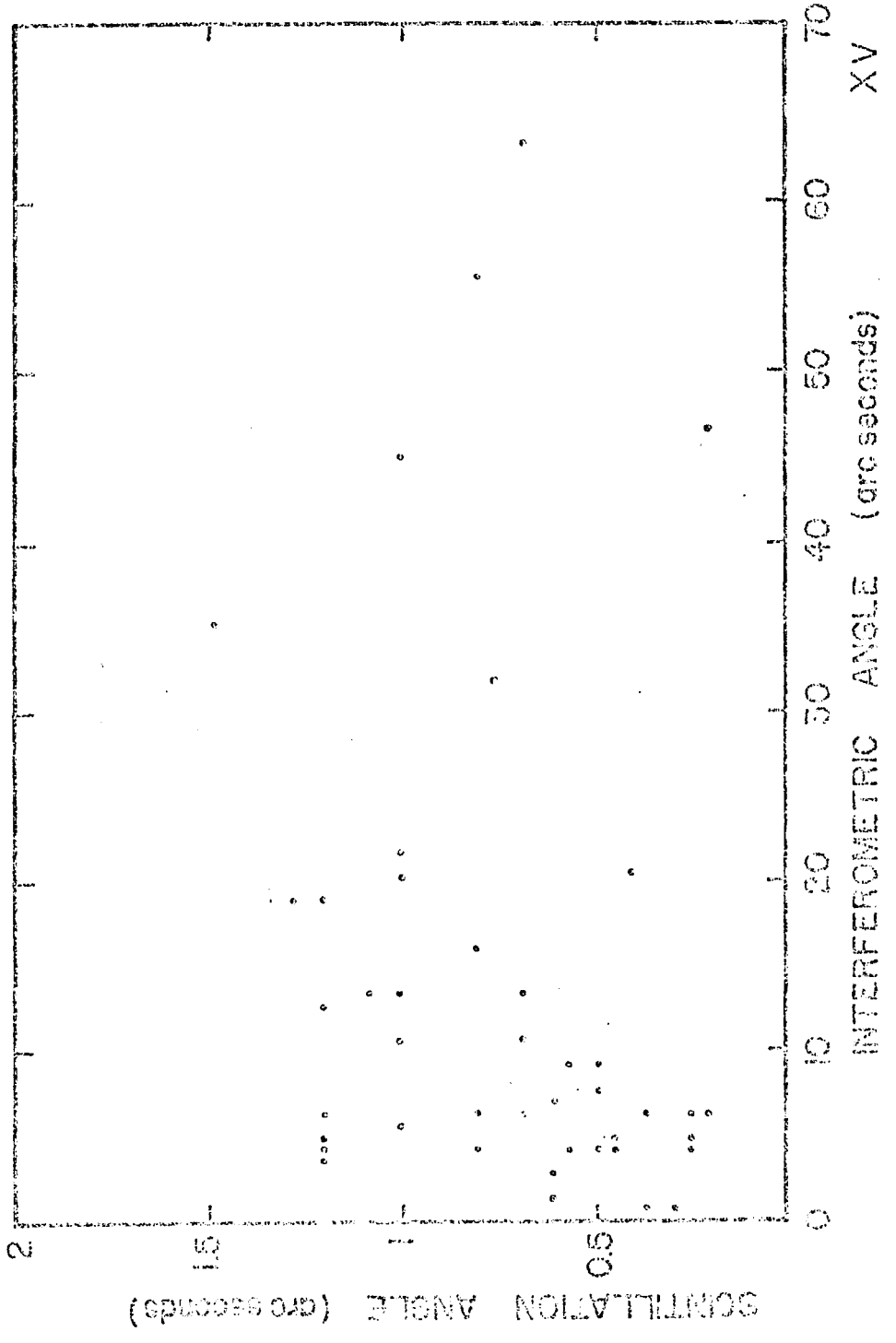
INTERFEROMETRIC ANGLE (arc seconds)
0
10
20
30
40
50
60
70
XV
SCINTILLATION ANGLE (arc seconds)
2
1.5
1
0.5

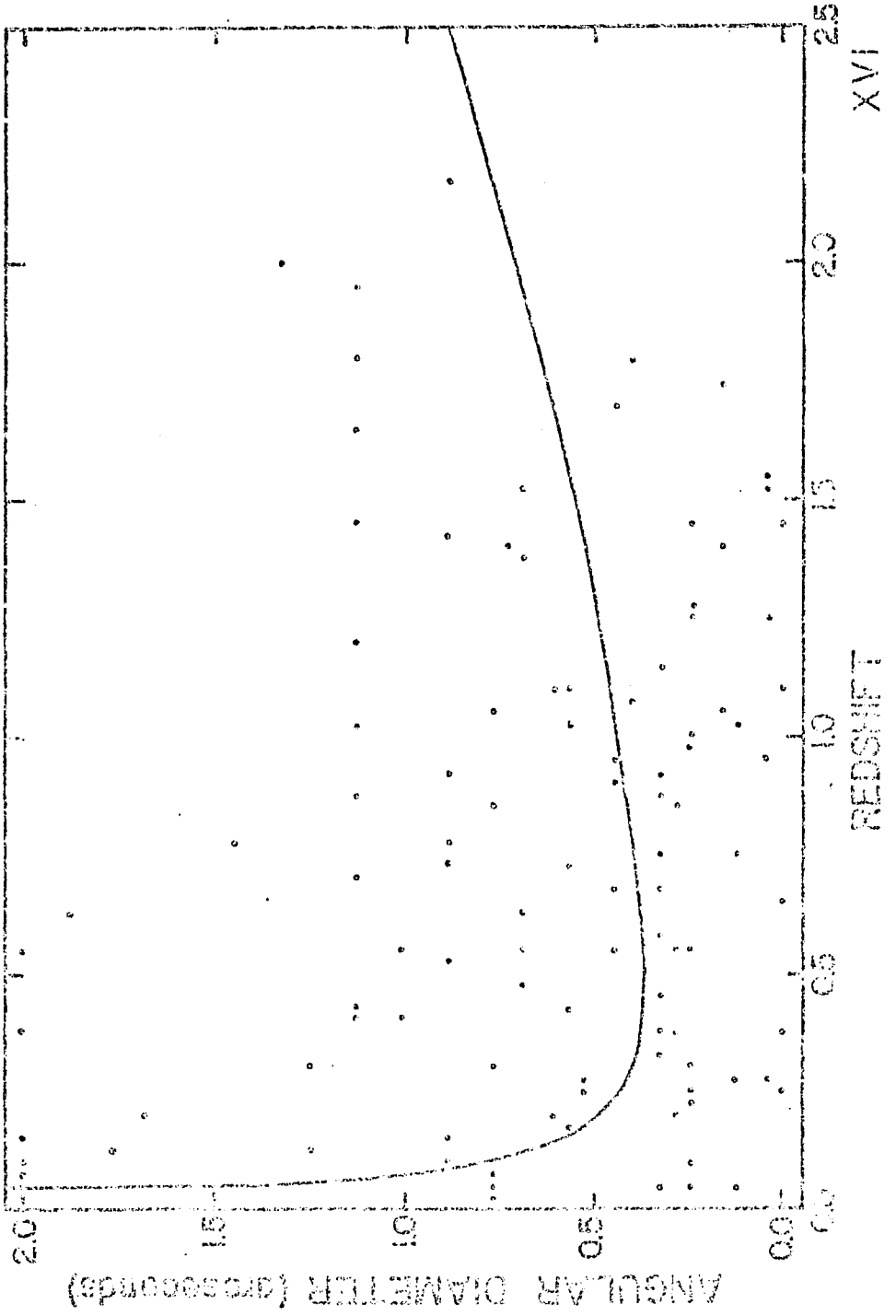
ANGULAR DIAMETER (arcseconds)
2.0
1.5
1.0
0.5
0.0
REDSHIFT
0.0
0.5
1.0
1.5
2.0
2.5
XVI

SECTION D

COSMOLOGICAL TESTS OF A SCALE-COVARIANT THEORY OF GRAVITATION: m-z, θ_m-z, θ_i-z, AND N(m)-m

SECTION D: SCALE COVARIANT TESTS

I. INTRODUCTION

In previous papers (Canuto et al. 1977, Canuto and Hsieh 1978b; hereafter referred to as papers I and II respectively) the theoretical structure of scale covariant gravitation was introduced so that gravitational phenomena can be studied in atomic units, assuming quite generally that the gravitational and atomic dynamical units are related through the scaling function $\beta(x)$. It was emphasized that Einstein's theory of gravitation remains unaltered if one limits oneself to using gravitational clocks. However, when observations are made and recorded with atomic instruments, one goes beyond the realm of purely gravitational dynamics. The function $\beta(x)$ was thus explicitly introduced to parametrize our ignorance of the correct coupling of gravitation to atomic dynamics over large cosmological scales. It was argued that any variation of the gravitational constant G must be interpreted as a relative variation of gravitational and atomic dynamics. Furthermore, such a variation does not contradict the improved experimental confirmation of Einstein's general relativity.

Along with the new formalism, we derived new conservation laws which must be adhered to in place of the standard conservation laws. In fact, the inconsistency of studying the effects of varying G with the imposition of the standard conservation laws has been repeatedly pointed out (see e.g., this work, Section B). A careful examination of the thermodynamic laws consistent with the scale covariant gravitation was given in paper II, where a semi-classical description of particles and photons in terms of the geometrical parameters of the scale covariant theory can be found. It was furthermore demonstrated in the above paper that a consistent analysis of the radiation problem allows one to interprete the observed background radiation as remnant of an

equilibrium radiation of an earlier epoch, just as in standard cosmology (see also Canuto and Hsieh, 1978a).

Papers I and II will serve as a foundation upon which the astrophysical analysis will be based.

In the present paper we consider well known cosmological observations and see if they are in agreement with the predictions of the scale covariant theory. Before entering into a detailed discussion, we indicate here some qualitative features peculiar to the scale covariant framework, normalizing our description to the well known standard cosmology.

First, it must be noted that the fundamental cosmological observations such as redshift and luminosity measurements are of atomic nature. To deduce from these measurements the geometrical structure of the Universe as determined by gravitation, one must first disentangle the relation between atomic and gravitational dynamics. That is, one must know the scaling function $\beta(t)$ (see this work, Section 5 for a thorough discussion of observational and theoretical determinations of the time derivatives of β). Specifically, if the metric (in atomic units) describing the cosmological space-time has the Robertson-Walker form, the time variation of the scale factor $R(t)$ being governed by equation (2.1) below, depends not only on gravitational dynamics but also on the time evolution of the function β. Thus, only if $\beta(t)$ is known, can one deduce the true geometrical structure of the Universe. The latter is still characterized by $\overline{H}_o$ and $\overline{q}_o$, defined in the usual manner in terms of the gravitational metric. Clearly, it is $\overline{H}_o$, $\overline{q}_o$ and not H_o, q_o, defined in terms of the atomic metric, which are directly related to the purely gravitational parameters such as the curvature of space, k, eq. (2.8).

Hence, the theoretical estimates of Appendix A should be used as a guide to the evolutionary effects and for this reason, in many tables and graphs below, we give results for different values of the evolutionary index e defined in eq. (7.8).

The use of QSO's as cosmological probes has been another controversial subject in standard cosmology. Treating the QSO as objects at distances indicated by their redshifts, we use the observed slope of the N-m relation to determine the evolutionary index for these objects. When such an evolution is used to evaluate the magnitude-redshift relation, we obtain theoretical m-z curves which fit the data points representing the QSO's. When we apply a similar procedure using standard cosmology, the fitting of the data is less successful.

Having thus given a preview of the highlights of the present paper as a general orientation, we proceed with the details of the analysis by first solving the cosmological equations for each choice of the scaling function. Luminosity and angular diameters are then derived as functions of the observed redshift. Except when analytic solutions can be obtained, results are presented in tabular form. Comparisons with existing data are then made and presented in figures.

II. COSMOLOGY

As shown in previous papers, Einstein equations in atomic units and for a Robertson-Walker metric read (I, Eq. 3.2 : in this paper we shall take $\Lambda = 0$)

$$\left(\frac{\dot{R}}{R} + \frac{\dot{\beta}}{\beta}\right)^2 + \frac{k}{R^2} = \frac{8\pi}{3} G\rho \qquad (2.1a)$$

$$\frac{\ddot{R}}{R} + \frac{\ddot{\beta}}{\beta} + \frac{\dot{\beta}\dot{R}}{\beta R} - \frac{\dot{\beta}^2}{\beta^2} = -\frac{4\pi G}{3}(3p + \rho) \qquad (2.1b)$$

where the derivatives are taken with respect to atomic time, t. $R(t)$ is the scale factor and p, ρ and G are in general functions of the scale function β which depends on the chosen gauge. If one decides to work in the so-called Einstein gauge, $\beta = 1$, then the atomic and Einstein times, $\beta\, dt = d\bar{t}$, coincide. The dots in Eqs. (2.1) would then represent derivatives with respect to $\bar{t}$. Clearly, if $\beta = 1$, all the β terms disappear and Eqs. (2.1) reduce to the familiar Einstein equations. It is the contention of our theory that the assumption $\beta = \text{const.}$, usually made in cosmology, and leading to no difference between Einstein and atomic times (except for a time independent large numerical factor) is unproven and should be tested by using observational data.

For that reason, we have extended the theory so as to incorporate a non-constant β. The extra terms in Eqs. (2.1) represent precisely this contribution. Should it turn out that the data can be fitted only with $\beta = \text{const.}$, we would have legitimized this gauge choice, heretofore made a priori. In this sense our theory does not change the

physics underlying Einstein theory, neither does it substitute Einstein equations with new ones. Rather, it investigates under which circumstances the assumption of a constant β is actually verified, if at all. The scale over which β varies is the age of the Universe and therefore the effect of β can be felt significant only if one extends the analysis to high red-shift objects so that a good portion of the Universe is actually investigated. From now on, quantities referring to Einstein units will be denoted by a bar.

With $\bar{R}(\bar{t}) = \beta R(t)$, $d\bar{t} = \beta(t)dt$, it is easy to derive the following relations, ($\beta_o = 1$)

$$\bar{H}_o = H_o + h_o \; ; \; h_o = (\dot{\beta}/\beta)_o \; , \; Q_o = -(\ddot{\beta}\beta/\dot{\beta}^2)_o \tag{2.2}$$

$$\frac{k}{\bar{R}_o^2} = (2\bar{q}_o - 1)\,\bar{H}_o^2 = \left(\frac{\rho_o}{\rho_c} - \frac{\bar{H}_o^2}{H_o^2}\right) H_o^2 \tag{2.3}$$

$$\frac{\rho_o}{\rho_c} = 2\bar{q}_o \left(\frac{\bar{H}}{H}\right)^2 \tag{2.4}$$

$$\bar{q}_o = q_o \left(\frac{H_o}{\bar{H}_o}\right)^2 + (1 + Q_o)\left(\frac{h_o}{\bar{H}_o}\right)^2 - \frac{h_o H_o}{\bar{H}_o^2} \tag{2.5}$$

where

$$\bar{q}_o = -\left(\frac{\bar{R}''\bar{R}}{\bar{R}'^2}\right)_o ; \quad q_o = -\left(\frac{\ddot{R}R}{\dot{R}^2}\right)_o ; \quad \left(' = \frac{d}{d\bar{t}} \; ; \; \cdot = d/dt \right)$$

From Einstein's equations (2.1), one can also derive the following energy conservation law (I, Eq. 2.38)

$$\dot{\rho} + 3\,\frac{\dot{R}}{R}\,(\rho + p) = -\rho\,\frac{(G\beta)^{\cdot}}{G\beta} - 3p\,\frac{\dot{\beta}}{\beta} \tag{2.6}$$

For an equation of state of the form

$$p = c_s^2\,\rho$$

Eq. (2.6) can be integrated exactly with the result (see I, Eq. 2.3).

$$\rho = \rho_o \left(\frac{R_o}{R}\right)^{3(1+c_s^2)} \cdot \frac{G_o}{G(\beta)} \cdot \frac{1}{\beta^{1+3c_s^2}} \tag{2.7}$$

We now have all the necessary ingredients to study the behavior of the scale factor R(t) vs. t.

A) *World models*

Substituting Eq. (2.7) in (2.1), and integrating we obtain ($c_s^2 = o$)

1) $k = 0$:

$$\beta(t)\ \frac{R(t)}{R_o} = \left\{\frac{3}{2}\ \overline{H}_o\ \int_o^t \beta(t)\ dt\right\}^{2/3} \tag{2.8}$$

$$\frac{8\pi}{3}\ G_o\ \rho_o = \frac{k}{R_o^2} + \overline{H}_o^2 \equiv A = B + \overline{H}_o^2$$

2) $k = -1$:

$$\beta(t)\ \frac{R(t)}{R_o} = \frac{A}{2B}\ (\cosh\psi - 1)\ ;\ \int_o^t \beta(t)\ dt = (A/2B^{3/2})\ (\sinh\psi - \psi) \tag{2.9}$$

$$A/2B = \overline{q}_o\ (1 - 2\overline{q}_o)^{-1}\ ;\ A/2B^{3/2} = \overline{q}_o/\overline{H}_o\ (1 - 2\overline{q}_o)^{3/2}$$

3) $k = +1$:

$$\beta(t)\ \frac{R(t)}{R_o} = \frac{A}{2B}\ (1 - \cos\theta)\ ;\ \int_o^t \beta(t)\,dt = (A/2B^{3/2})\ (\theta - \sin\theta)$$

$$A/2B = \bar{q}_o\ (2\bar{q}_o - 1)^{-1}\ ;\ A/2B^{3/2} = \bar{q}_o/\bar{H}_o\ (2\bar{q}_o - 1)^{3/2} \qquad (2.10)$$

Numerical solutions for R(t) vs. t are presented in Tables 1-4 for different values of $\bar{q}_o$.

B) Radiation dominated universe: $c_s^2 = 1/3$

1) $k = 0$:

$$\beta(t)\ R(t)/R_o = \left\{2\ \bar{H}_o \int_o^t \beta(t)\,dt\right\}^{1/2} \qquad (2.11)$$

2) $k = -1$:

$$\beta(t)\ R(t)/R_o = \left(\frac{2\bar{q}_o}{1 - 2\bar{q}_o}\right)^{1/2} \left\{\left[1 + \frac{1 - 2\bar{q}_o}{\sqrt{2\bar{q}_o}}\ \bar{H}_o \int_o^t \beta(t)dt\right]^2 - 1\right\}^{1/2} \qquad (2.12)$$

3) $k = +1$:

$$\beta(t)\, R(t)/R_o = \left(\frac{2\bar{q}_o}{2\bar{q}_o - 1}\right)^{1/2} \left\{\left[1 + \frac{2\bar{q}_o - 1}{\sqrt{2\bar{q}_o}}\, \bar{H}_o \int_o^t \beta(t)dt\right]^2 - 1\right\}^{1/2} \qquad (2.13)$$

C) The age of the matter dominated era, t_o.

This age can easily be determined by putting $t = t_o$, $R = R_o$, ($\beta_o = 1$), in the upper limit of the integrals (2.8)-(2.10), thus getting

$k = 0$:

$$t_o\, H_o = \frac{2}{3} \left\{ \frac{1}{\left(1 + \frac{h_o}{H_o}\right) \int_o^1 \beta(x)\, dx} \right\} \equiv \frac{2}{3}\, I(\beta) \qquad (2.14)$$

$k = +1$:

$$t_o\, H_o = \frac{\bar{q}_o}{(2\bar{q}_o - 1)^{3/2}} \left[\cos^{-1}\left(\frac{}{\bar{q}_o} 1\right) - \frac{1}{\bar{q}_o} (2\bar{q}_o - 1)^{1/2}\right] I(\beta) \qquad (2.15)$$

$k = -1$:

$$t_o\, H_o = \left[(1 - 2\bar{q}_o)^{-1} - \bar{q}_o\, (1 - 2\bar{q}_o)^{-3/2} \cosh^{-1}\left(\frac{1}{\bar{q}_o} - 1\right)\right] I(\beta) \qquad (2.15)$$

If we put $\beta = 1$, (2. .16) reduce to the well known expressions in Einstein units, i.e. $\bar{t}_o \bar{H}_o$. We th .. obtain in general,

$$\bar{t}_o = t_o \int_o^1 \beta(x)\, dx \qquad (2.17)$$

an expression which relates the age t_o in Einstein and atomic units. Values of $t_o H_o$ are presented in Tables 1-4.

III. THE RED-SHIFT

As proved in II (Eq. 3.14), the measured red-shift should be defined as

$$1 + z = \frac{R_o}{R} \tag{3.1}$$

i.e. as a function of the scale factor in atomic units. Within the present theory, the ratio of the scale factors in Einstein units is a convenient symbol and not a physically meaningful quantity. We shall denote it by z,

$$1 + z = \frac{\bar{R}_o}{\bar{R}} \tag{3.2}$$

However, since $\beta R(t) = \bar{R}$, it follows that

$$\beta(1 + z) = 1 + z \tag{3.3}$$

We shall find it convenient to express intermediate results in terms of z instead of z. However, physical results will always be expressed in terms of z.

IV. THE SCALE FUNCTION $\beta(t)$

As we have already discussed in great detail in the previous papers, the function $\beta(t)$ cannot be determined from within the theory as we have formulated it. External considerations must be used which can vary depending on which data are deemed most significant. In the previous papers we discussed different functional dependences of β on t, represented by a single function

$$\beta(t) = \left(\frac{t_o}{t}\right)^{\epsilon} \quad , \quad \epsilon = \mp 1; \mp 1/2 \tag{4.1}$$

corresponding to the following gauges

$$G \sim \beta^{-1}\ ,\ \beta,\ \beta^{-2}\ ,\ \beta^{2} \tag{4.2}$$

If $G \sim t^{-1}$, the first two gauges are the ones proposed by Dirac in 1938 and 1973 respectively. The third one was proposed by Canuto and Hsieh (1978) whereas the fourth one was discussed for the first time in the previous paper, II.

V. THE COMPLETE SOLUTION

a) General Relations

Using (2.17), (4.1), (2.14)-(2.16), we now obtain

$$t_o = \bar{t}_o\,(1-\epsilon) \quad , \quad H_o\, t_o = (1-\epsilon)\ \bar{H}_o\, \bar{t}_o + \epsilon \tag{5.1}$$

Since it is easier to evaluate $\bar{H}_o\ \bar{t}_o$ than $H_o\ t_o$, we shall use (5.1) as the equation defining $H_o\ t_o$. The relation (2.5) between $\bar{q}_o$ and q_o can also be considerably simplified. It becomes

$$\frac{k}{R_o^2} = \left[\frac{\rho_o}{\rho_c} - \left(1 - \frac{\epsilon}{H_o\, t_o}\right)^2\right] H_o^2 = (2\bar{q}_o - 1)\ \bar{H}_o^2$$

$$\frac{\rho_o}{\rho_c} = 2q_o + \frac{2\epsilon}{H_o\, t_o}\left[1 - \frac{1}{H_o\, t_o}\right] \tag{5.2}$$

$$q_o = \bar{q}_o \left(\frac{\bar{H}_o}{H_o}\right)^2 + \frac{\epsilon}{(H_o\, t_o)^2} - \frac{\epsilon}{H_o\, t_o}$$

b) The Analytic case: $k = 0$, $\bar{q}_o = 1/2$.

The case $k = 0$ can be treated analytically and we shall therefore present the results corresponding to it before giving the full numerical solution. We present only the zero pressure case, since these results are the ones of physical interest for the purposes of the present paper.

From Eq. (2.8) we obtain

$$R(t) = R_o \left(\frac{t}{t_o} \right)^r \quad , \quad r \equiv \tfrac{1}{3} (2 + \epsilon) \tag{5.3}$$

Since $\bar{H}_o \, \bar{t}_o$ is equal to 2/3 [Sec (2.17) with $\beta = 1$], it follows from (5.1) or (5.3) that

$$H_o \, t_o = \tfrac{1}{3} (2 + \epsilon) \quad , \quad \bar{H}_o = H_o \, \frac{2(1 - \epsilon)}{2 + \epsilon} \tag{5.4}$$

From (5.2) we finally obtain

$$q_o = \frac{1 - \epsilon}{2 + \epsilon} \tag{5.5}$$

or

$$H_o \, t_o \, q_o = \frac{1 - \epsilon}{3}$$

At the same time, from (3.3) we derive

$$1 + \mathcal{Z} = (1 + z)^{\frac{2 - 2\epsilon}{2 + \epsilon}} \quad , \qquad \beta(t) = (1 + z)^{\frac{3\epsilon}{2 + \epsilon}} \tag{5.6}$$

Explicitly

$$k = 0, \quad \bar{q}_o = 1/2$$

ϵ	$R(t)$	$H_o t_o$	q_o	$\beta(t)$	$1 + \mathcal{Z}$	
-1	$t^{1/3}$	1/3	2	t	$(1 + z)^4$	(5.7)
+1	t	1	0	t^{-1}	const.	(5.8)
-1/2	$t^{1/2}$	1/2	1	$t^{1/2}$	$(1 + z)^2$	(5.9)
+1/2	$t^{5/6}$	5/6	1/5	$t^{-1/2}$	$(1 + z)^{2/5}$	(5.10)

where t is normalized to t_o and $R(t)$ to R_o.

In spite of having $q_o = 0,\ 1/5,\ 1$ and 2, the four cases correspond to $\bar{q}_o = 1/2$ and, as we shall see, $\bar{q}_o$ and not q_o is the deceleration parameter determined from the m vs. z relation (see 7.7 and 7.11).

c) The full solution

Equations (2.8)-(2.10) were solved numerically and the results are presented in Tables 1-4. The procedure is as follows. Since the physically significant parameter is the curvature k, we first specify values of $\bar{\bar{q}}_o$, which in spite of having lost its direct physical meaning in our interpretation, is nonetheless a convenient parameter whose values indicates whether k = -1, 0, +1, Eq. (2.3).

Given a value of $\bar{\bar{q}}_o$ (first column), we then solve Eqs. (2.14)-(2.16) with $\beta = 1$, so as to get $\bar{\bar{H}}_o$ $\bar{t}_o$ (3rd column). With this information we then compute H_o t_o (Eq. 5.1), (4th column) and finally q_o, Eq. 5.2 (second column). Equations (2.8)-(2.10) can then be solved. We present in column 7 and 8 the function $R(t)/R_o$ vs. t/t_o, as well as the red-shift z, Eq. (3.1) (6th column) and z, Eq. (3.2) (5th column). Finally, in column 9 we present $\delta(t)$, which can then be read against R/R_o or t/t_o or z.

The values corresponding to $\bar{\bar{q}}_o = 1/2$ (k = 0), can be checked against the analytic expressions given by Eqs. (5.3)-(5.10).

d) Look-back time

An important parameter in any cosmology is the look-back time, defined as

$$\tau = t_o - t = \left(1 - \frac{t}{t_o}\right) t_o \qquad (5.11)$$

From column 8 of Tables 1-4, we can construct the function τ/t_o vs. z. For the four cases $\epsilon = \pm 1, \pm 1/2$, the curves τ/t_o vs. z are presented in Figures 1, 2, 3, and 4, for two values of $\bar{q}_o = 0$ and 1, i.e. for an open and closed Universe. These Figures should be compared with the one presented by Sandage for the case of ordinary cosmology (Sandage 1961b)

c) Small look-back times

The case of small look-back times can be worked out explicitly and it is therefore of interest because it yields a simple relation between the pairs of variables z, H_o and α, $\bar{H}_o$. From Eq. (4.1) we have

$$\beta(t) = 1 - (t_o - t) h_o - \tfrac{1}{2} Q_o h_o^2 (t_o - t)^2 + \ldots \qquad (5.12)$$

From (3.1) we obtain the expression for $t_o - t$, namely

$$t_o - t = \frac{z}{H_o} \left[1 - (1 + \tfrac{1}{2} q_o) z\right] + \ldots$$

so that

$$\beta(t) = 1 - \frac{h_o}{H_o} z + \frac{h_o}{H_o} \left(1 + \frac{1}{2} q_o - \frac{1}{2} Q_o \frac{h_o}{H_o}\right) z^2 + \ldots \qquad (5.13)$$

Substituting (5.13) into (3.3), we now obtain

$$z = z \left\{ 1 + \frac{h_o}{H_o} + \left[\left(1 + \frac{1}{2} Q_o \right) \frac{h_o}{H_o} - \frac{1}{2} q_o \right] \frac{h_o}{H_o} z + \dots \right\} \qquad (5.14)$$

which on the basis of both expressions (5.1) can be rewritten as

$$z = z \frac{\overline{H}_o}{H_o} + \frac{\epsilon}{2 H_o \overline{H}_o t_o} \left(q_o + \frac{\epsilon - 1}{t_o H_o} \right) z^2 + \dots \qquad (5.15)$$

The range of validity of this approximation can be checked using the exact values of z vs. z presented in the Tables [and Eq. (5.6) for the $k = 0$ case]. Some general relationship can already be reached at the level of (5.15). Since $\overline{H}_o = H_o - \epsilon/t_o$, [Eq. (2.2) with (4.1)] $\overline{H}_o > H_o$ for $\epsilon < 0$ and so

$$z > z \qquad (5.16)$$

Conversely, for the cases $\epsilon > 0$, $\overline{H}_o < H_o$ and so

$$z < z \qquad (5.17)$$

These two conclusions are borne out by the numerical values of z and z listed in Tables 1-4.

VI. THE HORIZON

A concept of great importance in cosmology is that of the horizon, particle horizon and event horizon (Rindler 1956)

Following Rindler, we shall define the proper distance of the particle horizon (i.e. the farthest object from which we can receive signals) as

$$d_{PH}(t) = R(t) \int_0^t \frac{dt}{R(\bar{t})} \tag{6.1}$$

Since $\beta\, dt = d\bar{t}$ and $\beta\, R(t) = \bar{R}(\bar{t})$, the integral can be transformed into an expression in Einstein units. The integration can then be performed. The final result valid for any k, is

$$d_{PH}(t) = R(t) \left(\frac{c}{\bar{H}_o \bar{R}_o}\right) \frac{2}{(1 - 2\bar{q}_o)^{1/2}} \operatorname{Arsinh} \left(\frac{1 - 2\bar{q}_o}{2\bar{q}_o} \frac{\bar{R}}{\bar{R}_o}\right)^{1/2} \tag{6.2}$$

For $2\bar{q}_o < 1$, it can be further transformed to

$$k = -1: \qquad \frac{d_{PH}(t)}{R(t)} = \frac{c}{\bar{H}_o \bar{R}_o} \cdot \frac{1}{\sqrt{1 - 2\bar{q}_o}} \cdot \psi \tag{6.3}$$

We note that with a prescribed β, the cosmological equations (2.1) become a proper set of second order differential equations so that the scale covariant theory can be subjected to cosmological tests just as general relativity is tested with standard cosmology. The objectives are also similar: firstly, one must demonstrate the compatibility of the observed data with the predictions of the theoretical model. (Other attempts to prove the consistency of $G \sim t^{-1}$ with the m vs. z relation have notoriously failed. See the discussion.) If that is achieved, one then proceeds to determine the parameters which characterize the model, namely $\overline{H}_o$ and $\overline{q}_o$. The functional forms of β considered have been derived from various impositions of gauge conditions. Hence the cosmological tests must be considered as tests of the specific gauge conditions.

It is natural at this point to ask whether cosmological observations can be used as a constraint on the scaling function $\beta(t)$ and thus constitute an alternative observational determination of β. We can anticipate the results: for all scaling functions of the forms given by (4.1), there exist theoretically allowed parameters which make the theoretical predictions compatible with observation. (Whether we should prefer an increasing or decreasing $\beta(t)$ vs. t, must be based on purely gravitational tests as discussed in part XV).

A common feature that plagues all cosmological investigations is the evolutionary correction i.e., the intrinsic variation of the sources. As is well known, the inclusion of evolutionary correction has caused difficulties over the interpretation of the cosmological data, for the truly geometrical effects are not easily separated from the evolutionary effects. To a large extent, these uncertainties persist in the scale covariant framework. Even though the evolutionary effects can be estimated, as we have done in Appendix A, to what extent the various evolutionary processes are operative is not known.

Analogously, for $2\bar{q}_o > 1$,

$$k = +1: \qquad \frac{d_H(t)}{R(t)} = \frac{c}{\bar{H}_o \bar{R}_o} \frac{1}{\sqrt{2\bar{q}_o - 1}} \cdot \theta \tag{6.4}$$

where we have used Eqs. (2.9) and (2.10).

Finally for $k = 0$,

$$\frac{d_H(t)}{R(t)} = 2\left(\frac{c}{\bar{H}_o \bar{R}_o}\right)\left(\frac{\bar{R}}{\bar{R}_o}\right)^{1/2} = 2\left(\frac{c}{\bar{H}_o \bar{R}_o}\right)\beta^{1/2}(t)\left(\frac{R(t)}{R_o}\right)^{1/2} \tag{6.5}$$

a) Analytic case: $k = 0$.

Using Eqs. (5.3) and (4.1) for R(t) and $\beta(t)$ and (5.4), Eq. (6.5) can be re-written as

$$d_H(t) = \left(\frac{2+\epsilon}{1-\epsilon}\right) \frac{c}{\bar{H}_o} \left(\frac{t}{t_o}\right) \tag{6.6}$$

Explicitly,

$\epsilon = -1$

$$d_H(t) = \frac{3}{2} ct \; ; \quad d_H(\bar{t}) = 3c\bar{t} = \frac{3ct\beta}{2} = \beta(t)\, d_H(t) \tag{6.7}$$

Analogously for

$\epsilon = \pm 1/2$

$$d_H(\bar{t}) = \beta d_H(t) \tag{6.8}$$

where $d_H(\bar{t}) = 3c\bar{t}$ corresponds to standard cosmology. The relation (6.7) or (6.8) is clearly valid also for the $1 > \epsilon > 0$ case. We can therefore conclude that

$$\frac{d_H(\bar{t})}{d_H(t)} \quad \begin{cases} < 1 & \epsilon = -1 \ , \ \epsilon = -1/2 \\ > 1 & 1 > \epsilon > 0 \ . \end{cases} \tag{6.9}$$

b) The $k = \pm 1$ cases.

Due to the implicit nature of the R(t) vs. t function, we can only present asymptotic relations. Numerical values of $d_H(t)$ can however be computed using the value of $\bar{q}_o$ and $R(t)/R_o$ given in the Tables. For the $k = -1$ case and for large development angles ψ, we obtain from (2.9)

$$\beta(t) \quad \frac{R(t)}{R_o} \rightarrow \frac{\bar{q}_o}{1 - 2\bar{q}_o} \quad \frac{1}{2} \quad e^{\psi} \tag{6.10}$$

$$\int_o^t \beta(t)\, dt \rightarrow \frac{1}{\bar{H}_o} \quad \frac{\bar{q}_o}{(1 - 2\bar{q}_o)^{3/2}} \quad \frac{1}{2} \quad e^{\psi}$$

$$\frac{R(t)}{R_o} \rightarrow (1 - 2\bar{q}_o)^{1/2} \quad \bar{H}_o \quad \frac{\int_o^t \beta(t)\, dt}{\beta(t)} \tag{6.11}$$

We now have from (6.3)

$$d_H(t) = \frac{c}{H_o}\left(\frac{R(t)}{R_o}\right)\frac{1}{(1-2\bar{q}_o)^{1/2}}\,\psi \;\rightarrow\; \frac{c\int_o^t \beta(t)\,dt}{\beta(t)}\,\psi \qquad (6.12)$$

or using (4.1)

$$d_H(t) \;\rightarrow\; \frac{ct}{1-\epsilon}\,\psi \qquad (6.13)$$

or

$$\begin{aligned} d_H(t) &= \tfrac{1}{2}\,ct\,\psi = \beta^{-1}\,d_H(\bar{t}) \qquad (\epsilon = -1) \\ d_H(t) &= \tfrac{2}{3}\,ct\,\psi = \beta^{-1}\,d_H(\bar{t}) \qquad (\epsilon = -1/2) \end{aligned} \qquad (6.14)$$

An analogous relation holds true for the case $0 > \epsilon > 1$. The general conclusions (6.9) are therefore still valid.

VII. THE m-z RELATION

We now proceed to derive the magnitude vs. red-shift relation making use of results obtained in paper II. Radiation propagating freely through space can be represented by the energy-momentum tensor

$$T^{\mu\nu} = E k^{\mu} k^{\nu}$$

where k^{μ} is the tangent vector of the photon path. It has been shown (see Eqs. (3.23) and (3.25) of II) that along the beam of radiation,

$$E A \beta^{-\pi} g = \text{constant}$$

where A is the cross section of the beam. For radiation emerging radially from the source, A takes on the value of the area of concentric spherical surfaces. For a R-W metric

$$A = 4\pi r^2 R^2$$

and hence

$$4\pi E r^2 R^2 \beta^{-\pi} g = \text{constant} \tag{7.1}$$

Next, we note that the apparent luminosity, being equal to the observed flux is given by

$$\ell = c \rho_{\gamma} = c T^{\mu\nu} u_{\mu} u_{\nu} = c E (u_{\mu} k^{\mu})^2$$

$$= c E \frac{\nu^2}{\beta^2}$$

where in the last equality, Eq. (6.5) of II has been used. Thus we can write (7.1) as

$$\frac{4\pi}{c} \ell \nu^{-2} \beta^{2 - \pi} g r^2 R^2 = \text{constant} \tag{7.2}$$

But, as we approach the source,

$$\lim_{r \to 0} \quad 4\pi r^2 R^2 \ell = L(t) \tag{7.3}$$

where $L(t)$ is the intrinsic luminosity at the time of emission, t. The above two Equations yield

$$\ell_{obs.} = \frac{L(t)}{4\pi} \frac{1}{r_{obs}^2 R_{obs}^2} \left(\frac{\beta_{em}}{\beta_{obs}}\right)^{2-\pi_g} \left(\frac{\nu_{obs}}{\nu_{em}}\right)^2$$

$$= \frac{L(t)}{4\pi r_{obs}^2 R_{obs}^2} \frac{1}{(1+z)^2} \left(\frac{\beta_{em}}{\beta_{obs}}\right)^{2-\pi_g} \tag{7.4a}$$

where r_{obs} is the radial coordinate distance from the emitter to the observer. If β is normalized such that $\beta = 1$ at the point of observation, we finally have

$$\ell = \frac{L(t)}{4\pi r_e^2 R_o^2} \frac{1}{(1+z)^2} \beta^2 G(\beta) \tag{7.4b}$$

where we have dropped the subscript obs from ℓ and called $r_{obs} = r_e$, and $R_{obs} = R_o \equiv R(t_o)$. It is easy to reduce (7.4b) to the case of ordinary cosmology: in fact it is sufficient to put $\beta = 1$ and $G(\beta) = 1$. It is in fact understood that $G(\beta)$ is normalized to today's value. We want to note at this point that the gauge condition $G\beta^2 = 1$, which makes ρ_γ (Eq. 3.7) independent of β, also makes ℓ independent of the scale factor β, at least explicitly. An alternative derivation of (7.4b) will be presented in Appendix C.

The comoving radial coordinate r_e of the light source is obtained by solving the equation

$$\int_0^{r_e} \frac{dr}{(1 - kr^2)^{\frac{1}{2}}} = \int_{t_e}^{t_o} \frac{cdt}{R(t)}$$

Since the integrand of the r.h.s. can be transformed to Einstein units by the change of variables $\beta dt = d\bar{t}$, $\beta R(t) = \bar{R}(\bar{t})$, and since $\bar{R}(\bar{t})$ satisfies the ordinary Einstein equation, we obtain, upon integrating, the following result

$$\frac{\bar{H}_o}{c} \bar{R}_o (1 + z) r_e = F(z, \bar{q}_o) \tag{7.5}$$

with

$$F(z, \bar{q}_o) = \frac{1}{\bar{q}_o^2} \left\{ \bar{q}_o z + (\bar{q}_o - 1) \left[\sqrt{1 + 2\bar{q}_o z} - 1 \right] \right\} \tag{7.6}$$

or alternatively

$$= z \left[1 + z \frac{1 - \bar{q}_o}{1 + \bar{q}_o z + \sqrt{1 + 2\bar{q}_o z}} \right] \tag{7.6a}$$

where (7.6a) is an algebraic manipulation of (7.6) (Terrell, 1977) which facilitates a great deal the computation in the limit of $\bar{q}_o \to 0$.

We recall that the quantity z was introduced as a symbol for $\bar{R}_o/\bar{R} - 1$ and is not a measurable quantity. The advantage of going to Einstein units when evaluating the previous integral is that it yields a familiar expression for r_e, which however must be re-expressed in terms of the physical parameters H_o, q_o, and z. Use of (7.5) and (3.3) thus yields for (7.4)

$$\ell = \frac{L(t)}{4\pi (c/\bar{H}_o)^2} \cdot \frac{G(\beta)}{F^2(z, \bar{q}_o)} \tag{7.7}$$

We note that no approximation has been made in the derivation of this expression. Before we change ℓ to m, we make explicit the dependence of the absolute luminosity L(t) on β. Let us write in general

$$L(t) = L_o \beta^e(t) \tag{7.8}$$

where the index "e" stands for evolution and will be discussed in the Appendices. At the same time, G(6) will be written as [See I, discussion preceding Eq. (2.44)].

$$G(6) = G_o \beta^{-\pi(6)} \equiv G_o \beta^{-g} \tag{7.9}$$

If one demands that $G \sim 1/t$, Eq. (4.1) and (7.9) imply that

$$g e = -1 \ . \tag{7.10}$$

As discussed in the previous papers, $\pi(G)$ is the power of G under scale transformations. With (7.8) and (7.9), we finally have from (7.7) ($\mathcal{L} = 10^{-2m/5} \times 2.52\ 10^{-5}$ ergs. cm^{-2} sec^{-1} ; $L = 10^{-2M/5} \times 3.62 \times 10^{35}$ ergs sec^{-1})

$$m = 5 \lg F(z, \bar{q}_o) - \frac{5}{2} (e-g) \lg \theta(t) + 5 \lg \left(\frac{H_o}{\bar{H}_o} \right) + m_o \qquad (7.11)$$

$$m_o = M - 97.45 + 5 \lg (c/H_o) = M + 42.38 - 5 \lg(H_o/100) \qquad (7.12)$$

where M is the absolute magnitude, and H_o is measured in units of 100 km sec^{-1} Mpc^{-1}.

In column 10 of Tables 1-4 we present the function $F(z, \bar{q}_o)$. In Tables 5-8 we present the values of m with $m_o = 0$ for four values of e. From Eq. (7.11) it is clear that the m vs. z relation will yield $\bar{q}_o$, not q_o. Results are presented in Figs. 5-8.

a) The analytic case: k = 0

Since in the k = 0 case we have an explicit expression for R(t), Eq. (5.3), we shall derive the m vs. z relation directly and show that it is indeed a particular case of the general expression (7.7). To this end, we compute r_e directly using Eq. (5.2). We obtain after a short computation

$$r_e = \frac{r}{1-r} \frac{c}{H_o R_o} \left\{ 1 - (1+z)^{\frac{r-1}{r}} \right\} \qquad (7.13)$$

Introducing (7.13) and the second of (5.6) into (7.4), we obtain

$$\ell = \frac{L(t)}{4\pi(c/H_o)^2}\ G(\beta)\ \left(\frac{\epsilon - 1}{\epsilon + 2}\right)^2\ \frac{(1+z)^{4(\epsilon-1)/(\epsilon+2)}}{\left[1 - (1+z)^{(\epsilon-1)/(\epsilon+2)}\right]^2} \tag{7.14}$$

On the other hand, from (7.6) and the first of (5.6), we have

$$F(z, \bar{q}_o = 1/2) = 2\left[1 + z - \sqrt{1+z}\right] = 2(1+z)^{2(1-\epsilon)/(2+\epsilon)}\left[1 - (1+z)^{(\epsilon-1)/(\epsilon+2)}\right] \tag{7.15}$$

Use of (7.15) and the second of (5.4), shows that (7.7) is indeed identical to (7.14). In particular, from (7.11) and (7.15), we derive making use of (5.4) and (5.6)

$\epsilon = -1$:

$$m = 5\lg z + 5\lg 2(2+z)(1+z)^2 + \frac{15}{2}(\epsilon - 2)\lg(1+z) + 5\lg 1/4 + m_o \tag{7.16}$$

$\epsilon = -1/2$:

$$m = 5\lg z + \frac{5\epsilon}{2}\lg(1+z) + 5\left(1 - \frac{1}{2}\epsilon\right)\lg(1+z) + m_o \tag{7.17}$$

$\epsilon = +3/2$

$$m = 5\lg\left[(1+z)^{1/5} - 1\right] + \lg(1+z) - \frac{3}{2}(\epsilon - 2)\lg(1+z) + 5\lg 3 + m_o \tag{7.18}$$

Eqs. (7.16-7.18) for the case $\alpha = -1$, [Eqs. (7.9)-(7.10)], and $m_o = 0$ are tabulated in Tables 5-8.

VIII. THE EFFECTIVE DECELERATION PARAMETER

Since the physically most important feature of the present theory consists of having disentangled atomic from gravitational times, it is to be expected that the higher the time derivative one considers, the more pronounced the effect will be.

We shall illustrate this phenomenon by studying the m vs. z relation in the limit of small z's, in which case the exact relation (7.7) can be rewritten in a form that depends on measurable quantities only.

At the same time, an effective curvature q_o^* will be defined which clearly displays the desired effect.

For small z's, the function $F(z, \bar{q}_o)$, (7.6) can be written as

$$F(z, \bar{q}_o) \cong z\left[1 + \tfrac{1}{2}(1 - \bar{q}_o)z\right] \tag{8.1}$$

Using (7.8), (7.9), (8.1), (5.13) and (5.14), eq. (7.7) can be transformed to the familiar form

$$\ell = \frac{1}{4\pi}\left(\frac{H_o}{c}\right)^2 \frac{L(t_o)}{F^2(z, q^*)} \tag{8.2}$$

where the effective curvature q^* is defined as

$$q^* = \bar{q}_o\left(1 + \frac{h_o}{H_o}\right)^2 - \frac{h_o}{H_o} - (1 + \bar{q}_o)\left(\frac{h_o}{H_o}\right)^2 - (e \cdot g)\ \frac{h_o}{H_o} \tag{8.3}$$

a) The Standard Case

Eq. (8.3) can be reduced to the standard case. To that end we put $\epsilon \to 0$, ($t_E \equiv \bar{t}$) $g \to 0$, $H_o \to \bar{H}_o$, $h_o \to 0$, $Q_o \to 0$, but $e\epsilon = \eta$. In fact,

$$L(t) \sim \beta^e \sim t^{-e\epsilon} \sim t_E^{-\eta} \tag{8.4}$$

We obtain

$$q^*_{s.c.} = \bar{q}_o + \frac{1}{\bar{H}_o \bar{t}_o}\eta = \bar{q}_o - \frac{1}{\bar{H}_o}\left(\frac{\dot{L}}{L}\right)_o \tag{8.5}$$

a well-known expression in standard cosmology.

b) Present Cosmology

We shall rewrite (8.3) so as to exhibit a form that will help us compare it with the standard case. We shall write

$$q^* = \bar{q}_o\left(\frac{\bar{H}_o}{H_o}\right)^2 + (g-1)\frac{h_o}{H_o} - (1+Q_o)\left(\frac{h_o}{H_o}\right)^2 + \frac{1}{H_o t_o}\eta \tag{8.6}$$

Contrary to (8.5), where $\bar{q}_o$ is multiplied by unity, here we have a magnifying effect due to $\bar{H}_o/H_o$ which makes the q^* vs. $\bar{q}_o$ even more nonlinear than usual. To this, we must add the two extra terms depending entirely on the first and second derivatives of β. For future use, we shall present (8.6) for $k = o$, $\bar{q}_o = 1/2$. Using (8.4) we obtain

$$\epsilon = -1 \qquad q^* = -1 + 3\eta \tag{8.7a}$$

$$\epsilon = -1/2 \qquad q^* = 1 + 2\eta \tag{8.7b}$$

$$\epsilon = +1/2 \qquad q^* = \frac{1}{5}(13 + 3\epsilon) \tag{8.7c}$$

$$\epsilon = 1 \qquad q^* = 3 + \eta \tag{8.7d}$$

c) The Value of η

Using (A.22), (A.13) and (B.7), we obtain

$$c\epsilon \equiv \eta = \epsilon(g-1)x + \frac{\alpha - x}{\alpha - 1}(1 + \epsilon g\delta) - \epsilon g\delta + \epsilon\gamma\frac{1-x}{1-\alpha} + \frac{R}{R+1}\left[\epsilon(g-1) + 1 + \epsilon g\delta + \right.$$

(evol.)

$$\left. + \frac{\nu\epsilon}{\alpha - 1} + (1 + \epsilon g\delta)\cdot\frac{\alpha}{1-\alpha}\right] + \epsilon(g-1) - \frac{1}{2}\cdot\frac{1}{1 - t_c/t_o} \tag{8.8}$$

(dyn. fr.)

When $\epsilon \to 0$, $g \to 0$ we obtain

$$\eta = \frac{\alpha - x}{\alpha - 1} + \frac{R}{R+1}\cdot\frac{1}{1-\alpha} - \frac{1}{2}\cdot\frac{1}{1 - \bar{t}_c/\bar{t}_o} \tag{8.9}$$

(evol.) (dyn. fr.)

a well-known expression recently discussed by Gunn and Tinsley (1976).

d) The Complete Solution

Even though we have derived an expression for $\eta = e\epsilon$, it would not be convenient to use it at this stage since we want to stress general properties of our cosmology. We shall therefore solve eq. (8.6) for different values of η. The resulting q^* vs. $\bar{q}_o$ curves are shown in Figures 9-12 together with the ones corresponding to (8.5). Examination of (8.3) shows that in the present cosmology in addition to the intrinsic luminosity variation, there is also the evolution due to the relative variation of gravitational and atomic force strengths (whose effects can also be seen from eq. (7.4b)). This is expected: by studying the gravitational evolution of the Universe through atomic instruments, we have no a priori reason to assume we can see clearly the gravitational dynamics, in this case characterized by the parameter $\bar{q}_o$. Instead, we should allow for distortions as if looking through a lens, which may be magnifying or reducing depending on the evolution of the scaling function. This is most easily seen from the first term on the right hand side of (8.3). If β is an increasing function of time, h_o is positive and the multiplicative factor $\left(1 + \frac{h_o}{H_o}\right)^2$ is greater than unity. In this case, atomic instruments amplify small differences in the geometrical structure, given by $\Delta\bar{q}_o$. The reverse is true if β is a decreasing function of time. Of course, when β is prescribed as a function of the cosmic times, h_o becomes a function of the age of the Universe, which in turn is an implicit function of $\bar{q}_o$. The "lens effect" thus becomes more complex. This "lens effect" can be seen from Figure 9-12 by comparing the slopes of the full curves with those of standard cosmology (dashed lines). For a given observational uncertainty in q^*, a steep slope reduces the uncertainty in $\bar{q}_o$.

For positive ϵ, the solid curves generally have slopes smaller than those of standard cosmology. Such positive or negative "magnification" of the gravitational dynamical effects through the atomic lens can also be seen in Figures 5-8 and 13-20, where curves corresponding to $\bar{q}_{\circ} = .1$ and $.5$ are presented.

In each case, the separation between the two curves is enhanced if $\epsilon < 0$ and reduced if $\epsilon > 0$.

It is also of interest to see from Figures 9-12 how an uncertainty in η affects the determination of $\bar{q}_0$, given an observed q^*.

Here again, for a family of more or less horizontal curves, a small shift in η causes a large shift in $\bar{q}_0$. This has been the situation in standard cosmology and it presents an obstacle preventing the determination of the true curvature of space. For positive ϵ, the situation has not improved. For negative ϵ on the other hand, there are regions where a change in η produces relatively unimportant changes in $\bar{q}_0$.

IX. METRIC ANGULAR DIAMETERS

Consider two events at the points $A(r_e, \theta_e, \varphi_e)$ and $B(r_e, \theta_e + \Delta\theta_e, \varphi_e)$ occurring at the same time t_e and let the observer be located at $(0, 0, 0)$ at the time t_o. The two emission events are separated by a local distance y.

The metric angular diameter θ_m is defined as

$$\theta_m = \frac{y}{r_e \, R(t_e)} \tag{9.1}$$

Using (7.5), (5.1) and (3.3), (9.1) becomes

$$\theta_m = \theta_o \left(\frac{H_o t_o - \epsilon}{H_o t_o} \right) \frac{\beta(t) (1+z)^2}{F(z, \bar{q}_o)} \tag{9.2}$$

where

$$\theta_o = 8.6'' \left(\frac{y}{250 \text{ kpc}} \right) \left(\frac{H_o}{50} \right) \text{ Arcsec} \tag{9.3}$$

Using the values of z, β and $F(z, \bar{q}_o)$ vs. z given in Tables 1-4, θ_m can be computed from (9.2). The numerical values quoted in Tables 5-8 correspond to $y = 250$ kpc and $H_o = 50$ km sec^{-1} Mpc^{-1}. We have not included a possible z dependence of the radius y. A scaling of the form $y(z) = y(0)\,(1 + z)^n$ can be easily superimposed on the values quoted in the Tables once a particular model has been chosen. The results are presented in Figures 13-16.

a) The analytic case: $k = 0$

Using (5.4), (5.6) and (7.15), θ_m can be expressed as

$$\theta_m = \theta_o \left(\frac{1 - \epsilon}{2 + \epsilon} \right) \frac{1 + z}{1 - (1 + z)^{(\epsilon - 1)/(\epsilon + 2)}} \tag{9.4}$$

For $\epsilon = 0$, (9.4) reduces to the well-known result in ordinary cosmology corresponding to the Einstein-de Sitter Universe. Equation (9.4) can be compared with the values quoted in Tables 5-8.

X. ISOPHOTAL ANGLES

In order to derive the isophotal angular diameters θ_i, we shall first define the surface brightness B as

$$B = \mathcal{L}/\theta_m^2 \ , \tag{10.1}$$

where $\mathcal{L}$ is given by (7.4). Using (9.1), we now have

$$B \sim (1 + z)^{-4} \ L(t) \ \beta^2 \ G(\epsilon) \ y^{-2} \tag{10.2}$$

The determination of θ_i is usually made adopting a formula (due to Hubble) giving the variation of B vs. θ, namely

$$\theta_i/\theta_m \sim B^{1/p} \qquad (p \simeq 2) \tag{10.3}$$

We then have

$$\frac{\theta_i}{\theta_m} \sim (1+z)^{-4/p} \left\{ \frac{L(t)\, \beta^2\, G(\beta)}{y^2} \right\}^{1/p} \tag{10.4}$$

and using (9.1) (with $p = 2$)

$$\theta_i \sim \left\{ \frac{L(t)\, \beta^2\, G(\beta)}{r_e^2\, (1+z)^2} \right\}^{1/2} \tag{10.5}$$

Comparing (10.5) with (7.4), we obtain the final result

$$\lg \theta_i = -\frac{1}{5} m + \text{const.} \tag{10.6}$$

The values of $\lg \theta_i$ are presented in Figures 17-20.

XI. DISTANCES

From (7.4) and (9.1) we can derive d_L, the luminosity distance as well as d_A, the angular diameter distance as

$$d_L = \frac{r_e}{R(t_e)\, \beta^{\frac{2+c}{2}}\, G^{1/2}}, \quad d_A = r_e\, R(t_e) \tag{11.1}$$

so that

$$\frac{d_A}{d_L} = \frac{1}{(1+z)^2} \beta^{\frac{2+e}{2}} G^{1/2}(\beta) \tag{11.2}$$

Using Eq. (5.6) for β in the $k = 0$ case, we obtain

$e = -1$ $(g = 1)$

$$\frac{d_A}{d_L} = \frac{1}{(1+z)^2} (1+z)^{-\frac{3}{2}(1+e)} \tag{11.3}$$

$e = -1/2$ $(g = 2)$

$$\frac{d_A}{d_L} = \frac{1}{(1+z)^2} (1+z)^{-e/2} \tag{11.4}$$

$e = +1/2$ $(g = -2)$

$$\frac{d_A}{d_L} = \frac{1}{(1+z)^2} \cdot (1+z)^{\frac{3}{5}(2+e/2)} \tag{11.5}$$

$c = .92$ $(g = -1.087)$

$$\frac{d_A}{d_L} = \frac{1}{(1+z)^2} \cdot (1+z)^{1.459 + .4726\,c} \tag{11.6}$$

Another way of expressing the experimental results is to say that the luminosity distance increases slowly with z (and even decreases after a maximum) and the angular distance increases quickly with z. This means that a cosmology in which d_A/d_L is a strong function of z is a good candidate for the tests. We have, using Eqs. (11.2), (7.9), (5.1), and (5.3)

$$\frac{d_A}{d_L} = (1+z)^{-2 + \frac{(2+c)\,\varepsilon + 1}{2\,t_o\,H_o}} \tag{11.7}$$

which is only an approximation for $z \sim 0$. For $\bar{q}_o = 0$ or $1/2$ Eq. (11.7) is exact. We want the exponent to be as large as possible and positive.

XII. THE N(m) vs. m RELATION

A test that is becoming increasingly important is the number count, i.e. the number of sources (per square degree) brighter than apparent magnitude m. The most widely used form of this test is in reference to optical quasars.

A formula of the type

$$\lg N(m) = a + bm \tag{12.1}$$

if often employed for its simplicity: the discussion then concentrates on the value of the parameter b predicted by the theory vs. the one obtained by fitting (12.1) to the data.

For a Euclidean space b = .6; all Friedman universes with $\Lambda = 0$ predict a value of b less than .6. However, evidence has been repeatedly adduced for values in excess of .6: Braccesi and Formiggini (1969) have concluded that b = .72; Sandage and Luyten (1969) suggested b = .75, although Setti and Woltjer (1973) have concluded that all the data until 1973 were actually consistent with b = .6. In the most recent work on the subject, Green and Schmidt (1978) have presented what they believe to be a clear indication of a value of b much larger than any of the ones proposed so far: in fact their analysis indicates b = .93, a value impossible to reconcile with any purely geometrical cosmology. Strong evolutionary trends in the number of quasars are then invoked as the logical implication of such results.

In this section we shall derive the N(m) vs. m relation pertaining to the present cosmology and we shall then discuss the corresponding values of b.

To that end, let us first derive N(z), the number of sources as a function of red-shift. If we start with a R-W metric (in atomic units)

$$ds^2 = dt^2 - R^2(t) \left\{ \frac{dr^2}{1 - kr^2} + r^2 \, d\Omega^2 \right\} \tag{12.2}$$

by virtue of the transformation

$$du = \frac{dr}{\sqrt{1 - kr^2}} \quad , \quad u = (-k)^{-1/2} \ \text{Arsinh} \ [(-k)^{1/2} \ r] \tag{12.3}$$

we obtain

$$ds^2 = dt^2 - R^2(t) \ \{ du^2 + \Sigma^2(u) \, d\Omega^2 \} \tag{12.4}$$

where

$$r = \Sigma(u) = (-k)^{-1/2} \ \sinh \ [(-k)^{1/2} \ u] \tag{12.5}$$

The volume element computed from (12.1) is

$$dv = \sqrt{g} \ dr \, d\theta \, d\phi = R^3(t) \ (1 - kr^2)^{-1/2} \ r^2 \, dr \, \sin\theta \, d\theta \, d\phi \tag{12.6}$$

and consequently the total number of sources is given by

$$N = 4\pi\, n_o\, R_o^3 \int_o^u du\, \Sigma^2(u) \quad , \quad (n(t)\, R^3(t) = \text{const.}) \tag{12.7}$$

The number of sources per square degree is then

$$N = N/Q \tag{12.8}$$

where Q is the total number of square degrees in the sky. Integration of (12.7) yields

$$N = \frac{N_o}{4}\, (-k)^{-3/2}\, \{\sinh 2y - 2y\} \tag{12.9}$$

where

$$N_o = \frac{4\pi\, n_o\, R_o^3}{Q} \quad ; \quad y = (-k)^{1/2}\, u \tag{12.10}$$

Using (12.3), (7.5) and (2.5) to express r in terms of $\bar{q}_o$ and z, we finally obtain

$$y = \text{Arsinh}\left[(1 - 2\bar{q}_o)^{1/2}\, \frac{F(z, \bar{q}_o)}{1+z}\right] \tag{12.11}$$

Eqs. (12.9) and (12.11) solve the problem of finding N vs. z, since the relation between z and z has already been given in Tables 1-4. Eqs. (12.3) and (12.11) are formally identical to the ones in standard cosmology: however, in the present context

z is not to be identified with the observed red-shift, which is the atomic one, z. The $N(z)$ vs. z relation is therefore different in the present context than in standard cosmology.

Explicitly, we have

$$k = 0 \qquad N = \frac{1}{3} N_o u^3 = \frac{1}{3} \frac{N_o c^3}{\bar{H}_o^3 R_o^3} \left[\frac{F(z, 1/2)}{1+z} \right]^3 \tag{12.12}$$

$$k = -1 \qquad N = \frac{1}{4} N_o (\sinh 2y - 2y) \quad ; \quad y = \operatorname{Arsinh} \left[\sqrt{1-2\bar{q}_o} \; \frac{F(z, \bar{q}_o)}{1+z} \right] \tag{12.13}$$

$$k = +1 \qquad N = \frac{1}{4} N_o (2y - \sin 2y) \quad ; \quad y = \operatorname{Arsin} \left[\sqrt{2\bar{q}_o - 1} \; \frac{F(z, \bar{q}_o)}{1+z} \right] \tag{12.14}$$

Let us now use (7.11) to eliminate z in favor of m. We have

$$10^{.2 (m - m_o)} = F(z, \bar{q}_o) \, \beta^{\frac{g-e}{2}} \left(\frac{H_o}{\bar{H}_o} \right) \tag{12.15}$$

a) Small look-back times

In this case, Eqs. (11.9) and (12.11) reduce to

$$N = \frac{4\pi}{3} \frac{n_o c^3}{H_o^3} \left(\frac{H_o}{\overline{H}_o}\right)^3 \left\{\frac{F(\overline{q}_o, z)}{1+z}\right\}^3 \tag{12.16}$$

where, using (8.1)

$$\frac{F(\overline{q}_o, z)}{1+z} = z\left[1 - \frac{1}{2}(1+\overline{q}_o)z\right] \tag{12.17}$$

Finally using (5.15), we obtain

$$N = \frac{4\pi}{3} \frac{n_o c^3}{H_o^3} z^3 [1 - 3\Lambda z] \tag{12.18}$$

where

$$\Lambda \equiv \frac{1}{2}(1+\overline{q}_o) \frac{\overline{H}_o}{H_o} - \frac{\epsilon}{2 H_o t_o}\left(q_o + \frac{\epsilon - 1}{t_o H_o}\right) \frac{H_o}{\overline{H}_o} \tag{12.19}$$

Let us now use ℓ as derived in (8.2), i.e. ($L_o \equiv L(t_o)$)

$$\left(\frac{H_o}{c}\right)\left(\frac{L_o}{4\pi\ell}\right)^{1/2} \equiv \chi = z[1 + \tfrac{1}{2}(1 - q^*)z] \tag{12.20}$$

where we have again made use of (8.1) to express $F(z, q^*)$ for small z. Eliminating z between (12.20) and (12.18) we obtain

$$N = \frac{4\pi}{3} n_o \left(\frac{L_o}{4\pi \ell}\right)^{3/2} \left\{1 - \frac{3}{2} x \left[1 - q^* + (1 + \bar{q}_o) \frac{\overline{H}_o}{H_o} - 2B \frac{H_o}{\overline{H}_o}\right]\right\} \quad (12.21)$$

where

$$B \equiv \frac{\epsilon}{2 H_o t_o} \left(q_o + \frac{\epsilon - 1}{t_o H_o}\right)$$

Contrary to the well-known case in standard cosmology, the correction to the Euclidean case does depend on the curvature $\bar{q}_o$. In the case of standard cosmology, $\epsilon \to 0$, $g \to 0$, $H_o \to \overline{H}_o$, we recover from (12.21), using (8.5)

$$N = \frac{4\pi}{3} n_o \left(\frac{L_o}{4\pi \ell}\right)^{3/2} \left\{1 - \frac{3\overline{H}_o}{c} \left(\frac{L_o}{4\pi \ell}\right)^{1/2} \left[1 + \frac{1}{2\overline{H}_o} \left(\frac{L'}{L}\right)_o\right]\right\} \quad (12.22)$$

a well-known expression in standard cosmology. Equation (12.21) can be further simplified. In fact, using expressions (2.5) and (8.3), one can show that the square parenthesis in (12.21) in equal to

$$2 - \frac{e(2 + e - g)}{H_o t_o}$$

so that finally we have

$$N = \frac{4\pi}{3} n_o \left(\frac{L_o}{4\pi \ell} \right)^{3/2} \left\{ 1 - 3x \left[1 - \frac{e(2 + e - g)}{2 H_o t_o} \right] \right\} \qquad (12.23)$$

This expression clearly indicates that a slope greater than the Euclidean one can be obtained as long as the value in the square bracket is negative.

XIII. THE SLOPE OF THE lgN(m) vs. m CURVE FOR QSO AND THEIR m vs. z RELATION.

Since evolutionary effects are very important, one cannot derive any reliable m vs. z relation for QSO without them.

However, due to the still uncertain nature of the physics of QSO, the evaluation of evolutionary effects is very uncertain since it is too model dependent.

For the case of elliptical galaxies we computed e, see eq. (7.8), using the best model presently available and the results shown in Figs. 5-8 are satisfactory. However, there is no compelling reason why such values of e should also apply to QSO in general and the dotted curves in the Figures should not be extrapolated much further than the region where they belong.

This leaves us with the problem of estimating e for QSO. We proceed as follows. We demand that e satisfies the lgN(m) vs. m relation with a given slope b determined by observations. For purpose of illustration we shall take b = .75, an average value among the ones quoted before.

Once e is so determined, we shall use it to construct the m vs. z relation for QSO.

To understand the results better, we shall apply such a procedure first to the case of standard cosmology and then to our case.

We shall show that within our cosmology the resultant m vs. z relation gives a better fit than the one of standard cosmology.

Instead of presenting a full numerical solution to this problem, we shall employ the k = 0 case since we can work out the problem entirely analytically.

Using (5.6), eq. (12.15) becomes

$$10^{.2(m - m_o)} = F(z, 1/2)\,(1+z)^p \left(\frac{H_o}{\bar{H}_o}\right) \tag{13.1}$$

where

$$p \equiv \frac{3}{4}\,\frac{\epsilon(q - e)}{1 - \epsilon} \tag{13.2}$$

so that finally from (12.12) we obtain

$$N(m) = \frac{1}{3}\,N_o \left(\frac{c}{H_o R_o}\right)^3 10^{.6(m - m_o)}\,(1+z)^{-3-3p} \tag{13.3}$$

or

$$\lg N(m) = .6m - 3(p+1)\lg(1+z) + \text{const.} \tag{13.4}$$

The slope of the lg N(m) vs. m curve can then be derived to be

$$\text{slope} = \frac{d\,\ell n\,N}{dm} = \frac{.6}{1 - 2(p+1) + 2(p+1)\,(1+z)^{1/2}} \tag{13.5}$$

a) Standard cosmology

In order to recover the expression pertaining to standard cosmology, we must a) identify z with the observed red-shift b) put $q \to 0$, $\epsilon \to 0$, i.e. $\bar{H}_o \to H_o$ but keep the product ϵe finite, say η, so that (see 8.4)

$$L(t) \sim \beta^{e} \sim t^{-ce} \sim t_E^{-\eta} \sim (1+z)^{\frac{3}{2}\eta} \tag{13.6}$$

The value of p becomes

$$p = -\frac{3}{4}\eta \tag{13.7}$$

(13.5) remains unaltered with p given by (13.7); (13.1) becomes now

$$m = m_o + 5\lg F(z, 1/2) - \frac{15}{4}\eta \lg(1+z) \tag{13.8}$$

with

$$F(z, 1/2) = 2\left[1 + z - \sqrt{1+z}\right]$$

Let us now look for a value of η such that the slope (13.5) is .75, a value intermediate among the ones quoted above. We obtain Table 9, which upon insertion in (13.8) yields Table 10.

Since for small z's, eq. (13.8) becomes identical to eq. (4) of Sandage (1972c), where m_o has been fitted to be 20.625, the magnitude m without η would be in the range 23-24.5, too high a value to fit even the envelope of the QSO's, as clear from Figs. 5-8. The addition of the evolutionary term η, determined for the slope of the lgN(m) vs. m relation, helps a great deal since it reduces column 2 of Table 10 by about 3 magnitudes. However, the final result (last column of Table 10) is still too high to fit the data.

In general, eliminating η between (13.5) and (13.8) we obtain

$$m = m_o + 5\lg F(z, 1/2) + 5\left\{\frac{\alpha - .6}{2\alpha - 2\alpha(1+z)^{1/2}} - 1\right\}\lg(1+z) \qquad (13.9)$$

where α is the slope (13.5).

b) Present cosmology

When the same procedure is followed within the present cosmology, one gets better results. The relation (13.5) becomes, using (5.6) to eliminate z' in favor of z,

$$\text{slope} = \frac{.6}{1-2(p+1)+2(p+1)(1+z)^{\frac{1-\epsilon}{2+\epsilon}}} \tag{13.10}$$

or

$\epsilon = -1$

$$\text{slope} = \frac{.6}{1+2(p+1)(z^2+2z)} \quad ; \quad 8p = 3(\epsilon-1) \tag{13.11}$$

$\epsilon = -1/2$

$$\text{slope} = \frac{.6}{1+2(p+1)z} \quad ; \quad 4p = \epsilon-2 \tag{13.12}$$

Analogously, for $\epsilon = -1$ and $\epsilon = -1/2$, (13.1) is given by eqs. (7.16) and (7.17).

Let us now require again that the slope be .75. We obtain for ϵ

Table 11. Using these values in (7.16) and (7.17), we obtain Table 12.

A considerable improvement exists over the corresponding values of $m - m_o$ of column 3, Table 10. In fact, we subtract more from m_o. As an example, let us take $z = 2$, $\lg z = 5.8$. We obtain

Standard cosmology	Present cosmology
$m = m_o - .68$	$m = m_o - 1.89$ $(\epsilon = -1)$
	$m = m_o - 1.35$ $(\epsilon = -1/2)$

Since $m_o \simeq 21$, when these values are reported in Figures 5-8, we get a better fit to the data with the present cosmology. The cases corresponding to $\epsilon > 0$ are indistinguishable from those of the case standard. In conclusion, we can say that the method of determining the evolutionary parameter ϵ from the slope of the lgN vs. m relation for QSO and then using it in the m vs. z relation, yields a better fit in the present than standard cosmology.

The previous derivation could lead one to conclude that we have excluded density evolution in favor of luminosity evolution only. This however is not the case. To prove our point, let us suppose that we add a factor ρ^s to (12.12) to simulate a density evolution. The derivation of (13.5) then follows: The relation (13.2) between the parameter p in (3.5) and e is now changed to

$$p = -\frac{1}{2}\,\frac{\varepsilon}{1-\varepsilon}\left[\frac{3}{2}e - \frac{3}{2}q + s\right] \qquad (13.13)$$

The parameter s affects p in the same way as 3/2e does, and, just as in standard cosmology, one can interpret the results in terms of luminosity or density evolution or as a combination of the two.

XIV. RESULTS

(a) The m vs. z relation

$\epsilon < 0$.

The cases $\epsilon = -1$ and $\epsilon = -\frac{1}{2}$ are presented in Figs. 5 and 6, dashed lines. The solid line corresponds to standard cosmology with $\bar{q}_o = 1$ and no evolutionary effects. The observational points of Figs. 5-8 are taken from Fig. 3 of Sandage 1972a. The value of the parameter m_o of Eq. (7.11) is fitted to be $m_o = 21.03$. Several comments are in order concerning Figs. 5 and 6.

First of all, the $k = 0$, $\bar{q}_o = .5$ case, corresponding to the original Dirac model, Eq. (5.7), has been repeatedly criticized for yielding $q_o = 2$, a value considered too high to fit the m vs. z relation.

This conclusion was based on an incorrect derivation of the m vs. z relation within the context of this new cosmology. We now see that since the m vs. z relation depends on $\bar{q}_o$ and not q_o, a value of $q_o = 2$ is perfectly acceptable since it can still correspond to an open Universe.

Secondly, contrary to the case of standard cosmology, the m vs. z curves are very sensitive to a change in $\bar{q}_o$. In fact, a change from .1 to .5 has a very distinct effect on the slope of the curves. In standard cosmology, the two curves corresponding to $\bar{q}_o = .1$ and $\bar{q}_o = .5$ are practically indistinguishable below $m \sim 20$.

The higher sensitivity in our case makes it possible to get a good fit even with an open Universe, say with k = 0, something not possible in standard cosmology, where a bending towards lower m's, like the one characterizing the $\bar{q}_o = .5$ curve, can be achieved only with a large $\bar{q}_o$ (>6), i.e. with a closed Universe, as seen from Fig. 1 of Sandage (1961a).

$\epsilon > 0$

The cases $\epsilon = +\frac{1}{2}$ and $\epsilon = .92$ are represented in Figs. 7 and 8, dashed lines.

For any given z, both the $\bar{q}_o = .1$ and $\bar{q}_o = .5$ cases correspond to lower m's than they would in standard cosmology with the same $\bar{q}_o$. In fact, the solid line corresponds to $\bar{q}_o = 1$, i.e. a closed Universe.

(b) Angular Diameters, θ_m vs. z.

The cases $\epsilon = -1$ and $\epsilon = -\frac{1}{2}$ are presented in Figs. 13 and 14, dashed lines.

As in the m vs. z case, we also note that within the present theory in the $\epsilon = -1$ case a sizable difference exists between $\bar{q}_o = .1$ and $\bar{q}_o = .5$. In standard cosmology, a much less pronounced difference exists between curves I and II.

When ϵ is positive, the predictions of the present cosmology become less sensitive to the value of $\bar{q}_o$, to the point where no difference exists between $\bar{q}_o = .1$ and $\bar{q}_o = 1$, when $\epsilon \to 1$, Fig. 16. In that sense the contrast between Fig. 13 ($\epsilon = -1$) and Fig. 16 ($\epsilon = .92$) is very instructive. An open Universe with $\bar{q}_o = .1$ does provide a satisfactory fit to the data in the $\epsilon < 0$ cases; the $\bar{q}_o = .5$ case is not as satisfactory. For positive ϵ, no preferable $\bar{q}_o$ exists.

The differences between the present theory and the standard one, as displayed in Figs. 13-16 are mainly due to the disentangling of atomic and gravitational times. In that sense they constitute a purer cosmological probe than others, where astrophysical effects intervene very heavily.

For negative ϵ, we conclude that values of $\bar{q}_o$ greater than $\frac{1}{2}$ (closed Universe) would fit the data very poorly. For positive ϵ, both closed as well as open Universes are acceptable.

(c) Isophotal Angles, θ_i vs. z.

The isophotal angles θ_i vs. z given by Eq. (10.6) are presented in Figs. 17-20, dashed lines.

The observational points as well as the full lines are taken from Fig. 5 of Sandage (1972b). The number labelling each curve is the value of $\bar{q}_o$. The value -1 corresponds to the steady state. Figures 17-20 are very instructive since they clearly show the sensitivity of the curves to the values of $\bar{q}_o$. In standard cosmology, a value of $\bar{q}_o = 2.5$ yields a lesser slope than does $\bar{q}_o = .5$ in the present theory. From this circumstance stems our hope of being able to discern a value of $\bar{q}_o$.

For negative ϵ, an open Universe fits the data certainly better than a closed one, which would predict angles too large for a given red-shift. This same feature characterizes the metric diameters. The deterioration of the fit as $\bar{q}_o$ passes $\frac{1}{2}$ becomes less evident as ϵ becomes positive. It is interesting that for the isophotal as well as for the metric angles the sensitivity of the results to $\bar{q}_o$ that characterizes negative ϵ progressively disappears as ϵ goes through zero ($\beta \to 1$, standard case) and becomes positive.

As the extreme case $e \sim 1$, the curves are totally insensitive to $\bar{q}_o$.

(d) The N(m) vs. m relation for QSO.

As explained in the text, the present impossibility of computing theoretically the evolutionary parameter e for QSO has been circumvented in this paper by requiring that e be such as to give a satisfactory lg N(m) vs. m relation. When such an e is used in the m vs. z relation, we derive a curve that nicely follows the envelope of the QSO data. This again happens only if $e < 0$. For positive e this procedure leads to results that are not better than those of standard cosmology, where a very satisfactory fit cannot be achieved. (See paragraph XIII).

XV. DISCUSSION

Even though it might be clear by now, we want to stress once more that the scale covariant cosmology does not provide just one curve for the m vs. z relation, which would make the acceptability or rejection of the theory a simple matter of comparison with the data. Such is the case for the steady state cosmology. As stated in the introduction, our objective is analogous to that of standard cosmology, namely the determination of the geometrical parameters that characterize the nature of space-time. However, the central idea of our work is the recognition that observations made with atomic instruments do not necessarily yield the geometrical parameters unless specific assumptions are made regarding the relation between atomic and gravitational dynamics, a relation that we have embodied in the function $\beta(t)$. Once a particular form of the scaling function $\beta(t)$ is chosen, the analysis of the data can be carried out exactly as in standard cosmology, employing the newly derived m vs. z relation, eq. (7.11). Given this framework, we can now assess the viability of the scale covariant cosmology.

The canonical test is given by the m vs. z relation using elliptical galaxies. From Figs. 5-6, we can appreciate the relation between the observed data and the theoretical predictions.

In the past, the m vs. z relation was employed to discriminate against possible variations of G. For example, Tinsley and Barnothy (1973) concluded that at least one version of Hoyle-Narlikar (HN) theory yields an m vs. z relation incompatible with the data. (See however Canuto and Narlikar (1979) for an extensive comparison of the HN theory with observations). Even though the HN theory has in common with the present one a varying G, its structure is very different as are its physical assumptions and no easy comparison is therefore possible.

In the present theory, for positive ϵ, all the tests yield results very similar to the ones in stardard cosmology, in the sense of being insensitive to $\bar{q}_o$.

For negative ϵ, however, the fit to the data becomes certainly better since one can discriminate between an open and a closed Universe. Positive and negative ϵ behave therefore in very distinct manners. Given the historical importance of the m vs. z relation vis a' vis the variation of G and the impression created by the work cited (see also Maeder 1977), we can conclude that among the many possible theoretical structures one can devise to account for a G(t), the present one, based on a scale covariance, yields results which are either equal or better than the ones of standard cosmology.

We have completed a description of scale covariant cosmology and have seen how it compares with a host of observations. The fact that none of the scaling functions $\beta(t)$ we have chosen can be ruled out by the available data is remarkable. In fact it was not our main thrust to achieve a fit to the data superior to those attempted so far.

Rather, our first aim was to show that the data are compatible with a non-constant $\beta(t)$, provided every ingredient in the computation is calculated consistently with the theory. This aim has been accomplished.

It therefore follows from the present work that there exists a consistent alternative interpretation of the cosmological data.

To drive home this point, we shall give the following further illustration. For a given observed H_o (see 7.11 and 7.12), we can define a "critical density"

$$\rho_c = \frac{3 H_o^2}{8\pi G} \tag{15.1}$$

From (2.4) we have

$$\frac{\rho_o}{\rho_c} = 2\bar{q}_o \left(1 + \frac{h_o}{H_o}\right)^2 \tag{15.2}$$

Thus, from the observed average density and the value of ρ_c, as computed from H_o, we cannot deduce directly the curvature of space.

If $\epsilon < 0$, $h_o > 0$. For a given (observationally determined) ρ_o/ρ_c, the corresponding value of $\bar{q}_o$ is smaller than for $\epsilon = 0$, i.e. standard cosmology. This favors an open Universe. The opposite is true if $\epsilon > 0$.

This altogether different relation between the amount of matter in the Universe and the curvature of space is perhaps the main feature of this new cosmology.

Since (15.2) depends critically on ϵ, do we have any way to choose between $\epsilon < 0$ and $\epsilon > 0$?

As discussed elsewhere (Canuto, Hsieh and Owen 1978), present data on time variation of the Moon angular velocity ($n = \Omega = 2\pi/P$)

$$\frac{\dot{n}}{n} = \frac{\dot{n}_a - \dot{n}_t}{n} \tag{15.3}$$

($\dot{n}_a$ and $\dot{n}_t$ are the atomic and tidal contributions), seem to indicate a non-null positive result. In fact, the data presently known for the Moon read (the units are arcsec per century^2)

$$\begin{aligned}
\dot{n}_t &= -30.0 \pm 3 && \text{(Muller, 1978)} \\
\dot{n}_a &= -21.7 \pm 3.6 && \text{(Van Flandern, 1978)} \\
\dot{n}_a &= -24.6 \pm 1.6 && \text{(Calame and Mulholland, 1978)} \\
\dot{n}_a &= -23.8 \pm 4 && \text{(Williams et al., 1978)}
\end{aligned} \tag{15.4}$$

Since in the present theory $\frac{\dot{n}}{n}$ is directly given by $\frac{\dot{\beta}}{\beta}$ (see Eq. 4.21 of I with GMβ = const., Eq. I, 2.50), a positive $\frac{\dot{n}}{n}$ implies

$$\dot{\beta} > 0 \tag{15.5}$$

i.e. $c < 0$, because of (4.1).

Should (15.4) be confirmed by future analysis, it would then follow that the bulk of the cosmological tests presented in this paper favor an open Universe.

Finally, a comment is in order concerning the radiation dominated Universe, characterized by the occurrence of nucleosynthesis. With the present knowledge of scale covariant cosmology, we are in no position to make any sensible statement. Throughout our work we have learned that even the most elementary relations can be changed by the presence of $\beta(t)$, see for example II, Eq. (2.15).

The study of nucleosynthesis necessitates ingredients like Fermi-Dirac distributions, invariant phase-space, reaction rates etc. that must be rederived in a manner consistent with the premises of the theory. This problem is now under study.

Appendix A. Evolutionary Corrections

a) Stellar Evolution

We shall first study the contribution to the parameter e, due to stellar evolution. Work by Maeder (1977) has already been published which treats the case when G and M are functions of time. Maeder has analyzed the two gauges 1) $M \sim t^2$, $G \sim t^{-1}$ and $M \sim t^0$, $G \sim t^{-1}$. We shall generalize his treatment so as to have results valid for an arbitrary gauge. To that end, let us call t the epoch at which a given photon leaves a galaxy and t_1 the time at which the galaxy is born. All times are computed from t = 0. The so-called one burst model for formation of elliptical galaxies is here adopted, as in all previous computations of this kind.

The contribution of dwarf stars to the total luminosity is written as

$$L_d = \int_{M_L(t)}^{M_t(t)} \frac{dN(t)}{dM(t)} \, \ell_{M(t)} \, dM(t) \qquad (A.1)$$

where $M_t(t)$ is the turnoff mass at time t; $M_L(t)$ is the lower mass limit at time t; dN/dM is the mass spectrum and $\ell_{M(t)}$ the luminosity of a star of mass M(t). We shall write in general

$$\ell_{M(t)} = M^{\alpha}(t) \; G^{\delta}(t) \; \ell^{\gamma} \qquad (A.2)$$

where the coefficient α, δ, and γ depend on the type of opacity and nuclear reactions employed. The Salpeter mass function at time $t = t_0$, i.e.

$$\frac{dN}{dM} \propto M^{-(1+x)} \tag{A.3}$$

must be generalized at $M = M(t)$. Using the general relation [See I, Eq. 2.50]

$$G(\beta)\ M\beta = \text{const.} \tag{A.4}$$

we obtain

$$M(t) \propto \beta^{-1}(t)\ G^{-1}(\beta) \tag{A.5}$$

so that (A.3) gets generalized to

$$\frac{dN(t)}{dM(t)} \propto M^{-(1+x)}(t)\ [\beta(t)\ G(\beta)]^{-x} \tag{A.6}$$

In general the main sequence lifetime τ scales like

$$\tau \propto M(t)/\ell(t) \sim M^{1-\alpha}(t)\ G^{-\delta}(\beta)\ \beta^{-\gamma} \tag{A.7}$$

Therefore

$$M(t) \propto \tau^{\frac{1}{1-\alpha}} \quad G^{\frac{\delta}{1-\alpha}} \quad (\beta) \quad \beta^{\frac{\gamma}{1-\alpha}} \tag{A.8}$$

For a particular mass $M_f(t)$, one has $\tau = t - t_1$, and so

$$M_f(t) \propto t^{\frac{1}{1-\alpha}} \quad G^{\frac{\delta}{1-\alpha}} \quad \left(1 - \frac{t_1}{t}\right)^{\frac{1}{1-\alpha}} \quad \beta^{\frac{\gamma}{1-\alpha}} \tag{A.9}$$

Maeder, like all the other authors, has neglected the t_1/t factor.

Inserting (A.6) and (A.2) into (A.1) and integrating, one gets

$$L_d \propto \beta^{\gamma-x} G^{\delta-x} (\beta) \left[M^{\alpha-x}(t) \right]_{M_L(t)}^{M_f(t)} \tag{A.10}$$

Since the main contribution comes from the upper limit, we finally have

$$L_d \propto t^{-\frac{\alpha-x}{\alpha-1}} \quad G^{\delta\frac{1-x}{1-\alpha}-x} \quad \beta^{\gamma\frac{1-x}{1-\alpha}-x} \tag{A.11}$$

The equivalent expression for ordinary cosmology, with $G = \text{const.}$ and $\beta = 1$ can be easily retrieved: the result coincides with that derived by Tinsley, (1976).

Using now Eq. (4.1) and (7.9), we can rewrite (A.11) in the form (7.8), i.e.

$$L_d(t) \sim \beta^{e_d}(t) \tag{A.12}$$

We have then

$$e_d = (g-1)\,x + \frac{1}{\epsilon}\,\frac{\alpha - x}{\alpha - 1}\,(1 + \epsilon g \delta) - g\delta + \gamma\,\frac{1-x}{1-\alpha} \tag{A.13}$$

For the commonly used value $x = 1$, e_d becomes independent of α, γ and δ, i.e.,

$$e_d = g - 1 + \frac{1}{\epsilon} \tag{A.14}$$

Since we further assume that $G \simeq \frac{1}{t}$, $\qquad g\epsilon = -1$: e_d then becomes

$$e_d = -1 \tag{A.15}$$

Following other authors, we also include the effect due to red-giants. Here too, we follow and generalize Maeder's results. Let l_g and τ_g be the mean luminosity and mean lifetime in the red giant phase. The contribution to L can be written as

$$L_g = \tau_g\, l_g \left| \frac{dN(t)}{dM(t)} \right| \left| \frac{dM_f(t)}{dt} \right| . \tag{A.16}$$

Using (A.6) and (A.9), we then have

$$L_g \propto \tau_g l_g \; t^{-1 - \frac{x}{1-\alpha}} \; \beta^{-x - \gamma \frac{x}{1-\alpha}} \; G^{-x - \delta \frac{x}{1-\alpha}} \left[1 + \delta \frac{\dot{G}}{G} t + \gamma \frac{\dot{\beta}}{\beta} t \right] \qquad (A.17)$$

or using (7.9)

$$L_g \propto \tau_g l_g \; t^{-1 - \frac{x}{1-\alpha}} \; \beta^{-x - \gamma \frac{x}{1-\alpha}} \; \beta^{gx + \delta g \frac{x}{1-\alpha}} \left[1 + (\gamma - \delta g) \frac{\dot{\beta}}{\beta} t \right] \qquad (A.18)$$

In order to recover Tinsley's expression, one has to posit $G = \text{const.}$ and $\beta = 1$ in either (A.17) or (A.18). From here on, we shall neglect the second term in the parenthesis with respect to unity. Transforming (A.18) into an expression containing only β, we have ($\tau_g l_g \sim \beta^{-1} G^{-1} \sim \beta^{g-1}$, see A.7)

$$L_g \propto \beta^{e_g} \qquad (A.19)$$

where

$$e_g = (g-1)(x+1) + \frac{1}{\epsilon} + \frac{x}{\epsilon(1-\alpha)} (1 + \epsilon g \delta) - \frac{x\gamma}{1-\alpha} \qquad (A.20)$$

For the total luminosity, we finally write

$$\frac{d \ln L}{d \ln \beta} = e \tag{A.21}$$

where

$$e = e_d + \left(\frac{R}{R+1}\right) e_1$$

$$e_1 = g - 1 + g\delta + \frac{1}{\epsilon}\left[1 + (1 + \epsilon g \delta)\ \frac{\alpha}{1-\alpha}\right] + \frac{\gamma}{\alpha - 1} \tag{A.22}$$

For $\epsilon g = -1$, (A.22) reduces further to

$$e_1 = -1 - \frac{1}{\epsilon}\ \frac{\alpha - \delta}{\alpha - 1} + \frac{\gamma}{\alpha - 1} \tag{A.23}$$

The important remark to be made concerning (A.23) is that the last positive term largely cancels the first one, leaving only the small contribution of the second term, $|\alpha - \delta| < \alpha - 1$.

b) Dynamical Friction

A different type of evolution that can affect the luminosity is represented by dynamical friction. The phenomenon, first described by Chandrasekhar (1943) in the context of stellar dynamics, has been recently applied to globular clusters and formation of galactic nuclei by Tremaine, Ostriker and Spitzer (1975). Ostriker and Tremaine (1975) have pointed out that the same mechanism may be operating in clusters of galaxies, where a small galaxy is dragged into the nucleus by the collective action of the field galaxies and thereby disrupted. The computation of the increase in mass and therefore luminosity of the giant galaxy has been performed by several people besides the references quoted above (see for example, Lecar 1974). The result is

$$M_E(t_E) \propto G_E^{-1/2} \; m_E^{1/2} \; t_E^{1/2} \tag{B.1}$$

where we have included sub-indices E to indicate that the quantities entering this expression are to be understood in Einstein units. In fact, the equations used to arrive at (B.1) involve only gravitational quantities and no atomic constants; here m_E is the mass of the galaxy eventually to be disrupted by tidal forces. Let us generalize (B.1) to an arbitrary gauge. We first recall that (1, Eq. 2.50) for any object of mass M, the following relation holds

$$\beta_A \; M_A \; G_A = \beta_E \; M_E \; G_E \tag{B.2}$$

We therefore have, using $dt_E \equiv d\bar{t} = \beta(t)\,dt$

$$M_A \propto \frac{\beta_E\ G_E}{\beta_A\ G_A}\ \frac{(M_A\ \beta_A\ G_A)^{1/2}}{(\beta_E\ G_E)^{1/2}}\ \frac{\left(\int_{t_c}^{t} \beta(t)\,dt\right)^{1/2}}{G_E^{1/2}} \qquad (B.3)$$

or finally ($\beta_E = 1$)

$$M \propto \frac{1}{\beta G(\beta)}\ \left(\int_{t_c}^{t} \beta(t)\,dt\right)^{1/2} \qquad (B.4)$$

where we have suppressed the index A; the time t_c can be taken to be zero (as originally done by Ostriker and Tremaine), or more realistically as a given fraction of the Hubble time. In fact galaxies did not form at $t = 0$, but after decoupling. We shall leave t_c undetermined for the time being.

(B.4) is the generalization of Eq. (8) of Tremaine et al. to our cosmological framework. We must note that (B.4) is exact to the same extent to which Tremaine et al. is. In fact, our generalization has not introduced any approximations. We can now write, for the contribution to L by dynamical friction, the expression

$$L_{dy.\ fr.} \propto \beta^{E-1}\ \left(\int_{t_c}^{t} \beta(t)\,dt\right)^{1/2} \qquad (B.5)$$

For small look back times, we can approximate the bracket so that

$$L_{dy.\ fr.} \sim \beta^{g-1}(t) \left\{ 1 - \frac{1}{2} \frac{\nu}{H_o t_o} \frac{1}{1 - t_c/t_o} \right\} \qquad (B.6)$$

Using now (5.13) we finally get

$$L_{dy.\ fr.} \sim \beta^{g-1}(t) \ \beta^{-\frac{1}{2\epsilon} \frac{1}{1 - t_c/t_o}} \qquad (B.7)$$

APPENDIX C. THE m-z RELATION

We shall now present an alternative derivation of the magnitude vs. redshift relation using a Robertson-Walker metric:

$$ds^2 = dt^2 - R^2(t) \left[\frac{dr^2}{1 - kr^2} + r^2(d\theta^2 + \sin^2\theta \, d\varphi^2) \right]$$

The tangent vector of a photon path, extending from the origin radially outwards, can be written as (see II, Eq. 2.26)

$$k^\mu = \frac{\nu_0}{\beta R} \left(1, \frac{(1 - kr^2)^{1/2}}{R}, 0, 0 \right) \tag{C.1}$$

where ν_0 is a constant. We recall that (C.1) satisfies the null in-geodesic equation. The energy-momentum tensor of radiation emerging from the source, located at the origin, can be represented by

$$T^{\mu\nu} = E k^\mu k^\nu \tag{C.2}$$

The modified energy momentum conservation equation and the null in-geodesic equation imply (see Eqs. (2.36), (2.37) of II)

$$(E k^\mu)_{;\mu} = 0 = (E k^\mu)_{;\mu} + (1 - \pi_g) E k^\mu (\ln \beta)_{,\mu}$$

$$= \frac{1}{\sqrt{g}} (\sqrt{g} E k^\mu)_{,\mu} + (1 - \pi_g) E k^\mu (\ln \beta)_{,\mu}$$

where $\sqrt{g} = [-\det(g_{\mu\nu})]^{1/2}$. Making use of (C.1), the above equation can be rewritten as

$$\frac{\nu_o}{R^3}\left(\frac{E R^2}{\beta}\right)_{,t} + \frac{\nu_o}{R^2}\frac{(1-kr^2)^{1/2}}{r^2}\left(\frac{Er^2}{\beta}\right)_{,r}$$

$$+ (1-\pi_g)\, E\left(\frac{\nu_o}{\beta R}\frac{\beta_{,t}}{\beta} + \frac{\nu_o}{\beta R^2}(1-kr^2)^{1/2}\frac{\beta_{,r}}{\beta}\right) = 0$$

Next, we introduce the variables τ and ξ

$$d\tau = \frac{dt}{R(t)} \; ; \quad d\xi = \frac{dr}{(1-kr^2)^{1/2}}$$

so that the above equation becomes

$$\frac{\nu_o}{\beta^{1-\pi_g} R^4 r^2}\left[\mathcal{E}_{,\tau} + \mathcal{E}_{,\xi}\right] = 0$$

where

$$\mathcal{E} \equiv E R^2 r^2 \beta^{-\pi_g}$$

Hence

$$\mathcal{E} = \mathcal{E}(\tau - \xi) \; . \qquad \text{(C.3)}$$

Since on a null path $\tau - \xi$ is constant, $\mathcal{E}$ is a conserved quantity along the beam of radiation. Next we note that the observed flux, which is equivalent to the apparent luminosity, is given by

$$\ell = c\rho_\gamma = c\, T^{\mu\nu} u_\mu u_\nu = c\, E (u_\mu k^\mu)^2$$

$$= c\, E \frac{\nu^2}{\beta^2}$$

where Eq. (6.5) of II has been used. Thus, we can write Eq. (C.3) as

$$\frac{\ell_1}{c} \frac{\beta_1^{2-n_g}}{\nu_1^2} r_1^2 R_1^2 = \frac{\ell_2}{c} \frac{\beta_2^{2-n_g}}{\nu_2^2} r_2^2 R_2^2 .$$

Subscripts 1 and 2 denote different space time points along the beam of radiation. As we approach the source,

$$\lim_{r \to 0} 4\pi r^2 R^2 \ell = L ,$$

where L is the intrinsic luminosity. Hence,

$$\ell_{obs} = \frac{L}{4\pi} \left(\frac{\beta_{em}}{\beta_{obs}}\right)^{2-n_g} \left(\frac{\nu_{ob}}{\nu_{em}}\right)^2 \frac{1}{r_{obs}^2 R_{obs}^2}$$

$$\ell_{obs} = \frac{L}{4\pi \nu_{obs}^2 R_{obs}^2} \frac{1}{(1+z)^2} \left(\frac{\beta_{em}}{\beta_{obs}}\right)^{2-n_g} \qquad (C.4)$$

which coincides with (7.4a).

TABLE CAPTIONS D

Table 1. Values of z', z, $R(t)/R_o$, t/t_o, $\hat{\beta}(t)$ and F, eq. (7.6), for different values of $\bar{q}_o$: $\epsilon = -1$.

Table 2. Same as Table 1 for $\epsilon = -\frac{1}{2}$.

Table 3. Same as Table 1 for $\epsilon = \frac{1}{2}$.

Table 4. Same as Table 1 for $\epsilon = .92$. [This value is derived by requiring that the cosmological constant Λ computed from gauge field theory at early times and which scales like $\Lambda_o \hat{\beta}^2$, be compatible with today's value].

Table 5. Values of the apparent magnitude m (Eq. 7.11) and the metric diameter θ_m, Eq. (9.2), vs. the red-shift z for different values of $\bar{q}_o$, and the evolutionary parameter e, Eq. (7.8) : $\epsilon = -1$.

Table 6. Same as Table 5 for $\epsilon = -\frac{1}{2}$.

Table 7. Same as Table 5 for $\epsilon = \frac{1}{2}$.

Table 8. Same as Table 5 for $\epsilon = .92$.

Table 9. Values of the parameter η, eq. (13.8) that yield a slope of .75 in the lgN(m) vs. m relation.

Table 10. The m vs. z relation of standard cosmology (k = o) using the values of η determined in Table 9.

Table 11. Values of the evolutionary parameter e, Eq. (7.8), that yield a slope of .75 in the lgN(m) vs. m relation in the present cosmology. Two gauges are presented.

Table 12. The m vs. z relation (Eqs. 7.16 and 7.17) corresponding to the present cosmology with the evolutionary corrections from Table 11.

FIGURE CAPTIONS D

Figure 1. Look-back time (normalized to today) vs. z for $\bar{\bar{q}}_o = 0$ and 1 : $\epsilon = -1$.

Figure 2. Same as in Figure 1 for $\epsilon = -\frac{1}{2}$.

Figure 3. Same as in Figure 1 for $\epsilon = \frac{1}{2}$.

Figure 4. Same as in Figure 1 for $\epsilon = .92$.

Figure 5. The m vs. z diagram, see Eq. (7.11), for $\epsilon = -1$ and two values of $\bar{\bar{q}}_o = .1$ and $\frac{1}{2}$. The evolutionary parameter is $e = -1.5$. The value of the normalization m_o is 21.03 (the observational points are from Figure 3 of Sandage 1972a).

Figure 6. Same as in Figure 5, $\epsilon = -\frac{1}{2}$; $e = -1.7$.

Figure 7. Same as in Figure 5, $\epsilon = \frac{1}{2}$; $e = -1.0$.

Figure 8. Same as in Figure 5, $\epsilon = .92$; $e = -1.2$.

Figure 9. The effective deceleration parameter q^* as determined from the m vs. z relation, Eq. (5.2) as a function of the geometrical $\bar{\bar{q}}_o$ Eq. (8.3), for different values of the evolutionary parameter η, Eq. (8.4); $e = -1$.

Figure 10. Same as Figure 9 for $\epsilon = -\frac{1}{2}$.

Figure 11. Same as Figure 9 for $\epsilon = +\frac{1}{2}$.

Figure 12. Same as Figure 9 for $\epsilon = .92$.

Figure 13. The metric angular diameters vs. z, Eq. (9.2), for two values of $\bar{q}_o = .1$ and .5 (dashed lines). Predictions of standard cosmology are represented by full lines; $\epsilon = -1$. (The observational points are from Wardle and Miley 1974).

Figure 14. Same as Figure 13 for $\epsilon = -\frac{1}{2}$.

Figure 15. Same as Figure 13 for $\epsilon = \frac{1}{2}$.

Figure 16. Same as Figure 13 for $\epsilon = .92$.

Figure 17. Isophotal angular diameter θ_i vs. z, Eq. (10.6), for two values of $\bar{q}_o = .1$ and .5. The value of ϵ is the same as for Figure 5: $\epsilon = -1$. (The observational points are from Fig. 5 of Sandage 1972b).

Figure 18. Same as Figure 17 for $\epsilon = -\frac{1}{2}$.

Figure 19. Same as Figure 17 for $\epsilon = \frac{1}{2}$.

Figure 20. Same as Figure 17 for $\epsilon = .92$.

TABLE I , $\epsilon = -1$

$\bar{q}_o$	q_o	$\bar{f}_o\bar{H}_o$	f_oH_o	γ	z	R/Ro	f/fo	β	F
0.0	0.0	1.000	1.000						
				56.140	0.559	0.132	0.132	0.132	1331.970
				25.666	4.164	0.194	0.194	0.194	355.337
				14.291	3.370	0.240	0.240	0.240	150.724
				11.903	2.592	0.278	0.278	0.278	82.745
				9.256	2.203	0.312	0.312	0.312	52.096
				7.511	1.917	0.343	0.343	0.343	35.715
				6.273	1.697	0.371	0.371	0.371	25.946
				5.349	1.520	0.397	0.397	0.397	19.656
				4.63.	1.374	0.421	0.421	0.421	15.279
				4.063	1.256	0.444	0.444	0.444	12.313
				3.590	1.144	0.466	0.466	0.466	10.059
				3.211	1.052	0.487	0.487	0.487	8.304
				2.883	0.971	0.507	0.507	0.507	7.041
				2.604	0.898	0.527	0.527	0.527	5.993
				0.333	0.155	0.766	0.856	0.866	0.399
				0.250	0.118	0.894	0.894	0.894	0.281
				0.176	0.085	0.922	0.932	0.922	0.192
				0.111	0.054	0.949	0.969	0.969	0.117
				0.053	0.026	0.975	0.975	0.975	0.054
0.100	-0.042	0.846	0.693						
				199.572	3.979	0.201	0.025	0.025	1510.038
				84.965	2.466	0.340	0.045	0.045	589.494
				49.481	2.797	0.340	0.069	0.069	287.799
				31.019	2.741	0.423	0.097	0.097	158.634
				20.932	1.703	0.507	0.128	0.128	94.365
				14.829	1.457	0.291	0.162	0.162	59.008
				10.861	1.354	0.425	0.198	0.198	38.322
				8.144	1.180	0.499	0.238	0.238	25.517
				6.202	1.028	0.593	0.282	0.282	17.309
				4.770	0.892	0.529	0.328	0.328	11.804
				3.687	0.769	0.765	0.377	0.377	8.208
				2.849	0.656	0.[illegible]	0.430	0.430	5.727
				2.190	0.553	0.844	0.487	0.487	3.974
				1.663	0.457	0.938	0.547	0.547	2.736
				1.238	0.368	0.731	0.611	0.611	1.854
				0.890	0.285	0.778	0.680	0.680	1.218
				0.604	0.207	0.826	0.752	0.752	0.759
				0.366	0.103	0.892	0.830	0.830	0.426
				0.167	0.065	0.939	0.912	0.912	0.190
0.500	2.000	0.667	0.333						
				399.000	3.[illegible]	0.824	0.011	0.011	760.000
				59.501	1.739	0.359	0.[illegible]	0.[illegible]	105.485
				37.670	1.497	0.460	0.064	0.064	65.209
				28.872	1.338	0.[illegible]	0.078	0.078	48.813
				23.743	1.233	0.[illegible]	0.090	0.090	39.537
				20.307	1.150	0.465	0.101	0.101	33.469
				17.947	1.086	0.479	0.110	0.110	29.189
				2.[illegible]	0.361	0.735	0.397	0.397	3.[illegible]
				2.166	0.338	0.750	0.[illegible]	0.[illegible]	2.774
				1.949	0.310	0.763	0.[illegible]	0.[illegible]	2.663
				1.[illegible]	0.290	0.775	0.[illegible]	0.[illegible]	2.294
				1.607	0.271	0.787	0.[illegible]	0.[illegible]	1.[illegible]
				1.471	0.254	0.798	0.[illegible]	0.[illegible]	1.798
				1.350	0.238	0.808	0.527	0.527	1.655
				0.246	0.059	0.945	0.843	0.843	0.271
				0.[illegible]	0.047	0.955	0.872	0.872	0.210
				0.151	0.036	0.965	0.909	0.909	0.156
				0.100	0.025	0.975	0.927	0.927	0.106
				0.[illegible]	0.010	0.904	0.954	0.954	0.066
1.000	22.188	0.571	0.142						
				311.416	2.922	0.262	0.012	0.012	311.416
				78.784	1.719	0.368	0.034	0.034	78.784
				34.[illegible]	1.227	0.449	0.062	0.062	34.788
				19.271	0.936	0.517	0.095	0.095	19.271
				12.[illegible]	0.753	0.[illegible]	0.133	0.133	12.[illegible]
				8.153	0.595	0.628	0.174	0.174	8.133
				5.[illegible]	0.472	0.675	0.219	0.219	5.762
				4.221	0.394	0.717	0.267	0.267	4.221
				3.164	0.323	0.756	0.316	0.316	3.164
				2.403	0.269	0.791	0.371	0.371	2.403
				1.[illegible]	0.215	0.823	0.[illegible]	0.[illegible]	1.868
				1.423	0.173	0.853	0.484	0.484	1.423
				1.092	0.137	0.879	0.[illegible]	0.[illegible]	1.092
				0.830	0.107	0.903	0.[illegible]	0.[illegible]	0.830
				0.[illegible]	0.081	0.925	0.[illegible]	0.[illegible]	0.619
				0.447	0.059	0.944	0.[illegible]	0.[illegible]	0.447
				0.304	0.040	0.962	0.[illegible]	0.[illegible]	0.304
				0.185	0.024	0.976	0.[illegible]	0.[illegible]	0.185
				0.085	0.011	0.989	0.[illegible]	0.[illegible]	0.085

NPTS= 103 NPTS4= 19

TABLE 2, $\epsilon = -1/2$

$\bar{q}_o$	q_c	$\bar{t}_o\bar{H}_o$	t_oH_c	γ	z	R/R_o	t/t_o	β	F
0.0	0.0	1.000	1.000						
				56.140	13.035	0.067	0.067	0.200	163.070
				25.656	7.926	0.112	0.112	0.333	35.037
				13.391	5.717	0.149	0.149	0.338	150.726
				7.903	4.501	0.182	0.182	0.476	82.745
				4.256	3.721	0.212	0.212	0.496	57.056
				2.511	3.165	0.240	0.240	0.693	35.735
				0.273	2.754	0.266	0.266	0.519	25.986
				5.449	2.429	0.292	0.292	0.560	19.696
				4.634	2.165	0.316	0.316	0.582	16.370
				4.065	1.959	0.339	0.339	0.602	13.918
				3.598	1.795	0.362	0.362	0.621	12.059
				3.211	1.607	0.384	0.384	0.639	8.264
				2.683	1.421	0.405	0.405	0.670	7.041
				2.004	1.250	0.425	0.425	0.682	5.093
				0.373	0.211	0.625	0.625	0.502	0.385
				0.250	0.168	0.862	0.862	0.928	0.201
				0.176	0.124	0.897	0.897	0.767	0.192
				0.111	0.073	0.932	0.932	0.965	0.117
				0.053	0.035	0.966	0.966	0.983	0.054
0.100	0.078	0.846	0.770						
				199.572	16.089	0.059	0.087	0.085	1510.038
				86.965	12.404	0.088	0.616	0.127	568.594
				49.481	7.614	0.117	0.020	0.159	287.729
				31.019	5.752	0.149	0.046	0.231	105.638
				20.932	4.660	0.180	0.064	0.253	94.385
				14.629	3.895	0.213	0.088	0.197	56.632
				10.863	3.036	0.248	0.116	0.310	30.362
				8.166	2.510	0.285	0.148	0.365	29.617
				6.202	2.096	0.324	0.185	0.430	17.369
				4.770	1.763	0.365	0.229	0.463	13.998
				3.687	1.487	0.409	0.273	0.502	8.246
				2.849	1.254	0.456	0.325	0.517	5.727
				2.190	0.979	0.507	0.382	0.519	3.074
				1.662	0.791	0.561	0.447	0.609	2.720
				1.230	0.618	0.623	0.517	0.650	1.852
				0.899	0.481	0.688	0.594	0.773	1.218
				0.644	0.407	0.754	0.674	0.827	0.729
				0.362	0.208	0.829	0.780	0.863	0.427
				0.167	0.098	0.911	0.885	0.941	0.190
0.500	1.000	0.667	0.500						
				67.801	7.299	0.121	0.015	0.121	171.156
				40.430	5.237	0.155	0.024	0.155	69.906
				30.197	4.569	0.177	0.042	0.179	51.150
				24.535	4.051	0.198	0.059	0.198	40.902
				20.911	3.681	0.218	0.045	0.218	34.480
				18.348	3.397	0.237	0.092	0.237	29.655
				16.823	3.179	0.257	0.057	0.256	26.698
				2.429	0.819	0.540	0.292	0.569	3.154
				2.106	0.770	0.562	0.316	0.582	2.774
				1.949	0.737	0.580	0.337	0.592	2.563
				1.765	0.663	0.601	0.362	0.601	2.209
				1.607	0.617	0.619	0.384	0.619	1.955
				1.471	0.573	0.639	0.415	0.636	1.790
				1.350	0.533	0.658	0.423	0.652	1.653
				0.256	0.121	0.812	0.716	0.832	0.291
				0.191	0.098	0.913	0.852	0.914	0.240
				0.131	0.073	0.932	0.909	0.959	0.155
				0.106	0.052	0.951	0.943	0.981	0.102
				0.065	0.032	0.969	0.959	0.989	0.066
1.000	3.241	0.571	0.350						
				103.857	6.691	0.104	0.008	0.092	163.037
				42.991	5.260	0.161	0.020	0.162	62.491
				23.109	3.616	0.217	0.037	0.191	23.109
				14.297	2.803	0.272	0.076	0.241	14.297
				9.587	2.038	0.327	0.055	0.291	9.587
				6.793	1.621	0.381	0.116	0.340	6.703
				4.993	1.309	0.436	0.152	0.390	4.903
				3.679	1.052	0.491	0.192	0.439	3.679
				2.810	0.797	0.559	0.238	0.487	2.811
				2.178	0.611	0.593	0.287	0.536	2.179
				1.636	0.509	0.632	0.341	0.583	1.636
				1.311	0.380	0.685	0.359	0.632	1.311
				1.015	0.309	0.730	0.402	0.680	1.015
				0.777	0.221	0.775	0.529	0.727	0.777
				0.603	0.206	0.817	0.598	0.773	0.603
				0.423	0.145	0.858	0.682	0.819	0.423
				0.299	0.111	0.895	0.759	0.865	0.299
				0.177	0.072	0.933	0.834	0.911	0.177
				0.081	0.035	0.968	0.913	0.955	0.081

NPTS= 108 NPTS4= 19

TABLE 3 , $\epsilon = 1/2$

$\bar{q}_o$	q_o	$\bar{t}_o\bar{H}_o$	t_oH_o	γ	z	R/R_o	t/t_o	β	F
0.0	0.0	1.000	1.000	0.985	2.863	0.259	0.259	1.965	1.431
				0.925	2.715	0.269	0.269	1.923	1.358
				0.891	2.576	0.280	0.280	1.881	1.289
				0.856	2.445	0.290	0.290	1.836	1.222
				0.822	2.320	0.301	0.301	1.822	1.160
				0.790	2.203	0.312	0.312	1.793	1.101
				0.758	2.091	0.324	0.324	1.758	1.045
				0.720	1.985	0.335	0.335	1.728	0.993
				0.698	1.885	0.347	0.347	1.696	0.942
				0.670	1.789	0.359	0.359	1.670	0.895
				0.643	1.698	0.371	0.371	1.643	0.849
				0.616	1.612	0.383	0.383	1.616	0.806
				0.590	1.529	0.395	0.395	1.590	0.765
				0.565	1.451	0.408	0.408	1.565	0.725
				0.143	0.305	0.766	0.766	1.143	0.153
				0.111	0.235	0.810	0.810	1.111	0.117
				0.081	0.169	0.856	0.856	1.081	0.084
				0.053	0.108	0.903	0.903	1.053	0.054
				0.026	0.052	0.951	0.951	1.026	0.026
0.100	0.066	0.846	0.923	1.850	9.478	0.095	0.075	3.663	3.181
				1.693	8.131	0.110	0.087	3.477	2.803
				1.536	6.974	0.125	0.101	3.142	2.405
				1.393	5.976	0.143	0.118	2.915	2.103
				1.258	5.115	0.164	0.136	2.708	1.893
				1.132	4.369	0.188	0.158	2.513	1.691
				1.014	3.721	0.212	0.182	2.344	1.435
				0.904	3.159	0.240	0.210	2.195	1.241
				0.800	2.669	0.273	0.241	2.038	1.067
				0.703	2.241	0.309	0.275	1.903	0.911
				0.612	1.867	0.349	0.316	1.776	0.771
				0.527	1.539	0.394	0.362	1.663	0.645
				0.446	1.251	0.444	0.413	1.557	0.532
				0.371	0.999	0.500	0.470	1.453	0.430
				0.299	0.776	0.563	0.535	1.297	0.339
				0.232	0.581	0.633	0.608	1.283	0.256
				0.169	0.408	0.710	0.690	1.204	0.182
				0.109	0.255	0.797	0.782	1.131	0.119
				0.053	0.120	0.893	0.885	1.063	0.059
0.500	0.200	0.667	0.833	0.585	2.164	0.316	0.251	1.690	0.650
				0.583	2.156	0.317	0.252	1.692	0.650
				0.581	2.143	0.318	0.253	1.688	0.647
				0.579	2.133	0.319	0.254	1.684	0.645
				0.577	2.123	0.320	0.255	1.680	0.642
				0.575	2.112	0.321	0.256	1.676	0.640
				0.573	2.102	0.322	0.257	1.672	0.637
				0.440	1.488	0.402	0.338	1.728	0.480
				0.424	1.418	0.414	0.347	1.693	0.461
				0.408	1.351	0.425	0.359	1.670	0.442
				0.392	1.287	0.437	0.371	1.645	0.425
				0.377	1.226	0.449	0.383	1.616	0.407
				0.362	1.167	0.462	0.395	1.590	0.390
				0.348	1.111	0.474	0.408	1.565	0.374
				0.110	0.298	0.770	0.731	1.178	0.113
				0.089	0.237	0.808	0.774	1.136	0.091
				0.069	0.181	0.847	0.819	1.105	0.070
				0.050	0.139	0.886	0.865	1.076	0.050
				0.031	0.080	0.926	0.912	1.047	0.031
1.000	0.300	0.571	0.785	0.897	4.491	0.182	0.119	2.395	0.897
				0.817	3.914	0.204	0.137	2.702	0.817
				0.744	3.410	0.227	0.156	2.529	0.744
				0.675	2.969	0.252	0.176	2.379	0.675
				0.610	2.582	0.279	0.202	2.233	0.610
				0.550	2.241	0.309	0.229	2.096	0.550
				0.494	1.939	0.340	0.258	1.968	0.494
				0.441	1.675	0.374	0.291	1.855	0.441
				0.391	1.436	0.411	0.326	1.751	0.391
				0.345	1.225	0.450	0.365	1.654	0.345
				0.301	1.035	0.491	0.408	1.565	0.301
				0.259	0.868	0.535	0.455	1.485	0.259
				0.220	0.716	0.583	0.505	1.407	0.220
				0.183	0.580	0.633	0.561	1.338	0.183
				0.148	0.458	0.686	0.620	1.270	0.148
				0.115	0.348	0.742	0.685	1.208	0.115
				0.086	0.248	0.802	0.755	1.151	0.086
				0.055	0.157	0.864	0.831	1.097	0.055
				0.027	0.075	0.930	0.912	1.047	0.027

NPTS= 108 NPTSA= 15

TABLE 4 , ϵ = .92

$\bar{q}_o$	q_c	$\bar{t}_o\bar{H}_o$	t_oH_o	γ	z	R/R_o	t/t_c	β	F
0.0	0.0	1.000	1.000	0.149	4.676	0.176	0.176	4.940	0.160
				0.146	4.466	0.183	0.183	4.771	0.156
				0.142	4.253	0.190	0.190	4.560	0.152
				0.139	4.069	0.197	0.197	4.451	0.148
				0.135	3.882	0.205	0.205	4.360	0.144
				0.132	3.705	0.213	0.213	4.155	0.141
				0.128	3.531	0.221	0.221	4.015	0.137
				0.125	3.365	0.229	0.229	3.830	0.133
				0.122	3.206	0.238	0.238	3.750	0.129
				0.118	3.054	0.247	0.247	3.626	0.125
				0.115	2.907	0.256	0.256	3.503	0.122
				0.112	2.766	0.266	0.266	3.387	0.118
				0.109	2.631	0.275	0.275	3.275	0.115
				0.105	2.500	0.286	0.285	3.167	0.111
				0.034	0.521	0.657	0.657	1.471	0.035
				0.027	0.397	0.716	0.716	1.380	0.027
				0.020	0.284	0.779	0.779	1.259	0.020
				0.013	0.181	0.847	0.847	1.115	0.013
				0.007	0.086	0.921	0.921	1.079	0.007
0.100	0.012	0.848	0.988	0.243	23.379	0.041	0.039	19.621	0.260
				0.228	19.539	0.049	0.047	18.722	0.251
				0.214	18.311	0.058	0.056	18.257	0.235
				0.200	13.595	0.069	0.066	13.169	0.218
				0.186	11.310	0.081	0.079	10.976	0.202
				0.173	9.387	0.096	0.093	8.855	0.189
				0.160	7.768	0.116	0.111	7.561	0.171
				0.146	6.403	0.135	0.132	6.459	0.156
				0.133	5.254	0.160	0.156	5.545	0.141
				0.120	4.285	0.189	0.185	4.717	0.127
				0.108	3.467	0.224	0.220	4.034	0.113
				0.095	2.777	0.265	0.260	3.456	0.099
				0.083	2.195	0.313	0.308	2.952	0.085
				0.070	1.704	0.370	0.365	2.528	0.073
				0.058	1.289	0.437	0.432	2.163	0.060
				0.046	0.938	0.516	0.512	1.852	0.047
				0.035	0.642	0.609	0.605	1.587	0.035
				0.023	0.391	0.719	0.715	1.358	0.023
				0.011	0.179	0.843	0.846	1.106	0.011
0.500	0.027	0.667	0.973	0.084	3.324	0.231	0.222	3.991	0.085
				0.083	3.311	0.232	0.223	3.979	0.085
				0.083	3.297	0.233	0.224	3.967	0.085
				0.083	3.284	0.234	0.224	3.956	0.085
				0.083	3.271	0.235	0.225	3.944	0.084
				0.083	3.257	0.235	0.226	3.932	0.084
				0.082	3.244	0.236	0.226	3.921	0.083
				0.069	2.701	0.294	0.284	3.418	0.071
				0.068	2.698	0.303	0.293	3.405	0.069
				0.066	2.200	0.313	0.303	3.012	0.057
				0.064	2.103	0.322	0.313	2.917	0.055
				0.062	2.011	0.332	0.322	2.825	0.053
				0.061	1.922	0.342	0.332	2.736	0.051
				0.059	1.839	0.353	0.343	2.677	0.050
				0.023	0.503	0.685	0.668	1.470	0.023
				0.019	0.400	0.714	0.708	1.374	0.019
				0.015	0.304	0.767	0.761	1.285	0.015
				0.011	0.215	0.823	0.818	1.202	0.011
				0.007	0.133	0.882	0.875	1.123	0.007
1.000	0.036	0.571	0.964	0.135	13.080	0.371	0.065	12.210	0.135
				0.127	11.150	0.082	0.075	10.805	0.127
				0.119	9.530	0.095	0.087	9.614	0.119
				0.112	8.125	0.110	0.101	8.208	0.112
				0.104	6.905	0.126	0.118	7.152	0.104
				0.097	5.855	0.146	0.135	6.282	0.096
				0.089	4.948	0.168	0.158	5.492	0.089
				0.081	4.164	0.194	0.183	4.775	0.081
				0.074	3.487	0.223	0.211	4.177	0.074
				0.067	2.902	0.256	0.244	3.667	0.067
				0.060	2.396	0.295	0.282	3.245	0.060
				0.053	1.955	0.338	0.326	2.887	0.053
				0.046	1.575	0.388	0.376	2.582	0.046
				0.039	1.245	0.445	0.433	2.161	0.039
				0.032	0.959	0.510	0.499	1.897	0.032
				0.026	0.719	0.585	0.574	1.667	0.026
				0.019	0.494	0.669	0.659	1.456	0.019
				0.013	0.306	0.765	0.758	1.270	0.013
				0.006	0.142	0.875	0.871	1.133	0.006

NPTS= 108 NPTSA= 19

TABLE 5, $\epsilon = -1$

$\bar{q}_o$	z	$\epsilon=-2$ m	$\epsilon=-2$ θm	$\epsilon=-1$ m	$\epsilon=-1$ θm	$\epsilon=0$ m	$\epsilon=0$ θm	$\epsilon=1$ m	$\epsilon=1$ θm	$\epsilon=+2$ m	$\epsilon=+2$ θm
0.0											
	6.559	7.970	4.549	10.100	4.549	12.302	4.549	14.508	4.569	16.755	4.569
	4.164	5.699	6.667	7.831	6.667	9.964	6.667	11.946	6.667	13.929	6.667
	3.173	4.735	8.271	6.785	8.271	7.835	8.271	9.535	8.271	10.956	8.271
	2.592	3.518	9.628	5.307	9.628	6.095	9.628	8.084	9.628	9.472	9.628
	2.203	3.268	10.837	4.551	10.837	5.815	10.837	7.079	10.837	8.345	10.837
	1.917	2.772	11.949	3.923	11.949	5.097	11.949	6.259	11.949	7.422	11.949
	1.697	2.344	12.993	3.411	12.993	4.478	12.993	5.565	12.993	6.692	12.993
	1.520	1.952	13.990	2.956	13.990	3.959	13.990	4.962	13.990	5.966	13.990
	1.374	1.613	14.955	2.551	14.955	3.490	14.955	4.428	14.955	5.367	14.955
	1.250	1.306	15.898	2.187	15.898	3.067	15.898	3.948	15.898	4.828	15.898
	1.144	1.025	16.829	1.854	16.829	2.682	16.829	3.510	16.829	4.338	16.829
	1.052	0.780	17.755	1.550	17.755	2.327	17.755	3.107	17.755	3.887	17.755
	0.971	0.523	18.684	1.260	18.684	1.996	18.684	2.733	18.684	3.469	18.684
	0.898	0.295	19.620	0.991	19.620	1.687	19.620	2.383	19.620	3.079	19.620
	0.155	-4.025	68.050	-3.469	68.050	-2.712	68.050	-1.956	68.050	-1.200	68.050
	0.118	-4.023	85.412	-3.502	85.412	-2.341	85.412	-1.180	85.412	-0.139	85.412
	0.085	-5.553	114.214	-5.005	114.214	-4.176	114.214	-3.098	114.214	-2.009	114.214
	0.059	-6.321	171.649	-6.275	171.649	-6.216	171.649	-6.159	171.649	-6.102	171.649
	0.026	-7.926	343.662	-7.898	343.662	-7.870	343.662	-7.843	343.662	-7.815	343.662
0.100											
	3.979	1.917	13.988	5.930	13.886	9.943	13.886	13.955	13.886	17.968	13.886
	3.060	1.821	14.311	5.105	14.011	8.565	14.011	11.913	14.011	15.277	14.011
	2.457	1.659	12.881	4.558	12.881	7.457	12.881	10.355	12.881	13.254	12.881
	2.101	1.458	13.141	3.963	13.141	6.527	13.141	9.092	13.141	11.657	13.141
	1.799	1.229	13.661	3.454	13.661	5.679	13.661	7.904	13.661	10.129	13.661
	1.557	0.776	14.388	2.950	14.388	4.237	14.388	5.917	14.388	8.598	14.388
	1.354	0.710	15.302	2.560	15.302	3.722	15.302	5.078	15.302	7.733	15.302
	1.180	0.425	16.409	2.202	16.409	3.538	16.409	5.024	16.409	6.851	16.409
	1.024	0.124	17.716	1.880	17.716	2.876	17.716	3.252	17.716	5.628	17.716
	0.892	-0.176	19.269	1.615	19.269	2.626	19.269	3.637	19.269	4.648	19.269
	0.769	-0.534	21.121	1.324	21.121	1.542	21.121	2.640	21.121	3.698	21.121
	0.656	-0.807	23.309	0.819	23.309	0.934	23.309	1.050	23.309	2.700	23.309
	0.553	-1.298	25.865	-0.587	25.865	0.275	25.865	1.057	25.865	1.838	25.865	
	0.457	-1.719	28.774	-1.066	28.774	-0.494	28.774	0.286	28.774	0.901	28.774
	0.365	-2.204	34.677	-1.668	34.677	-1.138	34.677	-0.600	34.677	-0.065	34.677
	0.285	-2.769	41.844	-2.358	41.844	-1.910	41.844	-1.511	41.844	-1.091	41.844
	0.207	-3.466	53.551	-3.157	53.551	-2.848	53.551	-2.539	53.551	-2.250	53.551
	0.133	-4.610	76.639	-4.307	76.639	-4.005	76.639	-3.907	76.639	-3.595	76.639
	0.065	-5.909	145.336	-5.809	145.336	-5.769	145.336	-5.669	145.336	-5.509	145.336
0.500											
	3.472	-3.243	80.916	1.646	80.916	6.515	80.916	11.134	80.916	15.273	80.916
	1.782	-2.918	55.011	0.423	55.011	3.764	55.011	7.105	55.011	10.446	55.011
	1.497	-2.578	51.130	0.182	51.130	3.083	51.130	5.984	51.130	8.885	51.130
	1.338	-2.866	49.183	-0.130	49.183	2.656	49.183	5.432	49.183	8.178	49.183
	1.230	-2.883	47.982	-0.251	47.982	2.382	47.982	4.975	47.982	7.587	47.982
	1.150	-2.868	47.157	-0.317	47.157	2.121	47.157	4.614	47.157	7.107	47.157
	1.086	-2.820	46.558	-0.375	46.558	1.920	46.558	4.315	46.558	6.711	46.558
	0.361	-3.526	50.852	-0.841	50.852	-0.519	50.852	-0.196	50.852	0.488	50.852
	0.334	-3.611	52.348	-0.972	52.348	-0.734	52.348	-0.497	52.348	0.143	52.348
	0.310	-3.695	53.932	-1.116	53.932	-0.936	53.932	-0.756	53.932	-0.172	53.932
	0.288	-3.779	55.605	-1.259	55.605	-1.142	55.605	-1.026	55.605	-0.895	55.605
	0.271	-3.862	57.371	-1.382	57.371	-1.291	57.371	-1.201	57.371	-1.081	57.371
	0.254	-3.960	59.236	-1.510	59.236	-1.473	59.236	-1.437	59.236	-1.309	59.236
	0.238	-4.031	61.204	-1.645	61.204	-1.649	61.204	-1.653	61.204	-1.247	61.204
	0.059	-6.442	108.679	-6.253	108.679	-6.060	108.679	-5.868	108.679	-5.669	108.679
	0.047	-6.847	205.826	-6.758	205.826	-6.669	205.826	-6.580	205.826	-6.491	205.826
	0.036	-7.388	262.466	-7.272	262.466	-7.157	262.466	-7.042	262.466	-6.929	262.466
	0.025	-8.089	359.682	-7.998	359.682	-7.916	359.682	-7.834	359.682	-7.753	359.682
	0.016	-9.069	564.208	-9.018	564.208	-8.967	564.208	-8.915	564.208	-8.864	564.208
1.000											
	2.622	-6.509	265.657	-1.428	265.657	3.153	265.657	7.934	265.657	12.716	265.657
	1.719	-6.057	190.769	-2.348	190.769	1.281	190.769	4.950	190.769	8.619	190.769
	1.227	-5.870	158.780	-2.805	158.780	0.160	158.780	3.175	158.780	6.190	158.780
	0.930	-5.758	141.075	-3.058	141.075	-1.058	141.075	1.052	141.075	4.642	141.075
	0.738	-5.699	130.392	-3.208	130.392	-1.516	130.392	0.774	130.392	3.064	130.392
	0.593	-5.669	123.965	-3.275	123.965	-1.677	123.965	0.819	123.965	3.315	123.965
	0.482	-5.673	120.537	-3.325	120.537	-1.873	120.537	-0.250	120.537	0.916	120.537
	0.394	-5.706	119.069	-3.402	119.069	-2.062	119.069	-1.695	119.069	-0.005	119.069
	0.323	-5.769	120.643	-3.541	120.643	-2.276	120.643	-2.031	120.643	-0.780	120.643
	0.264	-5.865	123.955	-3.761	123.955	-2.761	123.955	-2.624	123.955	-1.647	123.955
	0.215	-5.975	127.687	-3.969	127.687	-3.174	127.687	-3.179	127.687	-2.275	127.687
	0.173	-6.130	138.369	-4.252	138.369	-3.554	138.369	-3.769	138.369	-2.979	138.369
	0.137	-6.327	150.948	-4.605	150.948	-3.963	150.948	-4.341	150.948	-3.679	150.948
	0.107	-6.577	169.628	-5.069	169.628	-4.502	169.628	-4.937	169.628	-4.241	169.628
	0.081	-6.890	195.913	-5.681	195.913	-5.013	195.913	-5.574	195.913	-5.135	195.913
	0.059	-7.295	237.663	-6.469	237.663	-5.822	237.663	-6.263	237.663	-5.996	237.663
	0.040	-7.856	309.089	-7.269	309.089	-6.753	309.089	-7.117	309.089	-6.671	309.089
	0.024	-8.678	454.078	-8.211	454.078	-7.952	454.078	-8.194	454.078	-8.035	454.078
	0.011	-10.115	893.646	-10.038	893.646	-9.961	893.646	-9.884	893.646	-9.807	893.646
NOTS= 104		NPTSA= 19		19		19		19		19	

TABLE 6, $\epsilon = -1/2$

$\bar{q}_o$	z	e=-2 m	e=-2 θm	e=-1 m	e=-1 θm	e=0 m	e=0 θm	e=1 m	e=1 θm	e=+2 m	e=+2 θm
0.0											
	13.835	9.527	6.696	10.791	6.696	12.255	6.696	13.719	6.696	15.183	6.696
	7.926	7.118	8.642	8.306	8.642	9.494	8.642	10.683	8.642	11.871	8.642
	5.712	5.810	9.585	6.210	9.585	7.008	9.585	8.207	9.585	9.405	9.585
	4.561	5.006	11.059	5.412	11.059	6.057	11.059	7.253	11.059	8.204	11.059
	3.731	4.348	11.981	5.115	11.981	6.019	11.981	7.051	11.981	7.709	11.981
	3.168	3.764	12.605	4.556	12.605	5.348	12.605	6.105	12.605	6.846	12.605
	2.755	3.318	13.066	4.060	13.066	4.752	13.066	5.472	13.066	6.190	13.066
	2.429	2.911	13.428	3.580	13.428	4.245	13.428	4.918	13.428	5.587	13.428
	2.166	2.590	13.721	3.176	14.561	3.802	14.961	4.427	14.961	5.053	14.961
	1.939	2.324	13.974	2.811	15.624	3.358	15.624	3.905	15.624	4.452	15.624
	1.746	1.925	14.276	2.475	16.276	3.050	16.276	3.592	16.276	4.135	16.276
	1.607	1.701	14.571	2.171	16.521	2.641	16.921	3.211	16.921	3.732	16.521
	1.471	1.395	14.568	1.885	17.569	2.376	17.568	2.867	17.561	3.359	17.569
	1.369	1.152	14.260	1.616	18.260	2.080	18.260	2.546	18.260	3.010	18.260
	0.211	-3.343	53.564	-3.264	53.564	-3.160	53.564	-3.035	53.564	-2.731	53.564
	0.100	-4.958	66.486	-3.877	66.486	-3.797	66.486	-3.716	66.489	-3.635	66.486
	0.114	-5.099	88.413	-4.645	88.413	-4.191	88.413	-4.062	88.413	-4.383	88.413
	0.073	-5.657	131.013	-5.649	131.013	-5.611	131.013	-5.572	131.013	-5.534	131.013
	0.053	-7.292	259.959	-7.274	259.959	-7.255	259.959	-7.236	259.959	-7.218	259.959
0.100											
	16.969	4.107	32.141	6.738	32.141	9.458	32.141	12.183	32.141	14.898	32.141
	10.404	3.795	24.074	6.038	24.074	8.280	24.074	10.523	24.074	12.765	24.074
	7.514	3.478	21.178	5.411	21.178	7.343	21.178	9.276	21.178	11.208	21.178
	5.752	3.155	19.322	4.865	19.322	6.575	19.322	8.285	19.322	9.995	19.322
	4.969	2.827	18.320	4.317	18.320	5.807	18.320	7.297	18.320	8.787	18.320
	3.695	2.491	17.638	3.811	17.638	5.130	17.638	6.450	17.638	7.770	17.638
	3.030	2.148	17.213	3.319	17.213	4.490	17.213	5.660	17.213	6.831	17.213
	2.516	1.797	17.003	2.834	17.003	3.872	17.003	4.910	17.003	5.947	17.003
	2.094	1.435	16.951	2.352	16.951	3.270	16.951	4.187	16.951	5.105	16.951
	1.743	1.061	16.969	1.868	16.969	2.675	16.969	3.482	16.969	4.290	16.969
	1.447	0.671	17.035	1.430	17.035	2.052	17.035	2.707	17.035	3.373	17.035
	1.174	0.261	20.501	0.982	20.941	1.494	20.941	2.007	20.941	2.519	20.941
	0.974	-0.179	22.459	0.346	22.459	0.867	22.459	1.388	22.459	1.909	22.459
	0.781	-0.618	24.582	-0.211	24.582	0.226	24.582	0.662	24.582	1.099	24.582
	0.612	-1.174	27.590	-0.816	27.590	-0.460	27.590	-0.103	27.590	0.253	27.590
	0.461	-1.776	32.137	-1.217	32.137	-1.217	32.137	-1.217	32.137	-1.217	32.137
	0.327	-2.510	39.757	-2.308	39.757	-2.213	39.757	-1.922	39.757	-1.722	39.757
	0.209	-3.309	55.669	-3.254	55.669	-3.219	55.669	-3.093	55.669	-2.969	55.669
	0.098	-5.082	101.185	-5.016	101.185	-4.949	101.185	-4.883	101.185	-4.816	101.185
0.500											
	7.298	-0.279	81.090	2.019	81.090	4.316	81.090	6.614	81.090	8.911	81.090
	5.437	-0.367	65.494	1.485	65.494	3.427	65.494	5.369	65.494	7.310	65.494
	4.572	-0.538	58.462	1.139	58.462	2.845	58.462	5.172	58.462	7.039	58.462
	4.053	-0.677	54.145	1.280	54.145	3.032	54.145	4.784	54.145	6.537	54.145
	3.691	-0.822	51.159	1.134	51.159	2.730	51.159	4.326	51.159	5.921	51.159
	3.379	-0.969	48.927	1.040	48.927	2.507	48.927	4.035	48.927	5.573	48.927
	3.176	-0.994	47.176	0.907	47.176	2.508	47.176	4.056	47.176	5.611	47.176
	0.892	-1.782	36.599	-1.017	36.599	-0.339	36.599	0.339	36.599	0.016	36.599
	0.772	-1.793	36.911	-1.167	36.911	-0.541	36.911	0.084	36.911	0.710	36.911
	0.717	-1.936	39.330	-1.399	39.330	-0.862	39.330	-0.325	39.330	0.212	39.330
	0.663	-1.927	39.852	-1.445	39.852	-0.963	39.852	-0.481	39.852	0.011	39.852
	0.615	-2.007	39.902	-1.577	39.902	-1.056	39.902	-0.536	39.902	-0.015	39.902
	0.572	-2.196	37.153	-1.705	37.153	-1.214	37.153	-0.723	37.153	-0.232	37.153
	0.533	-2.296	37.491	-1.830	37.491	-1.364	37.491	-0.898	37.491	-0.432	37.491
	0.121	-4.075	89.366	-4.711	89.366	-4.667	89.366	-4.623	89.366	-4.579	89.366
	0.096	-5.292	107.729	-5.193	107.729	-5.093	107.729	-4.994	107.729	-4.895	107.729
	0.073	-5.843	125.276	-5.707	125.276	-5.570	125.276	-5.434	125.276	-5.298	125.276
	0.052	-6.542	184.320	-6.493	184.320	-6.439	184.320	-6.385	184.320	-6.329	184.320
	0.032	-7.547	280.573	-7.513	280.573	-7.479	280.573	-7.444	280.573	-7.410	280.573
1.000											
	8.611	-2.200	200.462	0.304	200.462	3.069	200.462	5.833	200.462	8.177	200.462
	5.230	-2.226	131.604	-0.108	131.604	2.218	131.604	4.543	131.604	6.262	131.604
	3.616	-2.304	99.495	-0.475	99.495	1.325	99.495	3.120	99.495	4.914	99.495
	2.673	-2.314	81.220	-0.771	81.220	0.773	81.220	2.317	81.220	3.861	81.220
	2.036	-2.378	69.773	-1.037	69.773	0.304	69.773	1.645	69.773	2.986	69.773
	1.621	-2.453	62.233	-1.286	62.233	-0.114	62.233	1.057	62.233	2.227	62.233
	1.330	-2.540	57.195	-1.553	57.195	-0.459	57.195	0.634	57.195	1.728	57.195
	1.092	-2.605	53.520	-1.760	53.520	-0.859	53.520	0.029	53.520	0.922	53.520
	0.892	-2.702	52.011	-2.092	52.011	-1.222	52.011	-0.641	52.011	0.229	52.011
	0.699	-2.941	51.267	-2.254	51.267	-1.577	51.267	-0.899	51.267	-0.222	51.267
	0.569	-3.195	51.634	-2.555	51.634	-1.938	51.634	-1.318	51.634	-0.679	51.634
	0.463	-3.350	51.196	-2.711	51.196	-2.113	51.196	-1.515	51.196	-1.117	51.196
	0.369	-3.561	50.153	-3.132	50.153	-2.612	50.153	-2.092	50.153	-1.573	50.153
	0.291	-3.669	49.911	-3.295	49.911	-2.947	49.911	-2.599	49.911	-2.251	49.911
	0.224	-4.153	65.625	-4.015	65.625	-3.836	65.625	-3.657	65.625	-3.478	65.625
	0.176	-4.939	81.024	-4.823	81.024	-4.707	81.024	-4.592	81.024	-4.475	81.024
	0.116	-5.775	101.775	-5.670	101.775	-5.913	101.775	-5.760	101.775	-5.655	101.775
	0.077	-6.373	147.691	-6.271	147.691	-6.170	147.691	-6.069	147.691	-5.967	147.691
	0.037	-7.548	283.452	-7.447	283.452	-7.346	283.452	-7.349	283.452	-7.349	283.452
NPTS= 178	NPTS=	19		19		19		19		19	

TABLE 7, $\epsilon = 1/2$

		e=-2		e=-1		e=0		e=1		e=+2	
$\bar{q}_\theta$	z	m	θm	m	θm	m	θm	m	θm	m	θm
0.0											
	2.863	2.284	22.792	1.559	22.792	0.617	22.792	0.083	22.792	-0.651	22.792
	2.715	2.119	22.667	1.457	22.667	0.744	22.667	0.032	22.667	-0.681	22.667
	2.570	1.955	22.561	1.350	22.561	0.671	22.561	-0.020	22.561	-0.712	22.561
	2.445	1.941	22.476	1.270	22.476	0.598	22.476	-0.073	22.476	-0.775	22.476
	2.320	1.828	22.410	1.176	22.410	0.525	22.410	-0.127	22.410	-0.828	22.410
	2.203	1.715	22.363	1.083	22.363	0.451	22.363	-0.181	22.363	-0.879	22.363
	2.091	1.602	22.330	0.989	22.330	0.378	22.330	-0.236	22.330	-0.930	22.330
	1.985	1.486	22.309	0.895	22.309	0.304	22.309	-0.292	22.329	-0.980	22.329
	1.885	1.376	22.302	0.801	22.302	0.230	22.302	-0.349	22.302	-0.929	22.302
	1.789	1.263	22.376	0.706	22.376	0.149	22.376	-0.407	22.376	-0.984	22.376
	1.698	1.150	22.430	0.611	22.430	0.072	22.430	-0.467	22.430	-1.035	22.430
	1.612	1.036	22.507	0.515	22.507	-0.006	22.507	-0.527	22.507	-1.048	22.507
	1.529	0.922	22.606	0.419	22.606	-0.085	22.606	-0.589	22.606	-1.093	22.606
	1.451	0.808	22.729	0.321	22.729	-0.165	22.729	-0.652	22.729	-1.139	22.729
	0.306	-2.571	41.911	-2.716	41.911	-3.011	41.911	-3.306	41.911	-3.151	41.911
	0.235	-3.149	50.204	-3.263	50.264	-3.378	50.204	-3.492	50.204	-3.606	50.204
	0.164	-3.869	64.360	-3.949	64.360	-4.032	64.360	-4.115	64.360	-4.203	64.360
	0.109	-4.838	92.795	-4.888	92.795	-4.944	92.795	-5.000	92.795	-5.055	92.795
	0.052	-6.243	178.543	-6.456	178.543	-6.478	178.543	-6.505	178.543	-6.533	178.543
0.100											
	9.478	4.207	37.116	2.797	37.116	1.387	37.116	-0.022	37.116	-1.432	37.116
	8.131	3.651	34.573	2.606	34.573	1.280	34.573	-0.045	34.573	-1.371	34.573
	6.974	3.652	32.350	2.410	32.350	1.167	32.350	-0.076	32.350	-1.319	32.350
	5.976	3.359	30.414	2.207	30.414	1.054	30.414	-0.116	30.414	-1.276	30.414
	5.115	3.077	28.740	1.998	28.740	0.916	28.740	-0.175	28.740	-1.247	28.740
	4.369	2.783	27.308	1.780	27.308	0.777	27.308	-0.225	27.308	-1.226	27.308
	3.721	2.478	26.107	1.563	26.107	0.628	26.107	-0.307	26.107	-1.227	26.107
	3.159	2.163	25.130	1.346	25.130	0.466	25.130	-0.382	25.130	-1.231	25.130
	2.669	1.835	24.378	1.052	24.378	0.269	24.378	-0.494	24.378	-1.254	24.378
	2.241	1.492	23.863	0.793	23.863	0.095	23.863	-0.603	23.863	-1.302	23.863
	1.867	1.129	23.611	0.530	23.611	-0.120	23.611	-0.765	23.611	-1.379	23.611
	1.539	0.742	23.667	0.190	23.667	-0.362	23.667	-0.915	23.667	-1.467	23.667
	1.251	0.323	24.113	-0.157	24.113	-0.638	24.113	-1.118	24.113	-1.599	24.113
	0.999	-0.134	25.090	-0.568	25.090	-1.057	25.090	-1.547	25.090	-2.037	25.090
	0.776	-0.608	26.804	-1.098	26.804	-1.587	26.804	-2.077	26.804	-2.566	26.804
	0.581	-1.265	29.272	-1.935	29.272	-2.605	29.272	-3.274	29.272	-3.944	29.272
	0.409	-2.199	33.680	-2.911	33.680	-3.623	33.680	-4.336	33.680	-5.048	33.680
	0.260	-3.427	47.795	-4.211	47.795	-4.995	47.795	-5.779	47.795	-6.563	47.795
	0.120	-4.628	85.386	-5.696	85.386	-6.771	85.386	-7.828	85.386	-8.904	85.386
0.500											
	2.154	1.042	26.432	0.318	26.432	-0.838	26.432	-1.189	26.432	-1.939	26.432
	2.104	1.054	26.412	0.306	26.412	-0.843	26.412	-1.191	26.412	-1.939	26.412
	2.143	1.045	26.393	0.299	26.393	-0.847	26.393	-1.193	26.393	-1.939	26.393
	2.133	1.047	26.373	0.293	26.373	-0.851	26.373	-1.195	26.373	-1.939	26.373
	2.123	1.029	26.354	0.287	26.354	-0.855	26.354	-1.197	26.354	-1.939	26.354
	2.113	1.020	26.335	0.280	26.335	-0.859	26.335	-1.199	26.335	-1.939	26.335
	2.102	1.012	26.317	0.274	26.317	-0.863	26.317	-1.201	26.317	-1.939	26.317
	1.608	0.955	25.663	-0.041	25.663	-0.734	25.663	-1.386	25.663	-1.969	25.663
	1.418	0.807	25.676	-0.168	25.676	-0.843	25.676	-1.418	25.676	-1.993	25.676
	1.351	0.819	25.715	-0.138	25.715	-0.895	25.715	-1.452	25.715	-2.009	25.715
	1.287	0.829	25.780	-0.110	25.780	-0.953	25.780	-1.487	25.780	-2.020	25.780
	1.226	0.839	25.873	-0.085	25.871	-1.003	25.873	-1.525	25.873	-2.044	25.873
	1.167	-0.884	25.993	-0.056	25.993	-1.060	25.993	-1.564	25.993	-2.067	25.993
	1.111	-0.169	26.143	-0.031	26.143	-1.118	26.143	-1.605	26.143	-2.091	26.143
	0.298	-2.705	43.867	-2.916	43.867	-3.128	43.867	-3.339	43.867	-3.551	43.867
	0.237	-3.239	50.992	-3.350	50.992	-3.460	50.992	-3.570	50.992	-3.774	50.992
	0.181	-3.786	62.036	-3.858	62.036	-4.003	62.036	-4.112	62.036	-4.223	62.036
	0.129	-4.508	81.173	-4.557	81.173	-4.609	81.173	-4.745	81.173	-4.823	81.173
	0.068	-5.529	121.868	-5.575	121.868	-5.625	121.868	-5.675	121.868	-5.725	121.868
1.000											
	4.601	1.902	36.271	0.897	36.271	-0.107	36.271	-1.581	36.271	-2.455	36.271
	3.914	1.761	34.116	0.651	34.116	-0.369	34.116	-1.479	34.116	-2.559	34.116
	3.410	1.555	32.291	0.548	32.291	-0.469	32.291	-1.467	32.291	-2.475	32.291
	2.969	1.355	30.766	0.447	30.766	-0.525	30.766	-1.466	30.764	-2.403	30.764
	2.582	1.129	29.510	0.254	29.510	-0.602	29.510	-1.477	29.510	-2.345	29.510
	2.241	0.901	28.513	0.105	28.513	-0.700	28.513	-1.501	28.513	-2.301	28.513
	1.937	0.668	27.768	-0.065	27.768	-0.904	27.768	-1.538	27.768	-2.265	27.765
	1.673	0.420	27.274	-0.244	27.274	-1.021	27.274	-1.592	27.274	-2.262	27.274
	1.436	0.161	27.045	-0.447	27.045	-1.155	27.045	-1.663	27.045	-2.271	27.045
	1.225	-0.115	27.107	-0.692	27.107	-1.268	27.107	-1.755	27.107	-2.332	27.107
	1.036	-0.412	27.509	-0.998	27.509	-1.389	27.509	-1.871	27.509	-2.356	27.509
	0.869	-0.734	28.331	-1.361	28.331	-1.534	28.331	-2.017	28.331	-2.845	28.331
	0.716	-1.088	29.767	-1.759	29.767	-1.669	29.767	-2.200	29.707	-2.745	29.767
	0.580	-1.480	31.867	-1.741	31.867	-2.115	31.867	-2.425	31.867	-2.744	31.867
	0.458	-1.909	35.235	-2.204	35.235	-2.463	35.235	-2.722	35.235	-3.231	35.235
	0.346	-2.350	40.665	-2.675	40.665	-3.011	40.665	-3.348	40.665	-3.811	40.665
	0.248	-3.175	50.159	-3.327	50.159	-3.480	50.159	-3.632	50.159	-3.786	50.159
	0.157	-4.119	69.738	-4.215	69.738	-4.315	69.738	-4.416	69.738	-4.516	69.738
	0.075	-5.617	129.520	-5.687	129.520	-5.777	129.520	-5.826	129.520	-5.876	129.520
DPI= 100	NPTS=	19		19		19		19		19	

TABLE 8, ϵ=.92

$\bar{q}_o$	z	e=-2 m	e=-2 θm	e=-1 m	e=-1 θm	e=0 m	e=0 θm	e=1 m	e=1 θm	e=2 m	e=2 θm
0.0											
	4.476	3.090	28.667	1.356	28.207	-0.378	28.007	-2.113	28.007	-3.847	28.007
	4.466	3.081	27.571	1.346	27.571	-0.388	27.571	-2.389	27.571	-4.705	27.571
	4.263	2.911	27.157	1.252	27.157	-0.407	27.157	-2.080	27.157	-3.724	27.157
	4.069	2.660	26.764	1.109	26.764	-0.422	26.764	-2.044	26.764	-3.665	26.764
	3.963	2.738	26.392	1.104	26.392	-0.439	26.392	-2.023	26.392	-3.607	25.392
	3.743	2.536	26.040	1.085	26.040	-0.457	26.040	-2.008	26.340	-3.550	26.040
	3.521	2.547	25.709	1.033	25.709	-0.477	25.709	-1.986	25.709	-3.495	25.709
	3.365	2.447	25.399	0.975	25.399	-0.497	25.399	-1.969	25.399	-3.441	25.399
	3.200	2.341	25.107	0.916	25.107	-0.519	25.107	-1.954	25.107	-3.339	25.107
	3.054	2.234	24.840	0.856	24.840	-0.542	24.840	-1.940	24.840	-3.338	24.840
	2.907	2.156	24.591	0.795	24.591	-0.566	24.591	-1.926	24.591	-3.283	24.591
	2.760	2.057	24.363	0.732	24.363	-0.591	24.363	-1.917	24.363	-3.243	24.363
	2.631	1.956	24.157	0.668	24.157	-0.620	24.157	-1.908	24.157	-3.178	24.157
	2.500	1.853	23.971	0.602	23.971	-0.649	23.971	-1.901	23.971	-3.152	23.971
	0.521	-1.631	31.161	-1.650	31.161	-2.769	31.161	-3.888	31.161	-5.107	31.161
	0.427	-2.315	35.900	-2.345	35.900	-3.483	35.900	-4.017	35.900	-5.251	35.900
	0.284	-2.739	44.141	-2.989	44.141	-3.735	44.141	-5.488	44.141	-5.738	44.141
	0.181	-3.716	61.090	-3.804	61.090	-4.050	61.090	-4.216	61.090	-4.381	61.090
	0.080	-5.421	112.789	-5.403	112.789	-5.456	112.789	-5.569	112.789	-5.651	112.789
0.100											
	23.379	5.914	66.510	2.482	66.510	-0.550	66.510	-3.781	66.510	-7.313	66.510
	19.539	5.612	59.188	2.554	59.188	-0.505	59.188	-3.564	59.188	-6.621	59.188
	16.311	5.305	52.946	2.418	52.946	-0.467	52.946	-3.352	52.946	-6.237	52.946
	13.525	4.929	47.363	2.245	47.363	-0.437	47.363	-3.150	47.363	-5.862	47.363
	11.310	4.654	42.638	2.124	42.638	-0.416	42.638	-2.956	42.631	-5.550	42.638
	9.387	4.321	38.565	1.962	38.565	-0.435	38.566	-2.773	38.565	-5.161	38.566
	7.768	3.968	35.073	1.791	35.073	-0.405	35.073	-2.602	35.073	-4.799	35.073
	6.403	3.637	32.098	1.604	32.098	-0.419	32.098	-2.444	32.094	-4.467	32.094
	5.254	3.241	29.592	1.466	29.589	-0.448	29.589	-2.303	29.587	-4.157	29.592
	4.285	2.874	27.514	1.189	27.514	-0.468	27.514	-2.189	27.514	-3.864	27.514
	3.467	2.562	25.850	0.949	25.850	-0.565	25.850	-2.077	25.853	-3.593	25.850
	2.777	2.027	24.599	0.603	24.599	-0.662	24.555	-2.036	24.585	-3.350	24.599
	2.195	1.567	23.788	0.312	23.788	-0.724	23.788	-1.944	23.788	-3.163	23.788
	1.704	1.143	23.490	0.017	23.490	-0.967	23.490	-1.975	23.490	-2.982	23.490
	1.289	0.868	23.865	-0.369	23.865	-1.207	23.865	-2.065	23.865	-2.862	23.865
	0.938	-0.125	25.259	-1.106	25.259	-1.519	25.261	-2.233	25.253	-2.972	25.259
	0.642	-0.698	28.539	-1.497	28.539	-1.801	28.539	-2.502	28.539	-3.004	28.539
	0.391	-2.067	36.278	-2.320	36.278	-2.724	36.278	-3.058	36.278	-3.392	36.278
	0.179	-3.738	61.505	-3.995	61.505	-4.072	61.505	-4.239	61.505	-4.406	61.505
0.500											
	3.329	2.331	25.894	0.928	25.894	-0.674	25.894	-2.177	25.894	-3.680	25.894
	3.311	2.323	25.867	0.924	25.867	-0.676	25.867	-2.179	25.867	-3.679	25.867
	3.297	2.315	25.840	0.919	25.840	-0.677	25.840	-2.179	25.840	-3.677	25.840
	3.284	2.307	25.815	0.915	25.815	-0.679	25.815	-2.172	25.815	-3.665	25.815
	3.271	2.299	25.788	0.910	25.788	-0.680	25.788	-2.170	25.788	-3.660	25.788
	3.257	2.292	25.762	0.905	25.762	-0.682	25.762	-2.168	25.762	-3.655	25.762
	3.244	2.284	25.736	0.900	25.736	-0.683	25.736	-2.167	25.736	-3.650	25.736
	2.991	1.905	24.281	0.659	24.281	-0.817	24.281	-2.073	24.281	-3.329	24.281
	2.229	1.665	24.164	0.384	24.164	-0.911	24.164	-2.065	24.164	-3.220	24.164
	2.200	1.522	24.023	0.328	24.023	-0.866	24.023	-2.039	24.023	-3.213	24.023
	2.104	1.413	23.919	0.271	23.919	-0.922	23.917	-2.054	23.917	-3.187	23.919
	2.011	1.303	23.833	0.212	23.833	-0.980	23.833	-2.051	23.833	-3.182	23.831
	1.920	1.252	23.766	0.151	23.766	-0.964	23.766	-2.042	23.766	-3.169	23.769
	1.835	1.139	23.717	0.099	23.717	-0.980	23.717	-2.044	23.717	-3.113	23.717
	0.583	-1.241	31.674	-1.999	31.674	-2.367	31.674	-3.786	31.674	-3.624	31.674
	0.488	-2.021	35.436	-2.309	35.436	-2.711	35.436	-3.007	35.436	-3.483	35.436
	0.304	-2.627	42.370	-2.880	42.370	-3.152	42.370	-3.525	42.370	-3.897	42.370
	0.215	-3.259	53.695	-3.509	53.695	-3.739	53.695	-3.918	53.695	-4.159	53.695
	0.133	-4.367	78.025	-4.515	78.025	-4.603	78.025	-4.772	78.025	-4.930	78.025
1.000											
	13.065	4.778	48.673	2.643	48.673	-0.691	48.673	-1.428	48.673	-6.160	48.673
	11.180	4.500	43.960	1.974	43.960	-0.666	43.960	-3.240	43.960	-5.808	43.960
	9.538	4.213	40.171	1.698	40.171	-0.636	40.171	-3.071	40.171	-5.505	40.171
	8.134	3.961	36.967	1.605	36.967	-0.621	36.967	-2.905	36.967	-5.172	36.967
	6.925	3.681	34.140	1.503	34.140	-0.614	34.140	-2.752	34.140	-4.889	34.140
	5.895	3.382	31.710	1.382	31.710	-0.618	31.710	-2.595	31.710	-4.595	31.710
	4.998	3.159	29.635	1.280	29.635	-0.634	29.635	-2.428	29.635	-4.351	29.635
	4.209	2.931	27.862	1.031	27.862	-0.654	27.862	-2.312	27.862	-3.969	27.862
	3.487	2.656	26.407	0.843	26.407	-0.709	26.407	-2.262	26.407	-3.814	26.407
	2.942	2.463	25.253	0.670	25.253	-0.779	25.253	-2.161	25.253	-3.543	25.253
	2.365	1.969	24.411	0.451	24.411	-0.810	24.411	-2.124	24.411	-3.438	24.411
	1.966	1.647	23.909	0.168	23.909	-0.975	23.909	-2.098	23.909	-3.219	23.909
	1.575	1.183	23.805	-0.193	23.805	-1.124	23.805	-2.102	23.805	-3.080	23.805
	1.245	0.905	24.212	-0.502	24.212	-1.319	24.212	-2.125	24.212	-2.931	24.212
	0.959	-0.134	25.346	-0.859	25.346	-1.570	25.346	-2.275	25.346	-2.980	25.346
	0.710	-0.731	27.658	-1.306	27.658	-1.951	27.658	-2.576	27.658	-3.201	27.658
	0.494	-1.477	32.215	-1.922	32.215	-2.607	32.215	-2.803	32.215	-3.538	32.215
	0.306	-2.598	42.260	-2.874	42.260	-3.149	42.260	-3.485	42.260	-3.760	42.260
	0.162	-4.243	73.697	-4.361	73.697	-4.519	73.697	-4.657	73.697	-4.794	73.697
NPTS= 136	NPTS=	19		19		19		19		19	

TABLE 9

$\frac{z}{d}$	η
2	1.51
2.5	1.48
3	1.46
3.5	1.45

TABLE 10

ζ	$m-m_o(\eta=0)$	$m-m_o(\eta$ as in Table 9)
2	2.02	-.68
2.5	2.56	-.45
3	3.01	-.28
3.5	3.38	-.16

TABLE 11

z	$\epsilon = -1$	$\epsilon = -1/2$
2	-1.70	-2.2
2.5	-1.63	-2.16
3	-1.68	-2.13
3.5	-1.67	-2.11

TABLE 12

z	$m-m_o$ (= -1)	$m-m_o$ (= -1/2)
2	-1.35	-1.35
2.5	-1.75	-0.95
3	-1.70	-0.83
3.5	-1.63	-0.73

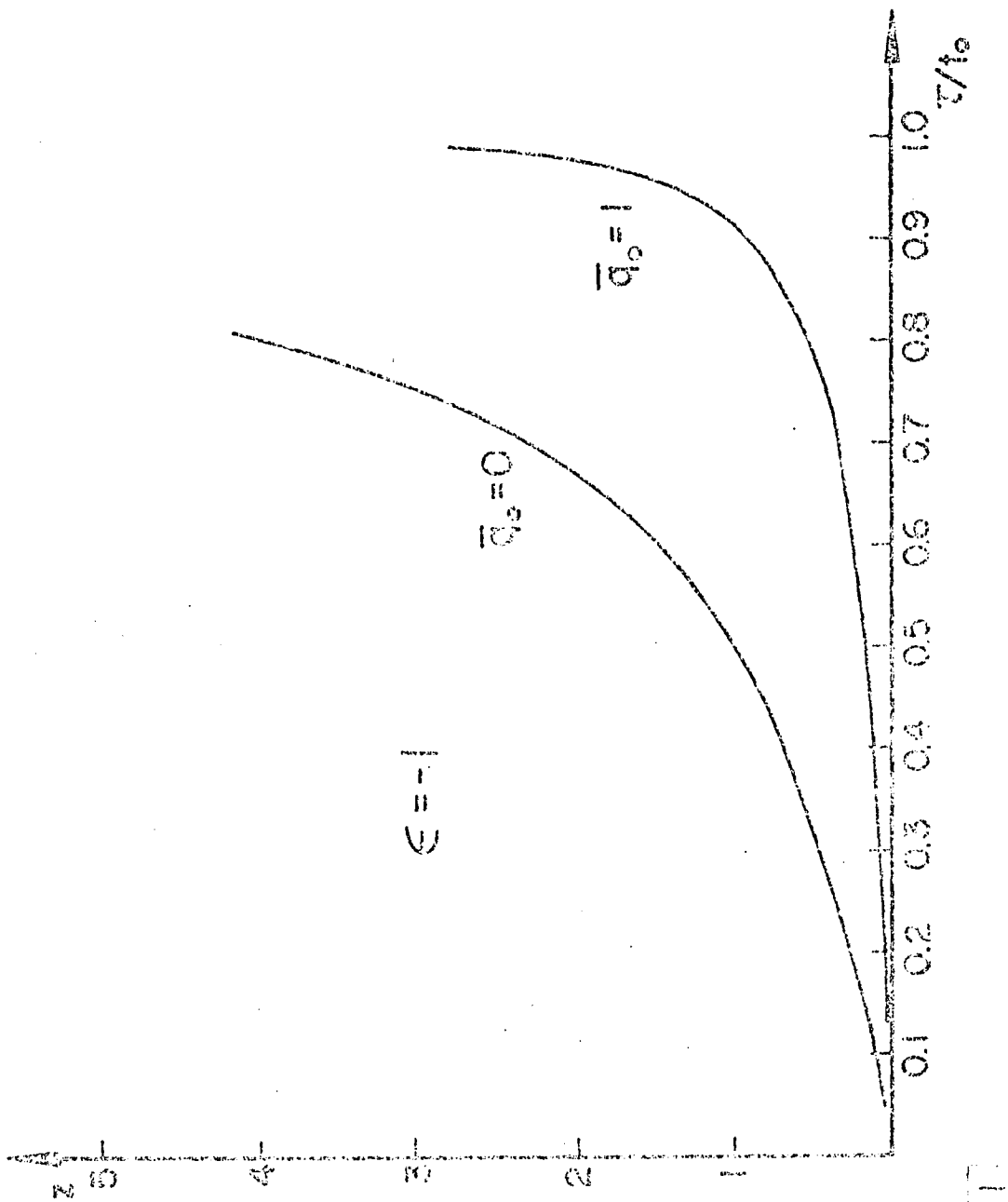
τ/τ_0
0.1
0.2
0.3
0.4
0.5
0.6
0.7
0.8
0.9
1.0
1
2
3
4
5
$\frac{\tau}{\tau_0} = 0$
$\frac{\tau}{\tau_0} = 0.9$

FIG. 1

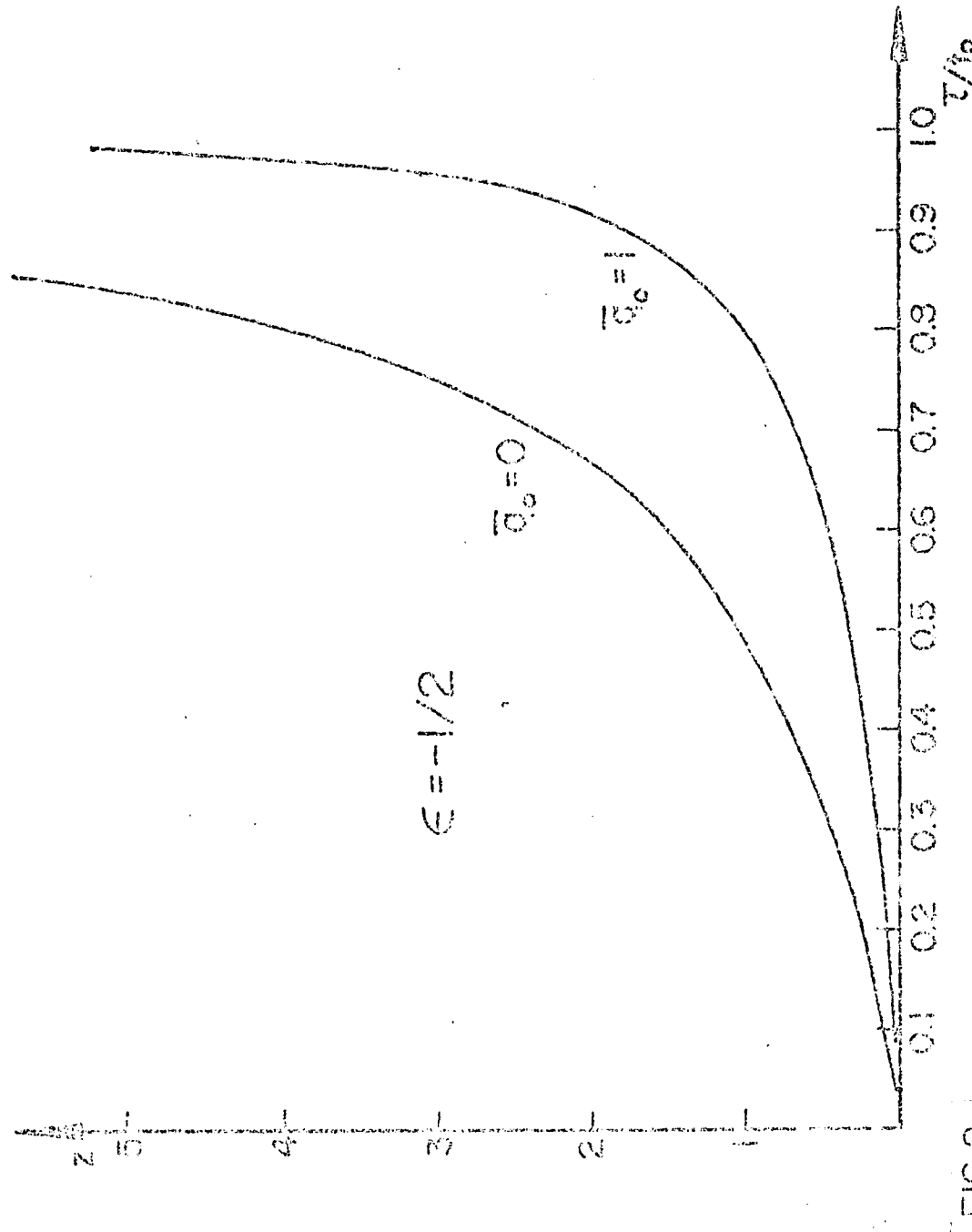
τ/τ_0
1.0
0.9
0.8
0.7
0.6
0.5
0.4
0.3
0.2
0.1
$\varepsilon = -1/2$
$\tau_0 = 0$
$\tau_0 = 1$
2
3
4
5
6

FIG. 2

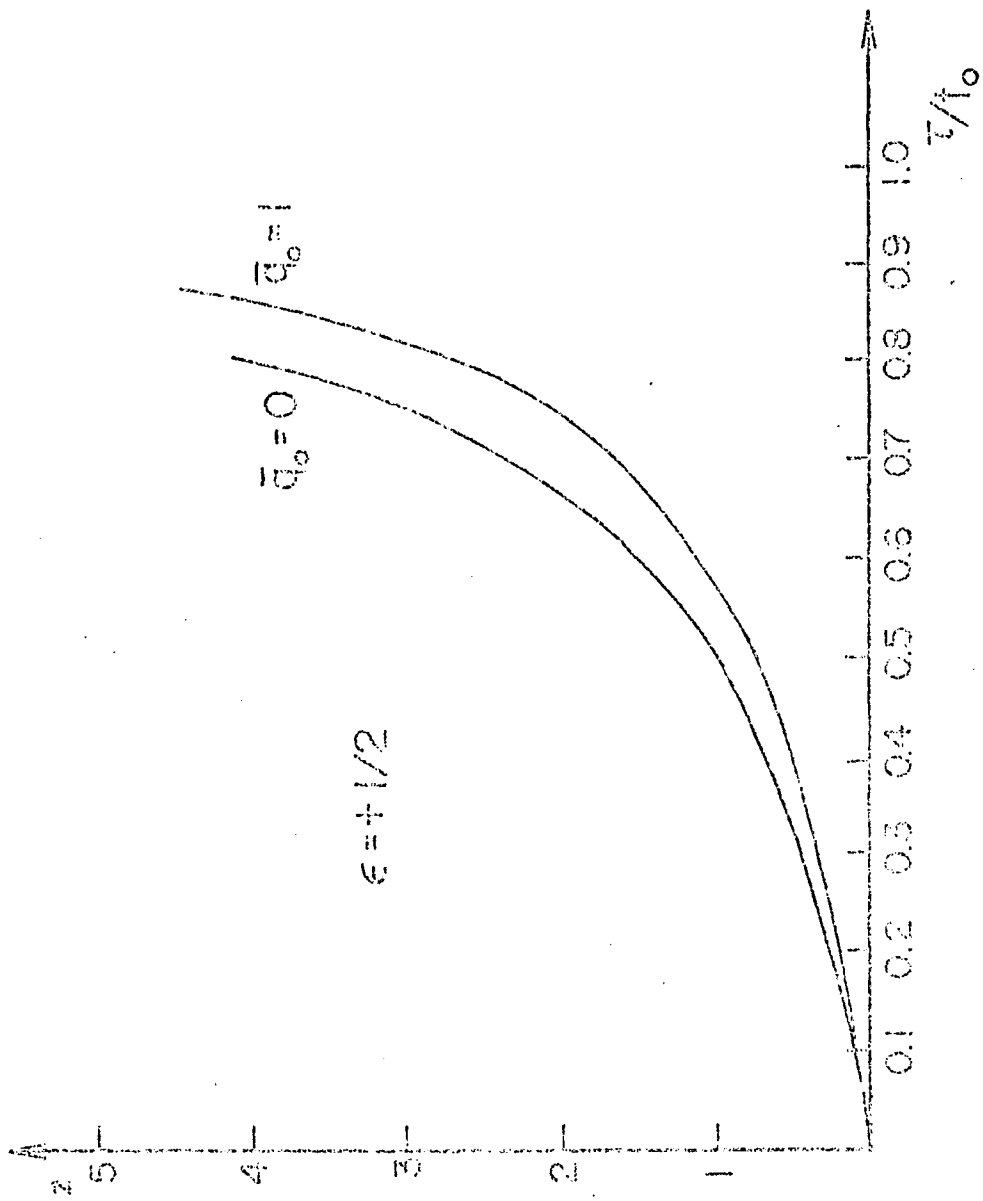
τ/τ_0
0.1 0.2 0.3 0.4 0.5 0.6 0.7 0.8 0.9 1.0
$\theta = 15°$
$\theta = 15°$
$\varepsilon = +1/2$
1 2 3 4 5

FIG. 4

FIG. 5

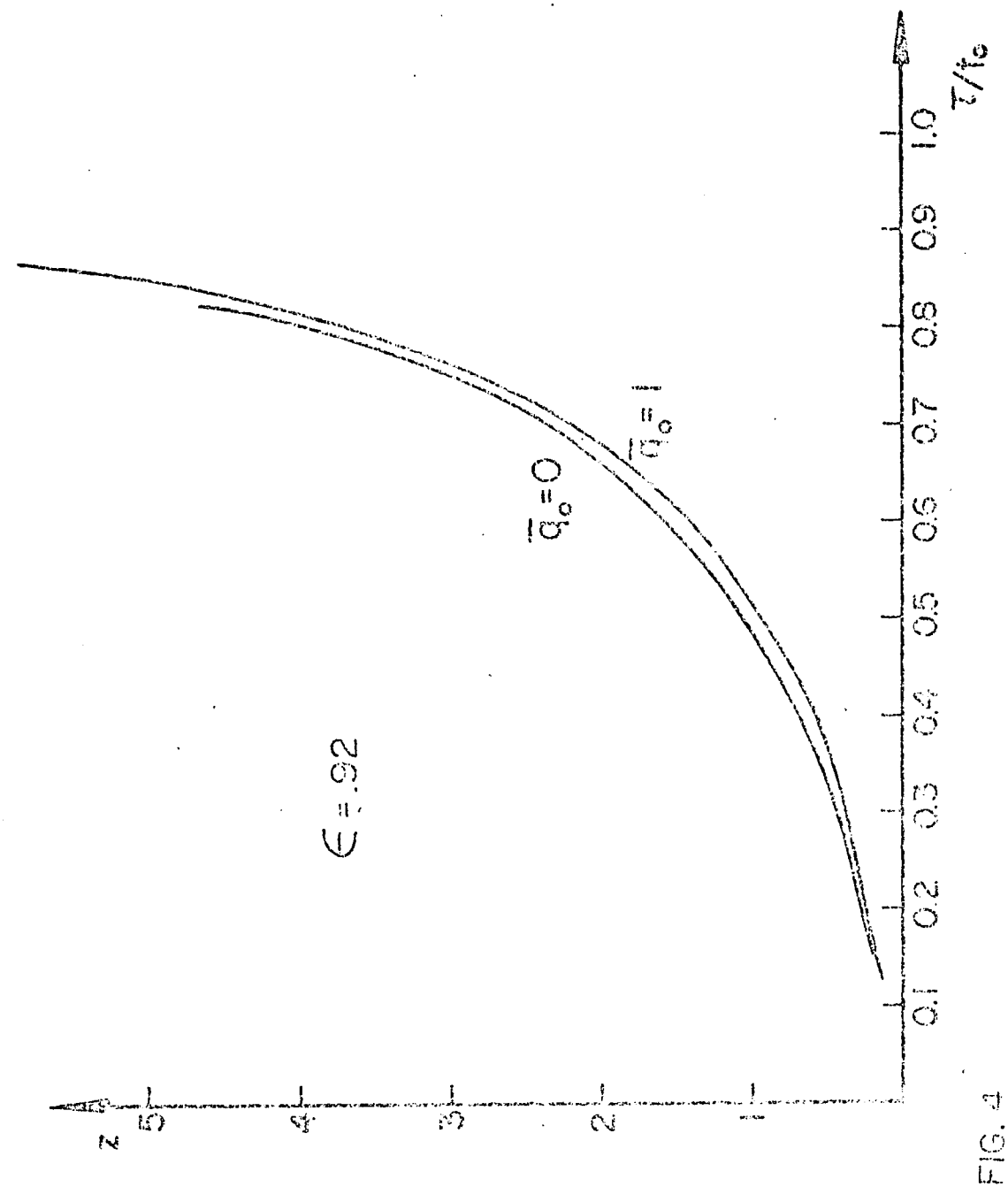
τ/t_0
0.1
0.2
0.3
0.4
0.5
0.6
0.7
0.8
0.9
1.0
$\overline{\theta_0}=0$
$\overline{\theta_0}=1$
$\epsilon=.92$
1
2
3
4
5
N

FIG. 1

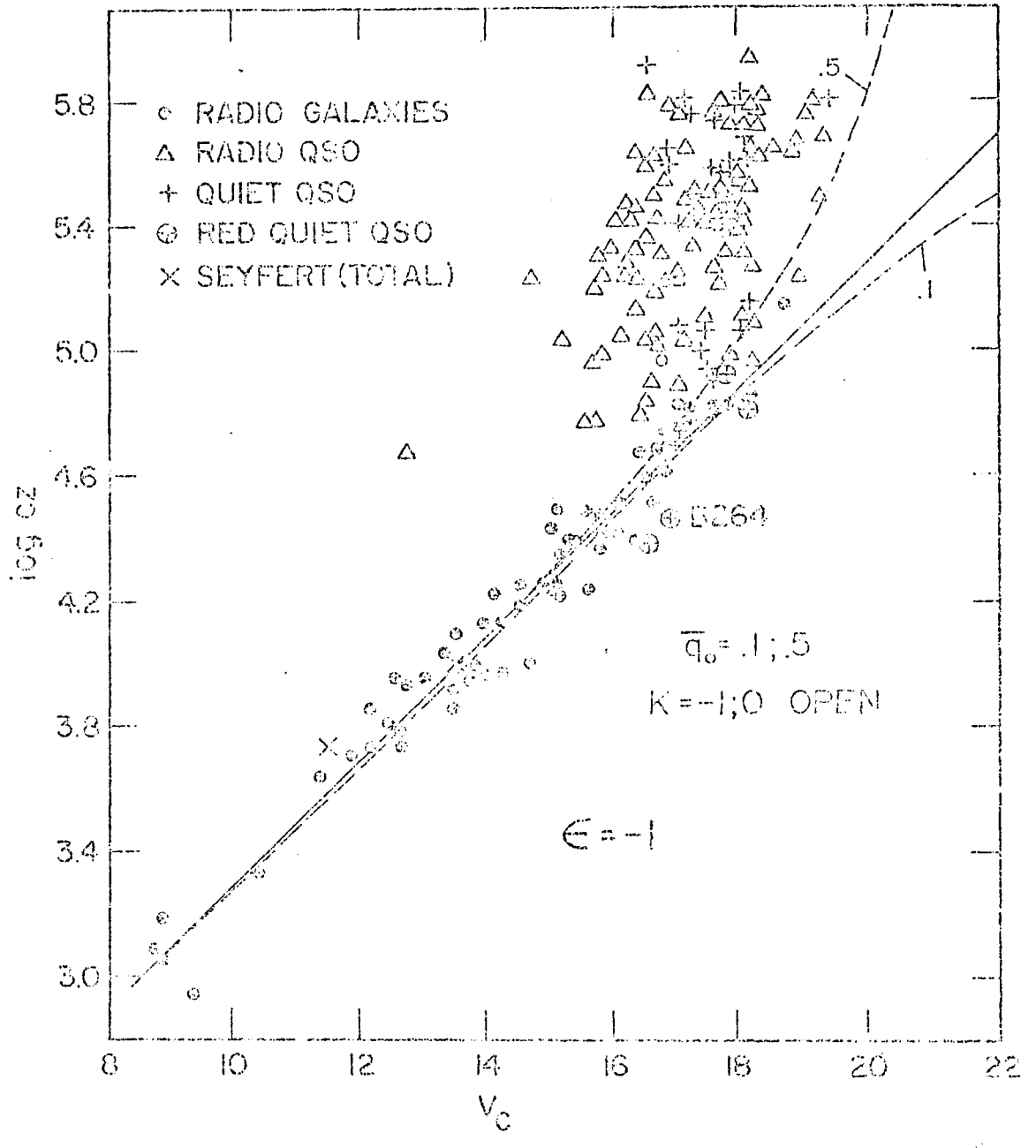
RADIO GALAXIES
RADIO QSO
QUIET QSO
RED QUIET QSO
SEYFERT (TOTAL)
.5
.1
5.8
5.4
5.0
4.6
4.2
3.8
3.4
3.0
log S
8
10
12
14
16
18
20
22
V_c
3C 295
$\overline{q}_o$ = .1 ; .5
K = -1 ; 0 OPEN
ϵ = -1

FIG. 5

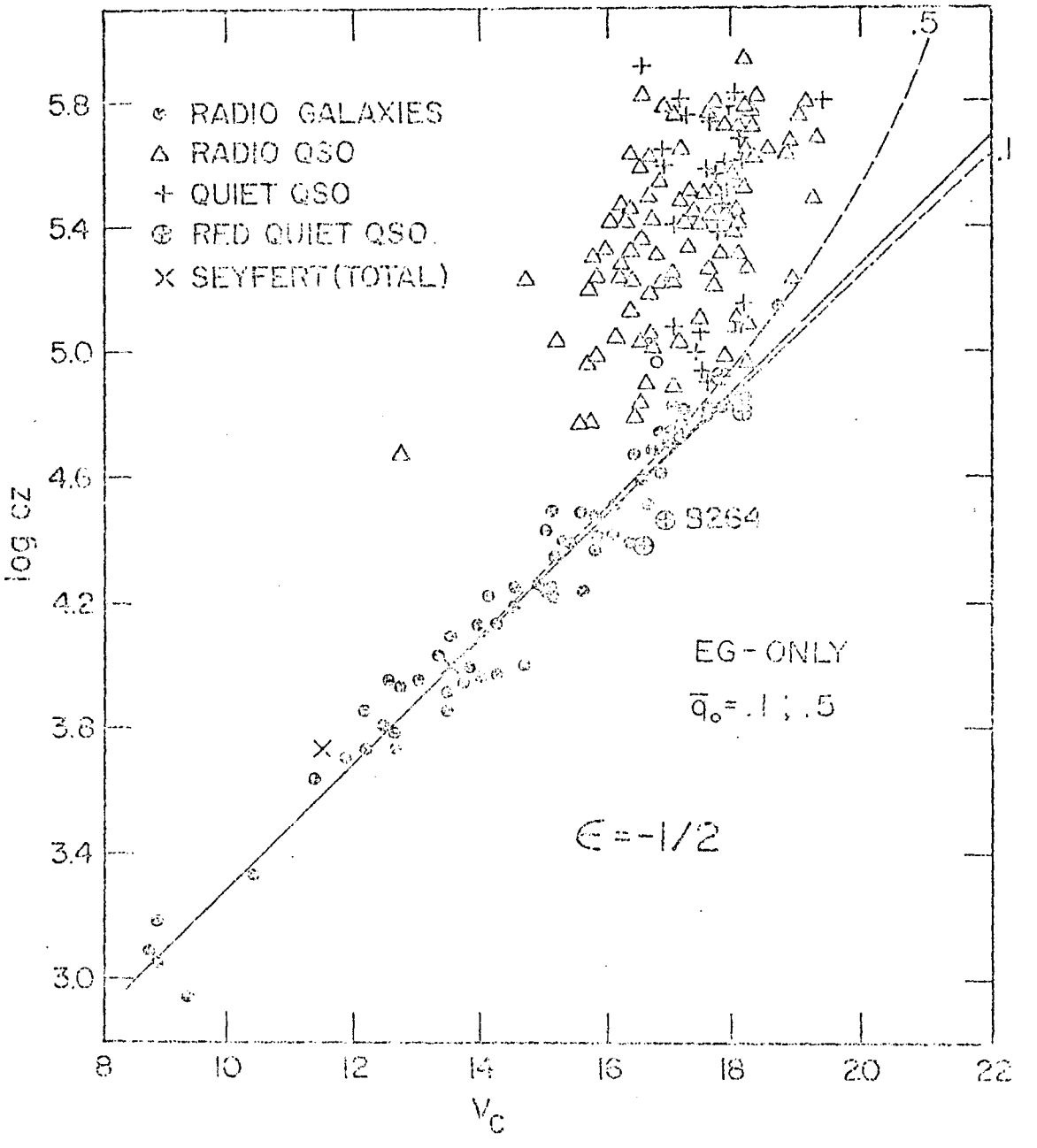
RADIO GALAXIES
RADIO QSO
QUIET QSO
RED QUIET QSO
SEYFERT (TOTAL)
3264
EG - ONLY
$\bar{q}_o = .1 ; .5$
$\epsilon = -1/2$
.5
.1
log cz
V_c
5.8
5.4
5.0
4.6
4.2
3.8
3.4
3.0
8
10
12
14
16
18
20
22

FIG. 6

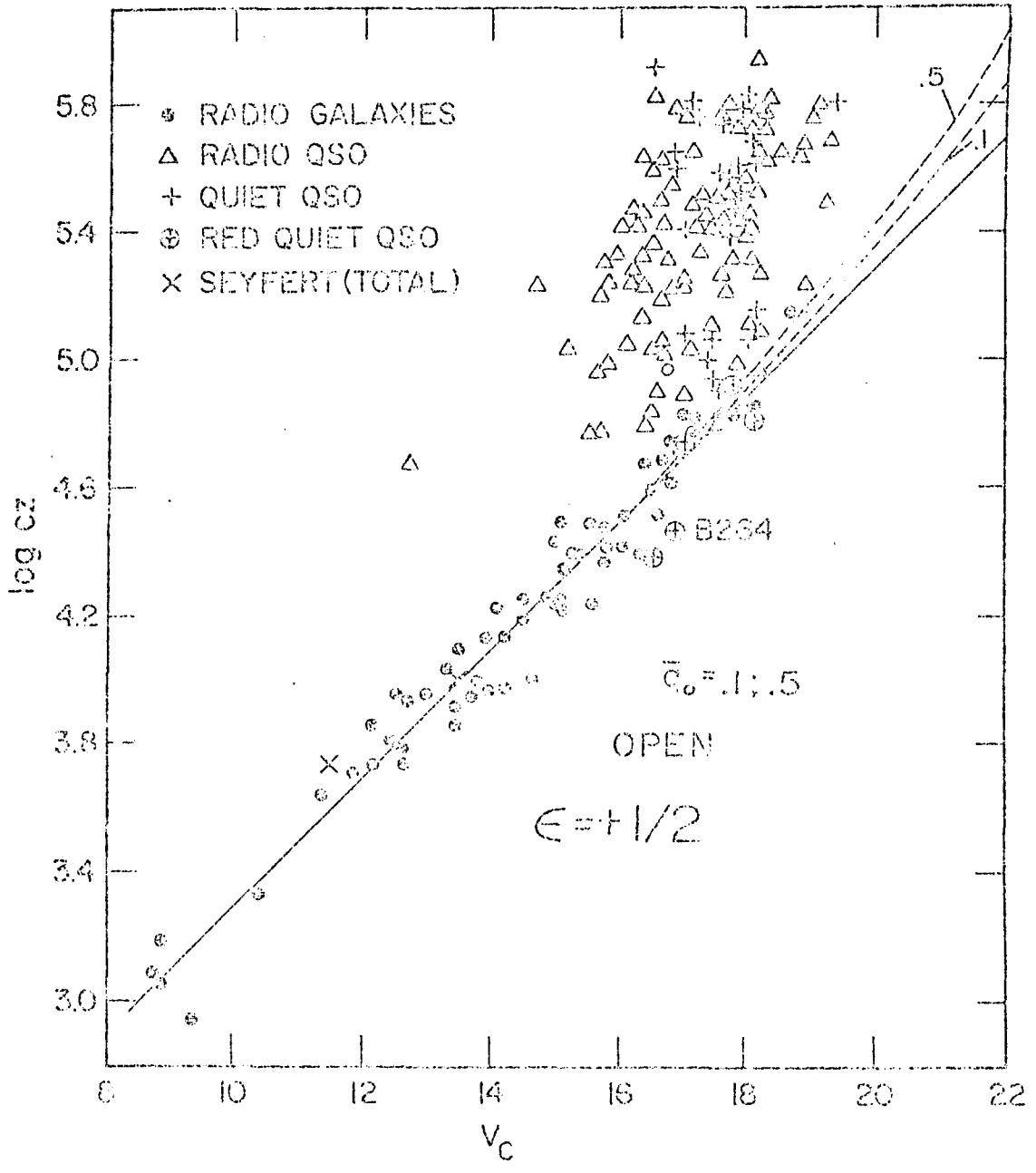
RADIO GALAXIES
RADIO QSO
QUIET QSO
RED QUIET QSO
SEYFERT (TOTAL)
.5
.1
B2134
$\bar{\sigma}_o$ = .1 ; .5
OPEN
ϵ = +1/2
log cz
V_c
5.8
5.4
5.0
4.6
4.2
3.8
3.4
3.0
8
10
12
14
16
18
20
22

FIG. 7

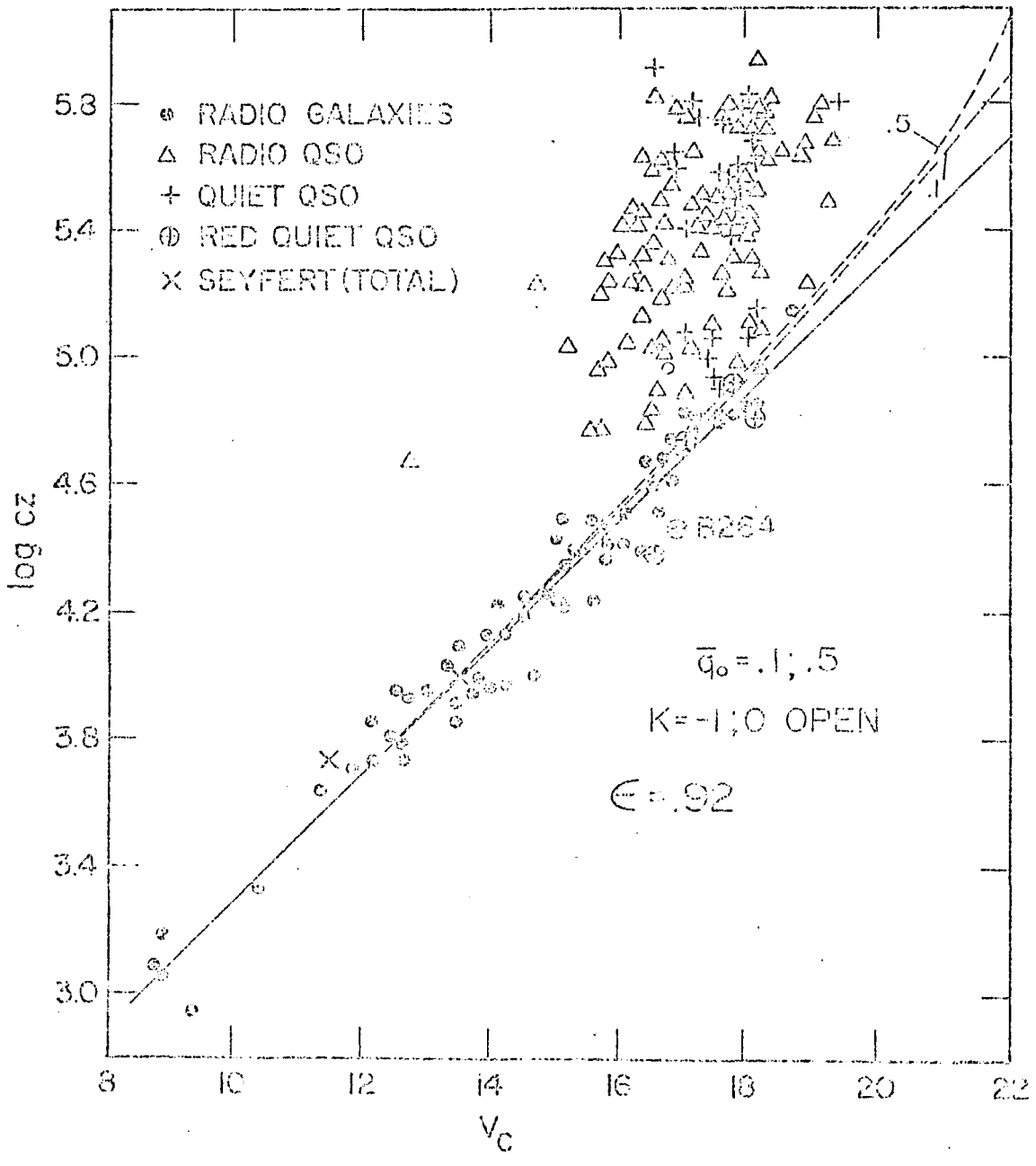
RADIO GALAXIES
RADIO QSO
QUIET QSO
RED QUIET QSO
SEYFERT (TOTAL)
.5
.1
3C 264
$\bar{q}_o = .1; .5$
K = -1; 0 OPEN
$\in = .92$
log cz
V_c
5.8
5.4
5.0
4.6
4.2
3.8
3.4
3.0
8
10
12
14
16
18
20
22

FIG. 9

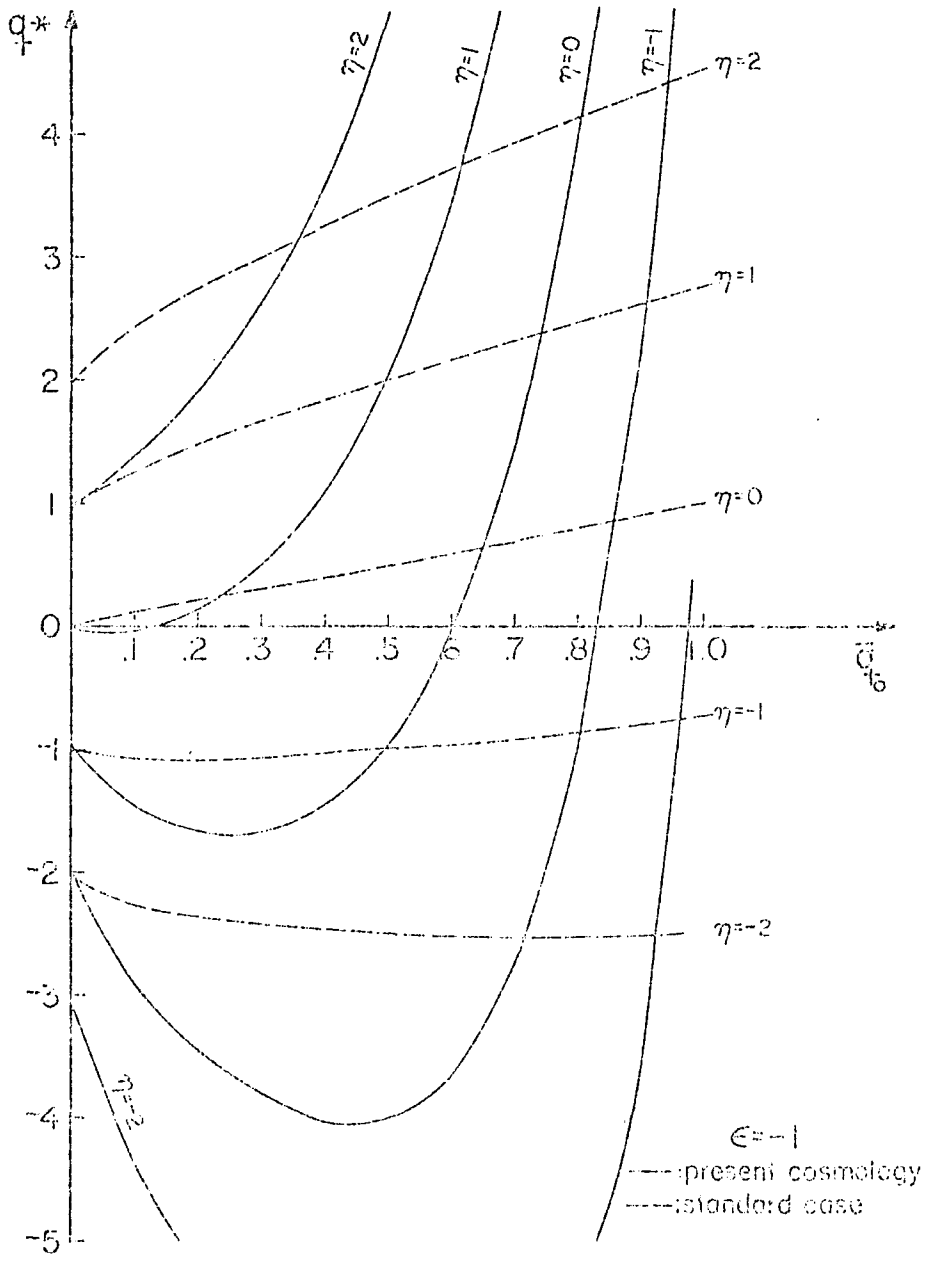
q*
4
3
2
1
0
-1
-2
-3
-4
-5
.1
.2
.3
.4
.5
.6
.7
.8
.9
1.0
$\frac{a}{a_0}$
$\eta=2$
$\eta=1$
$\eta=0$
$\eta=-1$
$\eta=-2$
$\epsilon=-1$
present cosmology
standard case

FIG. 9

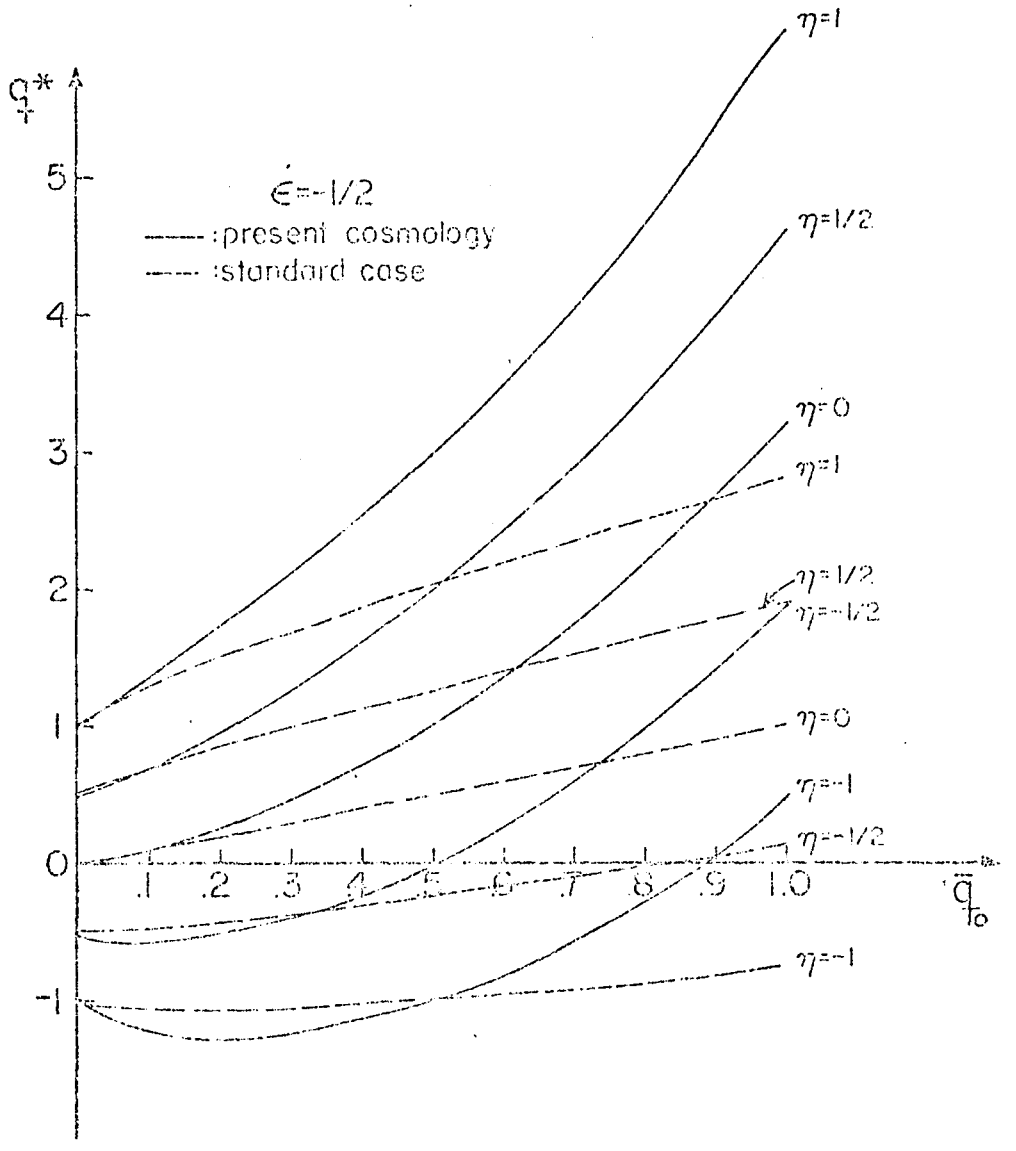
q_T^*
5
4
3
2
1
0
-1
ϵ=-1/2
——:present cosmology
---- :standard case
η=1
η=1/2
η=0
η=1
η=1/2
η=-1/2
η=0
η=-1
η=-1/2
η=-1
.1
.2
.3
.4
.5
.6
.7
.8
.9
1.0
$\bar{q}_{T_0}$

FIG. 10

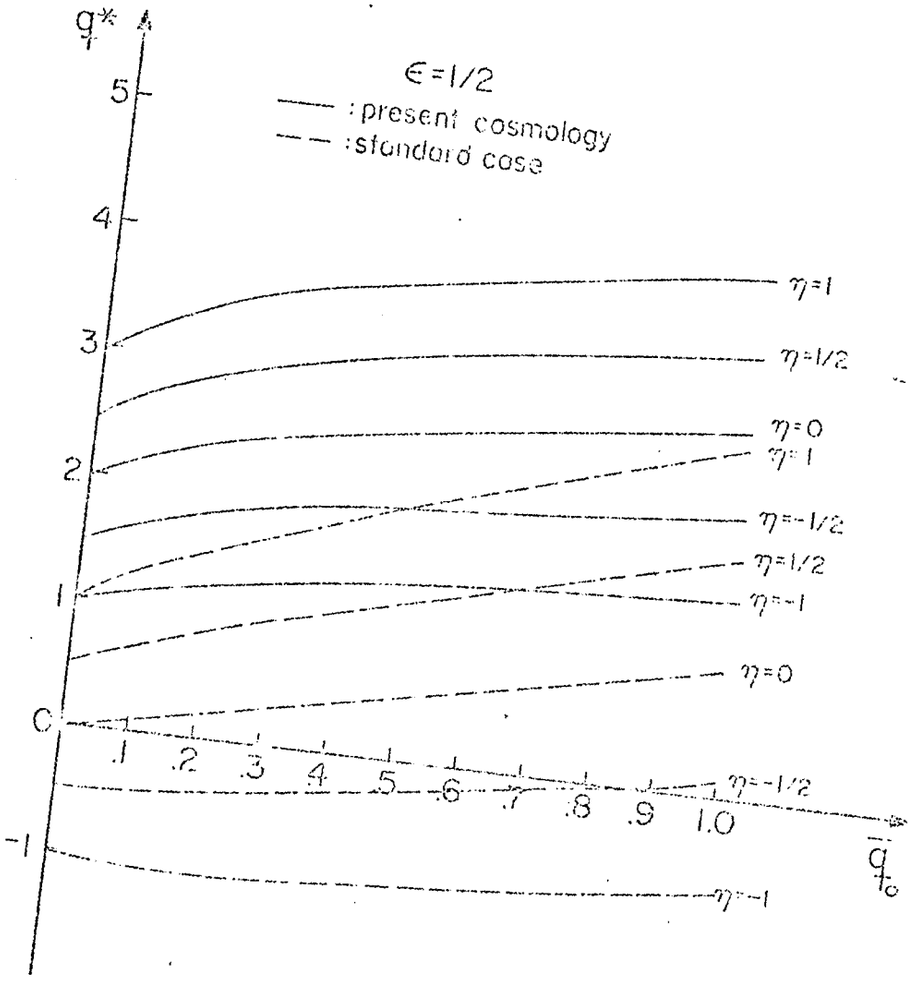
q*
5
4
3
2
1
0
-1
ε=1/2
: present cosmology
: standard case
η=1
η=1/2
η=0
η=1
η=-1/2
η=1/2
η=-1
η=0
η=-1/2
η=-1
.1
.2
.3
.4
.5
.6
.7
.8
.9
1.0
q0

FIG. 11

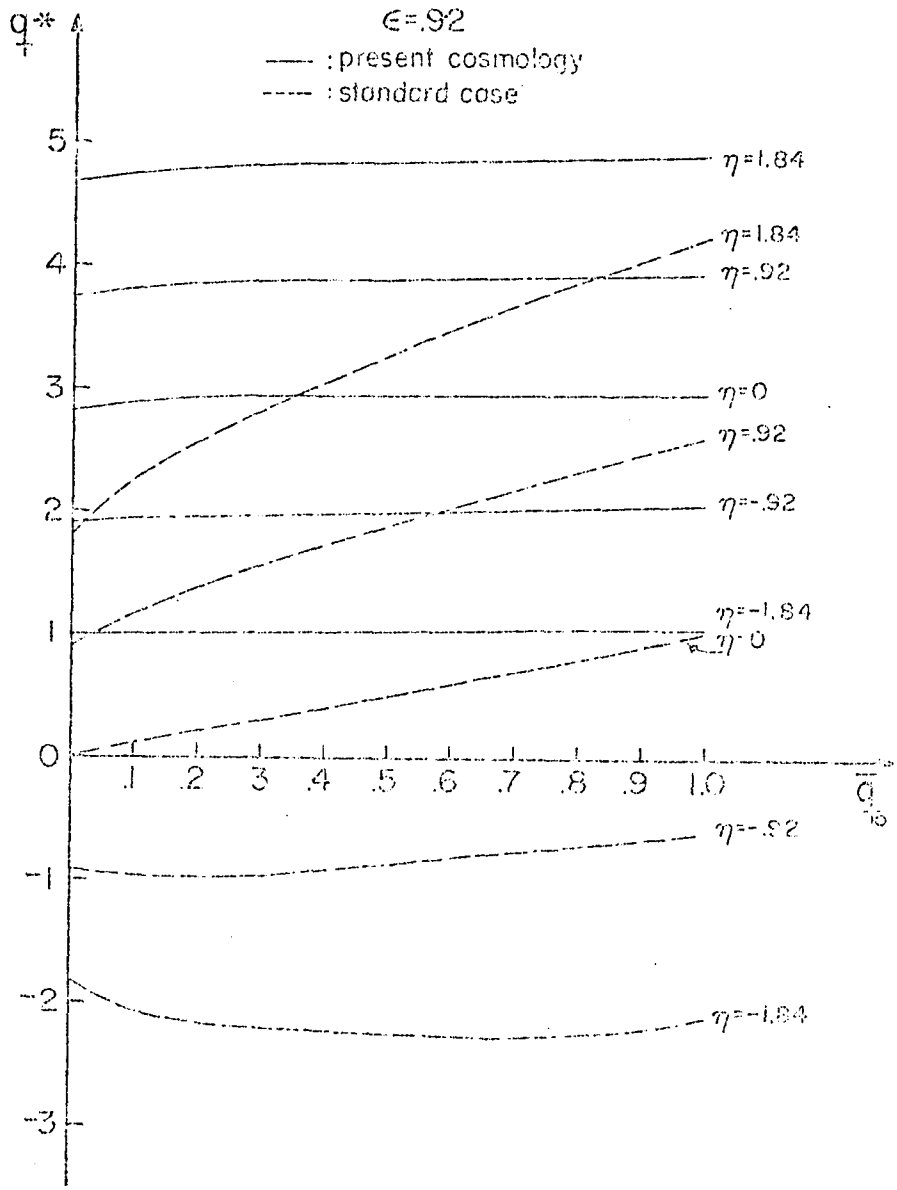
q_+^*
ϵ=.92
—— : present cosmology
---- : standard case
5
4
3
2
1
0
-1
-2
-3
η=1.84
η=1.84
η=.92
η=0
η=.92
η=-.92
η=-1.84
η=0
.1 .2 .3 .4 .5 .6 .7 .8 .9 1.0
$\bar{q}_{10}$
η=-.92
η=-1.84

FIG.12

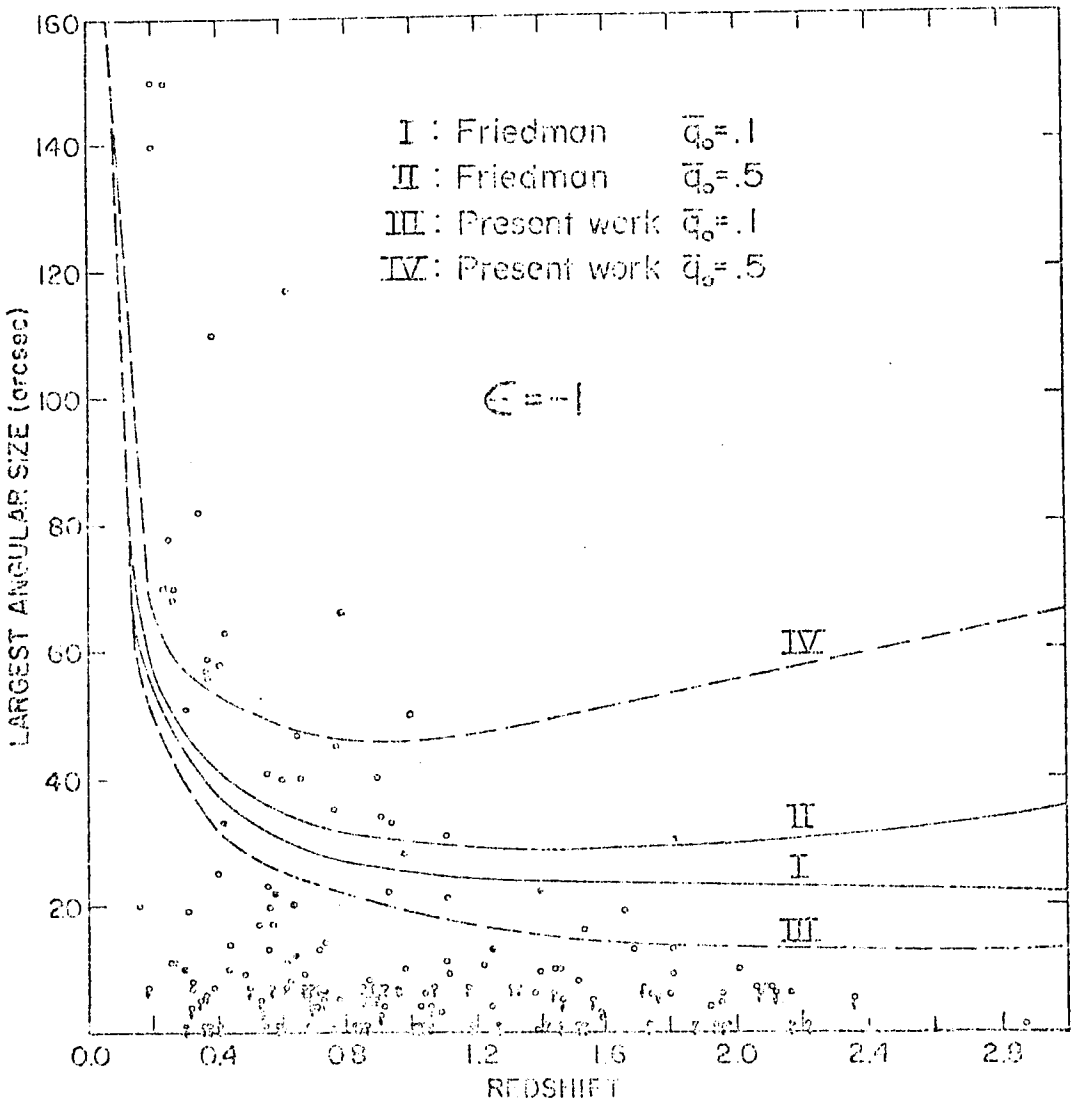
I : Friedman $\bar{q}_o$=.1
II : Friedman $\bar{q}_o$=.5
III : Present work $\bar{q}_o$=.1
IV : Present work $\bar{q}_o$=.5
ϵ = -1
LARGEST ANGULAR SIZE (arcsec)
REDSHIFT
160
140
120
100
80
60
40
20
0.0
0.4
0.8
1.2
1.6
2.0
2.4
2.8

FIG.13

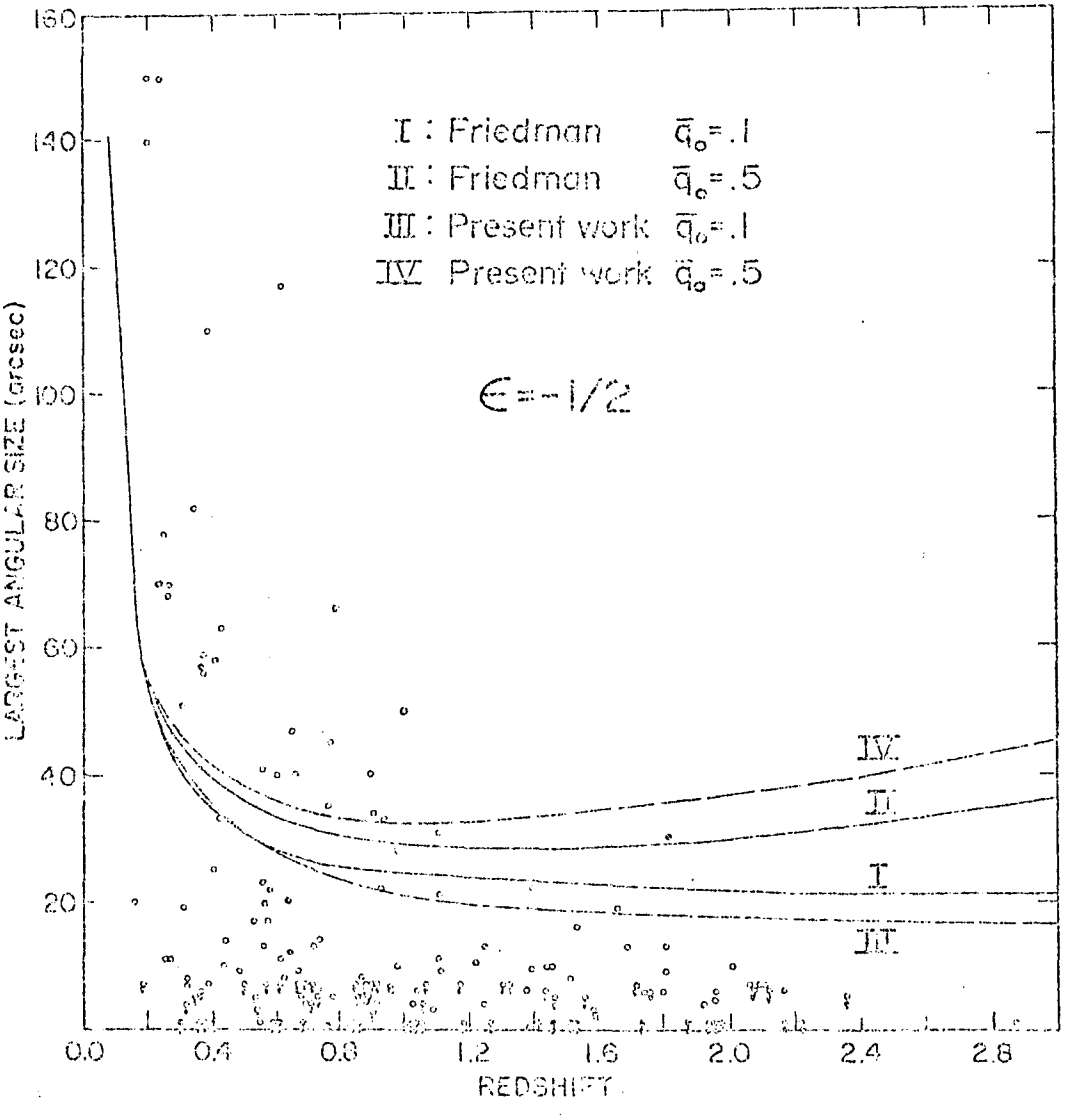
I : Friedman $\bar{q}_o = .1$
II : Friedman $\bar{q}_o = .5$
III : Present work $\bar{q}_o = .1$
IV Present work $\bar{q}_o = .5$
$\epsilon = -1/2$
LARGEST ANGULAR SIZE (arcsec)
REDSHIFT
160
140
120
100
80
60
40
20
0.0
0.4
0.8
1.2
1.6
2.0
2.4
2.8
IV
II
I
III

FIG. 14

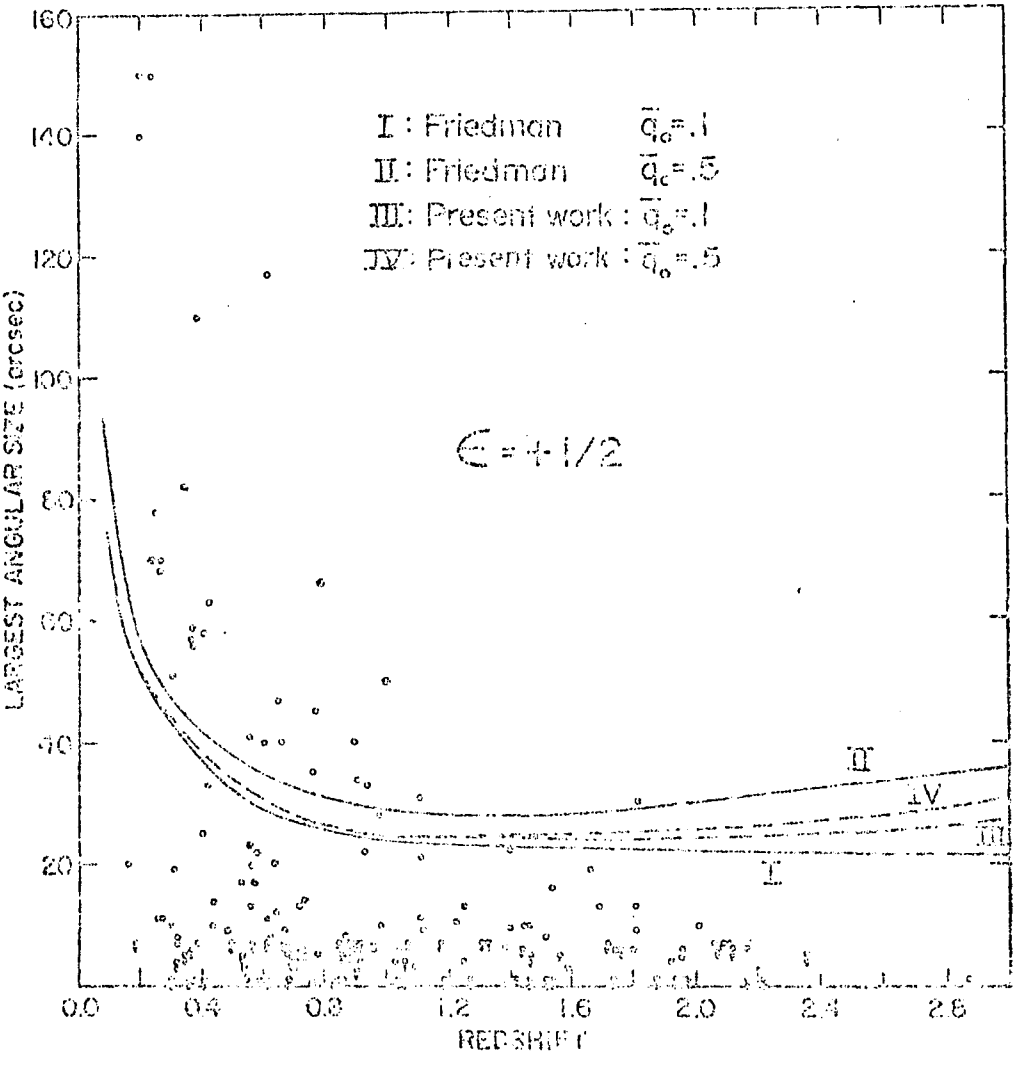
I : Friedman $\bar{q}_o$=.1
II : Friedman $\bar{q}_o$=.5
III : Present work : $\bar{q}_o$=.1
IV : Present work : $\bar{q}_o$=.5
ϵ = +1/2
LARGEST ANGULAR SIZE (arcsec)
REDSHIFT
160
140
120
100
80
60
40
20
0.0
0.4
0.8
1.2
1.6
2.0
2.4
2.8
I
II
III
IV

FIG.15

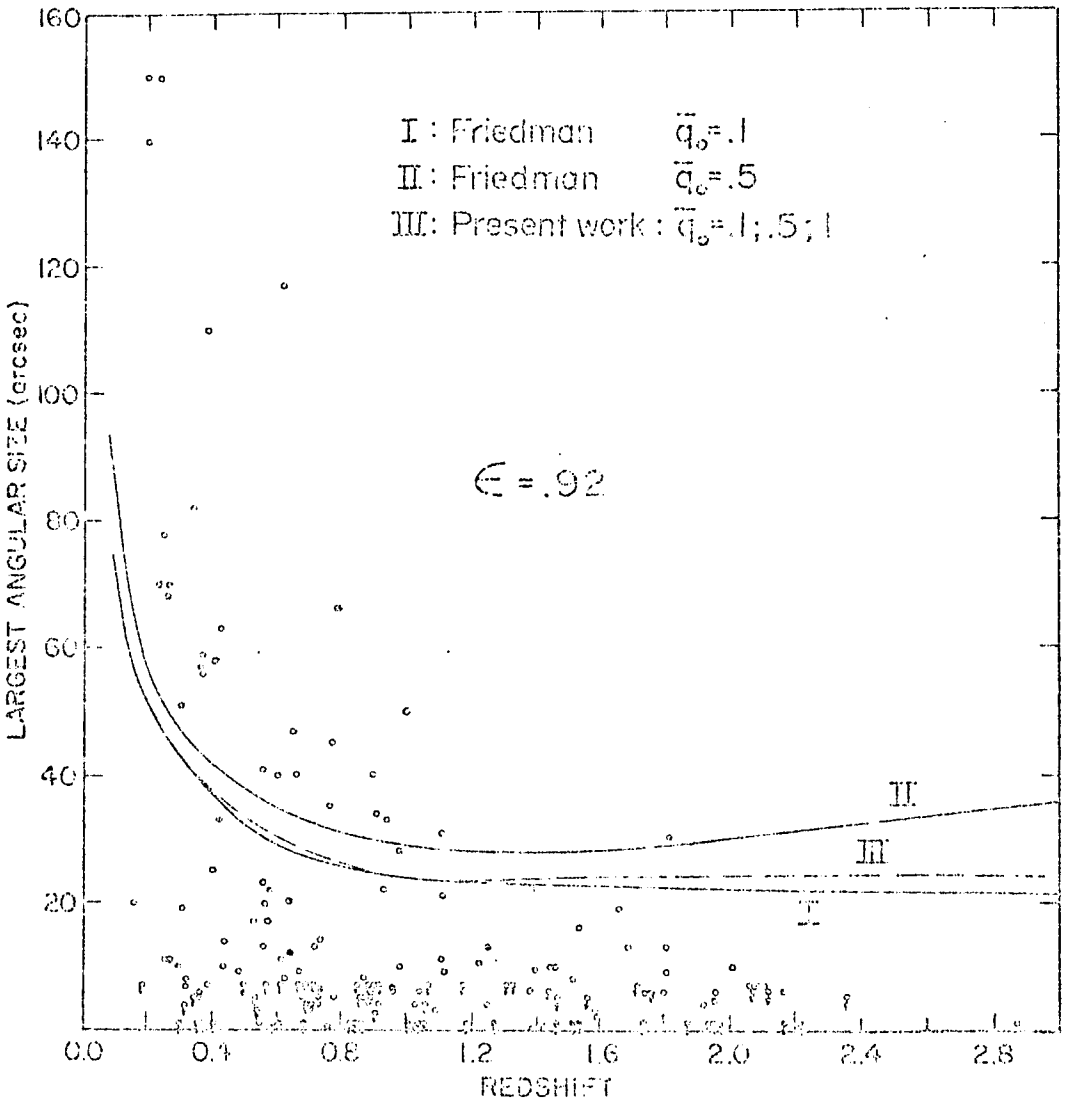
I : Friedman $\bar{q}_o$=.1
II : Friedman $\bar{q}_o$=.5
III: Present work : $\bar{q}_o$=.1; .5; 1
ϵ = .92
LARGEST ANGULAR SIZE (arcsec)
REDSHIFT
160
140
120
100
80
60
40
20
0.0
0.4
0.8
1.2
1.6
2.0
2.4
2.8
II
III
I

FIG. 15

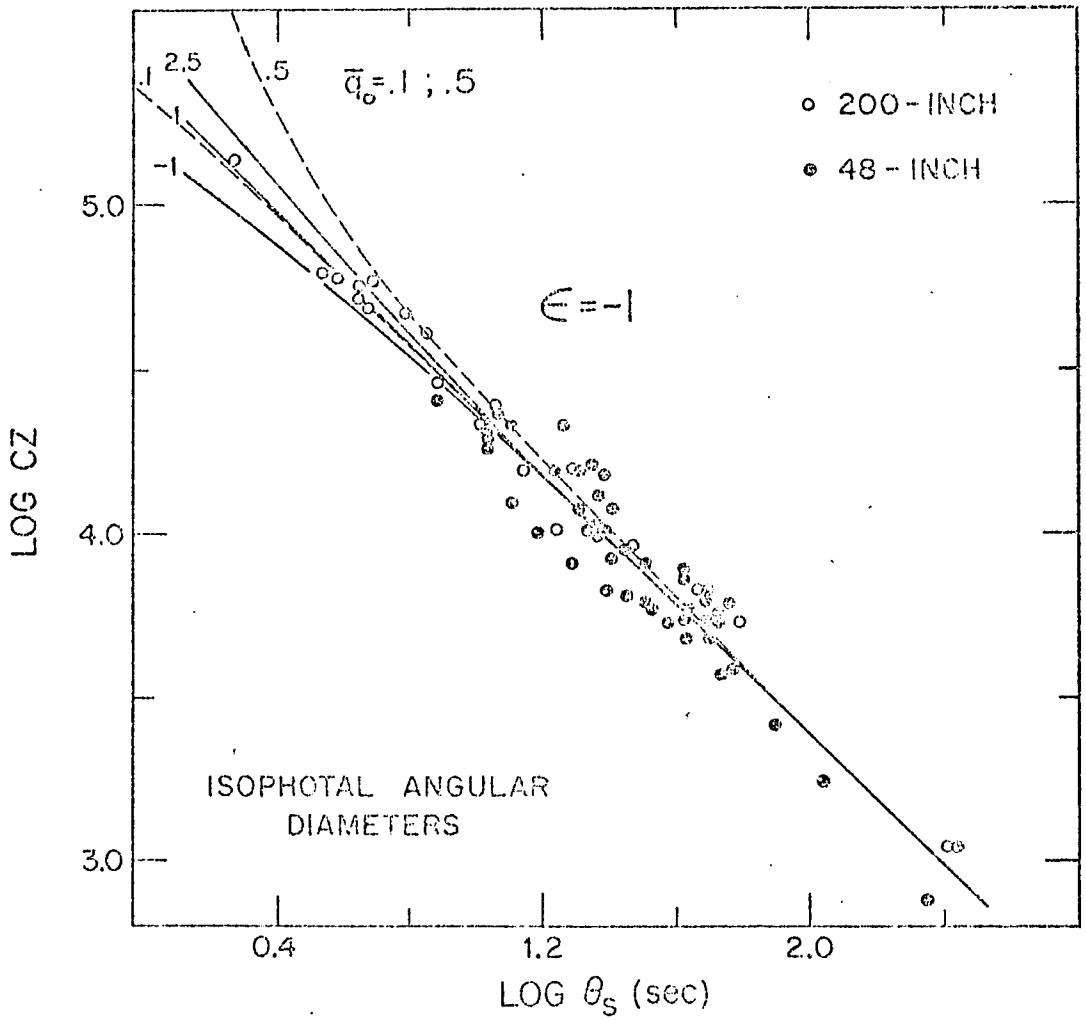
2.5
.5
.1
1
-1
$\bar{q}_o$=.1 ; .5
200-INCH
48-INCH
ϵ=-1
5.0
4.0
3.0
LOG CZ
ISOPHOTAL ANGULAR
DIAMETERS
0.4
1.2
2.0
LOG θ_s (sec)

FIG.17

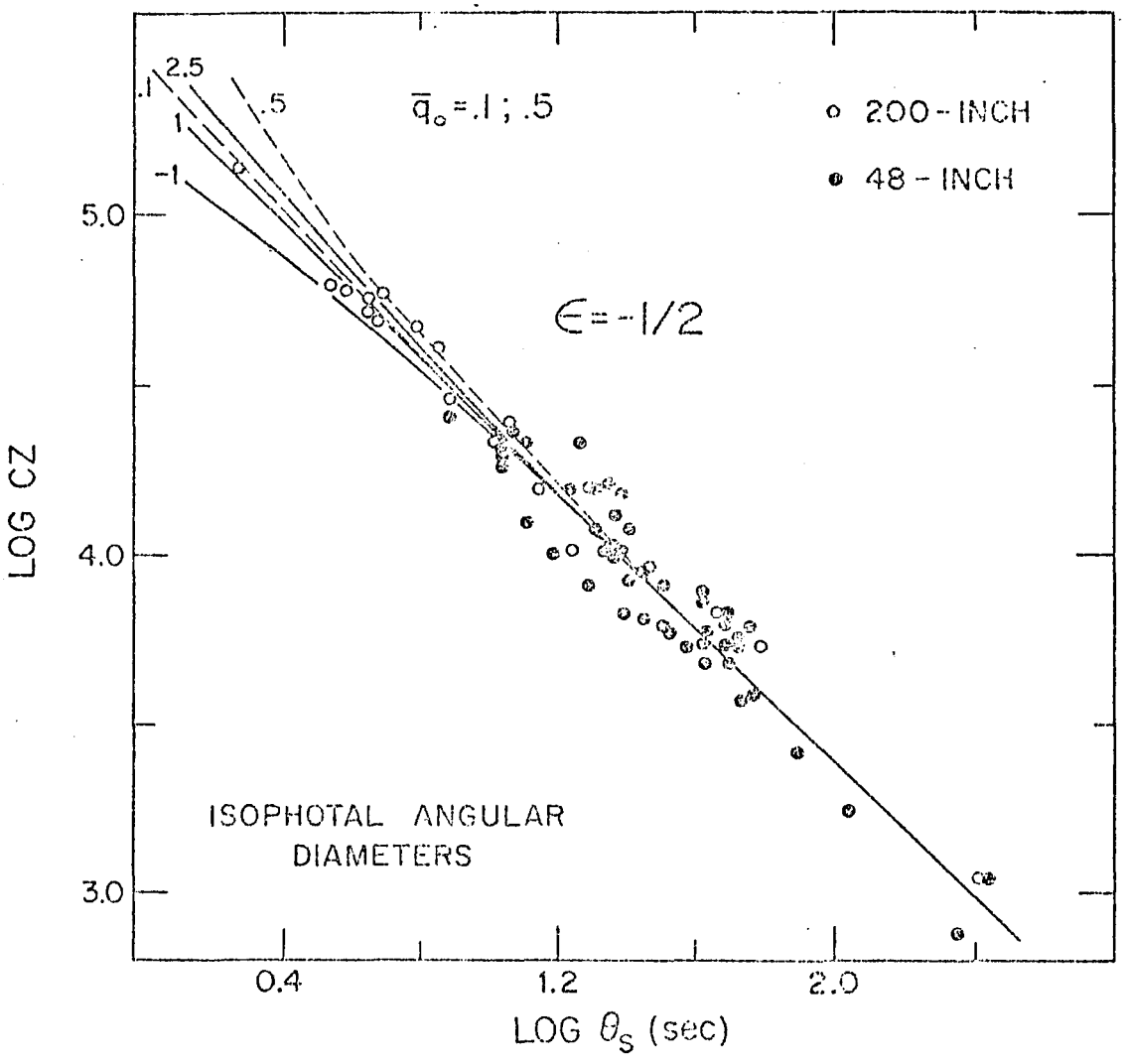
2.5
.1
.5
1
-1
$\bar{q}_o$=.1 ; .5
200-INCH
48-INCH
ϵ=-1/2
ISOPHOTAL ANGULAR
DIAMETERS
LOG CZ
5.0
4.0
3.0
0.4
1.2
2.0
LOG θ_S (sec)

FIG.15

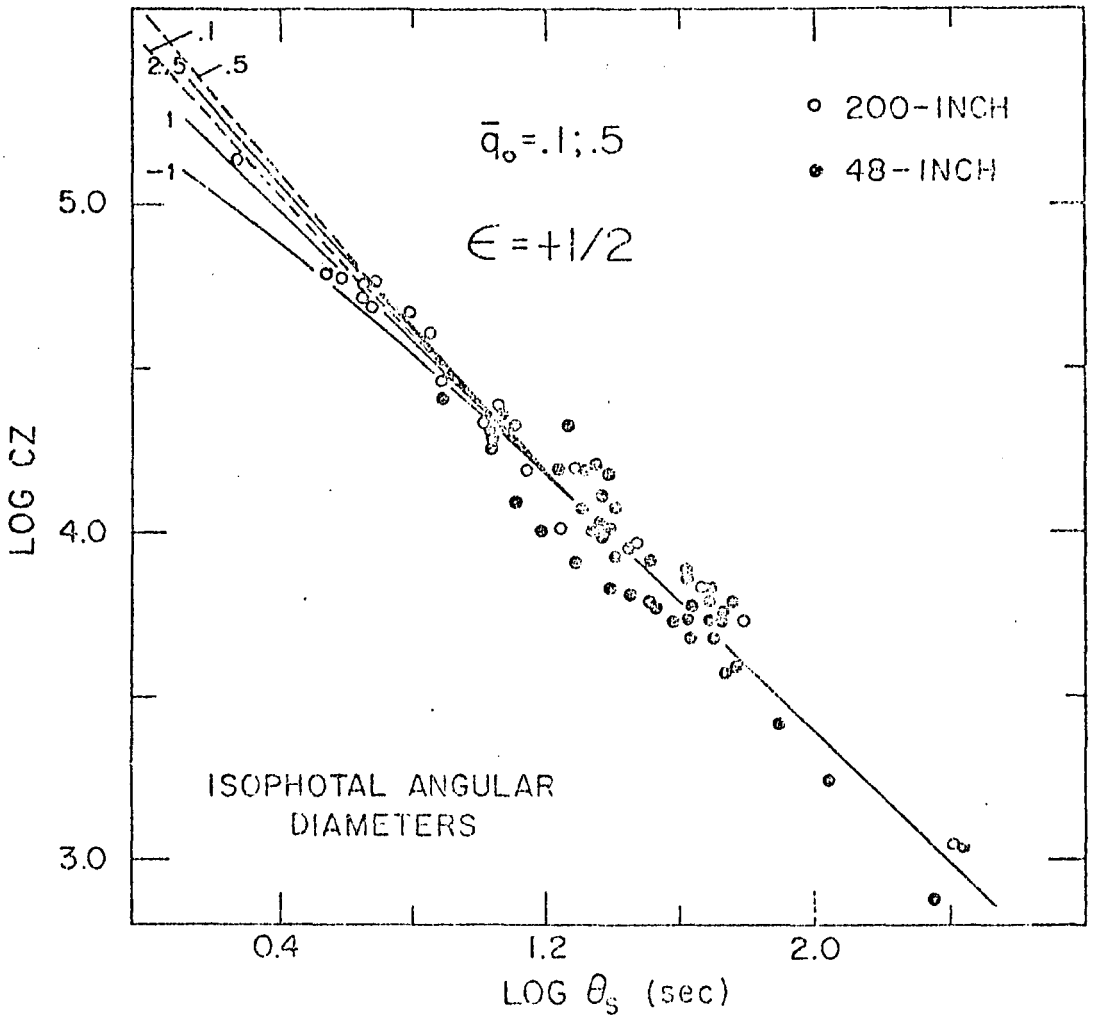
.1
2.5
.5
1
-1
$\bar{q}_o$=.1;.5
ϵ=+1/2
200-INCH
48-INCH
5.0
4.0
3.0
LOG CZ
ISOPHOTAL ANGULAR
DIAMETERS
0.4
1.2
2.0
LOG θ_s (sec)

FIG. 19

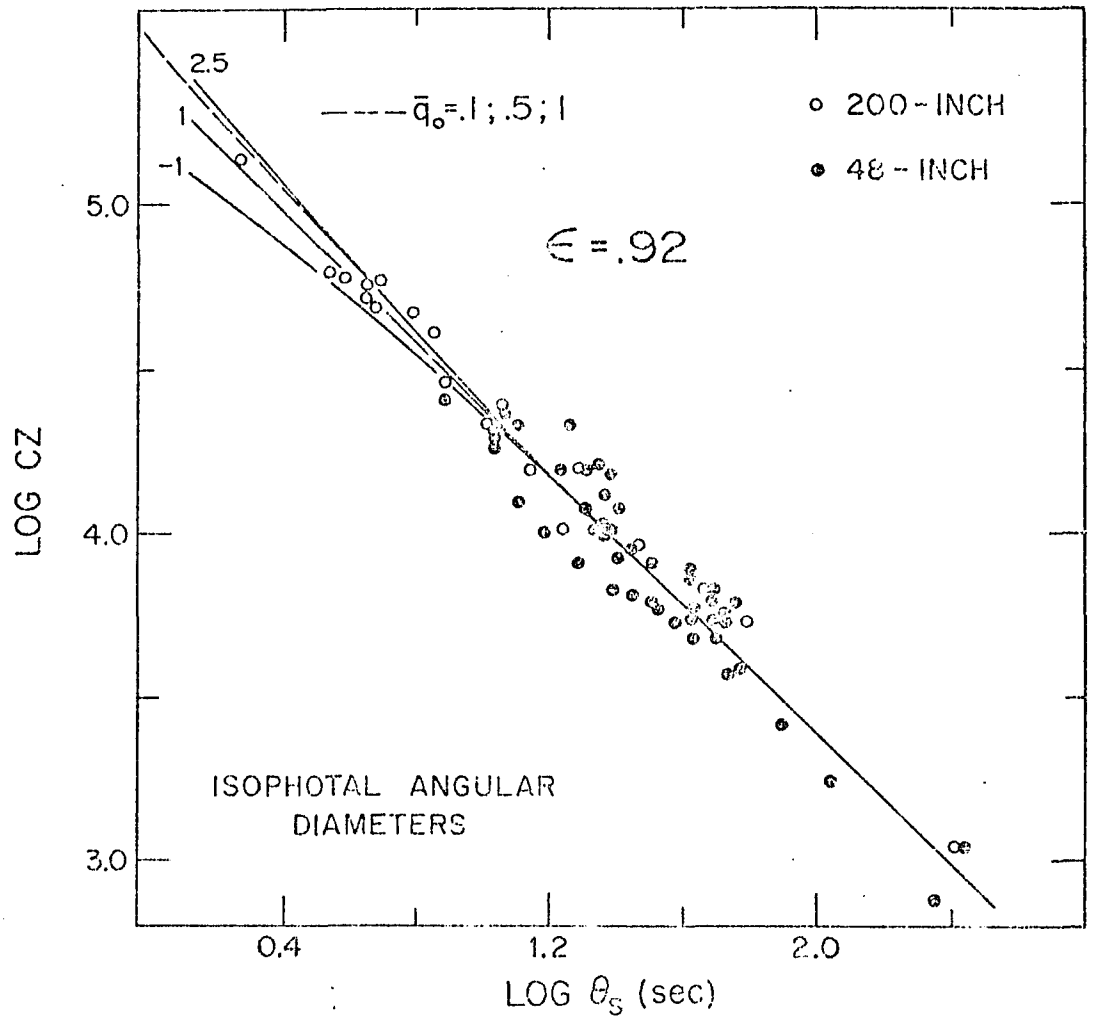
2.5
1
-1
$\bar{q}_o$=.1; .5; 1
200-INCH
48-INCH
ϵ=.92
ISOPHOTAL ANGULAR DIAMETERS
LOG CZ
5.0
4.0
3.0
0.4
1.2
2.0
LOG θ_S (sec)

FIG.29

SECTION E

lg N-lg S TEST

SECTION E: log N-log S

I. INTRODUCTION

It is the purpose of this paper to study the normalized, differential form of the log N - log S relation for radio sources within the framework of the scale-covariant cosmology developed and tested in previous papers. The formulation of the theory is described by Canuto et al., (1977, referred to as I); the formulation of thermodynamics and the 3°K background radiation is described by Canuto and Hsieh (1978, referred to as II). The magnitude-redshift test, the radio angular diameter-redshift test, and the optical number-magnitude test are described in Section D of this work. In D an improvement over non scale-covariant cosmology was obtained in fitting the data for a choice of parameters consistent with the present physical understanding of evolution. In the same paper a good fit to the large N vs. m slope for QSO's was also achieved. These tentative successes impel one to seek substantiation of the theory with further tests. The analysis of number counts, i.e. the number of sources having an observed flux greater than S, is an interesting case in point since fifteen years of model fitting under the assumptions of standard (non-scale-covariant) cosmology have yielded a discrepancy with the data which is rather insensitive to the parameters of that cosmology and which has been lumped into a free "evolutionary function" as described below. We shall demonstrate in this paper that the full covariant model needs to ascribe less of the fundamental form of the data to an "evolutionary function", which besides is not free at all. Indeed the standard theory does not depend sensibly on the deceleration parameter $\bar{q}_o$ while the scale-covariant theory can. This increases our confidence in the possibility of determining the curvature of the universe when all tests are in. For a similar sensitivity of the results to the value of $\bar{q}_o$, see the tests described in D.

Petrosian (1969), using the integrated N(S) count, found that the 3C data were consistent with the Lemaitre model with a uniform distribution of sources, but he had to use a $(1+z)^{1.5}$ evolutionary law to reconcile the 4C and 5C data with this model. Furthermore, the differential form of the test would have been superior statistically (Jauncey 1967 and 1975). The calculations for a $\bar{q}_o = \sigma_o = 1$ model required substantial evolution, namely, $(1+z)^{4 \pm 1}$.

Von Hoerner (1973) obtained a satisfactory fit by using a "flat" radio luminosity function (RLF), a density function , $(1+z)^3 F(z)$, made to order from the data and a relaxed redshift cut-off. A 'critical' luminosity function would require in addition a luminosity slope evolution to make the RLF flatter in the past (making it no longer really critical of course). A 'parabolic' RLF would require in addition a luminosity range evolution. His results were presented for a modified $\bar{q}_o = \sigma_o = 1$ model (taking advantage of the insensitivity to $\bar{q}_o$) and for a spectral index α equal to -1.

Wall, Pearson, and Longair (1977) using the Einstein-de Sitter model found their best fit for an evolutionary function $E(L, z)$ which depends on four parameters. They did not have the same success when they applied the model to a sample at higher frequencies containing a wider gamut of spectral indices, presumably because the RLF of steep sources which show up at high frequencies is different from that of those which show up at low frequencies.

Recently Robertson (1978) has presented a free-form iterative calculation of the luminosity distribution required to produce the observed differential log N - log S curve assuming an Einstein-de Sitter model, $\alpha = -.9$, and no evolution of luminosities inferior to a critical luminosity. His results approximate the $(1+z)^5$ power law (used in previous studies with a cutoff) up to $z \sim 2$, after which they level off and possibly decrease with z.

In all of the previous calculations, ad hoc evolutionary effects were assumed to fit the data. Their very existence rules out all simpler versions of the steady-state theory which have no room for evolution. Using the scale covariant theory, it turns out that part of the ad hoc evolution is accounted for by the new geometry, i.e. by the scale used, so that the large exponents like $(1 + z)^{4-5}$ are here reduced. It also turns out that in contrast to the standard case, most chosen scales when combined with the data, put constraints on the acceptable deceleration parameter $\bar{q}_o$.

In Part II we present a derivation of the log N - log S relation for the near region. This has the advantage of being easily interpretable and it can be made to produce the characteristically steep slope of -2.2 at high S in the quasar counts (Véron, 1966). This turns out to be possible if we use a model with a maximum in the effective luminosity distance ζ_L. The definition and behavior of ζ_L are explained in Part III and both new and old reasons for the observed luminosity-redshift distribution are offered.

In Part IV we present the derivation of the expression for the differential count and the conditions under which it is computed. In Part V we present several analytic cases.

Part VI is dedicated to the discussion of the RLF. We have performed computations a) by calculating the RLF within the context of the present theory and b) by "assuming" a RLF to allow comparison with previous results. The 177 sources used in this work are drawn mostly from the 4C survey and have known redshifts, spectral indices, and radio diameters. We also reran the program with a set compiled by Soltan (1978 a, b) with criteria of completeness. In order to make full use of the available information, we used the spectral index characteristic of each source instead of the common convenient practice of one average index for all sources.

In part VII we discuss the results, and in part VIII we present the final discussion.

II. THE NUMBER COUNT

The scale covariant theory as described in I, II and D, posits that the gravitational (or "Einstein") and electromagnetic (or "atomic") line elements, $d\bar{s}$ and ds, which form the basis of their respective dynamical theories are related by a time-dependent scale function $\beta(t)$,

$$d\bar{s} = \beta(t)\, ds \quad ; \quad \beta(t_o) \equiv 1 \ . \tag{2.1}$$

Equation (2.1) implies that gravitational and electromagnetic interactions did not always have the relative strengths observed today. All quantities calculated within the gravitational theory are indicated by a bar, except the redshifts which we denote by z. Quantities ultimately derivable from quantum electrodynamic theory or observed through atomic processes are unbarred including the redshift, z (see D Eqs. 3.1 and 3.2). The scale function β in (2.1) is a function of atomic time. Current research has concentrated on the consequences of assuming a general form

$$\beta(t) = (t_o/t)^{\epsilon} \qquad \epsilon = \pm 1, \ \pm 1/2 \ . \tag{2.2}$$

Two gauges, i.e. two values of ϵ were suggested by Dirac 1938 and 1974: $\epsilon = \pm 1$; and the other two by the present authors (H and D). $\bar{R}(\bar{t})$ appearing in Einstein's theory, is related to the scale factor $R(t)$ as it is observed through atomic processes, by the scale factor $\beta(t)$ [H, Eqs. 2.1-2.5].

The full solution of the gravitational equations written in atomic units as well as the behavior of $\beta(t)$, $R(t)$ vs. t and z can be found in D, Tables 1-4.

To find $dN(t_e)$, the total number of radio sources which emitted their light after time t_e, we must first find the number of galaxies enclosed between coordinates r_e and $r_e + dr_e$ at time t_e. If we assume a Robertson-Walker metric and if $n(t)$ is the number of galaxies per unit proper volume, we have

$$dN(t_e) = n(t)\ 4\pi\ r_c^2\ R^2(t)\ R(t)\ dr_e\ (1 - k\ r_c^2)^{-1/2} \quad . \tag{2.3}$$

If the radio source density depends only on expansion, i.e. there is no net creation or destruction of sources, then

$$n(t)\ R^3(t) = n_o\ R_o^3 \quad . \tag{2.4}$$

Using the relation

$$d\,r_e\ (1 - k\,r_e^2)^{-1/2} = c\ dt_e/R(t_e) \quad , \tag{2.5}$$

we find that the total number of sources that emitted their light after t_e is given by

$$N(>t_e) = 4\pi c\, n_o\, R_o^3 \int_{t_e}^{t_o} r_e^2(t)\, \frac{dt}{R(t)} \quad . \tag{2.6}$$

In the present section, we shall concentrate on the high flux regime. Expanding R(t) in the usual form

$$R(t) = R_o\, [1 - H_o(t_o - t) + \dots] \tag{2.7}$$

so that

$$r_e(t) = (c/R_o)\, [t_o - t + \tfrac{1}{2}\, H_o(t_o - t)^2] \quad , \tag{2.8}$$

we have

$$N(>t_e) = 4\pi n_o\, c^3 (t_o - t_e)^3 \left[1 + \frac{3}{2}\, H_o(t_o - t_e)\right] \quad . \tag{2.9}$$

If the source obeys a synchrotron-type power law

$$P(\nu_e)\, d\nu_e \sim \nu_e^{\alpha}\, d\nu_e \quad , \tag{2.10}$$

with the redshift law (D , 3.1)

$$\nu_e/\nu_o = 1 + z = \frac{R_o}{R(t_e)} \quad , \tag{2.11}$$

we obtain the radio bolometric correction

$$P(\nu_e)\, d\nu_e \sim \nu_o^{\alpha}\, R(t_e)^{-(1+\alpha)}\, d\nu_o \quad . \tag{2.12}$$

Within the scale covariant theory the universal gravitational "constant" G is written in general as (see I and II)

$$G = G_o\, \beta^{-n g} \equiv G_o\, \beta^{-g} \tag{2.13}$$

As far as evolution is concerned, we shall generalize the expression used in standard cosmology, namely

$$L(t) = L(t_o)\, (1+z)^{E} \tag{2.14}$$

to

$$L(t) = L(t_o)\, \beta^{e}(t) = L_o\, \beta^{e}(t) \quad , \tag{2.15}$$

For the inclusion of density evolution, see comment after eq. (4.4) and D , Section XIII). Then Eq. (D, 7.4) becomes

$$L_o/4\pi S = R_o^2\, r_e^2 \left(\frac{R_o}{R}\right)^{1-\alpha} \beta^{g-2-e} \tag{2.16}$$

Substituting the expansion (D, 5.12) for β

$$\beta(t) = 1 + \frac{\dot{c}}{c_o}\,(t_o - t) + \ldots \tag{2.17}$$

and (2.7) and (2.8), we obtain

$$t_o - t = \frac{1}{c}\left(\frac{L_o}{4\pi S}\right)^{1/2}\left[1 - \frac{(2-\alpha)}{2}\frac{H_o}{c}\left(\frac{L}{4\pi S}\right)^{1/2}(1 - C_1)\right] , \qquad (2.18)$$

where

$$C_1 \equiv \frac{\epsilon(2 + \epsilon - g)}{(2-\alpha) H_o t_o} . \qquad (2.19)$$

Substitution of (2.18) into (2.9) yields

$$N(>S) = \frac{4\pi n_o}{3}\left(\frac{L_o}{4\pi S}\right)^{3/2}\left[1 - \frac{3}{2}(1-\alpha)\frac{H_o}{c}\left(\frac{L}{4\pi S}\right)^{1/2}(1 - C_2)\right] \qquad (2.20)$$

with

$$C_2 \equiv \frac{\epsilon(2 + \epsilon - g)}{(1-\alpha) H_o t_o} = \frac{2-\alpha}{1-\alpha} C_1 .$$

In the optical case (obtained by setting $\alpha = -1$), (2.20) reduces to (1), (12.28) as expected. In the case of standard cosmology, $\epsilon = 0$ and $g = 0$, Eq. (2.20) reduces to Eq. (14.735) of Weinberg (1972) or to Eq. (13.36) of von Hoerner.

From (2.20) we can easily evaluate the slope of the N-S curve,

$$\text{slope} = \frac{S}{N}\frac{dN}{dS} = -\frac{3}{2}\left[1 - \frac{(1-\alpha)}{2}\frac{H_o}{c}\left(\frac{L_o}{4\pi S}\right)^{1/2}(1 - C_2)\right] .$$

Using the well-known expansion

$$H_o(t_o - t) \simeq z\,[1 - (1 + \tfrac{1}{2}\, q_o)\, z]$$

in (2.18), we finally obtain

$$\frac{H_o}{c}\left(\frac{I_o}{4\pi S}\right)^{1/2} = z\left\{1 + z\left[\left(\frac{2-\alpha}{2}\right)(1 - C_1) - (1 + \tfrac{1}{2}\, q_o)\right]\right\} \ ,$$

so that to first order in z

$$\text{slope} = \frac{S}{N}\,\frac{dN}{dS} = -\,\frac{3}{2}\left[1 - \frac{(1-\alpha)}{2}\,(1 - C_2)\, z\right] \qquad (2.21)$$

The first term in (2.21) reproduces the well-known Euclidian result, $S^{-3/2}$, whereas the term in parentheses represents the correction due to cosmology. The deceleration parameter appears in (2.21) through $H_o t_o$. The second term in brackets can be made positive if $C_2 > 1$, thus increasing the slope from -1.5 to perhaps -2.2, the observed values for quasars.[1] This can be achieved if

$$(1 - \alpha)\, H_o t_o < \varepsilon\,(2 + e - g) \qquad (2.22)$$

The values of e which produce a slope steeper than -1.5 assuming $\epsilon_g = -1$ and $\alpha = -.75$ are given in column A of Table 1. By multiplying e by the numbers in column D one obtains the equivalent E in standard cosmology for an assumed evolutionary function $(1+z)^E$, see (2.14) and part VII. In a real sample, the sources have a wide range of redshifts of course. When z becomes very small, the required $|e|$ for a slope of -2.2 is very large except for $\epsilon > 0$. We might not have to take such a stringent requirement as a slope of -2.2 (which comes from sources with large as well as small redshifts). We must realize that, once evolution is assumed, there is no reason to wish it to be small or large as long as it is consistent with the other tests and the model of physical evolution.

III. THE LUMINOSITY DISTANCE

Using (D, 7.5),

$$r_e = \frac{c}{R_0 H_0} \frac{F(z, \bar{q}_0)}{(1+z)} , \tag{3.1}$$

let us rewrite the exact expression (2.16) as

$$L_0 = 4\pi \left(\frac{c}{H_0}\right)^2 S \zeta_L^2(\beta) \tag{3.2}$$

where we have introduced the "luminosity distance"

$$\zeta_L(\beta) = F(z, \bar{q}_o)\,(1+z)^{-(1+\alpha)/2}\ \beta^{\varkappa}\ ;\ 2\varkappa = \varepsilon - 1 - \alpha - e \qquad (3.3)$$

which merely tries to incorporate into one expression evolutionary, geometrical, and bolometric factors contributing to the relationship between L and S.

Note that as given in Eq. (3.3), ζ_L is a function of z (the redshift in gravitational units, not that observed in atomic units) and of β which is usually given as a function of atomic time t. In standard cosmology, $\beta = 1$, $z = z$, and so (3.2) and (3.3) together reduce to the standard equations describing both the S-z diagram for any α and the m-z diagram if we take $\alpha = -1$. We note that for suitable choice of α, it is possible for the luminosity distance ζ_L to have a maximum, ζ_L^*, at redshift z_*. In standard cosmology, it is also possible to have a maximum in the luminosity distance but evolution must be very strong to make it occur at observable redshifts if $\bar{q}_o$ is not very large. The interest in a luminosity distance which is a slowly increasing function of z or which has even a maximum is that such a behavior seems indicated by the radio S-z diagram and by the integrated N(S) counts. The data can not yet establish its existence in the available redshift range $z \lesssim 3.5$, so if a maximum exists, it must be at $z > 2$ at least or else it would be more evident.

The presence of an observable maximum in standard cosmology would imply a closed universe and/or very strong evolution. However, because of the presence of the beam function $\beta(t)$, and the facts that $z \neq z$ and that our evolutionary function cannot in general be parametrized as $(1+z)^{\varepsilon}$, it is to be expected that

the value of z_* will be different in scale-covariant theory than in standard theory for the same $\bar{q}_o$. For some choices of ϵ and only moderate or null evolution it is possible to have ζ_L^* occur at observable or nearly observable z_* in an open universe. Thus for some scale choices, the S-z diagram corresponding to an open universe in our cosmology will look like the S-z diagram within a closed universe of standard cosmology. Similarly as the results for m vs. z and θ_m vs. z of paper D indicate, it is possible within our theory and an open universe to obtain results that in standard theory can only be obtained with a closed universe. For the θ_i vs. z test, as explained in D, the results of our theory can be simulated by standard theory by either a higher or lower q_o depending on the gauge ϵ and $\bar{q}_o$ chosen.

This explains the inconsistency of the results of the various cosmological tests (which require the angular distance to increase more slowly than the luminosity distance with z, as interpreted by standard theory but which require a unique $\bar{q}_o$ in the scale-covariant theory. These remarks become particularly important if it turns out that the measured deuterium abundance implies an open universe also in the new theory; this is a problem now under investigation.

A priori we should not expect the optical data to behave the same way. However, the steep slope of the N vs. m diagram can in fact imply a maximum in the bolometric distance as discussed in Part D, Sections XII and XIII. Also the m vs. z diagram combining the QSO and galactic data shows signs of a maximum, a circumstance which is variously interpreted as evidence for high $\bar{q}_o$, galactic evolution, misinterpretation of the redshift, or the unsuitability of QSO's for the test. The similarity of the behavior of the optical and radio data may be due to their physical connection which fortuitously is leading to similar evolutionary rates (perhaps density evolution would be easier to understand than

luminosity evolution in this context), or it may be that geometrical considerations and/or strong selection effects based on geometry are the dominant factors in both radio and optical flux distributions and a corrected (e.g. scale covariant) interpretation of space-time is in order.

Let us now study the cases $\bar{q}_o = 0,\ 1/2$ which can be treated analytically and the case $\bar{q}_o = 1$ in the limit of small z.

From Eq. (II, 3.3) we now have the exact results

$$1 + z = \beta(1 + z) = (1 + z)^{\frac{1}{1 - \varepsilon}} \quad ; \qquad \bar{q}_o = 0 \quad , \qquad \bar{H}_o\, \bar{t}_o = 1$$

$$1 + z = \beta(1 + z) = (1 + z)^{\frac{2 + \varepsilon}{2 - 2\varepsilon}} \quad ; \qquad \bar{q}_o = 1/2 \, , \qquad \bar{H}_o\, \bar{t}_o = 2/3 \, . \tag{3.4}$$

For $\bar{q}_o = 1$, since $R(\bar{t}) \sim \bar{t}^{\,H_o t_o}$ for $z << 1$, it follows that

$$1 + z = \beta(1 + z) \sim (1 + z)^{1 - \frac{1}{\bar{H}_o\, \bar{t}_o}\ \frac{\varepsilon}{\varepsilon - 1}} \quad ; \quad \bar{q}_o = 1, \quad \bar{H}_o\, \bar{t}_o = \pi/2 - 1 \, . \tag{3.5}$$

Using now (3.3) we can write

$$\zeta_L(z) = F(z,\ \bar{q}_o)\ (1 + z)^p \tag{3.6a}$$

where (1), 7.6a)

$$F(z,\ \bar{q}_o) = z + \frac{z^2(1 - \bar{q}_o)}{1 + \bar{q}_o\, z + \sqrt{1 + 2\bar{q}_o\, z}} \tag{3.6b}$$

and

$$2p = \frac{\epsilon(\epsilon + \alpha + 1 - g)}{(\epsilon - 1)\,\bar{\Pi}_o\,\bar{t}_o} - (1 + \alpha) \quad , \tag{3.7}$$

Using Eq. (3.6b), it is easy to find that the maximum of ζ_L occurs at

$$1 + z_* = \left(\frac{p}{2 + p}\right)^{1/2} \qquad p \le -2 \qquad \bar{\bar{q}}_o = 0$$

$$1 + z_* = \left(\frac{p + 1/2}{p + 1}\right)^{2} \qquad p \le -1 \qquad \bar{\bar{q}}_o = 1/2 \tag{3.8}$$

$$1 + z_* = \frac{p}{p + 1} \qquad p \le -1 \qquad \bar{\bar{q}}_o = 1$$

The values of ϵ corresponding to $p = -2$ and $-\infty$ (yielding $z_* = z = \infty$) are plotted as a function of ϵ for $\alpha = -.75$, in Figure 3a ($\bar{\bar{q}}_o = 0$) and for $\alpha = -.25$, $-.5$, and $-.75$ in Figure 3b ($\bar{\bar{q}}_o = 1/2$). The values of ϵ for the average spectral index $\alpha = -.75$ are presented in column B of Table 1. The region above the curve for $\epsilon < 0$ and below the curve for $\epsilon > 0$ is denoted Region I and corresponds to values of p for which ζ_L has no maximum at real, positive z. The remaining area is denoted Region II and corresponds to the condition for a maximum. We note that when $\bar{\bar{q}}_o = 1/2$, $\alpha = -1/2$ and when $\bar{\bar{q}}_o = 1$, $\alpha = -.7519$, $z \sim 0$, the division corresponds to the coordinate axes. In general as $|\alpha|$ becomes smaller or $\bar{\bar{q}}_o$ becomes greater, Region II becomes larger. As we penetrate deeper into Region II in all cases (taking ϵ farther from the boundary for the same ϵ), p becomes more negative, and z_* (as well as z_{*} becomes smaller.

Although $\epsilon = 0$ is not expected in the present cosmology, for the sake of understanding, the p values corresponding to no evolution are given in Table 2 as a function of α and ϵ. It is seen that except for unusually flat spectral indices and approximately for $\bar{q}_0 = 1$ in the local region, there is very little hope in the standard cosmology of finding p in Region II, a region so useful for understanding the S-z and m-z diagrams and the high slopes in the counts N(m) and N(high S). When $g\epsilon = -1$ and $\epsilon = 0$, we have

$$p = p(\epsilon = 0) + \frac{1}{2} \frac{\epsilon(\alpha + 2)}{(\epsilon - 1)\, \bar{\Pi}_0\, \bar{t}_0} \tag{3.9}$$

If $0 > \epsilon > 1$, the $\epsilon \neq 0$ contribution is positive and we are less likely to find a maximum for ζ_L at real positive z (Region II). If $0 < \epsilon < 1$, the contribution from the ϵ term is negative and we are more likely to be in Region II even without postulating any evolution.

Since we require that the maximum, if it occurs, occur at $2 < z_* < \infty$, we have calculated the combinations of (ϵ, e, α) which would yield $z_* = 2$ and present $e(z^* = 2)$ in column C of Table 1. When $\bar{q}_0 = 1$, we include only $\epsilon > 0$ because the z_* corresponding to $\epsilon < 0$ is too great for the approximation. Examination of columns C and B reveals that except for $\epsilon > 0$, for a given (ϵ, α), the e (and p) do not change significantly between $z_* = 2$ and $z_* = \infty$ and e is therefore fairly well determined if we accept the hypothesis that the solution is in Region II. We point out that, contrary to the case in standard cosmology, within the scale-covariant cosmology, z_* may occur at observable values (i.e. $z_* \lesssim 4$) even in an open universe. Requiring $z_* > 4$ then serves to restrict e to a small range between columns B and C.

We draw the reader's attention to the fact that for $\bar{q}_o = 1/2$, the condition that $z_* = \infty$, (that is, the boundary between Regions I and II, Eq. (3.7) and $p = -1$) coincides with the condition (2.23) that the N(S) slope be steeper than -1.5. For $\bar{q}_o = 0$, Eq. (2.23) has more solutions than Eq. (3.7) (compare columns A and B of Table 1) and some solutions in Region I will also produce a N(S) slope steeper than -1.5. This is important because we will find that the differential form of the N-S test requires solutions in Region I and there is no way for $\bar{q}_o = 1/2$ to satisfy both the differential and integrated tests simultaneously. On the other hand, for the $\bar{q}_o = 1$ case the solutions of (3.8) overlap those of (2.23) only when $\epsilon > 0$ and then the ϵ range is very narrow.

The very existence of a maximum in ζ_L poses some problems. In such cases for given L and S, there are two solutions of (3.2), z_1 and z_2 (where $z_1 < z_* < z_2$), and it is to be wondered why we don't observe many large z, especially when the corresponding space volumes are large and would contain many sources if uniformly distributed. Presumably ζ_L lumps all effects such as geometry, bolometric correction, and evolution. Since the light travel times would still be long even though ζ_L is "short", there may be focusing problems. Also ζ_L declines after its maximum slower than it rose, and a considerable region around the maximum might not be observable in present surveys, but barring unknown effects in an infinite open universe, sources with enormous redshifts would be observable (in fact, we should reexamine Olber's paradox). Possible explanations for their absence are:

A. The redshifts would be so great that the usual lines would be shifted out of the observed frequency range or observers are only looking for patterns around $z = 4$, not $z = 20$.

B. β^e is too simple to account for the variation of source density with z. In standard cosmology one just assumes that the evolution is turned off before z_c, that is radio sources may conveniently not exist or evolve before z_c, where $z_1 < z_* \leq z_c < z_2$. One should investigate whether something interesting is occurring at that time. Any observational effect of the reheating of the intergalactic gas is clearly pertinent. In some QSO models (Rees and Setti 1968), the source is quenched before it can be observed at high intergalactic densities.

C. If the universe is closed and finite with a finite number of sources, we would expect to observe only a finite number of sources on one side of the antipodes.

D. The geometry of the universe is such that ζ_I is asymptotic to its maximum at $z_* = \infty$ and the long asymptotic region is beyond our present instruments. Several problems are:

1. $z_* = \infty$ depends on α which is different for different sources.

2. $\bar{q}_o = 1/2$ would seem to be excluded because N - S is observed to be non-Euclidean. The choice $\bar{q}_o \sim 0$ seems manageable for both the integrated and differential

counts. The solutions $\bar{q}_0 > 1/2$, $z_+ = \infty$ may be acceptable; this is explanation C again of course.

E. There may be obscuring material in the early universe. The contribution of the obscured sources to the background radiation should be calculated.

F. For the same ϵ, c, $|p|$ increases with $|\alpha|$ so that flatter sources bring us further into Region II. This may be an expression of the flattening of observed sources with redshift. The "true" (ϵ, c) may be such that steep sources are in Region I and become progressively invisible with z and flat sources are near or into Region II. If the sources actually steepened with increasing z and the opposite observed weak correlation of flat sources with high z were a selection effect, the sources at high z would be invisible even though the sources fit at low z would imply some $z_+ < \infty$.

We remind the reader that the absence of sources with high redshift is also an outstanding problem in the non-scale-covariant cosmology which provides fewer explanations.

IV. THE DIFFERENTIAL COUNT

Let us first write the number of sources (per steradian) with luminosity between L and $L + dL$ as

$$n(L, r)\, dr = R^3(t_e)(1 - \tfrac{1}{3} r_e^2)^{-1/2} r_e^2\, dr_e\, \mathcal{L}(t_e, L)\, dL. \tag{4.1}$$

If in general we allow for a time variation of the number of sources, then we should write

$$n(t)\ R^3(t) = n_o\ R_o^3\ \ f(t)\ . \tag{4.2}$$

Then

$$n(L,\ r)\ dL\ dr = R_o^3\ (1 - k\ r_e^2)^{-1/2}\ \ r_e^2\ \ dr_e\ \ \Phi(t_o,\ L)\ dL\ , \tag{4.3}$$

where $\Phi(L)$ is the radio luminosity function. Using (3.1), (3.2), (3.3), and

$$\frac{dr_e}{dz} = \left(\frac{c}{\bar{H}_o\ \bar{R}_o}\right)\ (1 - k\ r_e^2)^{1/2}\ (1 + z)^{-1}\ (1 + 2\ \bar{q}_o\ z)^{-1/2}\ ,$$

and changing variables, (4.3) can now be expressed as

$$n(L,\ r)\ dL\ dz = 4\pi\ (c/\bar{H}_o)^5\ \left\{\frac{F^2\ (z,\ \bar{q}_o)\ f(t)\ \zeta_L^2(S)}{(1 + z)^3\ (1 + 2\ \bar{q}_o\ z)^{1/2}}\right\}\ \Phi(L)\ dS\ dz$$

$$\equiv 4\pi\ (c/\bar{H}_o)^5\ \ \zeta_n^4(S)\ \Phi(L)\ dS\ dz \tag{4.4}$$

$$\equiv n(S,z)\ \ dS\ dz$$

which defines ζ_n^4 as the expression in the curly brackets. The symbols ζ_L and ζ_n have been introduced to facilitate the comparison of our results with

the ones corresponding to standard cosmology as derived, for example, by von Hoerner, which can be recovered by putting $\beta = 1$, $z = z$. The exact expressions (4.4) and (3.3) constitute the basis for our future analyses.

Since, as we shall see later, the luminosity function can be written as

$$\phi(L) \sim L^{-(n+1)} \; ; \; L_m < L < L_M \quad , \tag{4.5}$$

we can use (3.3) to eliminate L and find the final expression for the number count normalized to the Euclidean value $n_E \sim S^{-3/2}$. Integrating $n(S, z)$ over z to get $n(S)$, we obtain

$$n_n(S) \equiv \frac{n(S)}{n_E(S)} = A S^{1.5-n} \int_{z_m}^{z_M} \frac{I(\beta)\, F^2(z, \bar{q}_0) G^{-2n}(z, \bar{q}_0, \beta)\, dz}{(1+z)^3 (1+2\bar{q}_0 z)^{1/2}} \tag{4.6}$$

where

$$A = \begin{cases} (3-2n)(4\pi c^2/H_0^2)^{1.5-n} \left\{ L_M^{1.5-n} - L_m^{1.5-n} \right\}^{-1} \; ; \; n \neq 1.5 \\ \{ \ell n (L_M/L_m) \}^{-1} \; ; \; n = 1.5 \; . \end{cases} \tag{4.7}$$

The upper and lower limits z_M and z_m depend on S via (3.2) once L_M and L_m are fixed.

The f(t) which we have included accounts for number density evolution. It can be formally absorbed into the general evolutionary term β^e (see 3.3). We will follow this procedure and not refer to f(t) again.

The solution of (3.3) and (3.2) for z_M and z_m must be found by iterative techniques in most cases. As S becomes smaller, ζ_L increases and it becomes increasingly difficult to find the limits. As p approaches region II, ζ_L increases more slowly with z and we must go to very high z. When $\epsilon < o$, $z < z$, but both z and z can go to ∞ as we approach the boundary of Region II. When we are in Region II, for some values of L and S, ζ_L may be larger than ζ_L^* and there will be no solution for z. Since this can occur for S which are no smaller than the observed values and since L_M comes from the M_L-M (as determined within the theory from the data) an inconsistency might be suspected until it is noted that the L_M calculated from the data was contributed by a datum associated with a much higher S and lower ζ_L than those being used for the limits of the integral in these cases. Therefore the very low S observations would be of sources with $L < L_M$ and we are allowed conceptually to lower L_M for low S so that $\zeta_L = \zeta_L^*$. When the lower limit L_m and S yield a ζ_L which leads to unphysical z's, this procedure of lowering L is not permissible since there are no L observed smaller than L_m; there is sufficient reason to reject the model corresponding to $(\epsilon, e, \alpha, \bar{q}_o)$. The most obvious culprit is α which would be raised.

The integration was performed by a) straight quadrature, b) δz steps, c) δm, δz steps, and d) Gaussian techniques and to as many steps (10^2 - 10^5) as necessary depending on the limits and function to stabilize the results.

V. ANALYTIC CASES

Using (3.3) we can rewrite (4.6) as

$$n_n(S) = A\, S^{\frac{3}{2} - n} \int_{z_m}^{z_M} \frac{F^{2-2n}(z, \bar{q}_o)\, S^{-2n\alpha}(z)\, dz}{(1+z)^{3-n(1+\alpha)}\,(1+2\bar{q}_o z)^{1/2}} \quad , \tag{5.1}$$

The limits z_m and z_M are again a solution of (3.2) and (3.8). We shall study here the cases when β can be expressed as a simple power law of the variable $(1+z)$, i.e.,

$$\beta = (1+z)^{\eta} \quad . \tag{5.2}$$

From Eqs. (3.4) and (3.5) we derive

$$\eta = \frac{\epsilon}{1-\epsilon} \quad ; \quad \bar{q}_o = 0$$

$$\eta = \frac{3\epsilon}{2(1-\epsilon)} \quad ; \quad \bar{c}_o = 1/2 \tag{5.3}$$

$$\eta = \frac{\epsilon}{1-\epsilon}\,\frac{1}{\bar{\Pi}_o \bar{t}_o} \quad ; \quad \bar{q}_o = 1 \; ; \; \bar{\Pi}_o \bar{t}_o = \frac{\pi}{2} - 1 \; ; \; z \sim 0 \quad .$$

Collecting the powers of $(1+z)$ we can rewrite (5.1) as

$$n_n(S) = A\, S^{\frac{5}{2} - n} \int_{z_m}^{z_M} F^{2-2n}(\bar{q}_o, z)\,(1+z)^{-3-2n\beta}\,(1+2\bar{q}_o z)^{-1/2}\, dz \quad , \tag{5.4}$$

where p is the same given by (3.7). Instead of specifying the parameters x(g, α, c) and ϵ separately, we shall discuss global cases corresponding to specific values of p (which arise from many combinations of the parameters $\bar{q}_o$, ϵ, c, and α) and $\bar{q}_o$. For convenience we shall use (3.2) to define

$$\zeta_L = \frac{\bar{H}_o}{c}\sqrt{\frac{L}{4\pi S}} \equiv \Lambda \ . \tag{5.5}$$

We present below the following cases: $\bar{q}_o = 0$: n = 1 (all p) and n = 2(p = - 1) and $\bar{q}_o = 1/2$: n = 1 (p = -2, -7/4, -4/3, -1, -1/2, -1/4, and 0). and n = 1.5 (p = - 4/3). We also have treated analytically the $\bar{q}_o = 1/2$ cases n = 1.5 (p = - 3/2, -7/6, -1, -5/6, and -2/3) and n = 2 (p = -5/4, -9/8, -1, -7/8, and -3/4) but do not present them here for simple reasons of space and because the reader after seeing the first few cases will be able easily to do these and many others himself.

1) Case A, $\bar{q}_o = 1/2$, p = -1

In this case of zero curvature, $\bar{H}_o \bar{t}_o = 2/3$, we have from Eq. (3.6b)

$$F(z, \bar{q}_o) = 2\,(1 + z - \sqrt{1+z}\,) \ . \tag{5.6}$$

Using (3.5), we have

$$\zeta_L = 2\left[1 - (1+z)^{-1/2}\right] \tag{5.6a}$$

or

$$1 + z_{m,\,M} = (1 - \tfrac{1}{2}\,\Lambda_{m,\,M})^{-2} \qquad (5.6b)$$

Substituting (5.6) in (5.4), we obtain

$$n_n = A S^{\frac{3}{2} - n} \int_{z_m}^{z_M} 2^{2-2n} (1+z)^{2n-3.5} \left[1 + z - \sqrt{1+z}\,\right]^{2-2n} dz \,. \qquad (5.7)$$

If $n = 1$, using (4.7) we find that $A = S^{-1/2} [\Lambda_M - \Lambda_m]^{-1}$ and

$$n_n = A S^{1/2} \int_{z_m}^{z_M} (1+z)^{-1.5}\, dz$$

$$= 1 \,; \qquad (5.8)$$

i.e., the model makes the same predictions as the Euclidean model.

Similarly if $n = 1.5$, and if we change variables to $y = \sqrt{1+z}$

$$n_n = A \int_{y_m}^{y_M} \frac{dy}{y(y-1)} = 1 \qquad (5.9)$$

Again, if $n = 2$, eq. (4.7) becomes $A = S^{1/2} [\Lambda_m^{-1} - \Lambda_M^{-1}]^{-1}$ and we find, with the same change of variables,

$$n_n = \tfrac{1}{2} A S^{-\frac{1}{2}} \int_{y_m}^{y_M} \frac{dy}{(y-1)^2} = 1 \qquad (5.10)$$

which is once more independent of S and L.

In general for $\bar{q}_o = 1/2$ and for any (g, c, α) which gives p = -1, the result is Euclidean and $z_* = \infty$. The value p = - 1 when $\bar{q}_o = 1/2$ corresponds to the boundary between Regions I and II and the e values which will give this Euclidean result are shown as a function of c for various α in Figure 1b and listed for α = - .75 in column B of Table I. When these are multiplied by column D, we obtain the corresponding E values if we write

$$L = L_o \beta^e = L_o (1+z)^E. \qquad (5.11)$$

2. Case B, $\bar{q}_o = o$

For $q_o = o$, we have $\bar{t}_o \bar{H}_o = 1$

$$F = z(1 + z/2) \qquad (5.12)$$

and

$$\zeta_L = F(1+2F)^{p/2} \qquad (5.13)$$

with

$$1 + z = (1 + 2F)^{1/2} \tag{5.14}$$

Substitution in (5.2) yields

$$n_n = A\, S^{3/2-n} \int F^{2-2n} (1 + 2F)^{-2-np}\, dF \tag{5.15}$$

(B1) If $p = -2/n$,

$$n_n(S) = \frac{A\, S^{\frac{3}{2} - n}}{3 - 2n} \left\{ F^{3-2n}(z) \right\}_{z_m}^{z_M}$$

and

$$A = F(1 + 2F)^{-1/n}$$

(B2) A particular case of B1 is $n = 1\,(p = -2)$, $F = A/(1 - 2A)$ and the upper limit A_M corresponds to $z_M = \infty$. A is given by (4.7), as already found in Case A. Then

$$n_n(S) = \left(\frac{A_M}{1 - 2A_M} - \frac{A_m}{1 - 2A_m} \right) \frac{1}{(A_M - A_m)}$$

$$= \left[\frac{L_M^{1/2}}{1 - \frac{H_o}{c}\sqrt{\frac{L_M}{\pi S}}} - \frac{L_m^{1/2}}{1 - \frac{H_o}{c}\sqrt{\frac{L_m}{\pi S}}} \right] \left(\frac{1}{L_M^{1/2} - L_m^{1/2}} \right) \tag{5.16}$$

which is a function of S and depends on the limits L_M and L_m of the RLF. The values of e satisfying this case are given as a function of e for various spectral indices in Figure 1a and tabulated for $\alpha = -.75$ in column E of Table 1 for $\bar{q}_o = o$. We are again on the boundary between Regions I and II.

(B3) Another subcase of B1 is: $n = 2$, $p = -1$:

$$F = \Lambda \left(1 + \sqrt{1 + \Lambda^2} \right)$$

$$n_n(S) = \left[\frac{L_m^{1/2}}{1 + \sqrt{1 + \frac{\bar{H}_o^2}{c^2} \frac{L_M}{4\pi S}}} - \frac{L_M^{1/2}}{1 + \sqrt{1 + \frac{\bar{H}_o^2}{c^2} \frac{L_m}{4\pi S}}} \right] \left(\frac{1}{L_M^{1/2} - L_m^{1/2}} \right)$$

This again depends on S, L_M and L_m.

We are in Region I.

(B4) If $n = 1$, $p \neq -1, -2$, then

$$1 + 2F = (1 - 2\Lambda)^{-1} \tag{5.17}$$

and

$$n_n(S) = \frac{(1 - 2\Lambda_M)^{p+1} - (1 - 2\Lambda_m)^{p+1}}{(\Lambda_M - \Lambda_m)(-2p - 2)} \tag{5.17a}$$

This expression is exact in both Regions I and II as long as $p \neq -1, -2$.

(B5) If $p = -2$ and $n = 1$, this case is the boundary case B2.

(B6) If $p = -1$ and $n = 1$,

$$n_n(S) = \tfrac{1}{2} A S^{1/2} \ln \frac{1 - (2\overline{H}_o/c)(L_m/4\pi S)^{1/2}}{1 - (2\overline{H}_o/c)(L_m/4\pi S)^{1/2}} \qquad (5.18)$$

This case corresponds to Region I. It has a flatter RLF than case B3 and consequently the graph of lg n vs. lg S appears more curved.

3. Case C, $\overline{q}_o = 1/2$, $p = -2$, $n = 1$

Again we are in Region II.

We find

$$n_n(S) = \frac{2}{3} \frac{(1 + z_M)^{3/2} - (1 + z_m)^{3/2}}{A_M - A_m} \qquad (5.19)$$

where the limits are given by

$$\tfrac{1}{2} A = (1 + z)^{-1} - (1 + z)^{-3/2} \qquad (5.19a)$$

which is easily solvable by simple methods.

4. Case D, $\bar{q}_o = 1/2$, $p = -1/4$, $n = 1$

Here we are in the more conventional Region I. We easily find from (5.2) that

$$n_n(S) = \frac{1}{2} \frac{(1+z_m)^{-2} - (1+z_M)^{-2}}{\Lambda_M - \Lambda_m} , \tag{5.20}$$

where the limits are obtained from

$$\tfrac{1}{2}\Lambda = (1+z)^{3/4} - (1+z)^{1/4} , \tag{5.20a}$$

which is an easily solvable cubic equation in the variable $(1+z)^{1/4}$.

5. Case E, $\bar{q}_o = 1/2$, $p = -1/2$, $n = 1$

We are again in Region I. Equation (5.2) reduces to

$$n_n(S) = \frac{2}{3} \frac{(1+\Lambda_m)^{-3} - (1+\Lambda_M)^{-3}}{\Lambda_M - \Lambda_m} . \tag{5.21}$$

since

$$\tfrac{1}{2}\Lambda = (1+z)^{1/2} - 1 . \tag{5.21a}$$

6. Case F, $\bar{q}_o = 1/2$, $p = 0$, $n = 1$

We are in Region I and

$$n_n(S) = \frac{2}{5} \frac{(1+z_m)^{-5/2} - (1+z_M)^{-5/2}}{\Lambda_M - \Lambda_m} , \tag{5.22}$$

where

$$2(1+z) = 1 + (1+2\Lambda)^{1/2} . \tag{5.22a}$$

7. Case G, $\bar{q}_o = 1/2$, $p = -4/3$, $n = 1.5$

We are in Region I, and the result is

$$n_n(S) = \frac{\ell n \left(\frac{1+x_M^3}{1+x_m^3} \right)}{\ell n \left(L_M / L_m \right)} \tag{5.23}$$

where

$$\tfrac{1}{3}\Lambda = x^2 - x^5 \tag{5.23a}$$

8. Case II, $\bar{q}_o = 1/2$, $p = -1.75$, $n = 1$

We are in Region II and

$$n_n(S) = \frac{z_M - z_m}{\Lambda_M - \Lambda_m} , \tag{5.24}$$

where z_M and z_m are solutions of

$$\tfrac{1}{2}\Lambda = (1+z)^{-3/4} - (1+z)^{-5/4} \tag{5.24a}$$

VI. THE RADIO LUMINOSITY FUNCTION

It is our purpose to show what scale covariance can accomplish with respect to the standard theory. If we fit the data by some special artifice in evolutionary and selection functions where the standard theory uses its own artifices, the separate contributions of the two theories are obscured. For this reason we fit the simplest RLF in conformity with previous practice, namely a truncated power law

$$\varphi = C \quad L^{-n} \quad , \quad L_{min} < L < L_{max}$$

$$0 \qquad , \quad L_{min} > L > L_{max}$$

where φ is the number of sources per unit volume with luminosities between L and 10L, which is related to Φ, the number of sources per unit volume with luminosities between L and L + dL and

$$\Phi \sim L^{-n-1} \equiv L^{\gamma},$$

with the same limits (Eq. 4.5).

The standard methods of calculating the RLF as outlined by Petrosian (1969) were used. The first method entails calculating the absolute luminosity L within the theory using Eqs. (3.2), (3.3), and (2.2). We use the best spectral index available for each source. When this is accomplished, the largest and smallest L become the limits used. At the same time the maximum redshift z_M at which the source luminosity could be observed at the flux limit of the survey ($3\ J_y$) is calculated; since $\varphi(z_M)$ is not known until z_M is known, an iterative routine must be used in general; we used our own, Wegstein's, Newton's and Moeller's (the same as used in finding the limits of the integral for n_p), finding our own most convenient for $\epsilon = -1$ and Wegstein's for $\epsilon = -1/2$. Since α differs from source to source for the same (ε, e) some sources have a maximum in ζ_L while others don't. When there is a maximum at $z_* < \infty$, there are two solutions for z_M, $z(M_1)$ and $z(M_2)$. The interest in finding z_M is to know the volume in which the source could be observed. If the sources are uniformly distributed and the universe is open, the observable volume is infinite when there is a maximum in ζ_L and a suitable number to represent infinity to a computer is chosen. If we are in Region II and the sources are uniformly distributed but the universe is closed, the appropriate closed volume must be used. If we assume that sources

don't appear before $z = 4$, we may use the volume up to the first $z(M_1)$ and add to it the volume between the second $z(M_2)$ and $z = 4$. Since, however, we don't believe in models with ζ_{L_*} at $z_* < 2$, it is unlikely that we will investigate a model with $z(M_2) < 4$, so it is sufficient to take volumes from $z = o$ to $z = z(M_1)$. We would do this even if we were trying to simulate selection effect IV, A.

The volumes in our theory are derived below. (See also III, Section XII).

The Robertson-Walker metric in atomic units is

$$\begin{aligned} ds^2 &= c^2\, dt^2 - R^2(t)\,[dr^2/(1 - k\, r^2) + r^2\, d\Omega^2] \\ &= c^2\, dt^2 - R^2(t)\,[d\chi^2 + \Sigma^2(\chi)\, d\Omega^2] \end{aligned} \tag{6.1}$$

where

$$r = \Sigma(\chi) = S(\sqrt{-k}\,\chi)/\sqrt{-k} = \sinh^{-1}(\sqrt{-k}\,\chi)/\sqrt{-k} \tag{6.2}$$

and

$$d\chi = \frac{dr}{(1-kr^2)^{1/2}} .$$

For photons $ds = 0$ and if $d\Omega = 0$ for convenience,

$$d\chi = \frac{c\, dt}{R(t)} , \tag{6.3a}$$

which, since dt and R(t) scale the same way, holds true in gravitational units, i.e.

$$d\chi = \frac{c\, d\bar{t}}{\bar{R}(\bar{t})} \tag{6.3b}$$

Just as in standard cosmology, this metric leads to

$$V(t_o, \chi) = 4\pi R_o^3 \int_o^{\chi} \Sigma^2(\chi')\, d\chi' , \tag{6.4}$$

with the limit given by

$$\chi = c \int_{\bar{t}_e}^{\bar{t}_o} \frac{d\bar{t}}{\bar{R}(\bar{t})} \tag{6.5}$$

where the limits $\bar{t}_o$ and $\bar{t}_e$ correspond to $z = o$ and z, which in turn corresponds to the emission redshift z in atomic units as in Eq. (3.4).

The values z, z, L (watt-sec), $V(Mpc^3)$, and V_{max} (Mpc^3) are given in Table 3.

Once the luminosities and maximum observable volumes are obtained, plots of lg L vs. lg z and lg L vs. lg z_M are made. Examples are given in Figures 2. The lg L axis is divided into overlapping one unit intervals, one-half unit apart, and the smallest $z_M = z_{MS}$ (corresponding to the weakest source in the interval when one spectral index is used as $\alpha = -.8$ in Petrosian 1969) is

found among the sources in each interval. The number of sources in the interval whose $z < z_{MS}$ is counted. This number is divided by the volume corresponding to z_{MS} to give φ for each L interval and a best fit of $\ell n\ \varphi = \ell n\ C - n\ \ell n\ L$ is made in order to find n. The second method of obtaining the RLF which we denote by an asterisk $\varphi^*(L)$ in order to differentiate it from the first one, is to sum up all the reciprocal volumes corresponding to the z_M in each interval and make the same power law approximation, $\lg \varphi^* = \lg C^* - n^* \lg L$. We found that n^* determined this way differed very little from n determined by the first method, n^* being generally slightly smaller than n.

In Table 4 we present the values of n that we have determined as a function of ϵ, $\bar{q}_o$, and c. As seen from the Table, the values of n cover quite a range from .2 to 2.4 depending on the chosen gauge and evolution. In Figure 3a-c we then present three typical RLF's for $\bar{q}_o = 0, +1/2$, and 1. We note that the RLF steepens as L increases and a power law is certainly only a first approximation just as in standard cosmology. We have chosen to present cases compatible with the data and this is partly responsible for the coincidence of the RLF's for different scales.

We reran our program with data compiled by Sutton (1973a,b) with criteria of completeness. His sample contains fewer high z sources, and has a higher n and thus a flatter N(S) curve for the same ϵ, $\bar{q}_o$, c. Nevertheless, the general conclusions of the paper are the same, even less evolution being required for the same results when $\epsilon < 0$.

VII. RESULTS

Using the values of the spectral index n so obtained, we have computed numerically the differential counts from (4.6).

In Figures 4a-4j we present the results for thirty selected cases, for the four gauges $\varepsilon = -1, -1/2, +1/2, .9$. For the first three gauges, we present the results for $\bar{q}_o = 0$, 1/2 and 1. For the last gauge, we only present the results for $\bar{q}_o = 0$ since, as seen from Table 4, the values of n are very insensitive to changes in $\bar{q}_o$. The theoretical curves are superposed on the same data used by von Hoerner (1973). We have fixed the normalization to be n_n (1 Jy) = 1.

The following comments are in order upon inspecting the results.

1) When ε is negative, the results depend sensitively on $\bar{q}_o$. When ε is positive, they do not. This same feature characterizes the tests studied in D .

2) It follows that for $\varepsilon < 0$, there is a clear deterioration of the fits as $\bar{q}_o$ increases.

3) For $\varepsilon < 0$, a closed Universe model does not fit the data.

4) For $\varepsilon > 0$, the data can be fitted with a closed or open Universe [see also paper III].

5) For each of the cases presented in Figures 4a-4j, we have selected the best fits and summarized the characteristic parameters in Table 5.

6) In the same Table we have also added a column giving the value of E, the evolutionary parameter as defined in standard cosmology, eqs. (2.14) and (2.15).

7) Such values of E are obtainable as a function of ε, ε, and $\bar{q}_o$ using (2.4) and (5.2). In the case of $\bar{q}_o = 0$ or 1/2, the relation is exact, whereas for other values of $\bar{q}_o$ is approximate.

We deduce

$$E = \frac{e}{H_o} \frac{s}{t_o} \tag{7.1}$$

The ratio E/e is also given in column D of Table 1 and the value of e which corresponds to E = 5 is given in the same table, column E.

VIII. DISCUSSION

Two major conclusions follow from our analysis. A self-consistent treatment of the parameters entering the problem, especially n, yields results that fit the data very satisfactorily, even when the "gravitational constant" G varies with time as t^{-1}.

When $e > 0$, the results are not very different from those of standard cosmology, whereas for $e < 0$ it is possible to discriminate between an open and a closed Universe. This does not happen in standard cosmology. Evolution of the sources is needed as in standard cosmology. In fact, our cosmology's main effect is the disentanglement of atomic from gravitational times, not the determination of a parameter like E or e which depends on the physics of the problem and only marginally on cosmology.

Even so, our cosmology brings in an amelioration. In fact, as seen from Table 5, the equivalent E needed here is less than the one usually posited in standard cosmology, as discussed in part 1. This means that our differentiation of z from z has accounted for part of what in standard cosmology is usually lumped under the name "evolutionary corrections". This is not totally unexpected since the luminosity is a function of G, which in turn is a function of t and therefore of z.

We can conclude by saying that the count of radio sources, much like the optical tests presented in Part D, not only does not forbid a varying G, but can be improved by it.

Table Captions

Table 1. Evolutionary parameter e defined in Eq. (2.15):

Column A: Values of e that give d lg N/d lg S < -1.5 (Eq. 2.23, $\alpha = -.75$).

Column B: Values of e that give $z_* = \infty$ (Eq. 3.7, $p = -1, -2$, $\alpha = -.75$).

Column C: Values of e that give $z_* = 2$, (Eqs. 3.4, 3.7, and 3.8, $\alpha = -.75$).

Column D: The ratio E/e in general as given by Eq. (7.1).

Column E: Values of e that give E = 5 (Eq. 7.1).

Table 2. Exponent p as a function of α and e when there is no evolution (e = 0) as given by Eq. (3.7). When p = -1 or -2 ($\bar{\alpha}_0 = 0$), we can expect the data if available to show a maximum in the luminosity distance which is not due to evolution but merely to the scale geometry and (constant) source spectral properties.

Table 3. We present the values from which the RLF is determined for typical cases. Luminosity is given in watts/Hz. Volumes are in $(\text{Mpc})^3$. These cases are presented in graphical form in Figure 2.

Table 4. The parameter n of the RLF for typical (z, $\bar{\alpha}_0$, e) investigated (for $\alpha = -.75$). Three digits are retained for easy reading but are obviously not statistically significant.

Table 5. For each ε, q_o investigated, with $\alpha = -.75$, we present the c which gave the best fit to the differential $N(S)$ data with the corresponding n, equivalent E as defined by Eq. (5.11), and ρ as given by Eq. (3.7).

Figure Captions E

Figure 1. Evolutionary parameter e vs. scale parameter ϵ satisfying Eq. (3.7) for p = -2 ($\bar{q}_{\epsilon} = 0$), Fig. 1a, and p = -1 ($\bar{q}_o = 1/2$), Fig. 1b, giving $z_* = \infty$.

Figure 2a-d. Log_{10} L (watts/Hz) vs. observed z (asterisks) and z_M (dots) from our data, corresponding to select cases from Fig. 3, detailed in Table 3.

Figure 3. The RLF corresponding to Table 5, some cases of which are further illustrated in Figures 2a-d and Table 2. They correspond to the following evolutionary parameters: Figure 3a (1) e = -1.28, (2) e = -4.5, (3) e = -35, (4) e = -.5. Figure 3b (1) e = -1.28, (2) e = -1.65, (3) e = -1.45, (4) e = -1.25. Figure 3c (1) e = -1.40, (2) b = -1.25. The RLF for $\bar{q}_o = 1$, e < 0 is not presented because the corresponding calculated lg N-lg S curve did not fit the data well.

Figure 4a-j. Log-Log plots of Eq. (5.1), N(S), the differential radio source counts normalized to Euclidean values. All curves are made to pass through the point (N,S) = (1, 1). Such vertical normalization is customary.

TABLE 1

EVOLUTIONARY PARAMETER e

$\bar{q}_o$	ϵ	$H_o t_o$	A	B	C	D	E
0	-1	1	-2.75	-6.75	-8.85	-1	-5
	-1/2	1	-3.50	-9.50	-9.96	-1/2	-10
	1/2	1	-0.50	1.50	3.50	1/2	10
	.92	1	-1.19	-1.01	.80	.92	5.435
	1	1	-1.25	-1.25		1	5
1/2	-1	1/3	-1.58	-1.58	-1.75	-3	-1.67
	-1/2	1/2	-1.75	-1.75	-2.75	-1	-5
	1/2	5/6	-1.08	-1.08	1.96	.6	8.333
	.92	.97	-1.24	-1.24	.66	.945	5.290
	1	1	-1.25	-1.25		1	5
1	-1	.1416	-1.25	-1.24		-7.06	-.708
	-1/2	.3562	-1.25	-1.24		-1.40	-3.56
	1/2	.7854	-1.25	-1.25	1.079	.637	7.854
	.92	.9651	-1.25	-1.25	.612	.953	5.248
	1	1	-1.25	-1.25		1	5

TABLE 2

VALUES OF THE PARAMETER p
AS DEFINED IN EQ.(3.7)

$\theta=0,\ g^*\xi=-1$

$\bar{q}_c$	Q/ε	-1.00	-.50	0.00	.50	.92
0.	-.25	-.438	-.584	-.875	-1.750	-10.94
	-.50	-.375	-.500	-.750	-1.500	-9.38
	-.75	-.312	-.416	-.625	-1.250	-7.81
	-1.00	-.250	-.333	-.500	-1.000	-6.25
.50	-.25	-.562	-.638	-1.125	-2.438	-16.22
	-.50	-.500	-.625	-1.000	-2.125	-13.94
	-.75	-.438	-.562	-.875	-1.812	-11.66
	-1.00	-.375	-.500	-.750	-1.500	-9.38
1.00	-.25	-.484	-.740	-1.251	-2.786	-18.89
	-.50	-.469	-.683	-1.126	-2.441	-16.24
	-.75	-.454	-.635	-1.001	-2.096	-13.59
	-1.00	-.438	-.594	-.876	-1.752	-10.95

$(\epsilon,\beta) = (-1.00, -3.50)$

$\bar{q}_o = 0$

Z	$\hat{z}$	LOG L	V(MPC3)	VM(MPC3)
0.02	0.051	25.5	.1360+08	.2340+09
0.03	0.055	25.9	.1580+08	.9650+09
0.06	0.113	26.5	.1390+09	.8930+10
0.07	0.134	26.1	.2270+09	.1790+10
0.07	0.141	26.0	.2580+09	.1330+10
0.08	0.154	25.9	.4000+09	.9280+09
0.08	0.171	27.1	.4481+09	.6610+11
0.10	0.206	26.2	.7450+09	.2260+10
0.11	0.220	26.6	.9860+09	.1180+11
0.12	0.252	26.8	.1390+10	.2180+11
0.13	0.277	26.8	.1670+10	.1680+11
0.14	0.293	27.0	.1940+10	.4470+11
0.15	0.307	26.9	.2550+10	.3758+11
0.16	0.341	27.8	.2910+10	.1080+13
0.16	0.343	27.0	.3088+10	.5640+11
0.17	0.362	26.9	.3400+10	.3670+11
0.18	0.404	27.5	.3520+10	.8540+12
0.19	0.418	26.6	.4955+10	.1690+11
0.20	0.430	27.3	.5320+10	.9370+11
0.20	0.440	27.8	.5838+10	.1960+12
0.20	0.440	27.3	.5650+10	.1160+12
0.21	0.476	27.8	.6891+10	.1520+12
0.24	0.535	27.3	.9210+10	.1170+12
0.24	0.537	26.6	.9350+10	.1098+11
0.24	0.538	27.0	.9352+10	.4050+11
0.25	0.560	26.7	.1020+11	.1560+11
0.26	0.578	27.7	.1120+11	.4830+12
0.26	0.588	25.9	.1170+11	.2370+11
0.26	0.593	27.3	.1220+11	.1440+12
0.27	0.608	26.7	.1250+11	.1395+11
0.27	0.618	27.6	.1320+11	.3170+12
0.30	0.665	28.2	.1700+11	.2250+11
0.30	0.676	26.7	.1770+11	.1770+11
0.31	0.686	27.7	.1830+11	.5760+12
0.31	0.710	27.5	.1990+11	.2540+12
0.32	0.742	27.4	.2260+11	.2100+12
0.32	0.750	27.3	.2110+11	.1390+12
0.33	0.780	27.2	.2310+11	.1090+12
0.34	0.806	27.5	.2510+11	.2160+12
0.35	0.852	27.5	.2860+11	.2670+12
0.35	0.858	26.9	.2650+11	.5980+11
0.37	0.869	27.6	.2930+11	.4000+12
0.37	0.869	27.0	.2990+11	.7570+11
0.37	0.869	28.3	.2990+11	.2760+13
0.37	0.877	27.3	.3060+11	.1140+12
0.37	0.880	27.7	.3050+11	.5660+12
0.37	0.880	27.6	.3038+11	.4270+12
0.38	0.913	27.0	.3400+11	.5440+11
0.39	0.937	27.5	.3470+11	.2830+12
0.41	0.975	27.4	.3938+11	.1930+12
0.41	0.982	27.5	.3960+11	.2140+12
0.41	0.991	27.7	.4060+11	.4010+12
0.42	1.016	27.4	.4300+11	.1440+12
0.43	1.031	28.1	.4440+11	.1550+13

$(\epsilon,\beta) = (-0.50, -4.50)$

$\bar{q}_o = 0$

$\hat{z}$	LOG L	V(MPC3)	VM(MPC3)
0.034	25.5	.1360+08	.2310+09
0.039	25.9	.1580+08	.9450+09
0.094	26.5	.1390+09	.8580+10
0.099	26.1	.2260+09	.1750+10
0.104	26.0	.2580+09	.1260+10
0.121	25.9	.3998+09	.9230+09
0.125	27.1	.4440+09	.6310+11
0.151	26.2	.7420+09	.2260+10
0.166	26.6	.9810+09	.1070+11
0.184	26.8	.1290+10	.2110+11
0.201	26.8	.1660+10	.1630+11
0.212	27.0	.1930+10	.4250+11
0.236	26.9	.2530+10	.3440+11
0.246	27.8	.2880+10	.1140+13
0.251	27.0	.3240+10	.5460+11
0.261	26.9	.3370+10	.3560+11
0.290	27.5	.4480+10	.2660+12
0.300	26.6	.4900+10	.1650+11
0.308	27.3	.5260+10	.9070+11
0.315	27.2	.5570+10	.1030+12
0.315	27.3	.5570+10	.1560+12
0.333	27.8	.6600+10	.1490+12
0.379	27.3	.9090+10	.1140+12
0.381	26.6	.9200+10	.1070+11
0.391	27.0	.9800+10	.3930+11
0.396	25.7	.1020+11	.1530+11
0.408	27.7	.1100+11	.4540+12
0.414	25.9	.1140+11	.2360+11
0.421	27.3	.1190+11	.1410+12
0.426	26.7	.1230+11	.1320+11
0.436	27.6	.1290+11	.3130+12
0.479	26.8	.1660+11	.2150+11
0.487	26.7	.1730+11	.1730+11
0.493	27.7	.1780+11	.5770+12
0.501	27.5	.1860+11	.2290+12
0.517	27.4	.2090+11	.2140+12
0.522	27.3	.2060+11	.1350+12
0.541	27.2	.2250+11	.1060+12
0.558	27.5	.2430+11	.2110+12
0.593	27.5	.2760+11	.2610+12
0.598	27.0	.2760+11	.5590+11
0.590	27.6	.2850+11	.3960+12
0.598	27.0	.2890+11	.7350+11
0.598	28.3	.2890+11	.2770+13
0.604	27.3	.2950+11	.1100+12
0.605	27.7	.2970+11	.5570+12
0.605	27.6	.2970+11	.4240+12
0.630	27.0	.3280+11	.5240+11
0.635	27.5	.3350+11	.2790+12
0.667	27.4	.3770+11	.1880+12
0.671	27.5	.3820+11	.2080+12
0.676	27.7	.3860+11	.3900+12
0.682	27.4	.4120+11	.1380+12
0.701	28.2	.4350+11	.1520+13

0.43	1.053	27.5	.4670+11	.3020+12
0.45	1.103	27.4	.5210+11	.1790+12
0.49	1.203	27.6	.6370+11	.3870+12
0.53	1.305	27.7	.7960+11	.5670+12
0.53	1.303	27.4	.8200+11	.2430+12
0.54	1.366	28.1	.8370+11	.2770+13
0.54	1.372	27.5	.8450+11	.2430+12
0.54	1.387	28.6	.8660+11	.1000+14
0.55	1.415	28.2	.9060+11	.2960+13
0.55	1.415	28.0	.9060+11	.9350+12
0.56	1.424	28.1	.9210+11	.1660+13
0.56	1.437	27.7	.9360+11	.5660+12
0.57	1.468	28.0	.9810+11	.1770+13
0.57	1.477	27.9	.9980+11	.1600+13
0.58	1.544	27.6	.1100+12	.1540+13
0.60	1.557	27.7	.1120+12	.4710+12
0.61	1.606	27.9	.1190+12	.8990+12
0.61	1.605	27.8	.1190+12	.6290+12
0.62	1.611	28.1	.1200+12	.1610+13
0.63	1.641	28.3	.1250+12	.3030+13
0.63	1.657	27.6	.1280+12	.3360+12
0.64	1.693	28.1	.1340+12	.9880+12
0.65	1.729	28.2	.1400+12	.2090+13
0.65	1.758	27.6	.1440+12	.3530+12
0.67	1.796	28.1	.1500+12	.1040+13
0.67	1.796	27.8	.1520+12	.1250+13
0.68	1.812	27.4	.1550+12	.2490+12
0.68	1.836	28.0	.1590+12	.3670+13
0.68	1.836	27.5	.1590+12	.3110+12
0.69	1.863	28.8	.1640+12	.3270+14
0.70	1.897	27.7	.1690+12	.3340+12
0.72	1.958	27.7	.1780+12	.8900+12
0.72	1.963	27.9	.1780+12	.1530+13
0.73	1.989	27.8	.1820+12	.3460+12
0.73	1.996	27.5	.1830+12	.2300+12
0.73	2.007	28.5	.1920+12	.4200+13
0.76	2.093	28.3	.2110+12	.6240+13
0.76	2.115	28.0	.2150+12	.9980+12
0.77	2.129	28.4	.2170+12	.3820+13
0.78	2.204	27.6	.2340+12	.2560+12
0.78	2.202	27.5	.2360+12	.3510+12
0.85	2.419	28.4	.2780+12	.1570+14
0.86	2.430	27.8	.2800+12	.1050+13
0.86	2.456	28.2	.2930+12	.6990+13
0.86	2.463	27.7	.2940+12	.8230+12
0.87	2.501	28.1	.3040+12	.1630+13
0.87	2.501	27.5	.3040+12	.6120+12
0.87	2.504	28.1	.3050+12	.3010+14
0.88	2.516	28.1	.3070+12	.1350+13
0.89	2.572	27.9	.3220+12	.9950+12
0.90	2.591	28.1	.3270+12	.1400+13
0.90	2.614	27.5	.3330+12	.5740+12
0.92	2.625	28.5	.3460+12	.1200+14
0.91	2.633	28.2	.3380+12	.2750+13
0.91	2.663	28.2	.3460+12	.2760+13
0.93	2.713	28.4	.3590+12	.3980+13
0.94	2.764	28.5	.3730+12	.7510+13
0.96	2.846	28.2	.3960+12	.2470+13
0.96	2.849	28.5	.3970+12	.9250+13
0.98	2.920	28.3	.4170+12	.3700+13
1.01	3.048	28.2	.4550+12	.2330+13

0.715	27.5	.4470+11	.2950+12	
0.748	27.4	.4970+11	.1630+12	
0.811	27.6	.5930+11	.3770+12	
0.889	27.7	.7070+11	.5640+12	
0.900	27.4	.7690+11	.2320+12	
0.907	28.1	.7840+11	.2360+13	
0.911	27.5	.7930+11	.2350+12	
0.920	28.6	.8110+11	.1040+14	
0.937	28.2	.8460+11	.2970+13	
0.979	28.0	.8560+11	.9980+12	
0.943	28.1	.8580+11	.1660+13	
0.950	27.7	.8750+11	.5460+12	
0.960	28.3	.9180+11	.1770+13	
0.978	27.9	.9260+11	.1380+13	
1.014	27.8	.1020+12	.1600+13	
1.022	27.7	.1030+12	.4490+12	
1.050	27.9	.1100+12	.8970+12	
1.050	27.8	.1100+12	.5960+12	
1.054	28.1	.1110+12	.1560+13	
1.071	28.3	.1150+12	.2020+13	
1.081	27.9	.1170+12	.8140+12	
1.102	28.1	.1210+12	.9220+12	
1.120	28.2	.1250+12	.1960+13	
1.137	27.6	.1320+12	.3220+12	
1.156	28.1	.1370+12	.1470+13	
1.162	27.8	.1380+12	.1260+13	
1.172	27.4	.1410+12	.2290+12	
1.183	28.0	.1450+12	.4180+13	
1.185	27.5	.1450+12	.2870+12	
1.201	28.8	.1490+12	.3760+14	
1.219	27.7	.1530+12	.8120+12	
1.256	27.7	.1550+12	.8870+12	
1.256	27.9	.1650+12	.1550+13	
1.273	27.4	.1700+12	.3260+12	
1.277	27.5	.1710+12	.2540+12	
1.283	28.5	.1730+12	.3020+13	
1.335	28.3	.1850+12	.6460+13	
1.346	27.9	.1930+12	.9130+12	
1.351	28.4	.1940+12	.3260+13	
1.346	27.6	.2030+12	.3180+12	
1.472	27.5	.2340+12	.3120+12	
1.514	28.4	.2460+12	.1790+14	
1.530	27.7	.2510+12	.4830+12	
1.536	28.2	.2560+12	.6570+13	
1.539	27.7	.2580+12	.7520+12	
1.550	28.1	.2650+12	.1670+13	
1.559	27.5	.2650+12	.5560+12	
1.561	29.1	.2660+12	.2750+14	
1.567	28.0	.2680+12	.1210+13	
1.598	27.9	.2800+12	.8960+12	
1.609	28.0	.2840+12	.1250+13	
1.621	27.6	.2890+12	.5100+12	
1.627	28.5	.2910+12	.1200+14	
1.631	28.2	.2930+12	.2540+13	
1.648	28.1	.2990+12	.2570+13	
1.675	28.4	.3100+12	.3580+13	
1.702	28.5	.3210+12	.6960+13	
1.745	28.2	.3390+12	.2190+13	
1.748	28.5	.3390+12	.4450+13	
1.786	28.2	.3550+12	.3430+13	
1.858	28.2	.3850+12	.2060+13	

TABLE 4

EXPONENT n OF RLF (EQ.4.5)

ϵ	$c/\tilde{q}_o$	0	1/2	1
-1	-4.50	1.55		
	-4.00			1.35
	-3.50	1.11	1.46	
	-1.56	.879	.759	
	-1.50	.876	.734	.399
	-1.45	.861	.726	
	-1.25	.822	.728	.270
	0.00	.735	.465	.257
	2.00	.640	.305	.192
-1/2	-6.00	2.04	1.91	
	-5.00	1.21	1.02	
	-4.50	1.14	1.12	
	-4.00	1.04		
	-1.65	.879	.886	
	- .80	.897	.776	.774
	0.00	.825	.795	.615
	2.00	.754	.583	.513
1/2	-2.00		.956	.959
	-1.25	.957	1.11	1.77
	-1.00	.928	1.15	
	- .50	1.07		1.44
	0.00	1.23	1.38	
	1.00	1.58	1.79	
.92	-2.00	1.03	1.03	1.03
	-1.40	1.05	1.05	1.05
	-1.25	1.07	1.07	1.07
	-1.20	1.08	1.09	
	- .50			2.08
	0.00	2.41	2.34	

TABLE 5

EVOLUTIONARY PARAMETER e (EQ. 2.15)
YIELDING BEST FIT OF DIFFERENTIAL LG N-LG S DATA

$\alpha = -.75$

$\bar{q}_0$	ϵ	e	n	E	p
0	-1.00	-3.50	1.110	3.50	-1.1875
	-0.50	-4.50	1.140	2.25	-1.1667
	0.50	-0.50	1.070	-0.25	-1.0000
	0.92	-1.28	1.070	-1.30	-0.4525
1/2	-1.00	-1.45	0.726	4.35	-0.9500
	-0.50	-1.65	0.866	1.65	-0.8750
	0.50	-1.25	1.110	-0.75	-0.8750
	0.92	-1.28	1.070	-1.32	-0.6938
1	0.50	-1.25	1.170	-0.24	-1.0010
	0.92	-1.40	1.050	-0.40	0.3101

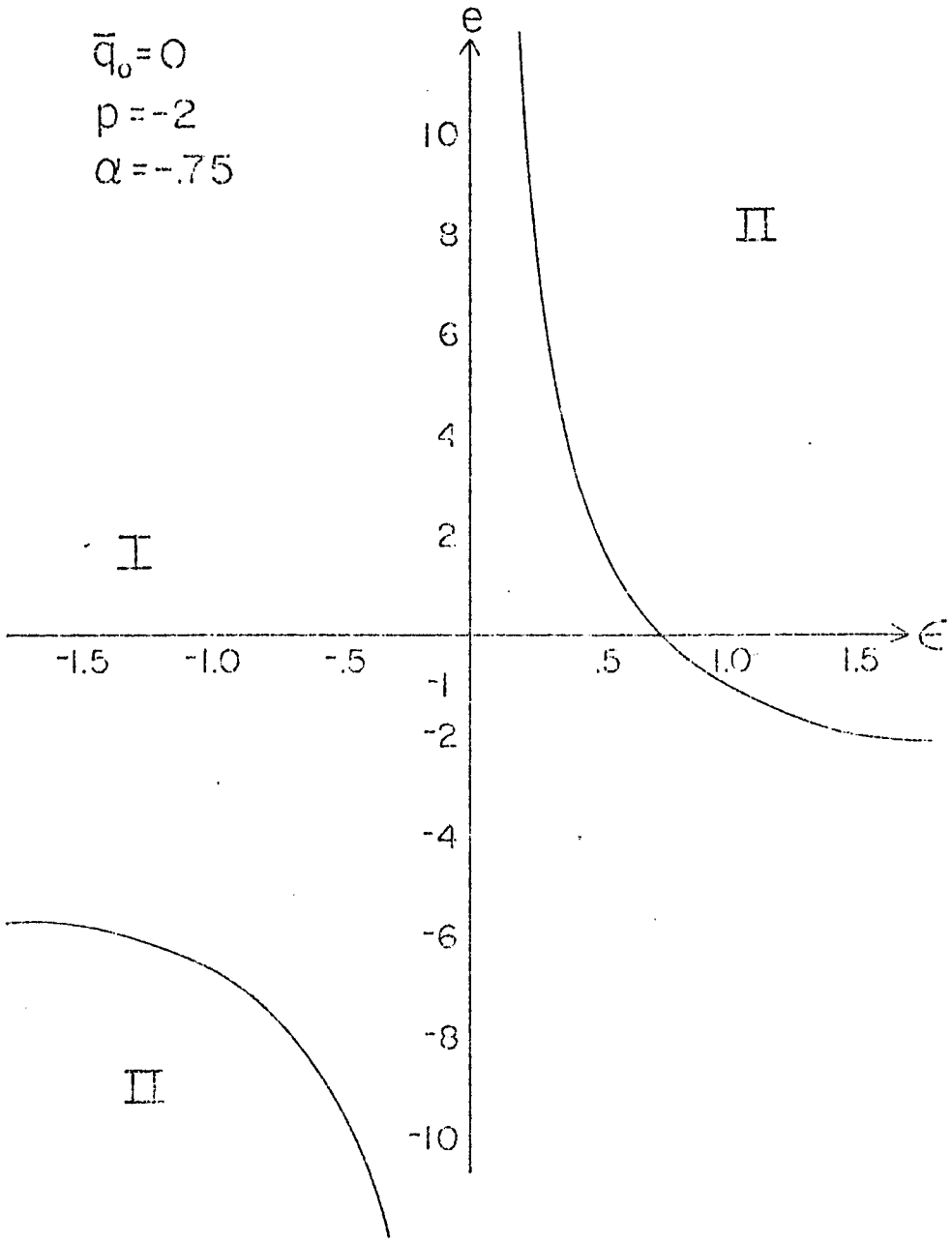
$\bar{q}_o = 0$
$p = -2$
$\alpha = -.75$
e
10
8
6
4
2
-1
-2
-4
-6
-8
-10
I
II
II
-1.5
-1.0
-.5
.5
1.0
1.5
ϵ

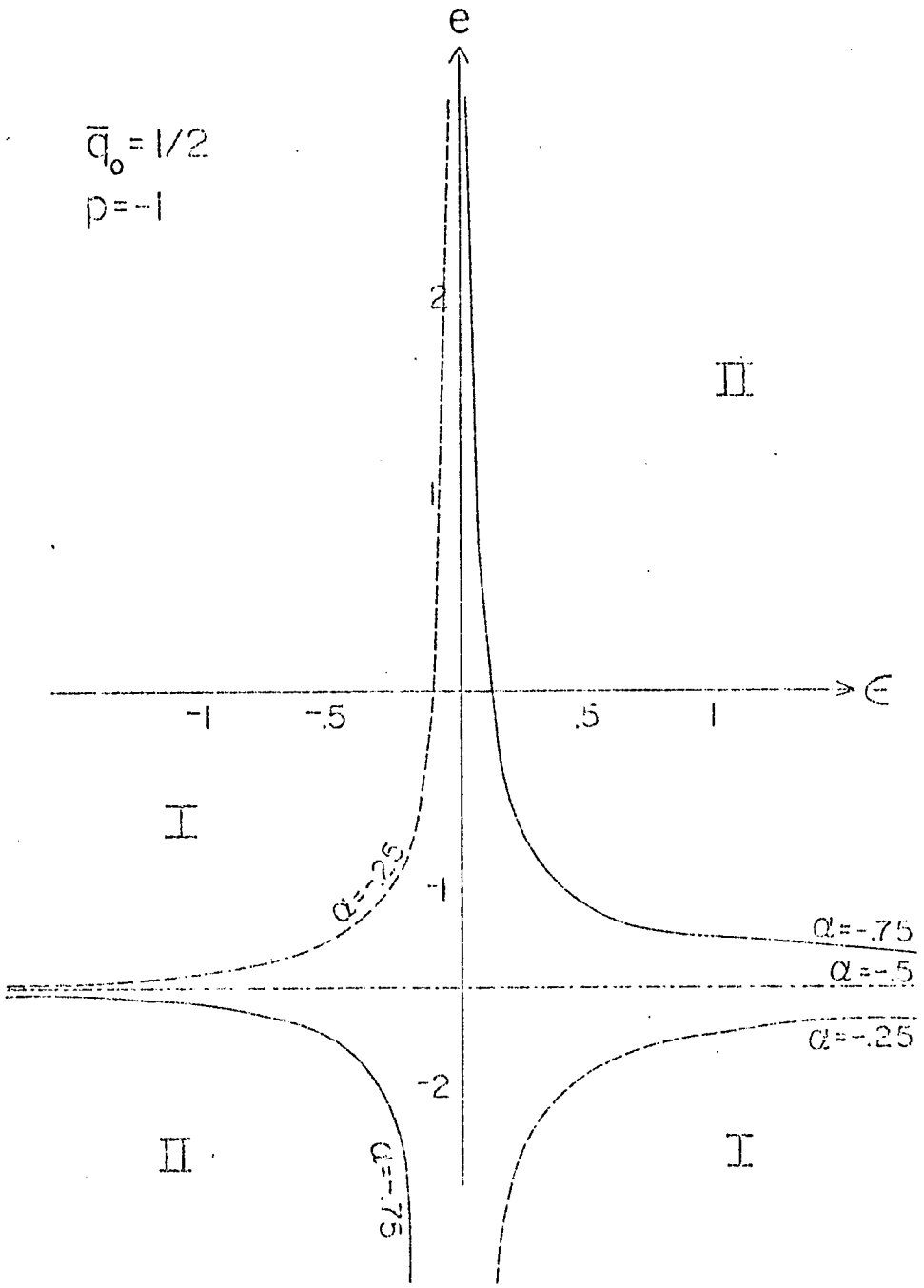
e
$\bar{q}_o = 1/2$
$p = -1$
2
1
-1
-2
-1
-.5
.5
1
ϵ
II
I
II
I
α=-.25
α=-.75
α=-.75
α=-.5
α=-.25

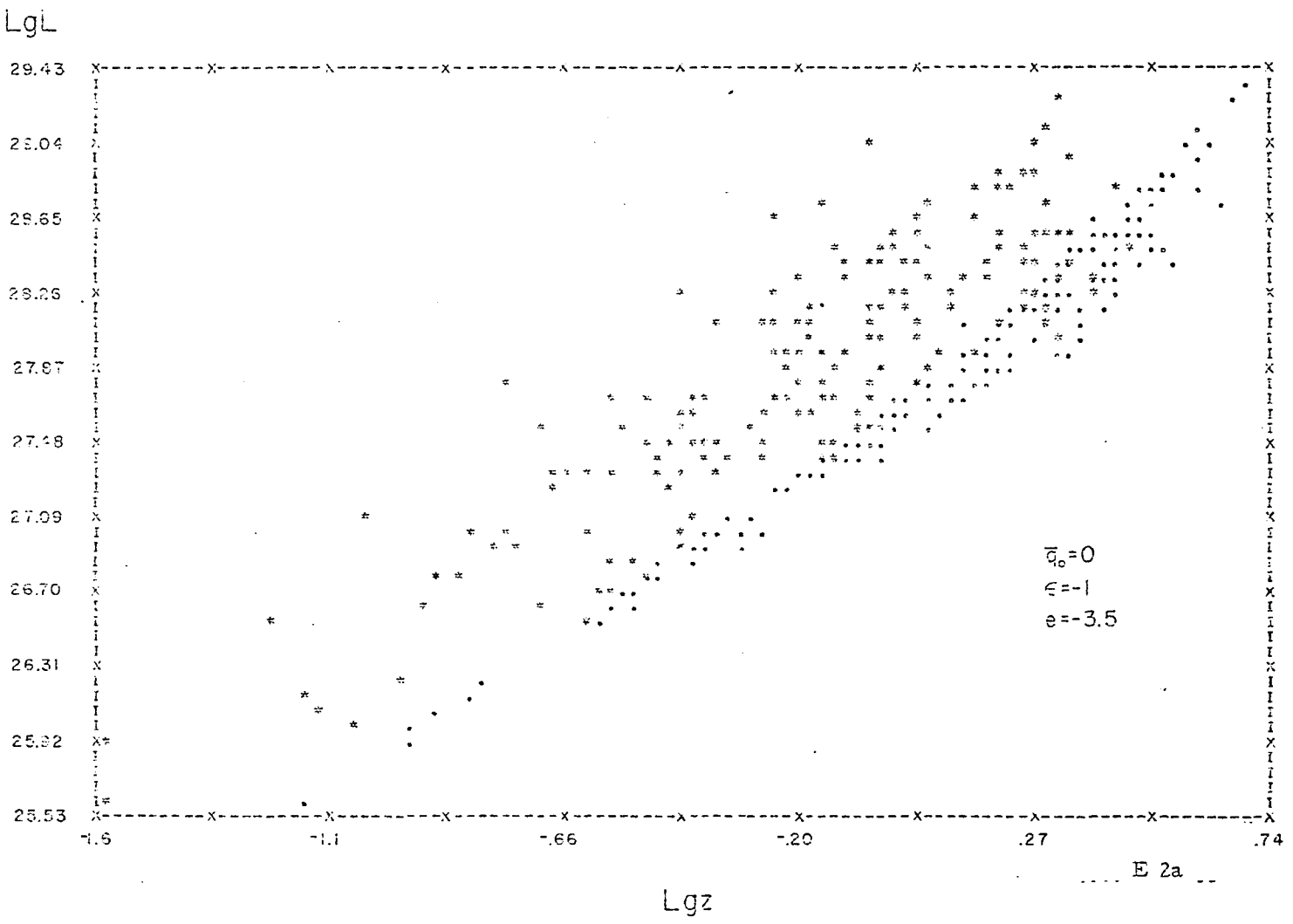
LgL
29.43
28.04
28.65
28.26
27.87
27.48
27.09
26.70
26.31
25.92
25.53
-1.6
-1.1
-.66
-.20
.27
.74
$\bar{\sigma}_0$=0
ϵ=-1
e=-3.5
E 2a
Lgz

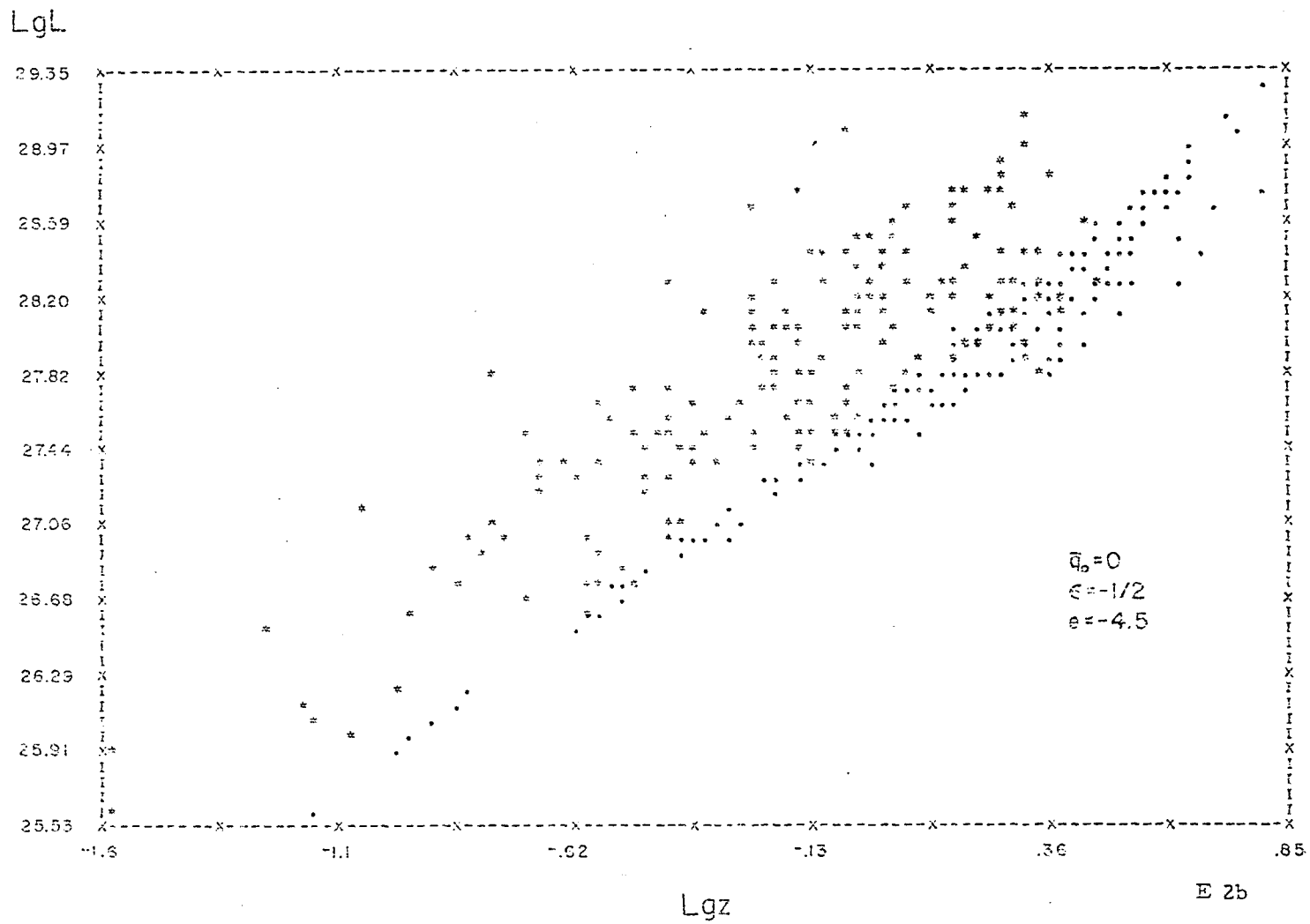
LgL
29.35
28.97
28.59
28.20
27.82
27.44
27.06
26.68
26.29
25.91
25.53
-1.6
-1.1
-.62
-.13
.36
.85
Lgz
$\bar{q}_b$=0
ϵ=-1/2
θ=-4.5

E 2b

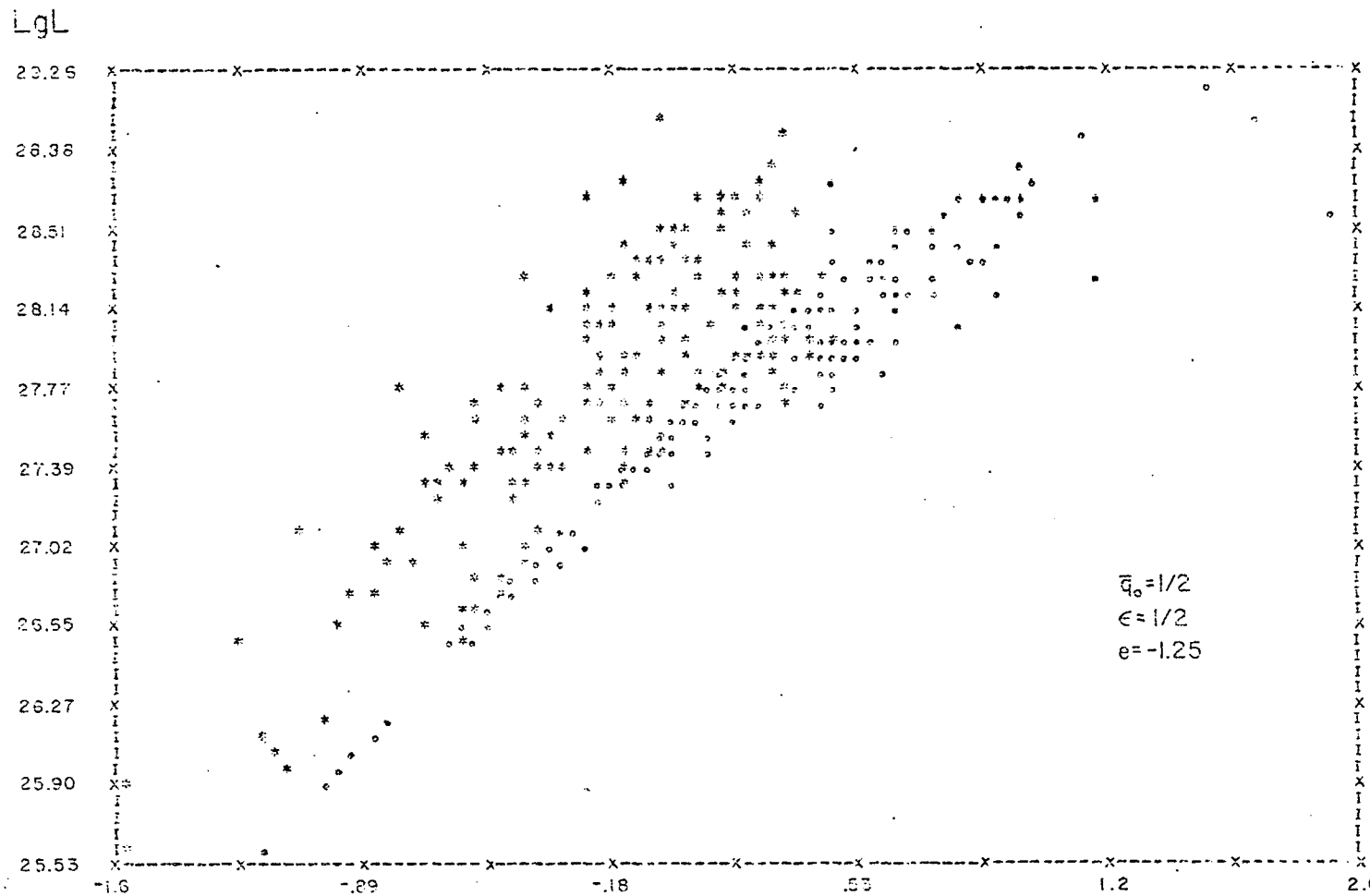
LgL
28.25
28.38
28.51
28.14
27.77
27.39
27.02
26.65
26.27
25.90
25.53
-1.6
-.89
-.18
.53
1.2
2.0
Lgz
$\bar{q}_o$=1/2
ϵ=1/2
e=-1.25

E 2c

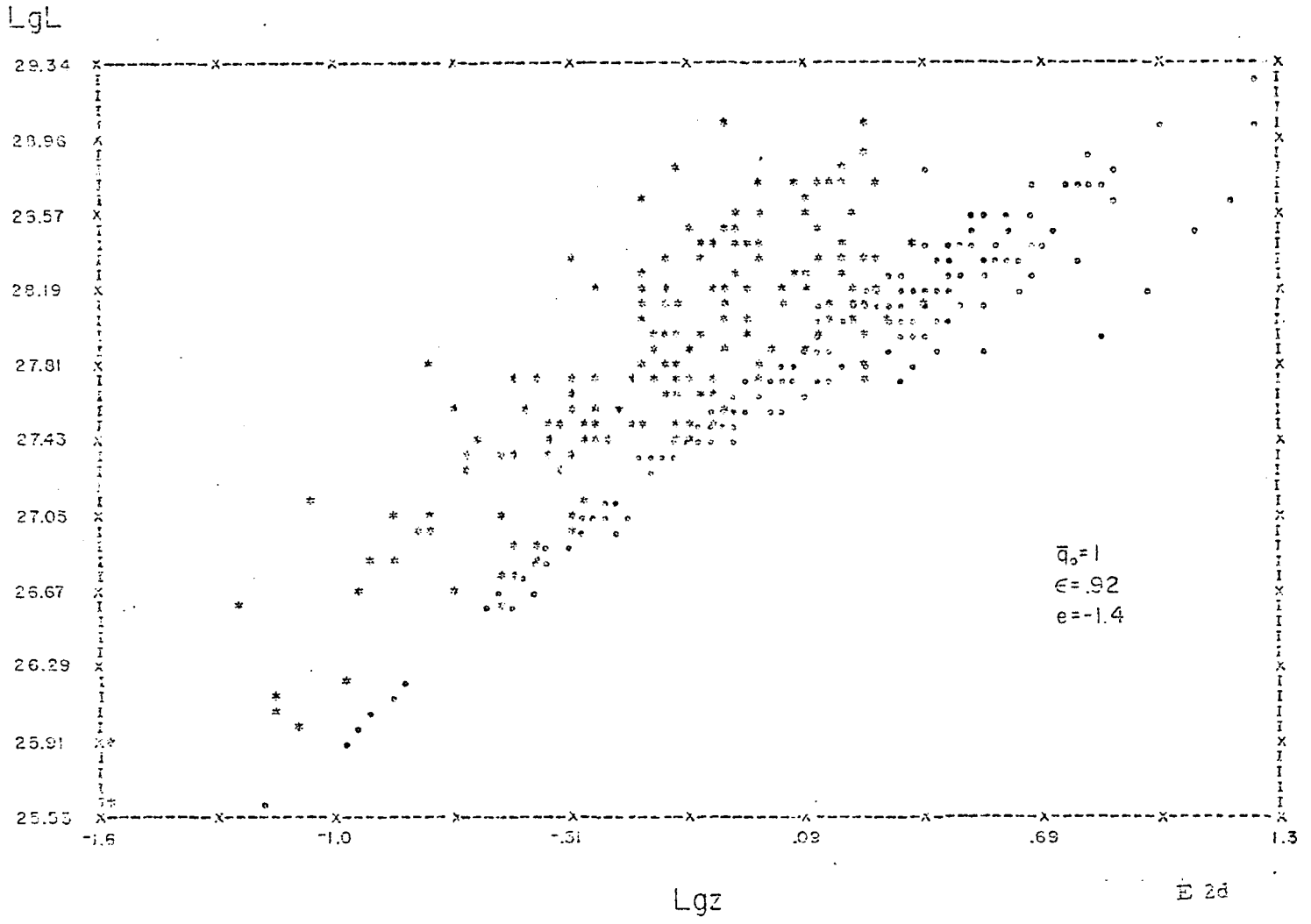
LgL
29.34
28.96
28.57
28.19
27.81
27.43
27.05
26.67
26.29
25.91
25.53
-1.6
-1.0
-.51
.09
.69
1.3
Lgz
$\bar{q}_o$=1
ϵ=.92
e=-1.4

E 2d

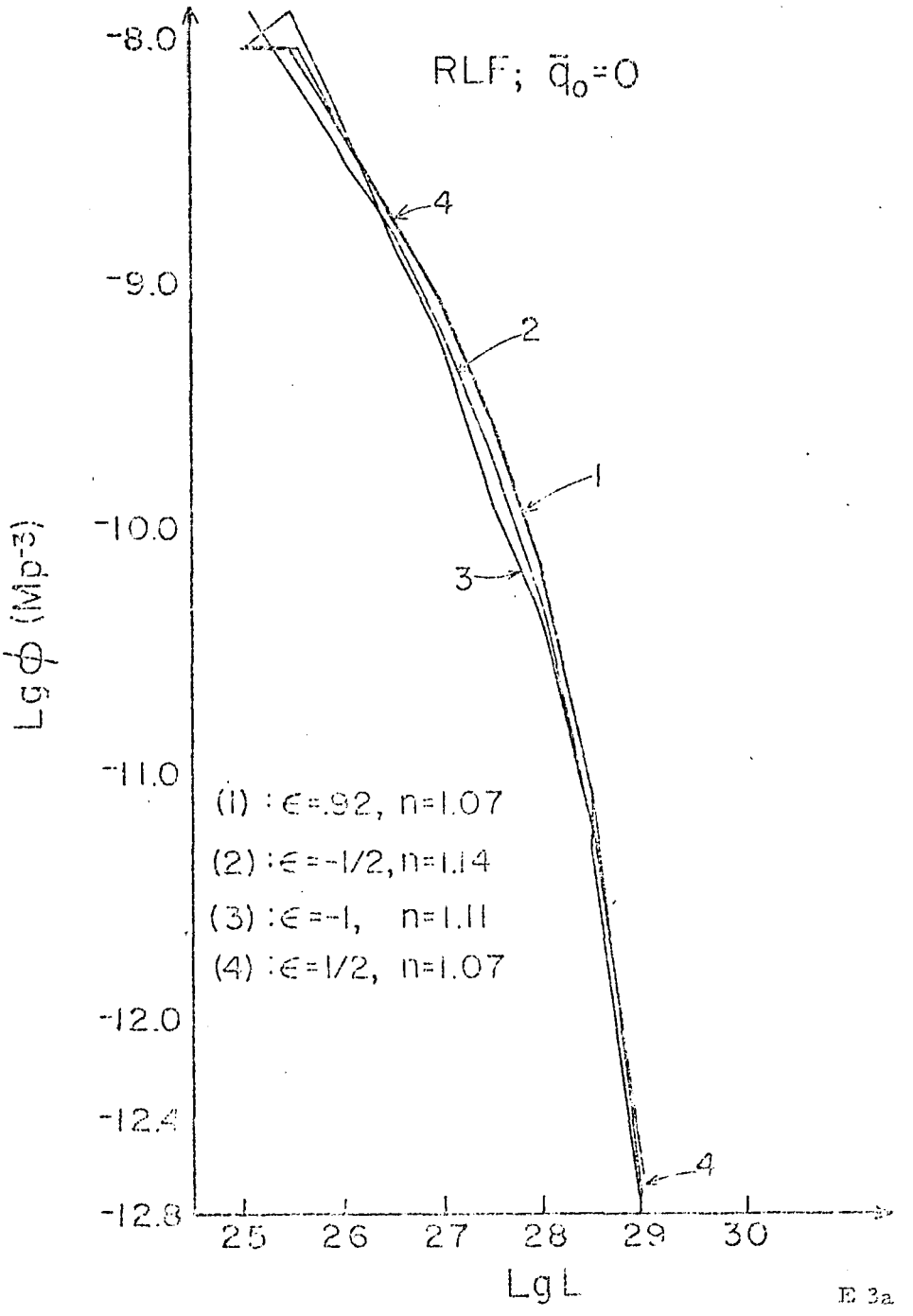
RLF; $\bar{q}_o$=0
-8.0
-9.0
-10.0
-11.0
-12.0
-12.4
-12.8
Lg φ (Mp^{-3})
25
26
27
28
29
30
Lg L
4
2
1
3
4
(1) : ∈=.92, n=1.07
(2) : ∈=-1/2, n=1.14
(3) : ∈=-1, n=1.11
(4) : ∈=1/2, n=1.07

E 3a

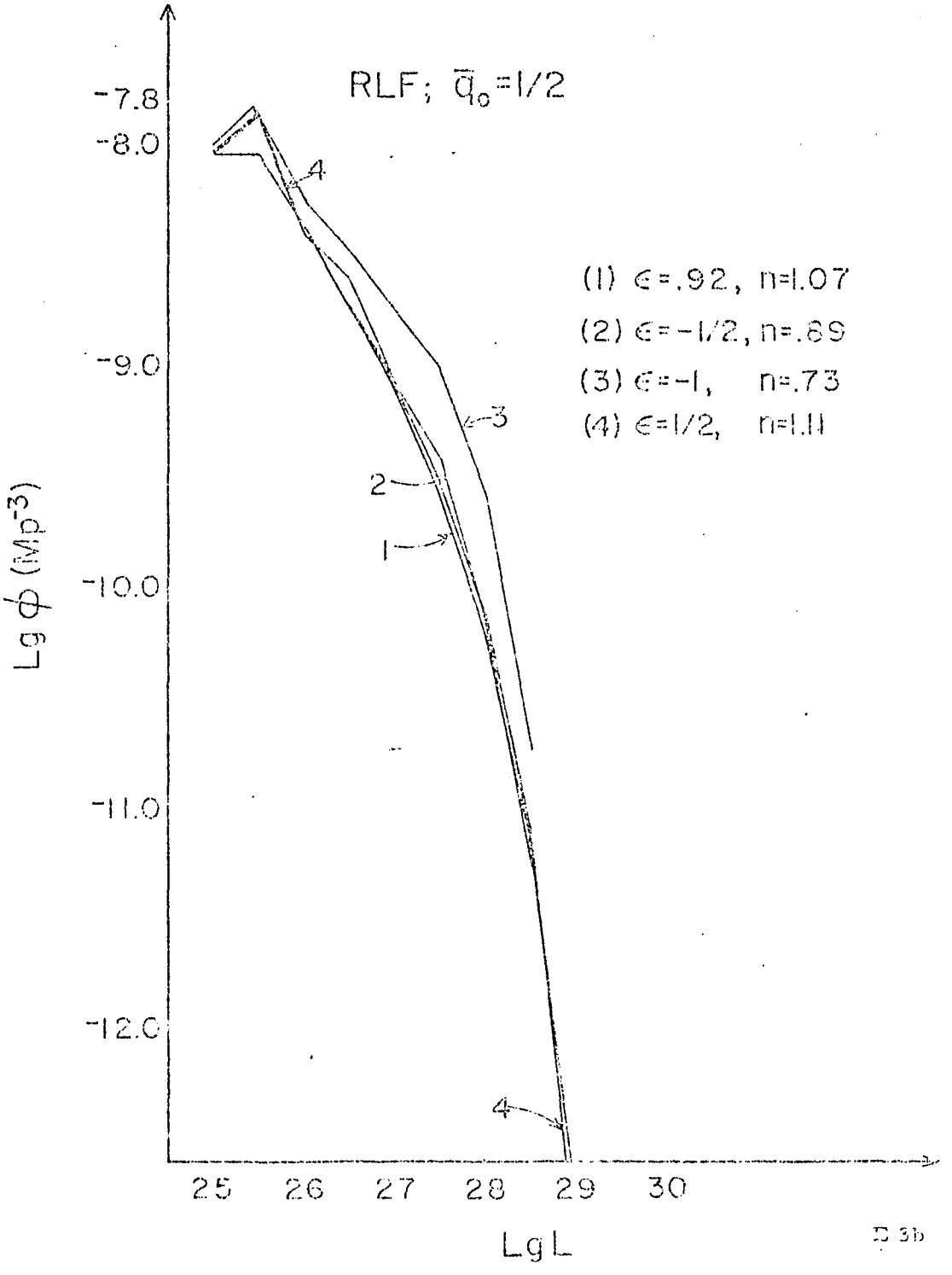
RLF; $\bar{q}_o$=1/2
(1) ϵ=.92, n=1.07
(2) ϵ=-1/2, n=.89
(3) ϵ=-1, n=.73
(4) ϵ=1/2, n=1.11
-7.8
-8.0
-9.0
-10.0
-11.0
-12.0
Lg φ (Mp^{-3})
25
26
27
28
29
30
LgL
1
2
3
4

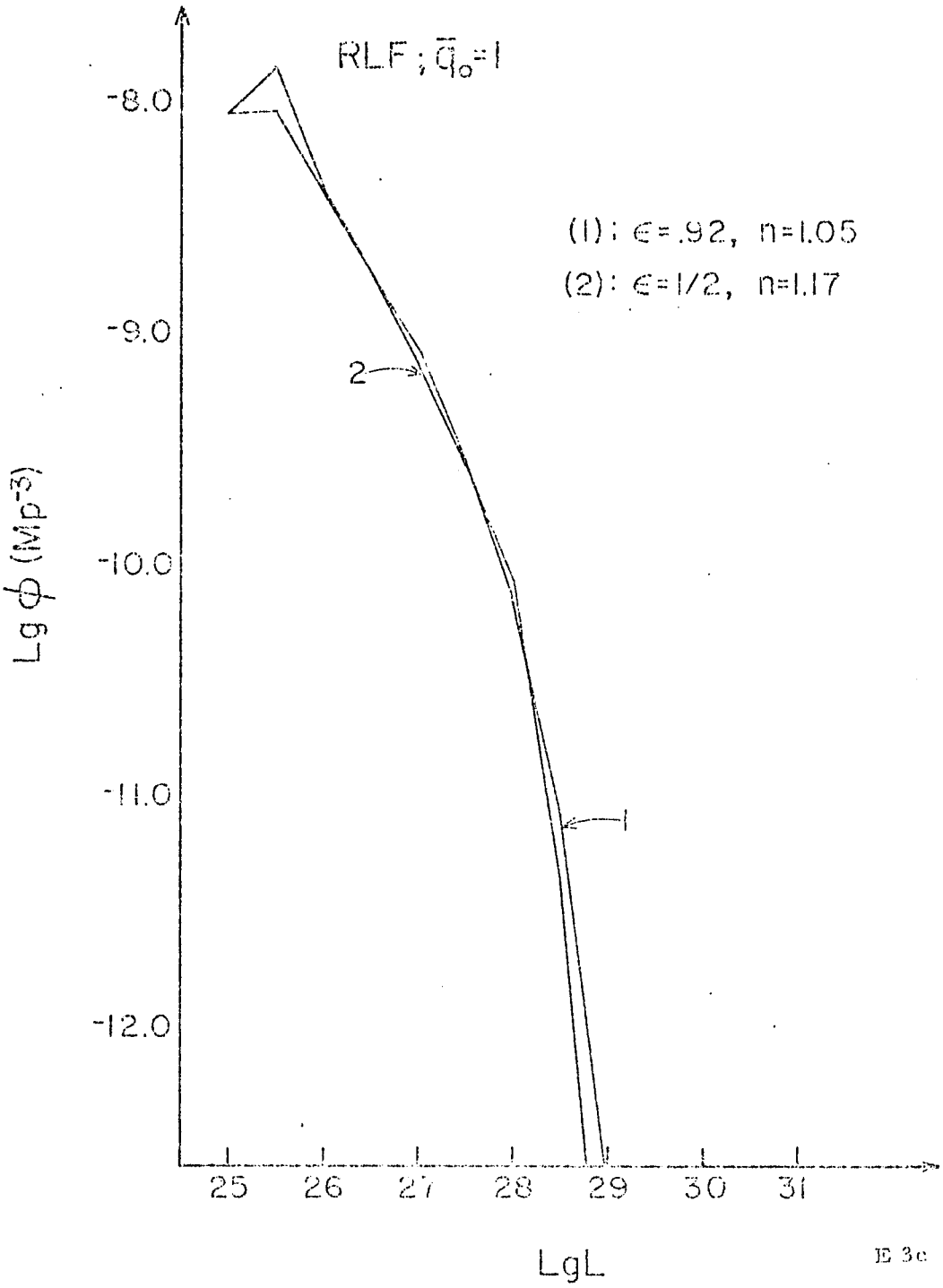
RLF ; $\bar{q}_o$=1
(1) : ∈=.92, n=1.05
(2) : ∈=1/2, n=1.17
-8.0
-9.0
-10.0
-11.0
-12.0
Lg φ (Mp^{-3})
25
26
27
28
29
30
31
LgL
1
2

E 3c

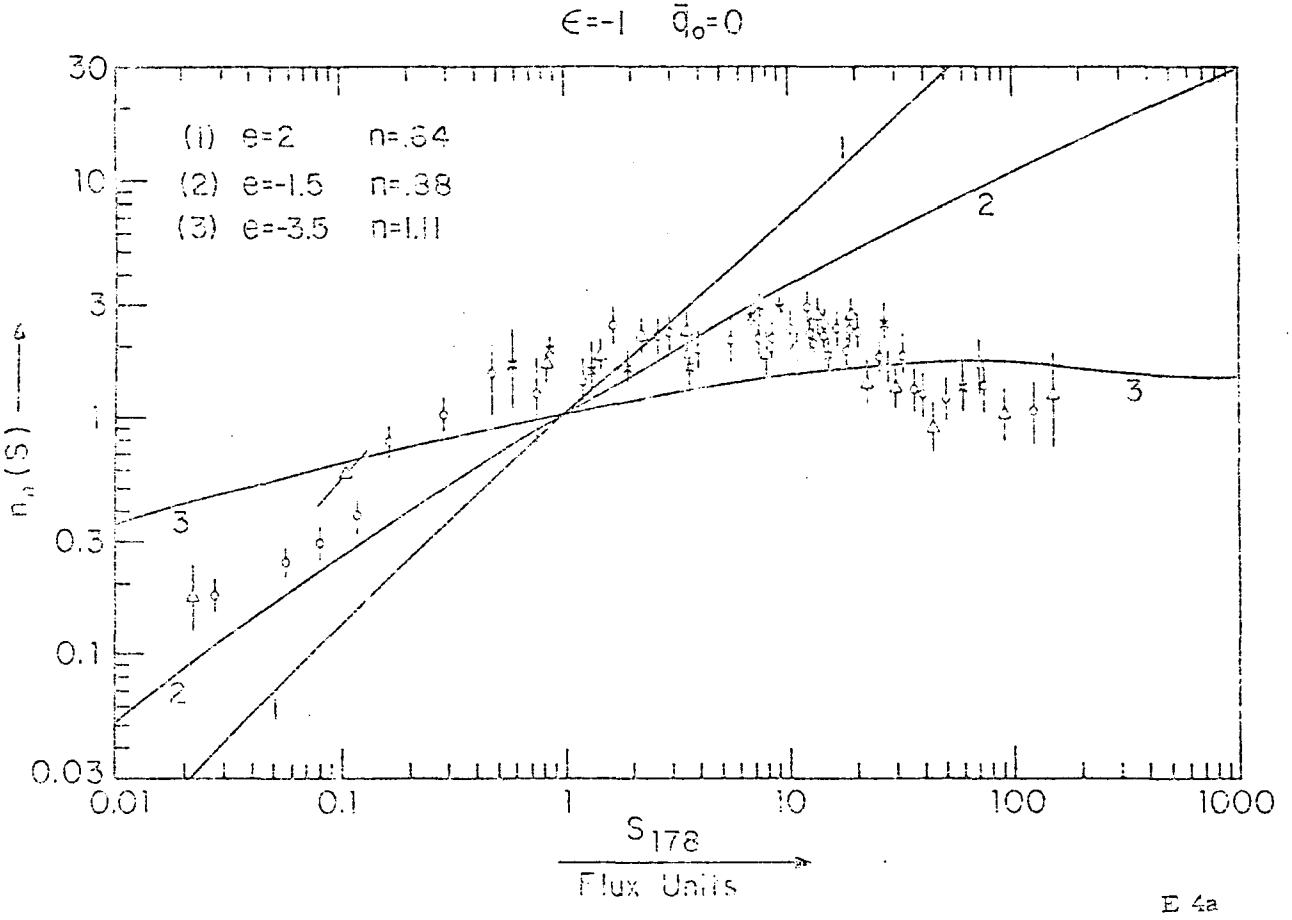
ϵ=-1 $\bar{q}_o$=0
(1) e=2 n=.64
(2) e=-1.5 n=.38
(3) e=-3.5 n=1.11
30
10
3
1
0.3
0.1
0.03
$n_n(S)$
0.01
0.1
1
10
100
1000
S_{178}
Flux Units
1
2
3

E 4a

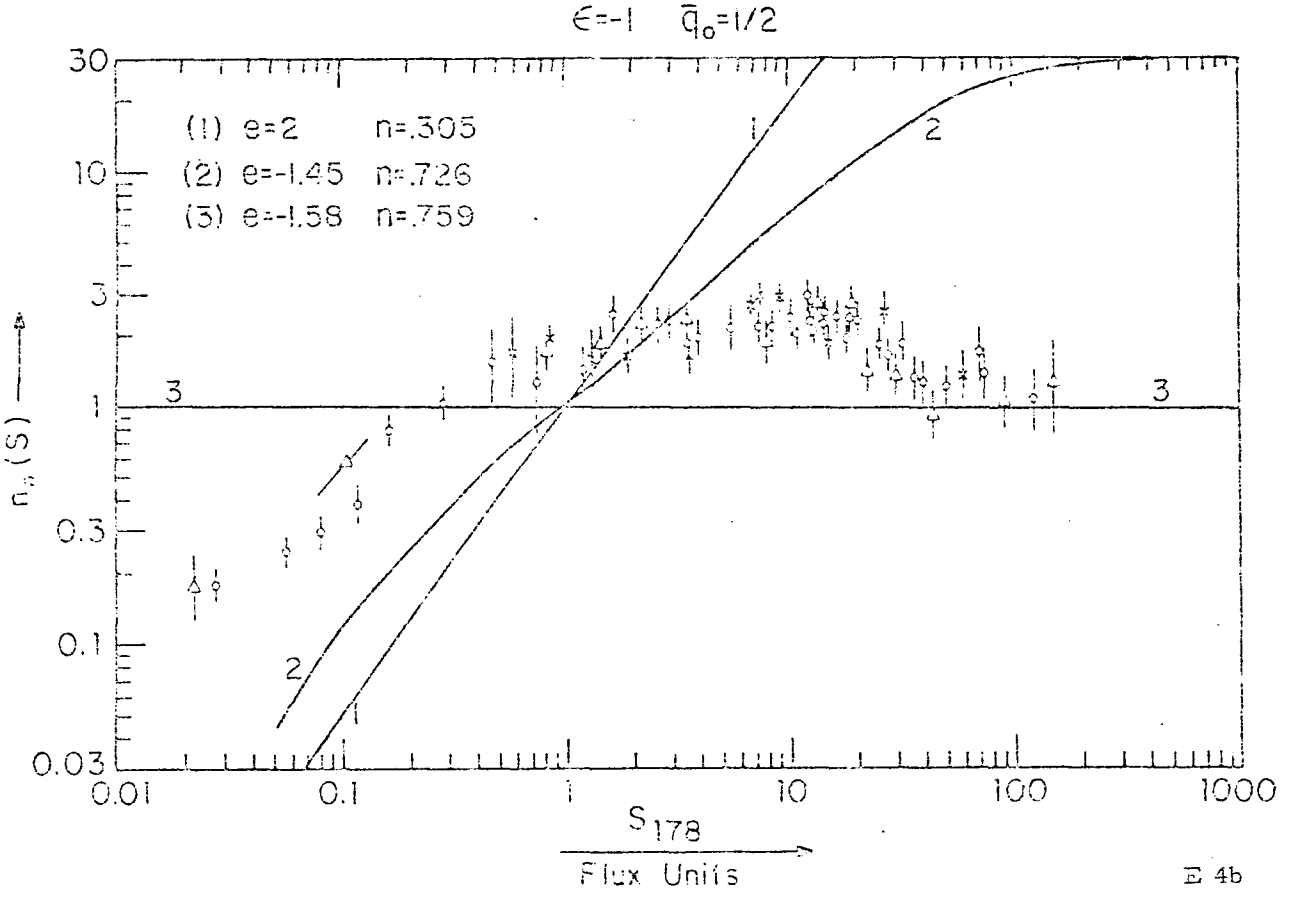
ϵ=-1 $\bar{q}_o$=1/2
(1) e=2 n=.305
(2) e=-1.45 n=.726
(3) e=-1.58 n=.759
30
10
3
1
0.3
0.1
0.03
0.01
0.1
1
10
100
1000
$n_{\nu}(S)$
S_{178}
Flux Units
1
2
3

E 4b

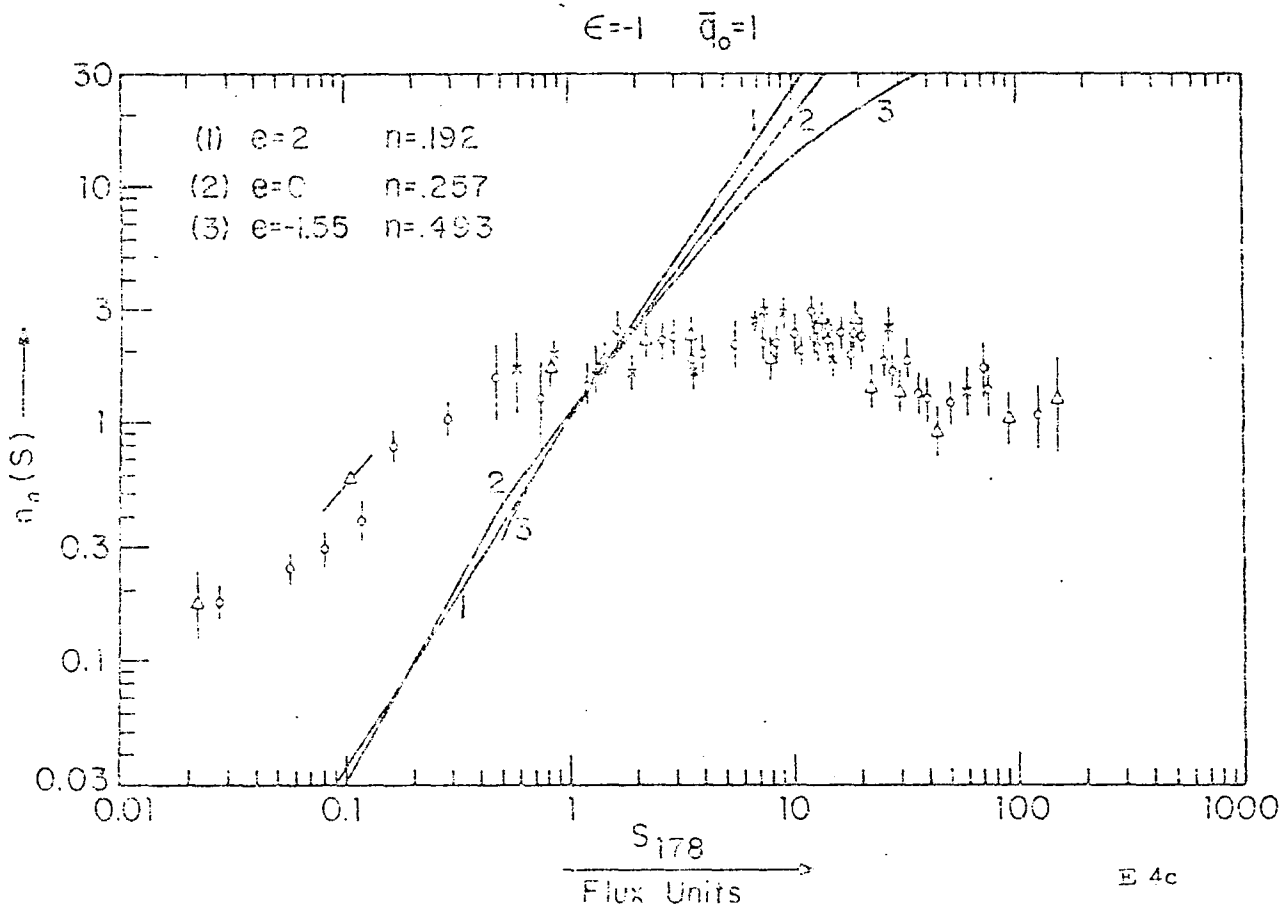
ϵ=-1 $\bar{a}_o$=1
(1) e=2 n=.192
(2) e=0 n=.257
(3) e=-1.55 n=.493
30
10
3
1
0.3
0.1
0.03
0.01
0.1
1
10
100
1000
$n_n(S)$
S_{178}
Flux Units
1
2
3

E 4c

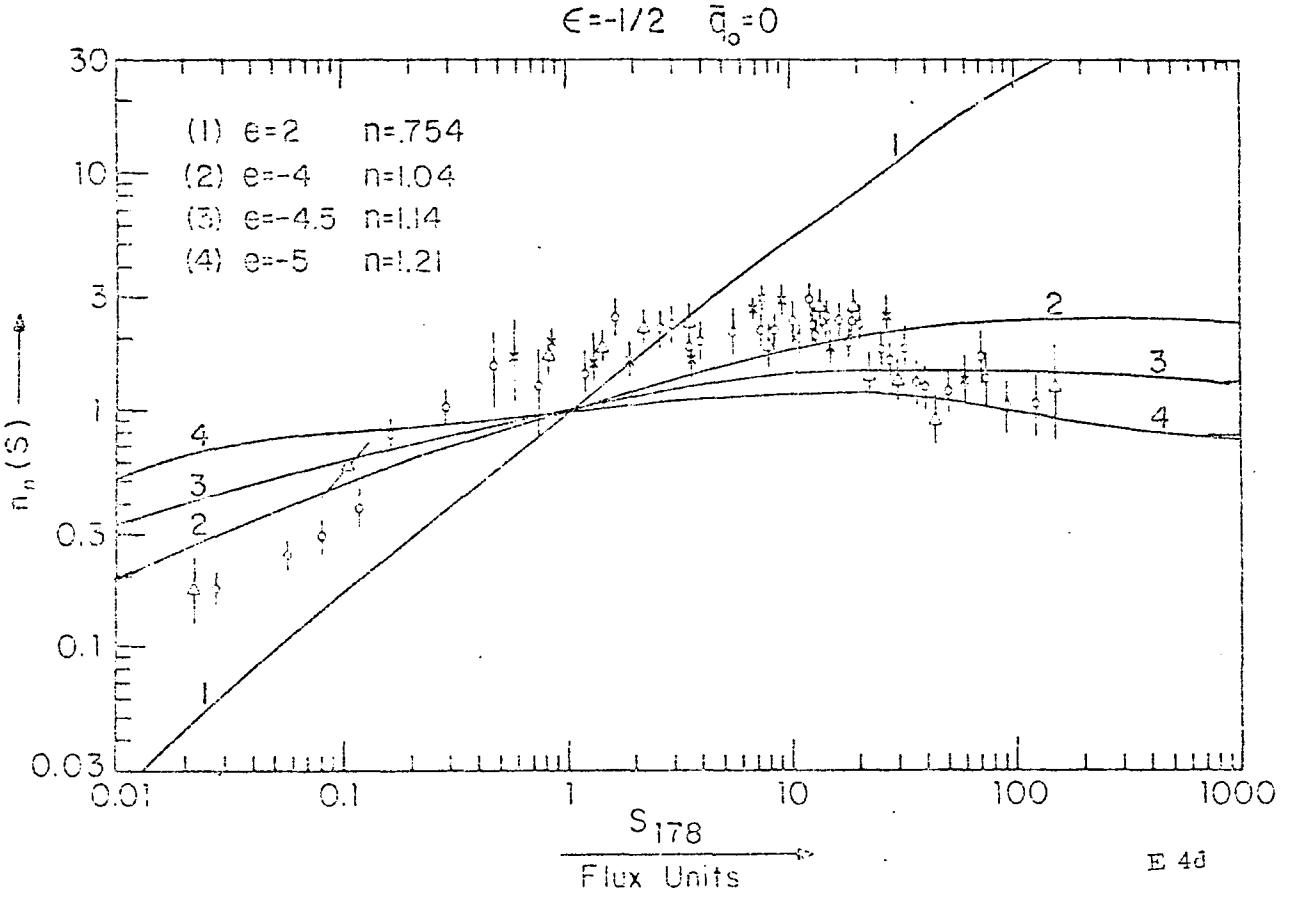
ϵ=-1/2 $\bar{a}_o$=0
(1) e=2 n=.754
(2) e=-4 n=1.04
(3) e=-4.5 n=1.14
(4) e=-5 n=1.21
$n_n(S)$
30
10
3
1
0.3
0.1
0.03
0.01
0.1
1
10
100
1000
S_{178}
Flux Units
E 4d

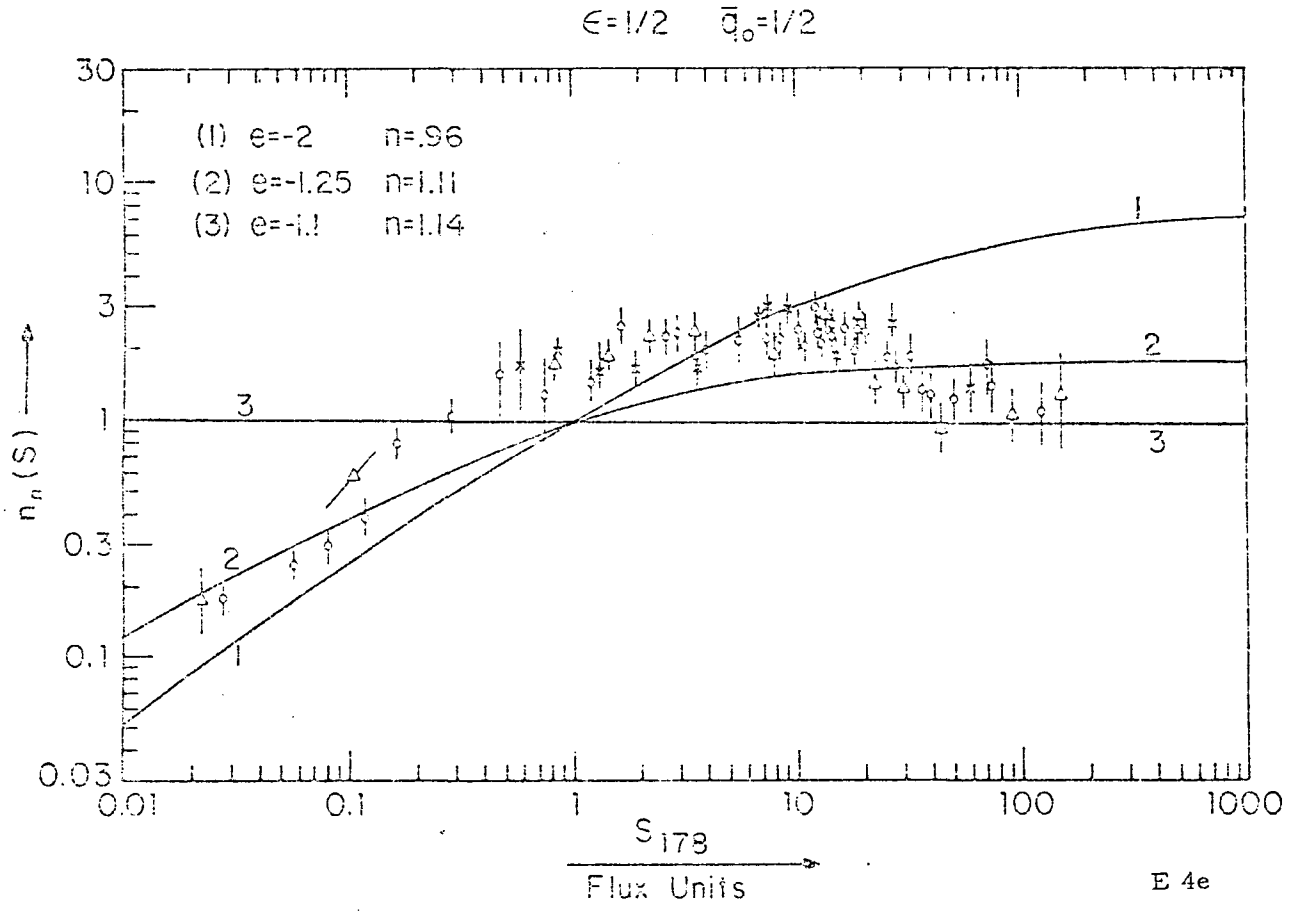
∈=1/2 $\bar{a}_0$=1/2
(1) e=-2 n=.96
(2) e=-1.25 n=1.11
(3) e=-1.1 n=1.14
30
10
3
1
0.3
0.1
0.03
$n_n(S)$
0.01
0.1
1
10
100
1000
S_{178}
Flux Units
1
2
3

E 4e

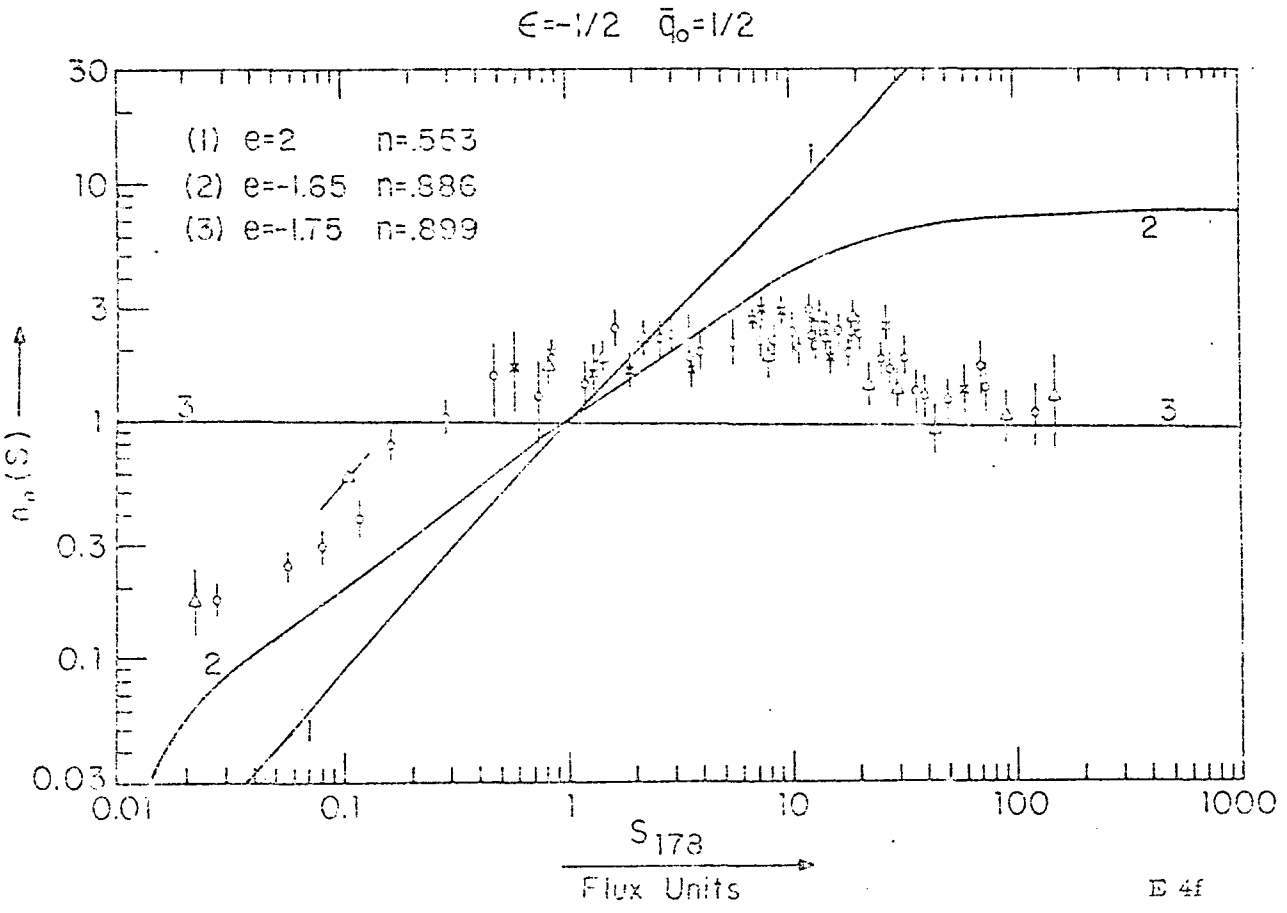
ϵ=-1/2 $\bar{q}_o$=1/2
(1) e=2 n=.553
(2) e=-1.65 n=.886
(3) e=-1.75 n=.899
30
10
3
1
0.3
0.1
0.03
$n_n(S)$
0.01
0.1
1
10
100
1000
S_{178}
Flux Units
1
2
3

E 4f

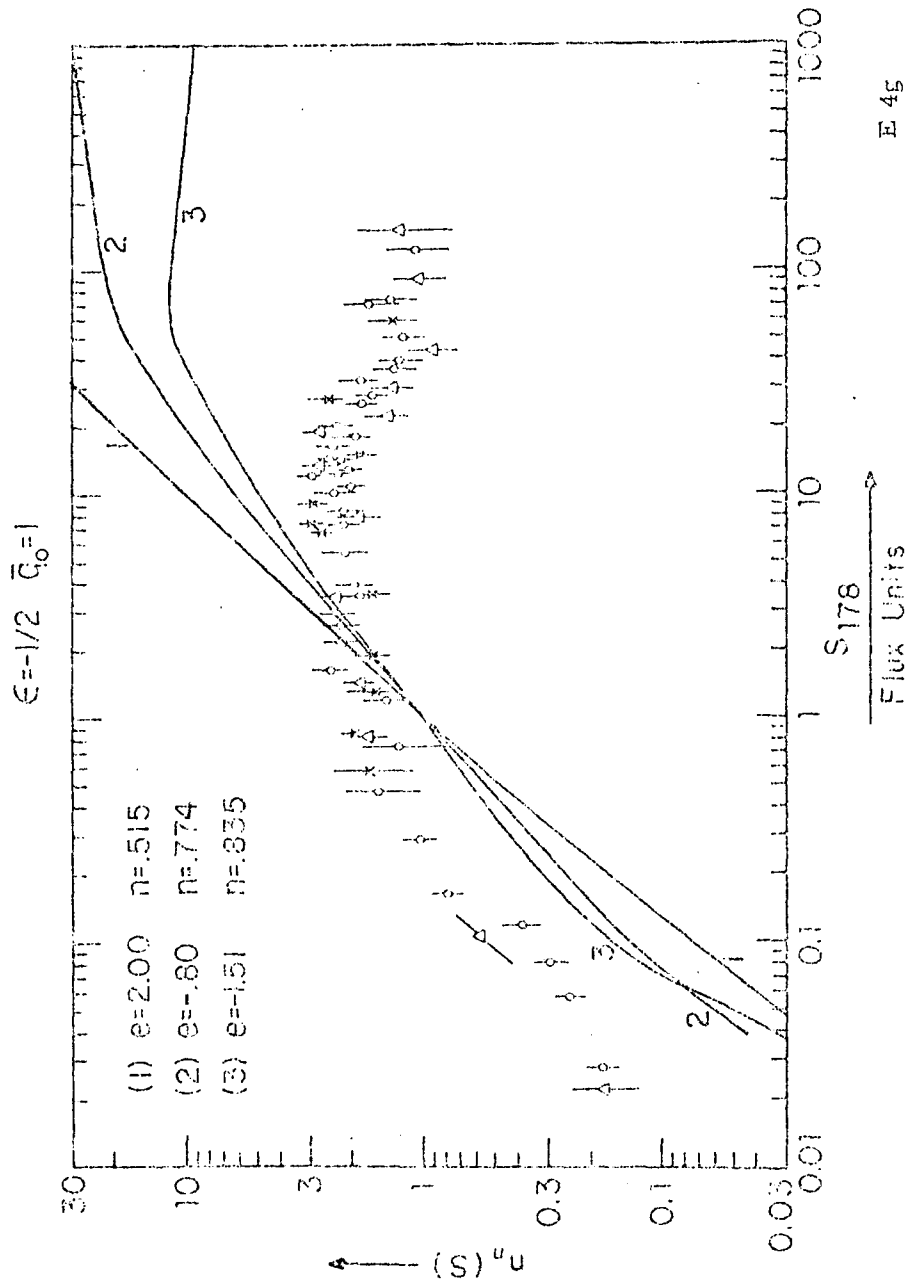
ε=-1/2 $\bar{G}_o$=1
(1) e=2.00 n=.515
(2) e=-.80 n=.774
(3) e=-1.51 n=.835
$n_u(S)$
S_{178}
Flux Units
E 45
1000
100
10
1
0.1
0.01
30
10
3
1
0.3
0.1
0.03

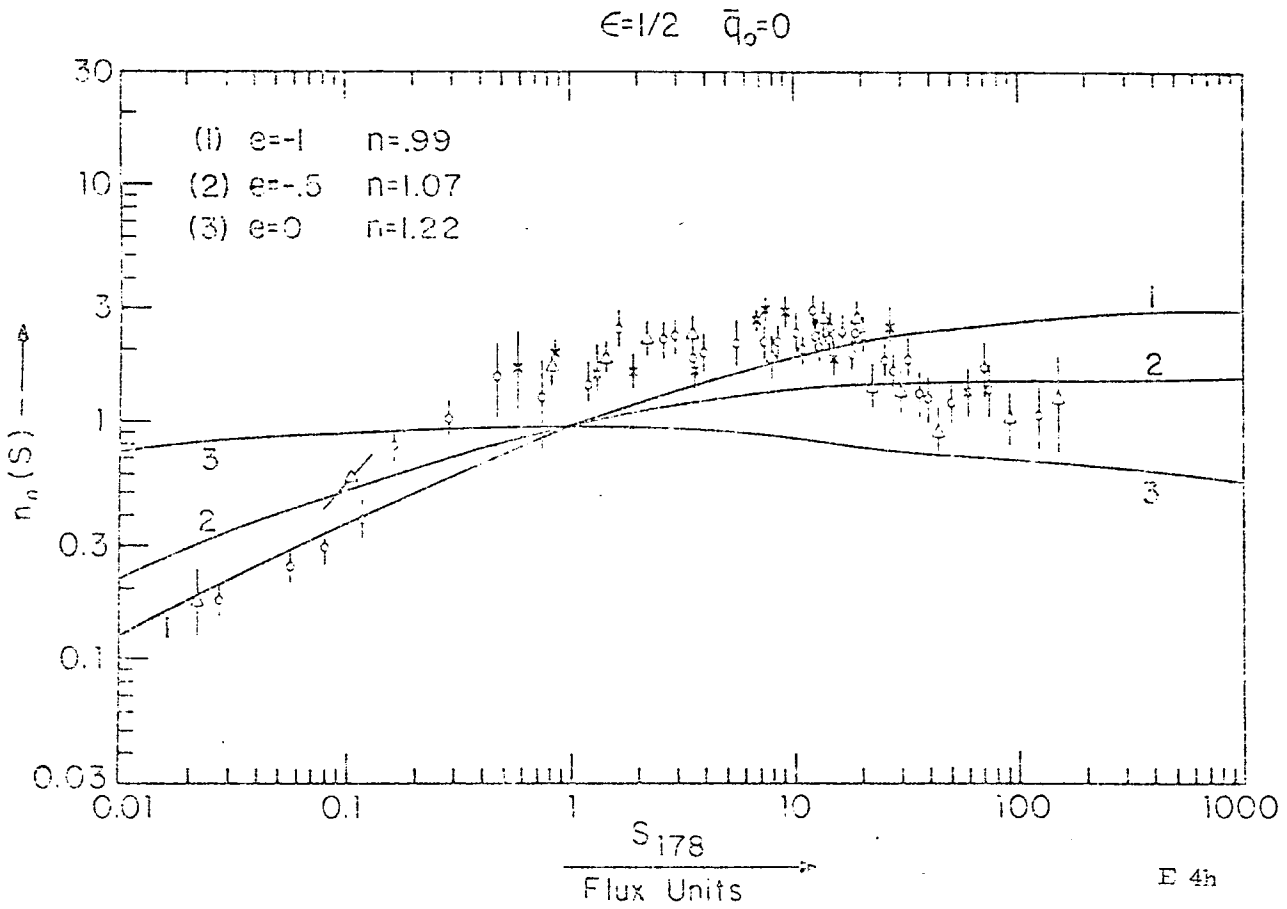
ϵ=1/2 $\bar{q}_o$=0
(1) e=-1 n=.99
(2) e=-.5 n=1.07
(3) e=0 n=1.22
30
10
3
1
0.3
0.1
0.03
0.01
0.1
1
10
100
1000
$n_o(S)$
S_{178}
Flux Units
1
2
3

E 4h

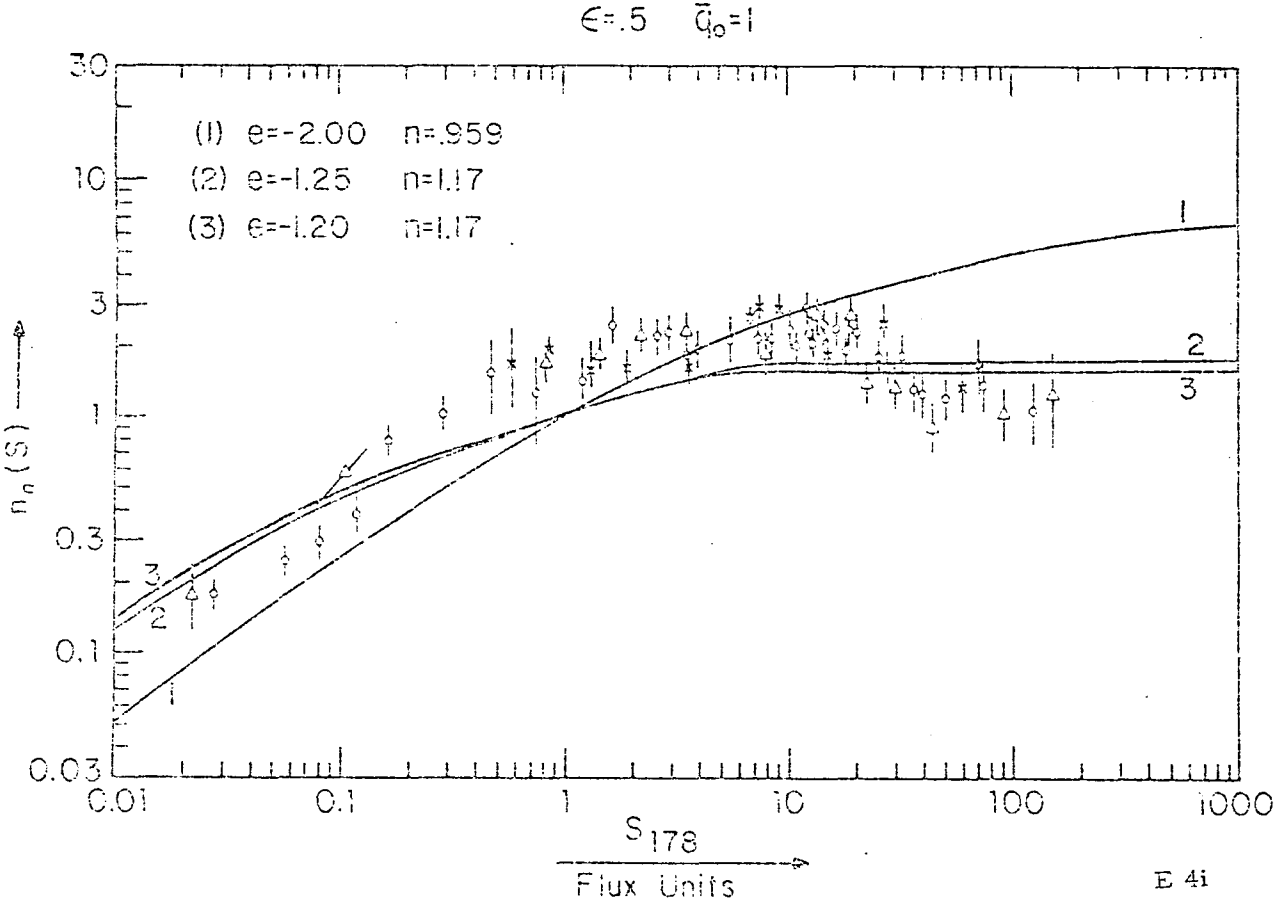
∈=.5 $\bar{q}_0$=1
(1) e=-2.00 n=.959
(2) e=-1.25 n=1.17
(3) e=-1.20 n=1.17
30
10
3
1
0.3
0.1
0.03
0.01
0.1
1
10
100
1000
$n_n(S)$
S_{178}
Flux Units
1
2
3

E 4i

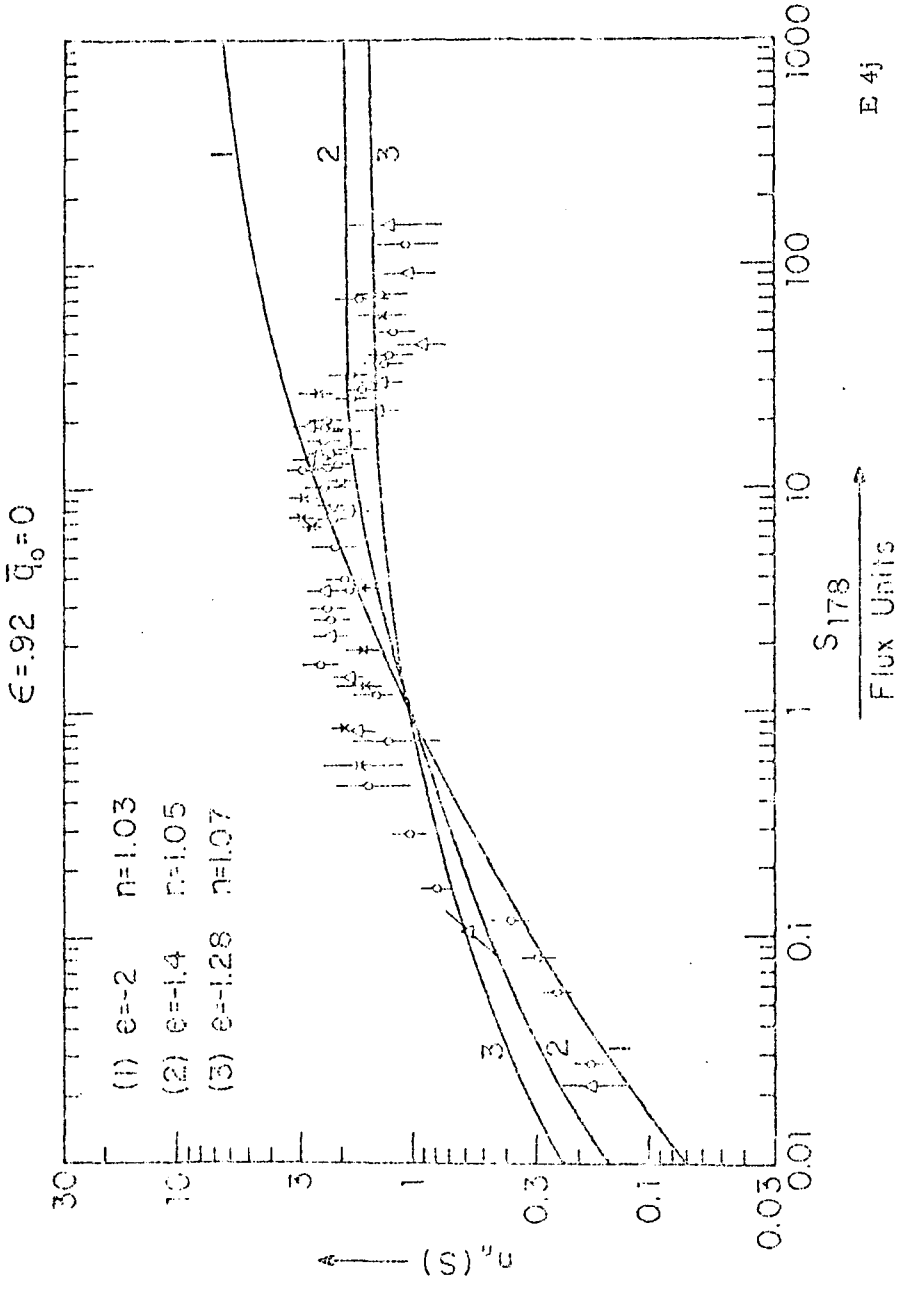
ε=.92 $\bar{q}_o$=0
(1) e=-2 n=1.03
(2) e=-1.4 n=1.05
(3) e=-1.28 n=1.07
$n_e(S)$
S_{178}
Flux Units
E 4j
30
10
3
1
0.3
0.1
0.03
0.01
0.1
1
10
100
1000

SECTION F

CONCLUDING REMARKS

F. CONCLUDING REMARKS

We have found throughout that in order to understand observations within standard cosmology either a very convoluted evolution of the sources or a peculiar geometry such as a local hole must be posited. Furthermore, the evolutions indicated by the different tests do not always agree. In addition the tests are not sensitive enough to differentiate world models, that is to determine q_o.

In the scale-covariant theory when G is allowed to vary, a gentler evolution is generally indicated, and tests such as m-z and N(m) and the differential and integrated forms of log N-log S are compatible. Furthermore, when the scale factor is an increasing function of time, it is possible to discriminate among models with different deceleration parameters. In such a case, the strong bending of the m-z curves (typical of a closed universe or strong evolution in standard cosmology) is predictable in an open universe with modest evolution. An open universe seems to be presently the most popular one in standard cosmology due to the observed deuterium abundance although it is not yet known how this abundance will be interpreted in scale-covariant cosmology. The currently favored scale is $\beta \sim t$.

Thus the cosmological geometrical tests are so far favorable to the interpretation of a non-constant scale function: indeed, there is no observational or theoretical consideration thus far which prohibits a small cosmological variation of G. To determine this within the framework of the tests considered was the purpose of this work. It is therefore of paramount importance to anyone interested in cosmology of field theory that the investigation of the validity of the physicists first guess, that G is constant, be carried further. Areas of future research are: (1) stellar structure, since this field seems less beset by the uncertainties which mask cosmological effects than those of galaxies, QSO's and tidally-perturbed planetary systems, (2) primal nucleosynthesis, (3) the development of the inhomogeneity spectrum when the Jean's mass evolves with an extra functional dependence $G^{-3/2}$, and (4) spatial regions of high energy density where G may not have decayed. Such research might give us clues of how to extend the theory beyond the asymptotic region and ultimately determine the constraints on a quantized, unified field theory.

BIBLIOGRAPHY

Bahcall, J.N. and Wills, R.E. 1973, Ap.J., 172, 699.

Baily, J.A. and Pooley, G.G. 1968, M.N.R.A.S., 138, 51.

Bennett, A.S. 1963, Mem.R.A.S., 68, 956.

Braccesi, A. and Formiggini, L. 1969, Astr. Ap., 3, 364.

Burbidge, G.R. and O Dell, S.L. 1973, Ap.J., 183, 759.

Burbidge, M. and Strittmatter 1972, Ap.J., 172, 137.

Burbidge, G., Crowne, A., and Smith, H.E. 1977, Ap.J. Supp., 33, 113.

Canuto, V., Hsieh, S.-H., and Adams, P.J. 1977, P.R. Letters, 39, 429

Canuto, V., Adams, P.J., Hsieh, S.-H., and Tsiang, E. 1977, Phys.Rev.D., 16 1643. (This paper is referred to as I.)

Canuto, V. and Hsieh, S.-H. 1978a, Ap.J., 224, 302.

Canuto, V., Hsieh, S.-H., and Adams, P.J. 1978, Phys.Rev.D, 18, 3577.

Canuto, V. and Hsieh, S.-H. 1979, Ap.J. (in press). (This paper is referred to as II.)

Canuto, V. and Narlikar, J.V. 1979 (preprint)

Chandrasekhar, S. 1943, Ap.J. 97, 255.

Christiansen, W. 1969, M.N.R.A.S., 145, 327.

Colla, G., Fanti, C., Fanti, R., Giora, I., Lala, C., and Ulrich, N. 1975, Astron. and Ap., 38, 209.

deVeny, J.B., Osborn, W.T., and James, K. 1975, Astron. Soc. of the Pacific, 33, No. 495 with Supplement.

deYoung, D.S. 1971, Ap.J., 167, 541.

Dirac, P.A.M. 1938, Proc.R.Soc.Lond., A165, 199.

Dirac, P.A.M. 1974, Proc.R.Soc.Lond., 5338.439.

Disney, 1976, Nature, 263, 573.

Dixon, R.S. 1970, Ap.J., Supp. 180, 20, 1.

Edge, D., Shakeshaft, J.R., McAdam, W.B., Archer, S., and Baldwin, J.E. 1963, Mem.R.A.S., 68, 37.

Elsmore, B., Ryle, M., and Leslie, P. 1963, Mem.R.A.S., 68, 611.

Gopal, Krishna, and Swarup 1977, M.N.R.A.S., 178, 265.

Gott III, J.R., Gunn, J.E., Schramm, D.N. and Tinsley, B.M. 1974, Ap.J., 194, 543.

Green, R.F. and Schmidt, M. 1978, Ap.J., 220, L1.

Gunn, J.E. 1978, in "Observational Cosmology", Geneva Observatory, edited by A. Maeder, L. Martinet, and G. Tammann.

Gunn, J.E. and Tinsley, B.M. 1975, Nature, 257, 454.

Hewish, A., Headhead, A.C.S., and Duffett-Smith, P.J. 1974, Nature, 232, 652.

Hills, J.G. 1977, M.N.R.A.S., 178, 1P.

von Hoerner, S. 1973, Ap.J., 186, 741.

Jauncey, D.L. 1967, Nature, 216, 847;
1975, Ann.Rev.Astr.Astrophys., 13, 23.

Lecar, M. 1974, I.A.U. Symposium #69, 161.

Longair, M.S. and MacDonald, J.S. 1969, M.N.R.A.S., 145, 309.

Maeder, A. 1977, Astr.Ap., 57, 125.

Mackay, C.D. 1973, M.N.R.A.S., 162, 1.

MacDonald, T.H., Kenderdine, S. and Neville, A.C. 1968, M.N.R.A.S., 138, 259.

MacDonald, M.S. and Miley, G.K. 1971, Ap.J., 164, 237.

McCrea, W.J. 1966, Ap.J., 144, 516;

1974, Comment on Van Flandern s talk in the VII Texas Symposium, Ann.N.Y.Acad.Sci., 262, 495;

1978, The Observatory, 98, 52.

McElhinny, M.W., Taylor, S.R., and Stevenson, D.J. 1978, Nature, 271, 367.

Miley, G.K. 1971, M.N.R.A.S., 152, 477.

Moffet, A. 1968, Brandeis Univ. Summer Inst. in Theor. Physics, Astrophys. and Gen. Rel., Vol. I.

Muller, P.M. 1978, in "On the Measurements of Cosmological Variations of the Gravitational Constant", ed. by L. Halpern, Univ. Press of Florida, Gainsville, Fla.

Narlikar, J.V. and Chitre, S.M., 1977, M.N.R.A.S., 180, 525.

Ostriker, J.P. and Tremaine, S.D. 1975, Ap.J., L113.

Pacholczyk, A.G. and Scott, J.S. 1976, Ap.J., 203, 313.

Petrosian, V. 1969 Ap.J., 155, 1029.

1976, Ap.J., 209, L1.

Readhead, A.C.S. and Hewish, A. 1974, Mem.R.A.S., 78, I,1.

Readhead, A.C.S. and Longair, M.S. 1975, M.N.R.A.S., 173, 333.

Reasenberg, R.D. and Shapiro, I., 1977 in "Experimental Gravitation", Roma, Academia Nazionale dei Lincei.

Reasenberg, R.D. and Shapiro, I. 1978, in "On the Measurement of Cosmological Variations of the Gravitational Constant", ed. by L. Halpern, Univ. Presses of Florida, Gainsville, Fla. (page 71).

Rees, M.J. and Setti, G. 1978, Nature, 219, 127.

Reinhardt, M. 1972, Ap. Letters, 12, 135.

Riley, P.A. and Pooley, G.G. 1975, Mem. R.A.S., 80, III, 105.

Rindler, W. 1956, Mont. Not. R.A.S., 116, 663.

Robertson, J.G. 1975, M.N.R.A.S., 182, 617.

Roeder, R.C. 1975, Nature, 255, 124.

Roxburgh, I.W. 1975, Nature, 261, 301.

Sandage, A. 1961a, Ap.J., 133, 355;

1961b, Ap.J., 134, 916;

1972a, Q.Jl., R.A.S., 13, 282;

1972b, Ap.J., 173, 485;

1972c, Ap.J., 178, 1;

1972d, Ap.J., 178, 25.

Sargent, W.L.W. 1973, Ap.J., 182, L13.

Schmidt, M. 1968, Ap.J., 151, 393;

1974, Ap.J., 193, 505, republished 195, Erratum.

Scott, E.L. 1951, Ap.J., 62, 248.

Setti, G. and Woltjer, L. 1973, Ann. N.Y. Acad. Sci., 224, 8.

Soltan, A. 1978, Acta Astronomica, 28, 1; ibid. 1978, 27, 339.

Stannard, D. and Neal, D.S. 1977, M.N.R.A.S., 179, 719.

Terrel, J. 1977, Am. J. of Physics, 45, 869.

Tinsley, B.M. 1976, Ap.J., 203, 63; ibid. 1976, 203, 63.

Tinsley, B.M. and Barnothy, J.M. 1973, Ap.J., 182, 343.

Tremaine, S.C., Ostriker, J.P. and Spitzer, L. 1975,

Ap.J., 196, 407.

van der Kruit, P.C. 1973, Ap. Letters, 15, 27.

Van Flandern, T. 1973 (private communication)

Véron, P. 1966, Ann. d As., 32, 231.

Wall, J.V., Pearson, T.J., and Longair, M.S. 1977,
I.A.U. Symp., 74, 269.

Wardle, J.F.C. and Miley, G.K. 1974, Astron. and Astrophys.,
30, 305.

Weinberg, S. 1972, John Wiley & Sons, Inc., Gravitation
and Cosmology.

Williams, J.G., Sinclair, W.S. and Yoder, C.F. 1978,
JPL preprint (June)

Zotov, N.V. and Davidson, W. 1973, M.N.R.A.S., 162, 127.